

Learning Following Brain Injury: Neural Plasticity Markers

Lead Guest Editor: Leeanne Carey

Guest Editors: Michael Nilsson and Lara Boyd





Learning Following Brain Injury: Neural Plasticity Markers

Neural Plasticity

Learning Following Brain Injury: Neural Plasticity Markers

Lead Guest Editor: Leanne Carey

Guest Editors: Michael Nilsson and Lara Boyd



Copyright © 2019 Hindawi. All rights reserved.

This is a special issue published in “Neural Plasticity.” All articles are open access articles distributed under the Creative Commons Attribution License, which permits unrestricted use, distribution, and reproduction in any medium, provided the original work is properly cited.

Editorial Board

Eckart Altenmüller, Germany
Shimon Amir, Canada
Victor Anggono, Australia
Sergio Bagnato, Italy
Laura Baroncelli, Italy
Michel Baudry, USA
Michael S. Beattie, USA
Alfredo Berardelli, Italy
Nicoletta Berardi, Italy
Michael Borich, USA
Davide Bottari, Italy
Clive R. Bramham, Norway
Katharina Braun, Germany
Kalina Burnat, Poland
Gaston Calfa, Argentina
Martin Cammarota, Brazil
Carlo Cavaliere, Italy
Sumantra Chattarji, India
Rajnish Chaturvedi, India
Guy Cheron, Belgium
Vincenzo De Paola, UK
Gabriela Delevati Colpo, USA

Michele Fornaro, USA
Francesca Foti, Italy
Zygmunt Galdzicki, USA
Preston E. Garraghty, USA
Paolo Girlanda, Italy
Massimo Grilli, Italy
Takashi Hanakawa, Japan
Anthony J. Hannan, Australia
Grzegorz Hess, Poland
George W. Huntley, USA
Alexandre H. Kihara, Brazil
Jeansok J. Kim, USA
Eric Klann, USA
Malgorzata Kossut, Poland
Feng Liu, China
Volker Mall, Germany
Stuart C. Mangel, USA
Diano Marrone, Canada
Aage R. Møller, USA
Jean-Pierre Mothet, France
Xavier Navarro, Spain
Martin Oudega, USA

Fernando Peña-Ortega, Mexico
Maurizio Popoli, Italy
Bruno Poucet, France
Mojgan Rastegar, Canada
Emiliano Ricciardi, Italy
Gernot Riedel, UK
Alessandro Sale, Italy
Marco Sandrini, UK
Roland Schaette, UK
Menahem Segal, Israel
Jerry Silver, USA
Naweed I. Syed, Canada
Josef Syka, Czech Republic
Yasuo Terao, Japan
Daniela Tropea, Ireland
Tara Walker, Australia
Christian Wozny, UK
Chun-Fang Wu, USA
Long-Jun Wu, USA
J. Michael Wyss, USA
Lin Xu, China

Contents

Learning following Brain Injury: Neural Plasticity Markers

Leeanne Carey , Michael Nilsson , and Lara Boyd 

Editorial (2 pages), Article ID 4838159, Volume 2019 (2019)

Correlated Resting-State Functional MRI Activity of Frontostriatal, Thalamic, Temporal, and Cerebellar Brain Regions Differentiates Stroke Survivors with High Compared to Low Depressive Symptom Scores

Peter Goodin, Gemma Lamp, Rishma Vidyasagar, Alan Connelly, Stephen Rose, Bruce C. V. Campbell, Tamara Tse , Henry Ma, David Howells, Graeme J. Hankey , Stephen Davis, Geoffrey Donnan, and Leanne M. Carey 

Research Article (12 pages), Article ID 2357107, Volume 2019 (2019)

MMP-9 Contributes to Dendritic Spine Remodeling Following Traumatic Brain Injury

Barbara Pijet , Marzena Stefaniuk, and Leszek Kaczmarek 

Research Article (12 pages), Article ID 3259295, Volume 2019 (2019)

Stroke Induces a BDNF-Dependent Improvement in Cognitive Flexibility in Aged Mice

Josh Houlton, Lisa Y. Y. Zhou, Deanna Barwick, Emma K. Gowing, and Andrew N. Clarkson 

Research Article (14 pages), Article ID 1460890, Volume 2019 (2019)

Finding the Intersection of Neuroplasticity, Stroke Recovery, and Learning: Scope and Contributions to Stroke Rehabilitation

Leeanne Carey , Alistair Walsh , Achini Adikari , Peter Goodin, Daminda Alahakoon, Daswin De Silva, Kok-Leong Ong, Michael Nilsson , and Lara Boyd 

Review Article (15 pages), Article ID 5232374, Volume 2019 (2019)

Motor Control System for Adaptation of Healthy Individuals and Recovery of Poststroke Patients: A Case Study on Muscle Synergies

Fady S. Alnajjar , Juan C. Moreno , Ken-ichi Ozaki, Izumi Kondo, and Shingo Shimoda

Research Article (13 pages), Article ID 8586416, Volume 2019 (2019)

White Matter Biomarkers Associated with Motor Change in Individuals with Stroke: A Continuous Theta Burst Stimulation Study

K. P. Wadden , S. Peters , M. R. Borich , J. L. Neva , K. S. Hayward, C. S. Mang , N. J. Snow, K. E. Brown, T. S. Woodward, S. K. Meehan , and L. A. Boyd 

Clinical Study (15 pages), Article ID 7092496, Volume 2019 (2019)

Editorial

Learning following Brain Injury: Neural Plasticity Markers

Leeanne Carey ^{1,2}, Michael Nilsson ^{1,3,4} and Lara Boyd ⁵

¹Occupational Therapy, School of Allied Health, Human Services and Sport, College of Science, Health and Engineering, La Trobe University, Bundoora, VIC 3086, Australia

²Neurorehabilitation and Recovery, Stroke, Florey Institute of Neuroscience and Mental Health, Heidelberg VIC 3084, Australia

³Faculty of Health and Medicine and Centre for Rehab Innovations, The University of Newcastle, Callaghan NSW 2308, Australia

⁴LKC School of Medicine, Nanyang Technological University (NTU), Singapore 308232

⁵Djavad Mowafaghian Centre for Brain Health, Faculty of Medicine, University of British Columbia, Vancouver, BC, Canada V6T 1Z3

Correspondence should be addressed to Leeanne Carey; l.carey@latrobe.edu.au

Received 23 June 2019; Accepted 23 June 2019; Published 2 September 2019

Copyright © 2019 Leeanne Carey et al. This is an open access article distributed under the Creative Commons Attribution License, which permits unrestricted use, distribution, and reproduction in any medium, provided the original work is properly cited.

Following a brain injury, individuals need to relearn lost skills, such as grasping, and learn new strategies to achieve goal-directed actions in daily activities. Yet the ability to learn and adapt is often disrupted. In this special issue, we called for new insights into the brain networks that support learning after brain injury, biomarkers of learning, and factors that may impact learning following brain injury.

In their review, L. Carey et al. developed and applied a novel methodology to identify key themes and topics to advance our thinking in relation to learning following brain injury, by searching the concepts of neuroplasticity, stroke recovery, and learning and finding the intersection of topics that link them. Using machine learning and natural language-processing technologies, the authors identified 23 intersecting themes (topics) from over a quarter of a million publications, with a time-linked pattern emerging. An important and unique feature of this approach was the ability to not only identify what is *common* across these contributing bodies of knowledge but also identify *gaps* in available literature. For example, while transfer of learning has been extensively researched in the learning literature, it did not emerge in relation to stroke recovery, neural plasticity, or their intersection. This highlights a gap in the knowledge base that informs stroke rehabilitation and also provides a clear direction for future research and potential applications from the field of learning. Overall, findings from this review identified foundation literature that may be synthe-

sised to advance a neuroscience informed approach to stroke rehabilitation.

To date, attention has largely been focused on motor learning after stroke. Building on this literature, F. Alnajjar et al. employed a computational approach to investigate the motor control system for adaptation in healthy individuals and in recovery poststroke. They aimed to determine whether neuromuscular control strategies are comparable between healthy individuals during their adaptation to an unfamiliar environment and stroke survivors during their recovery. Results revealed that computed muscle synergy characteristics changed both in healthy participants under unfamiliar environment conditions and in stroke survivors following motor recovery. The authors concluded that change in muscle synergies during recovery from moderate stroke most likely represents an adaptation of existing synergies, similar to what occurs in healthy individuals when neurons adapt to an unfamiliar environment. Further, a relationship between muscle synergies and energy consumption was found. Findings suggest that training leads to gradual adaptation to the new environment, with implications for energy consumption.

Knowledge of brain networks that support learning after brain injury is critical not only to advance knowledge of biomarkers of recovery facilitated by learning-based therapies but also to guide development of tailored interventions. K. Wadden et al. report on white matter biomarkers associated

with motor change in individuals with stroke. Individual variability is identified as a key issue in the application and effectiveness of adjunctive therapies, such as continuous theta burst stimulation (cTBS, i.e., repetitive brain stimulation), when paired with skilled motor practice. The authors investigated the white matter microstructure of a motor learning network, named the constrained motor connectome (CMC), as well as the corticospinal tract (CST) of lesioned and nonlesioned hemispheres. Individuals categorised as responders vs. nonresponders, based on change in motor behaviour, showed significant differences in the microstructural properties in the CMC, but not in CST. These findings revealed a potential new biomarker for training-facilitated motor recovery that extends beyond the CST alone. The relationship between the complex white matter motor network and the responsiveness of individuals to cTBS paired with motor practice was highlighted.

P. Goodin et al. looked beyond sensorimotor networks and brain structure to whole brain functional regions that may be important in learning and recovery. Factors such as mood, common poststroke, are associated with poorer recovery and worse cognitive outcomes and negatively impact response to rehabilitation in acute and subacute phases of recovery. The authors therefore sought to investigate the relationship between level of depressive symptom score and intrinsic brain activity in varying brain regions in 63 stroke survivors at 3 months poststroke. They investigated changes in low-frequency fluctuations in brain signals associated with poststroke depressive symptoms, specifically whether interaction effects might be observed. Significant interaction effects were found, involving frontostriatal and cerebellar regions, including insula. Further investigation is recommended given the role of these regions in sensorimotor processing and learning.

Two papers advance our understanding of potential biological markers of brain plasticity and learning through animal models of brain injury. J. Houlton et al. investigated the involvement of brain-derived neurotrophic factors (BDNF) in improving learning in aged mice after stroke. They established an animal model of stroke that induced delayed impairment in spatial memory. Spatial performance and memory were trained and monitored using a touchscreen and visual pairwise discrimination task. The treatment group received a BDNF decoy, TrkB-Fc. Aged mice exhibited greater stroke-induced cognitive deficits relative to young controls but also significant improvement in learning, which was dampened in the presence of the BDNF decoy. As concluded by the authors, these findings suggest age-related differences in recovery of cognitive function, with potential reopening of a critical window for recovery that is being mediated by BDNF. The role of BDNF in improving learning in aged mice after stroke was revealed.

B. Pijet et al. presented data on the influence of matrix metalloproteinase-9 (MMP-9) on dendritic spine density and morphology in an animal model of traumatic brain injury (TBI). The injury caused a marked decrease in spine density as well as spine shrinkage in the cerebral cortex ipsilateral to the injury, when compared to sham animals and the contralateral side, both one day and one week after the insult.

Decreased spine density was also observed in the dentate gyrus of the hippocampus. In mice lacking MMP-9, no effects of TBI on spine density and morphology were observed, further implying a role for MMP-9 in brain plasticity.

Through this special issue, we have sought to bring together a themed collection of new insights and pathways to the investigation of learning following brain injury, focusing on markers of neural plasticity. We thank the authors for their contributions and hope this issue serves to stimulate further research across multiple disciplines and fields of related research. Perhaps in a decade, a similar review to that conducted by L. Carey et al. may reveal a rich intersection of knowledge across the fields of neural plasticity, learning, and stroke recovery?

Conflicts of Interest

The authors declare that there is no conflict of interest regarding the publication of this article.

*Leeanne Carey
Michael Nilsson
Lara Boyd*

Research Article

Correlated Resting-State Functional MRI Activity of Frontostriatal, Thalamic, Temporal, and Cerebellar Brain Regions Differentiates Stroke Survivors with High Compared to Low Depressive Symptom Scores

Peter Goodin,^{1,2} Gemma Lamp,¹ Rishma Vidyasagar,¹ Alan Connelly,³ Stephen Rose,⁴ Bruce C. V. Campbell,² Tamara Tse ,^{1,5} Henry Ma,⁶ David Howells,^{7,8} Graeme J. Hankey ,⁹ Stephen Davis,^{2,7} Geoffrey Donnan,⁷ and Leanne M. Carey ^{1,5,7}

¹Neurorehabilitation and Recovery, Stroke, Florey Institute of Neuroscience and Mental Health, Melbourne Brain Centre-Austin Campus, Heidelberg, Victoria, Australia

²Department of Medicine and Neurology, Melbourne Brain Centre, Royal Melbourne Hospital, Parkville, Melbourne, Victoria, Australia

³Advanced Imaging, Florey Institute of Neuroscience and Mental Health, Melbourne Brain Centre-Austin Campus, Heidelberg, Victoria, Australia

⁴Australian e-Health Research Centre, CSIRO, Brisbane, Queensland, Australia

⁵Occupational Therapy, School of Allied Health, Human Services and Sport, College of Science, Health and Engineering, La Trobe University, Bundoora, Victoria, Australia

⁶Department of Medicine, School of Clinical Sciences, Monash University, Clayton, Victoria, Australia

⁷Department of Florey, University of Melbourne, Parkville, Victoria, Australia

⁸School of Medicine, University of Tasmania, Australia

⁹Medical School, University of Western Australia, Perth, Western Australia, Australia

Correspondence should be addressed to Leanne M. Carey; l.carey@latrobe.edu.au

Received 23 November 2018; Revised 11 May 2019; Accepted 29 May 2019; Published 28 July 2019

Academic Editor: Carlo Cavaliere

Copyright © 2019 Peter Goodin et al. This is an open access article distributed under the Creative Commons Attribution License, which permits unrestricted use, distribution, and reproduction in any medium, provided the original work is properly cited.

Background. One in three survivors of stroke experience poststroke depression (PSD). PSD has been linked with poorer recovery of function and cognition, yet our understanding of potential mechanisms is currently limited. Alterations in resting-state functional MRI have been investigated to a limited extent. Fluctuations in low frequency signal are reported, but it is unknown if interactions are present between the level of depressive symptom score and intrinsic brain activity in varying brain regions. **Objective.** To investigate potential interaction effects between whole-brain resting-state activity and depressive symptoms in stroke survivors with low and high levels of depressive symptoms. **Methods.** A cross-sectional analysis of 63 stroke survivors who were assessed at 3 months poststroke for depression, using the Montgomery-Åsberg Depression Rating Scale (MÅDRS-SIGMA), and for brain activity using fMRI. A MÅDRS-SIGMA score of >8 was classified as high depressive symptoms. Fractional amplitude of frequency fluctuations (fALFF) data across three frequency bands (broadband, i.e., ~0.01–0.08; subbands, i.e., slow-5: ~0.01–0.027 Hz, slow-4: 0.027–0.07) was examined. **Results.** Of the 63 stroke survivors, 38 were classified as “low-depressive symptoms” and 25 as “high depressive symptoms.” Six had a past history of depression. We found interaction effects across frequency bands in several brain regions that differentiated the two groups. The broadband analysis revealed interaction effects in the left insula and the left superior temporal lobe. The subband analysis showed contrasting fALFF response between the two groups in the left thalamus, right caudate, and left cerebellum. Across the three frequency bands, we found contrasting fALFF response in areas within the fronto-limbic-thalamic network and cerebellum. **Conclusions.** We provide evidence that fALFF is sensitive to changes in poststroke depressive symptom severity and implicates frontostriatal and cerebellar regions, consistent with previous studies. The use of multiband analysis could be an effective method to examine neural correlates of depression

after stroke. The START-PrePARE trial is registered with the Australian New Zealand Clinical Trial Registry, number ACTRN12610000987066.

1. Introduction

Post stroke, patients frequently experience motor, sensory, cognitive, and behavioural changes, all of which may impact recovery [1]. Changes to a stroke survivor's mood are also common [2], with depression as the most frequently reported psychiatric disorder following ischaemic stroke [3]. Post-stroke depression (PSD) is estimated to affect approximately one-third of survivors [4, 5], compared to about one-sixth of the nonstroke population [6, 7].

PSD is associated with poorer recovery prospects [8], including increased disability [9], worse cognitive outcomes [10–12], decreased quality of life [13], and increased risk of mortality [14]. In particular, PSD negatively impacts response to rehabilitation in acute and subacute phases of recovery [15]. However, our understanding of the potential mechanisms underlying the negative impact of depressive symptoms on recovery and rehabilitation is currently limited. Determining factors that may assist in the identification of those “at risk” of developing poststroke depression may aid in the recovery process and/or prediction of response to rehabilitation.

The value of biomarkers of stroke recovery that focus on brain structure and function has recently been highlighted in consensus-based recommendations [16]. Neuroimaging markers of depression may be used to provide new insight into neural mechanisms underlying depression, to predict the likelihood of future depressive symptoms, and/or to predict readiness to engage in treatment or treatment response. All are important reasons to identify stroke survivors with underlying vulnerabilities that may be “at risk” of developing depression.

One approach has been to investigate the relationship between lesion location and depression; however, despite a large number of studies, findings are equivocal [17–20]. These findings suggest that lesion location alone is unlikely to be an informative biomarker associated with PSD. A meta-analysis of behavioural, biochemical, and neuroimaging markers of PSD found associations with reduced cerebral blood flow and regional volume reductions [21].

In the broader literature of clinical depression, the disorder is not considered to be caused by independent, localised changes within specific brain regions but is thought to be partially due to disruption of communication between areas [22]. Several meta-analyses of fMRI cohort studies of clinical depression have found changes in brain activation and connectivity [23–25]. Findings highlight alteration of brain regions consistent with the current system-level models of depression. It may therefore be useful to examine biomarkers of PSD using resting-state methods that focus on intrinsic brain activity and whole brain [26].

Resting-state fMRI methods focus on low frequency fluctuations (LFF) present within the blood oxygen level-dependent (BOLD) signal (0.01 to ~0.1 Hz) [27] which in

part reflect intrinsic neuronal activity [28, 29]. Several methods have been developed that evaluate different aspects of the signal. For example, local or regional correlations between BOLD time series are able to be examined, collectively known as functional connectivity [30]. These functional connectivity analyses focus on temporal correlations of the BOLD signal.

The spectral (frequency) characteristics of signal within individual voxels during resting-state can also be examined, typically by taking the sum amplitude of low frequency fluctuations (ALFF) [31] or a ratio of LFF over the entire estimated spectra (fractional ALFF, fALFF) [32]. Of these two methods, fALFF has been shown to be robust against physiological artefacts and vascular effects [33, 34], which are common poststroke given changes to neurovasculature post-stroke [35].

While methods typically focus on the full LFF range, spectral measures allow the exploration of subbands, which have been suggested to be important for a scope of physiological and function processes within the brain [36, 37]. Wang et al. [38, 39] used fALFF to examine LFF and subbands of slow-5 (0.01–0.027 Hz) and slow-4 (0.027–0.07) in medication of naive participants with major depressive disorder over two studies. Both studies found similar changes in LFF measures when depressed participants were compared to controls.

Wang et al. [39] also found areas that displayed an interaction effect between controls and those with depression and subband signal changes. Their results showed that the areas of the left ventromedial prefrontal cortex, left inferior frontal gyrus, and bilateral precuneus showed changes in amplitude in the slow-5 band, but not slow-4. This suggests that examination of subbands may be useful in identifying regions that are associated with depressive symptoms. It also highlights the value of investigating for an interaction effect in brain regions.

To date, PSD studies of resting-state changes have not been widely employed, have focused on functional connectivity from specific regions, e.g., within the default mode network (DMN) and anterior cingulate, and have included participants of varying times post stroke. Results from these studies have been inconsistent. For example, Lassalle-Lagadec et al. [40] found correlations at 10 days post stroke between the depression score and the left middle temporal cortex and precuneus and at 3 months with the neostriatum. Vicentini et al. [41] found an association with the posterior cingulate cortex and depression score at approximately 1-month poststroke, while Liu et al. [42] failed to find any regional correlations of the posterior cingulate with a depression score in a cohort of chronic stroke survivors. More recently, Balaev et al. [43] explored changes in the default mode network and found changes post treatment. Only one study, by Egorova et al. [44], used voxelwise spectral analysis of fALFF and found mean differences between

depressed and nondepressed stroke survivors in the frontal and insular regions.

While examining main effects that can be informative for identifying brain regions for further examination, they give no information regarding how intrinsic activity in these regions may influence the individual depressive symptom score. Furthermore, finding regions that show differing response depending on regional activity may help identify potential biomarkers and predict severity of depressive symptoms [45, 46].

Our aim was to examine the interaction effects between the amplitude of whole-brain resting-state signal (using broadband and subband fALFF) and depressive symptom score, in stroke survivors with high and low levels of depressive symptoms. We hypothesised that there would be a significant interaction effect in frontolimbic regions with the depressive symptom score, such that the high depressive score group would show a positive association between the depressive symptom score and increases in regional brain signal response.

2. Methods

2.1. Participants. Sixty-three participants (44 female) with advanced imaging from the STroke imAging pRevention and Treatment (START) cohort [47] were included in the current study. Participants were three months post their first ischaemic stroke episode, diagnosed clinically, and confirmed via brain imaging. They were required to be medically stable, be 18 years or older, speak English, not have a significant disability prior to stroke, and be able to give informed consent. Stroke participants were excluded if they had a brainstem infarct, previous neurological dysfunction, or evidence of unilateral spatial neglect or were not suitable for MRI.

2.2. Clinical Data, Depression Symptom Assessment, and Group Formation. Data was obtained on age, sex, and history of depression prior to their stroke. Stroke severity was measured using the National Institute of Health Stroke Scale (NIHSS) [48]. We assessed for depressive symptoms using the structured interview guide for the Montgomery-Åsberg Depression Rating Scale (MÅDRS-SIGMA) [49]. The MÅDRS-SIGMA is a 10-item structured interview that enquires into participants' range of depressive symptoms including reported sadness, inner tension, concentration difficulties, and pessimistic thoughts. Each item is scored on a range from 0 (no symptoms present) to 6 (high levels of symptoms present). Total scores on the MÅDRS-SIGMA range from 0 to 60 with higher scores indicating higher levels of depressive symptoms. Participants were placed into low or high depressive symptom groups based on the MÅDRS-SIGMA cut-off score of >8. This cut-off was chosen as it has been shown to give the optimal sensitivity and specificity (0.85, 0.71, AUC = 0.91 [95%CI = 0.84–0.98]) for the classification of poststroke depression from a sample of 150 stroke patients [50].

2.3. MRI Acquisition. Imaging data was acquired on a 3 Tesla Siemens Trio scanner. Resting-state functional data was

acquired using an echo planar imaging (EPI) sequence over 7 minutes (TR = 3000 ms, TE = 30 ms, 3 mm isotropic voxels, 72×72 matrix, 44 slices, 216 mm FOV). Participants were instructed to "Close your eyes and rest. You do not need to think about anything in particular" and were also instructed that they should stay awake throughout the scan. Following the scan, this was confirmed by participant report. Resting-state acquisition was consistently conducted after a touch activation task to the fingertips.

A high-resolution 1 mm isotropic MPRAGE scan (TR = 1900 ms, TE = 2.55 ms, 256×256 matrix, 160 slices, 216 mm FOV) was collected for coregistration to the functional data, segmentation, and normalisation to MNI space. 2D FLAIR (fluid attenuation inverse recovery sequence; 1 mm isotropic, TR = 6000 ms, TE = 388 ms, 100 mm FOV) was acquired axially for delineation of infarcts.

2.4. Lesion Mask Creation. Axial FLAIR images were used to identify and draw a mask around the primary infarct hyperintensity using MRicron (<http://www.mccauslandcenter.sc.edu/mricro/mricron/index.html>). Masks were quality checked and modified as necessary by a neurologist (BC) to ensure they accurately represented the infarct.

2.5. Resting-State Preprocessing and Analysis. A customised data cleaning pipeline optimised for preprocessing of stroke data was constructed [51]. The pipeline used functions from DCMstack (<https://github.com/moloney/dcmstack>), Analysis of Functional NeuroImages (AFNI) [52], SPM12 v6685 (<http://www.fil.ion.ucl.ac.uk/spm/software/spm12/>), Advanced Normalization Tools (ANTs) [53], Numpy [54], Scipy [55], and Nibabel (<https://github.com/nipy/nibabel>), combined under the NiPy framework [56].

Anatomical image preprocessing consisted of segmentation using the new segmentation method and coregistration to the mean EPI image [51]. White matter and cerebrospinal fluid (CSF) masks were created by thresholding the segmented white matter and CSF images at 0.99 and eroding two times using a $3 \times 3 \times 3$ mm structure element to minimise partial volume effects. Normalisation to Montreal Neurological Institute (MNI) space was achieved by transforming an MNI space $3 \times 3 \times 3$ mm template image to subject space, then using the inverse transformation matrix to warp the T1 image from subject space to MNI space. Stroke participants had their FLAIR and lesion mask included in the pipeline, which were coregistered to the T1 image and coregistered to the EPI image [51].

Prior to preprocessing, we conducted systematic, visual quality inspection of each participant's resting-state data. Participants were excluded if their data were shown to have consistent, excessive motion or noticeable distortions. No participants were excluded on this basis. Preprocessing of EPI data included despiking, slice timing correction to the central slice, and realignment to the first volume. Motion and physiological related artefact were regressed from the data using the Friston 24 parameter model [57] and aCompCor [58], taking the top five components each for white matter and CSF mask extracted signals. The global signal from within the brain mask was also regressed. This can help

attenuate residual motion and physiological effects not removed by prior cleaning [59]. In connectivity-based measures, global signal regression is thought to alter the covariance structure of the data, introducing artefactual negative correlations [60, 61]. However, as fALFF is derived from voxel-based spectral data, there is no evidence that this step impacts individual or group measures. After cleaning, images were normalised to MNI space using the inverse transform matrix computed from the EPI space T1 image. The data were then smoothed using a 6 mm Gaussian kernel.

2.6. fALFF Calculation and Analysis. We employed fALFF broadband and subband (slow-5/slow-4) measures to examine for potential associations between the resting-state brain activity and poststroke depressive symptom score. fALFF maps were calculated using the method outlined by Zuo et al. [34]. Briefly, data were linearly detrended and using Fast Fourier Transform, converted to the frequency domain. The square root of the transform was used to convert the power spectra to spectral magnitude. fALFF was defined as the voxel-wise ratio of the sum of LFF data (~ 0.01 Hz to 0.08 Hz) over the sum of the entire spectra (~ 0 Hz to 0.33 Hz). Slow-5 and slow-4 bands were calculated by taking frequency bands from ~ 0.01 to 0.027 and 0.027 to 0.07 Hz, respectively, and dividing over the entire spectra. Participant fALFF maps were then z -scored by subtracting the global fALFF mean value from each voxel and divided by the global fALFF standard deviation.

Second level analysis was performed in SPM 12 using cluster-based familywise error correction (cFWE) to control multiple comparisons, with the cluster forming threshold set to $p < 0.001$ [62] and spatial threshold set to $p < 0.05$.

An interaction model of the group \times MÅDRS-SIGMA was used, which initially included covariates of age, sex, and NIHSS. No significant voxels were found for covariates (all cFWE > 0.05), so these were removed from the model and the data were reanalysed. Significant clusters were localised using the automatic anatomical labelling (AAL) atlas [63] as found in the Wake Forest University PickAtlas v3.0.5 [64, 65]. fALFF amplitudes for significant clusters were extracted and used in further analysis.

2.7. Statistical Analysis. Demographic data were analysed using the statistical package R [66] for between-group comparisons. We examined differences in sex membership and prestroke history of depression between groups using chi-square tests with p values simulated based on 10,000 reshuffles. Two sample t -tests were used to examine differences between groups for age and NIHSS.

2.8. Data Visualisation. fMRI data were visualised using mricroGL (<http://www.mccauslandcenter.sc.edu/mricrogl/>). Extracted fALFF data were visualised using Seaborn (<https://seaborn.pydata.org/>).

3. Results

3.1. Demographics. Demographic and clinical information for the low and high depressive symptom score groups is presented in Table 1.

TABLE 1: Demographic and clinical information for the low and high depressive symptom score groups.

Group	Low	High
n	38	25
Age (mean, SD)	64.68 (13.56)	59.28 (12.26)
Sex (no. of females)	28	19
MÅDRS-SIGMA score (mean, SD)	2.29 (2.31)	14.88 (6.67)***
History of depression	0/38 (0%)	6/25 (24%)**
Reported sadness (yes/no)	5/33 (13.1%)	15/10* (60%)
Reported discouragement (yes/no)	4/34 (10.5%)	15/10** (60%)
Reported loss of interest (yes/no)	3/35 (7.9%)	16/9** (64%)
On antidepressant medication (yes/no)	1/37 (2.6%)	3/22 (13.6%)
NIHSS (mean, SD)	0.58 (1.20)	0.84 (1.28)

* $p < 0.05$, ** $p < 0.01$, and *** $p < 0.001$. MÅDRS-SIGMA = Montgomery-Åsberg Depression Rating Scale using Structured Interview Guide.

Two sample t -tests showed no significant difference between the two groups for age ($t(55.06) = 1.64$, $p = 0.10$) or NIHSS ($t(49.01) = 0.81$, $p = 0.42$). Chi-square tests showed no significant difference between the groups for sex ($\chi^2 = 0.67$, $p = 0.57$).

The high depressive symptom score group showed a significantly increased MÅDRS-SIGMA score compared to the low group ($t(27.83) = 9.08$, $p < 0.001$), as expected. There were also significantly higher counts of reported sadness ($\chi^2 = 5.99$, $p = 0.021$), discouragement ($\chi^2 = 7.58$, $p = 0.012$), and loss of interest in daily activities ($\chi^2 = 7.72$, $p = 0.008$) in the high depressive symptom score group compared to low. No significant differences were observed between the low and high groups for counts of antidepressant usage ($\chi^2 = 2.23$, $p = 0.29$).

The high depressive symptom score group showed a greater number of participants with a prestroke history of depression ($\chi^2 = 10.08$, $p = 0.002$). There did not appear to be a significant difference in the MÅDRS-SIGMA score between those with a history of depression ($M = 20.00$, $SD = 8.53$) and those without ($M = 13.26$, $SD = 5.25$) in the subgroup analysis of the high depressive symptom score group ($t(6.25) = 1.83$, $p = 0.11$).

3.2. Lesion Overlap. The overlap of lesion locations across all participants and the groups is shown in Figure 1. Lesion locations across all participants showed the largest overlap in the left and right hemispheres, in an area including the internal capsule, corona radiata, and insula. Damage to the right hemisphere extended to lateral parietal regions. The low and high depressive symptom score groups showed the greatest overlap in the right internal capsule/corona radiata.

3.3. Functional Connectivity fALFF Results. Examination of the interaction between the group and MÅDRS-SIGMA score showed several regions across the three bands of interest that had an increased slope for the high depressive

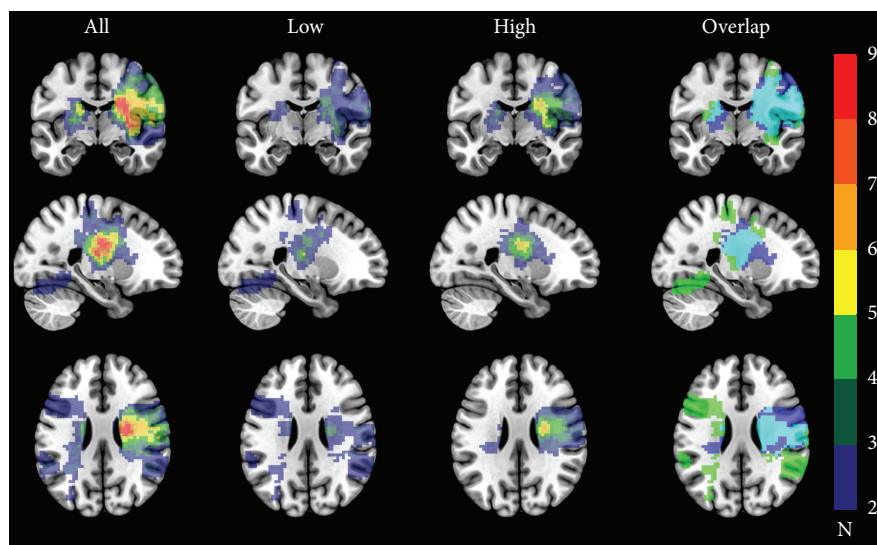


FIGURE 1: Overlap of lesion locations for all participants, low depressive symptom score group, high depressive symptom score group, and overlap of lesion location for the low and high groups. For columns All, Low, and High, cooler colours indicate lower numbers of participants with overlapping lesions, and warmer colours indicate higher numbers of participants with overlapping lesions. For the Overlap column, green = low depressive symptom score group, dark blue = high depressive symptom score group, and light blue = overlap between the two groups. All brain images are shown in neurological convention.

TABLE 2: Regions that showed significant group \times MÅDRS-SIGMA score interaction effects for broadband (0.01–0.08 Hz), slow-4 band (0.027 to 0.067 Hz), and slow-5 band (0.01–0.027 Hz) of interest. Peak voxel region, coordinates in the MNI space, cluster size (k) and statistical values (t , z , r^2 , and p) of regions are reported.

Region	MNI coords (xyz)	k	t/z	r^2	p
<i>Broadband</i>					
Left superior temporal lobe	-36 -39 27	72	5.06/4.59	0.30	0.006
Left insula	-30 21 -9	49	4.82/4.41	0.28	0.035
<i>Slow-4</i>					
Left thalamus	-15 -27 12	44	4.60/4.24	0.26	0.025
Right caudate	18 12 15	59	4.48/4.14	0.25	0.006
<i>Slow-5</i>					
Left cerebellum, posterior lobe	-30 -66 -24	45	4.28/3.98	0.24	0.030

symptom score group compared to the low depressive symptom score group. No significant increases or decreases in the slope were found for the low depression symptom score group. Cluster location, coordinates, and summary information for the three bands are shown in Table 2. R -squared values were calculated using the formula $r^2 = \sqrt{t^2/(t^2 + df)}$, where t is the peak voxel value of the cluster and df is the degrees of freedom. Regions and cluster interaction effects are presented in Figure 2.

4. Discussion

A significant *interaction effect* was observed between groups with low and high depressive symptoms. Our data showed that for the high depressive symptom score group, (those who scored greater than 8 on the MÅDRS-SIGMA), the increased symptom score was associated with increased fALFF amplitude in the left insula, superior temporal lobe, thalamus and cerebellum, and right caudate. Conversely, no

significant association was found between the fALFF amplitude and low depressive symptom score group. Such an interaction effect has not been previously described.

The interaction effect found adds a novel insight as it maps a linear relationship with signal changes in brain regions with depressive symptom scores, separable by low and high depressive symptoms. In addition, the fact that these differential effects were observed in the same regions for patients with and without depressive symptoms provides further support for a role for this set of regions in depression. For example, we observed an interaction effect in the insula. The insula has been extensively associated with depression in prior studies of nonstroke depression, yet it is unclear if insula is hyper- or hypoactivated, with variable reports depending on the use of positive or negative stimuli, the stage (first episode vs. repeated), or severity (major vs. subthreshold) of depression [67].

Our findings provide insight into how brain signal is differentially associated with the depression score in those with

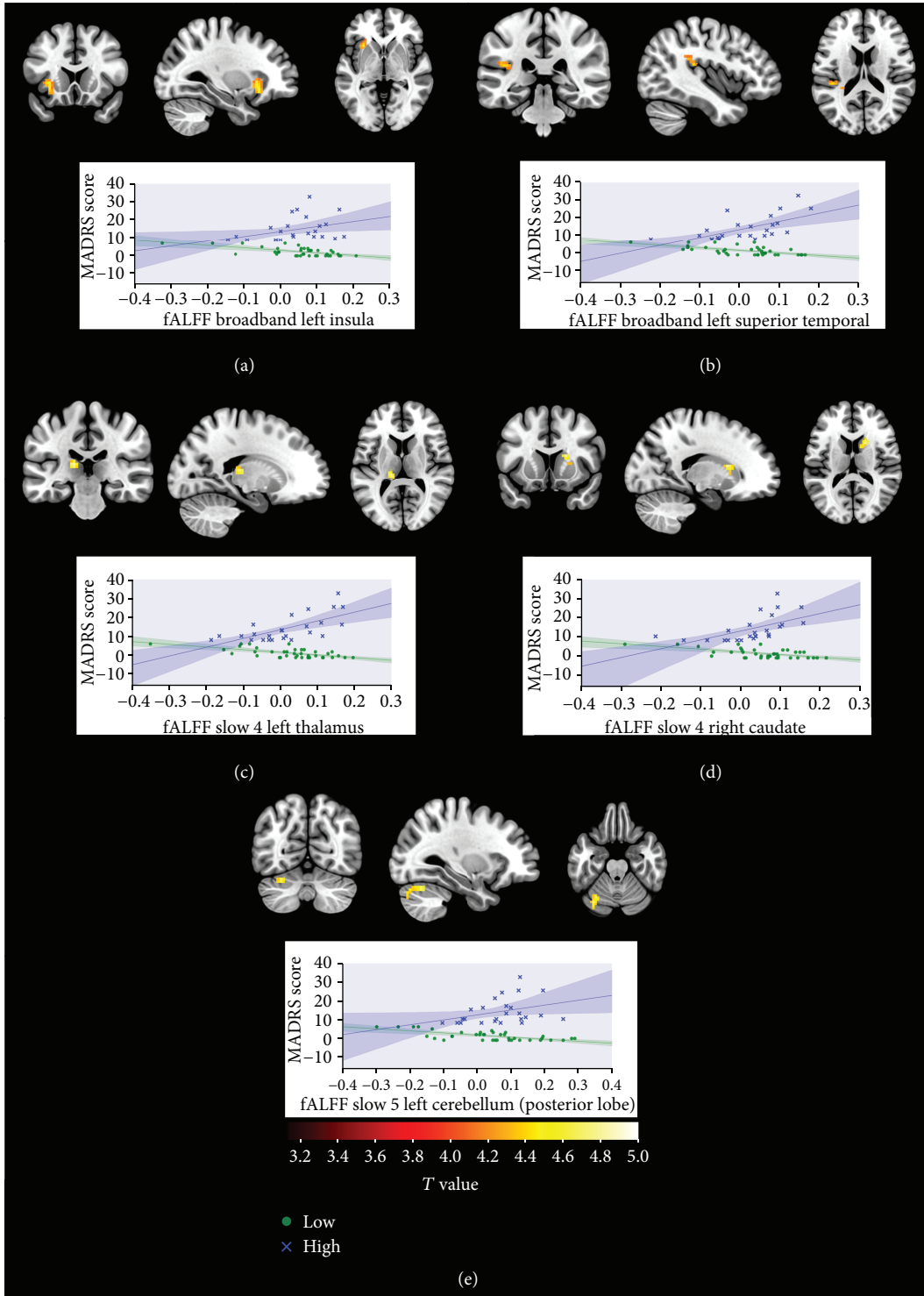


FIGURE 2: Cluster locations showing a significant interaction effect between the low and high depressive symptom score groups with the mean cluster fALFF response plotted against the MADRS-SIGMA score for broadband, slow-4 band, and slow-5 band (green represents low depressive symptom score group, blue represents high depressive symptom score group, and bands along regression line represent the 95% confidence interval). (a) Broadband: left insula. (b) Broadband: left superior temporal. (c) Slow-4: left thalamus. (d) Slow-4: right caudate. (e) Slow-5: left cerebellum. In the high depressive symptom group, high response from these regions was associated with an increased depressive symptom score. The low depressive symptom group showed no significant association between these regions and depressive symptom score. All brain images are shown in neurological convention.

and without depressive symptoms. Further, these results suggest that MÅDRS-SIGMA and fALFF analyses could potentially be used to identify individuals at risk of developing poststroke depression. This is important given the negative impact poststroke depression has been shown to have on the participation of everyday activities [68] and readiness to engage in the process of rehabilitation [8], which has also been shown to be negatively impacted [9–13]. Additionally, these results suggest that analysis using multiple fALFF frequency bands may be better than single band to study neural correlates of PSD.

In the nonstroke depression literature, alterations of resting-state activity to depressive symptoms have been well established [69] and may even allow for the exploration of different depressive subgroups [70]. Meta-analyses focusing on studies of resting-state changes in participants with depression have found associations with a large number of areas across the brain, including cortical, subcortical, and cerebellar locations, that show divergence of response from healthy controls [23–25].

Despite suggestions that resting-state methods may be a better approach to examine changes post stroke [71, 72], they have not been widely employed in PSD research. Most studies that have used functional connectivity have focused on specific regions of interest to investigate connectivity changes, e.g., from a default mode network and anterior cingulate [40–43, 73]. These studies showed inconsistent results, potentially due to differing times post stroke, methods used, and possible inclusion of artefact, a common issue with correlation-based methods [58] if not adequately controlled for. In our study, we utilised fALFF, which has been shown to be less susceptible to physiological artefact [34], performed a voxel-wise approach, and examined broad and subfrequency bands. We found significant differences in response to the depression score as a function of fALFF amplitude between those who presented with low depressive symptoms and those with high depressive symptoms.

The five significant clusters we found were located within the left insula, superior temporal lobe, thalamus, cerebellum, and right caudate. The insula, thalamus, and caudate are all part of the fronto-limbic-thalamic circuit [74], which is thought to be a major component in the neurocircuitry of depressive illness [22, 75–79]. The posterior superior temporal lobe and insula are also associated with social emotional processing [80], although the involvement of the superior temporal region with depression is currently not well understood [81]. The insula has extensive connections to fronto-limbic areas and has previously been linked to aberrant emotional and interoceptive processing in depression [67]. The insula is also reported to have a role in homeostasis through the regulation of sympathetic and parasympathetic systems [82], in salience and selective attention, especially during challenging tasks [83], in motor learning [84] and in motor recovery from stroke [85]. The cerebellum has long been known for connections with the somatomotor cortex [86, 87], but recently, subdivisions within the cerebellum have been discovered which are functionally connected with a wide range of cortical functional networks [88]. A recent voxel-based lesion symptom mapping study [89] also found

an association between the cerebellum and a measure of depressive symptoms, the geriatric depression scale. Interestingly, their results are also within a subdivision of the left superior cerebellum, which has been shown to have extensive functional connections to networks of the cerebrum including cognitive, emotional processing and salience networks [90].

Examination of fALFF amplitudes across several bands allowed us to uncover associations between regions and PSD that otherwise would have been hidden. Examining the frequency characteristics of signals is a widely used method in electromagnetic physiology research [91, 92], but has been slow to emerge within functional MRI analyses. Subbands within the low frequency resting-state range have previously been identified [36, 37], and the use of spectral methods such as fALFF has shown distinct spatial differences between them [34]. If broadband range alone had been examined, alterations within the caudate, thalamus, and cerebellum would not have been detected. This suggests that within the “resting-state range” of 0.01 to 0.08 Hz, different regions have unique oscillatory characteristics which are associated with depressive symptom severity. In the nonstroke depression literature, these areas are thought to be involved in cognitive and emotional modulation [93] and are considered to be central to the emotional dysregulation that is a hallmark of the condition [94–96].

The analysis performed in this study had similarities with that described by Egorova et al. [44]. Egorova et al. also investigated stroke survivors at 3 months post stroke, but used a different measure of depression (Patient Health Questionnaire-9), which had a lower proportion with depression (31%), and 40% of their depressed group (8/20) had a prior stroke. Only 2% (1/44) of the nondepressed group had a prior stroke, potentially impacting the findings. Egorova et al. reported mean differences between the low and high depressive symptom score groups in the dorsolateral prefrontal, precentral, and middle frontal regions. In contrast, we did not find any significant differences between the groups in frontal regions. Similar to our study, Egorova et al. found a significant association with the depression scores, in the left insula/superior temporal gyrus; however, in contrast, this was observed in the slow-4 subband and not the broadband as we reported. Further, our study found an interaction effect in both of these regions separately. Differences in the findings could be due to the difference in models used to examine the data. Egorova et al. examined only the group main effects, which in the General Linear Model framework compares the distance between slopes of the groups. In contrast, an interaction term examines differences in how the slopes interact with a third variable (in this case MÅDRS-SIGMA scores). We did not test group differences, as in the presence of a significant interaction effect interpretation of main effects may be misleading [97]. Thus, the studies asked different, but complementary, questions.

A caveat of our study is that the groups were determined by the cut-off score rather than a diagnosis made by a clinician. The cut-off score of >8 was used in this study to denote the high depressive symptom score. This cut-off, determined by Sagen et al. [50], had an AUC of 0.91 to correctly classify the depressed state of poststroke patients. However, it must be acknowledged that depression is a multifaceted disorder

with idiosyncratic presentation of symptoms and a simple cut-off score may incorrectly classify some individuals as depressed when they are not depressed and vice versa. Optimally, determination of group placement requires examination from a clinician trained to identify and make a diagnosis of mood disorders. A second caveat of this study is the presence of overlap between voxels that showed a significant interaction effect and voxels that were affected by lesion damage. These regions of overlap however occurred in voxels where 3 or less participants showed damage. This would have affected less than 8% of the total low MÅDRS-SIGMA group or less than 12% of the total high MÅDRS-SIGMA group and only in a subset of voxels where a significant interaction was found.

A few methodological issues and their potential impact are highlighted. A scanning acquisition time of 7 minutes was selected, following pilot protocol testing, to optimize comfort for the patient while achieving adequate signal-to-noise and robust findings. While longer acquisition periods may be recommended for resting-state functional connectivity analyses [98, 99], voxelwise methods based on BOLD frequency spectrum have been shown to reach a stable state around 5 minutes [100]. The impact of head motion on BOLD fluctuations was minimized by the following: careful preparation and support positioning of the patient; real-time monitoring of motion, with repeating scan if excessive motion was evident; systematic, quality inspection of each participant's resting-state data prior to inclusion in data analysis; motion regression and global signal regression (see Methods); and standardization (z -scoring) of ALFF and fALFF based on evidence that it serves to decouple amplitudes from head motion [100]. We did not censor periods of high motion from the analysis, as missing data may introduce artefact into the spectra [100]. Finally, delay in the hemodynamic response function of the BOLD response is identified as an issue impacting functional connectivity data analysis following stroke [101]. A potential advantage of using a frequency spectra analysis (rather than time domain analysis) is that the hemodynamic lag is not such an issue in spectral methods of analysis.

5. Conclusion and Implications

In summary, this study provides evidence that fALFF, a measure of resting-state activity, is sensitive to changes in poststroke depressive symptom severity and implicates the frontostriatal and cerebellar regions consistent with previous studies. Significant interaction effects between the resting-state fALFF values and MÅDRS-SIGMA score were observed in the left insula, superior temporal lobe, thalamus, and cerebellum and in the right caudate across several frequency bands. These regions showed differing activity patterns when coupled with the MÅDRS-SIGMA score between those who scored low on the MÅDRS-SIGMA compared to those who scored high. These results may be useful in identifying "at risk" individuals for PSD and guide further exploration of brain regions and networks vulnerable to altered functioning in PSD. Identification of "at risk" individuals has clinical implications for planning clinical pathways and as a factor

in the effectiveness of rehabilitation therapies due to impact on a patient's "readiness for change," which further impacts on when therapeutic interventions should be targeted.

Evidence of an interaction effect is also of value in better understanding the neural mechanisms underlying poststroke depression, in particular the association with the amplitude of resting signals of certain brain regions in different groups of patients. The possibility of manipulating brain signal activity in key areas, such as insula, to differentially impact depressive symptoms in stroke patients is appealing. Given the role of the insula in multimodal sensory and cognitive emotional processing, and in learning, the potential to influence brain signal activity through such experiences suggests a worthwhile area of investigation.

Data Availability

The neuroimaging and clinical data used to support the findings of this study are restricted by the Human Research Ethics Committee of Austin Health, Australia, in order to protect patients' confidentiality. Data may be made available from Dr. Leeanne Carey, l.carey@latrobe.edu.au, for researchers who meet the criteria for access to this confidential data.

Ethical Approval

The study was approved by the ethics committees covering the recruiting sites and the tertiary institutes involved in this study, i.e., Austin Health, Melbourne Health, Epworth Hospital, and La Trobe University Ethics Committees. The START program of research, which comprises START_EXTEND (NTA 0901 trial ID: NCT00887328) and START_PrePARE (NTA0902 trial ID: ACTRN12610000987066), is registered and approved by the Australian New Zealand Clinical Trials Registry.

Consent

All participants gave written informed consent before data collection began.

Disclosure

An earlier version of this research was presented at the 27th Annual Scientific Meeting of the Stroke Society of Australasia 23–25 August 2017, Queenstown, New Zealand. The abstract of the presentation is published in the proceedings as follows: [Goodin P, Lamp G, Tse T, and Carey L. Correlated resting-state activity of frontostriatal and cerebellar brain regions differentiates stroke survivors with high compared to low depressive symptom scores, International Journal of Stroke 2017, Vol. 12(3S), 22-23].

Conflicts of Interest

The authors have no conflict of interest to declare.

Acknowledgments

We acknowledge the contribution to this manuscript from the START team of investigators [47]. The authors would

like to thank all the participants who gave their time to take part in the study. The authors also wish to acknowledge lead investigators and study coordinators from the START recruiting sites. In particular, we acknowledge and thank those from the START-PrePARE recruiting sites: Austin Hospital (Helen Dewey), Epworth Hospital (Richard Geraty), Monash Medical Centre (Henry Ma), Royal Melbourne Hospital (Bruce C.V. Campbell), and Western Hospital (Tissa Wijeratne). We acknowledge the financial support for the conduct of the research from the Commonwealth Scientific and Industrial Research Organization (CSIRO) of Australia, Flagship Collaboration Fund through the Preventative Health Flagship, and the support for the analysis, write-up, and researchers from the James S. McDonnell Foundation 21st Century Science Initiative in Cognitive Rehabilitation–Collaborative Award (#220020413), NHMRC Centre of Research Excellence in Stroke Rehabilitation and Brain Injury (#1077898), NHMRC Program Grant Saving Brain and Changing Practice in Stroke (#1113352), Victorian Government's Operational Infrastructure Support Program, an Australian Research Council Future Fellowship awarded to LMC (#FT0992299), and a La Trobe University Post Graduate Scholarship and Florey student scholarship awarded to TT.

References

- [1] S. Stephens, R. A. Kenny, E. Rowan et al., "Neuropsychological characteristics of mild vascular cognitive impairment and dementia after stroke," *International Journal of Geriatric Psychiatry*, vol. 19, no. 11, pp. 1053–1057, 2004.
- [2] M. Herrmann and C.-W. Wallesch, "Depressive changes in stroke patients," *Disability and Rehabilitation*, vol. 15, no. 2, pp. 55–66, 1993.
- [3] G. R. Cojocaru, A. Popa-Wagner, E. C. Stanculescu, L. Babadan, and A.-M. Buga, "Post-stroke depression and the aging brain," *Journal of Molecular Psychiatry*, vol. 1, no. 1, p. 14, 2013.
- [4] M. L. Hackett and K. Pickles, "Part I: frequency of depression after stroke: an updated systematic review and meta-analysis of observational studies," *International Journal of Stroke*, vol. 9, no. 8, pp. 1017–1025, 2014.
- [5] M. L. Hackett, C. Yapa, V. Parag, and C. S. Anderson, "Frequency of depression after stroke," *Stroke*, vol. 36, no. 6, pp. 1330–1340, 2005.
- [6] L. Andrade, J. J. Caraveo-Anduaga, P. Berglund et al., "The epidemiology of major depressive episodes: results from the International Consortium of Psychiatric Epidemiology (ICPE) surveys," *International Journal of Methods in Psychiatric Research*, vol. 12, no. 1, pp. 3–21, 2003.
- [7] S. A. Riolo, T. A. Nguyen, J. F. Greden, and C. A. King, "Prevalence of depression by race/ethnicity: findings from the National Health and Nutrition Examination Survey III," *American Journal of Public Health*, vol. 95, no. 6, pp. 998–1000, 2005.
- [8] R. G. Robinson and R. E. Jorge, "Post-stroke depression: a review," *The American Journal of Psychiatry*, vol. 173, no. 3, pp. 221–231, 2016.
- [9] T. Pohjasvaara, R. Vataja, A. Leppävuori, M. Kaste, and T. Erkinjuntti, "Depression is an independent predictor of poor long-term functional outcome post-stroke," *European Journal of Neurology*, vol. 8, no. 4, pp. 315–319, 2001.
- [10] M. L. Kauhanen, J. T. Korpelainen, P. Hiltunen et al., "Post-stroke depression correlates with cognitive impairment and neurological deficits," *Stroke*, vol. 30, no. 9, pp. 1875–1880, 1999.
- [11] M. Kimura, R. G. Robinson, and J. T. Kosier, "Treatment of cognitive impairment after poststroke depression," *Stroke*, vol. 31, no. 7, pp. 1482–1486, 2000.
- [12] Y. Murata, M. Kimura, and R. G. Robinson, "Does cognitive impairment cause post-stroke depression?," *The American Journal of Geriatric Psychiatry*, vol. 8, no. 4, pp. 310–317, 2000.
- [13] J. Opara and K. Jaracz, "Quality of life of post-stroke patients and their caregivers," *Journal of Medicine and Life*, vol. 3, no. 3, pp. 216–220, 2010.
- [14] F. Bartoli, N. Lillia, A. Lax et al., "Depression after stroke and risk of mortality: a systematic review and meta-analysis," *Stroke Research and Treatment*, vol. 2013, Article ID 862978, 11 pages, 2013.
- [15] R. F. Villa, F. Ferrari, and A. Moretti, "Post-stroke depression: mechanisms and pharmacological treatment," *Pharmacology & Therapeutics*, vol. 184, pp. 131–144, 2018.
- [16] L. A. Boyd, K. S. Hayward, N. S. Ward et al., "Biomarkers of stroke recovery: consensus-based core recommendations from the Stroke Recovery and Rehabilitation Roundtable," *International Journal of Stroke*, vol. 12, no. 5, pp. 480–493, 2017.
- [17] S. K. Bhogal, R. Teasell, N. Foley, and M. Speechley, "Lesion location and poststroke depression: systematic review of the methodological limitations in the literature," *Stroke*, vol. 35, no. 3, pp. 794–802, 2004.
- [18] A. J. Carson, S. MacHale, K. Allen et al., "Depression after stroke and lesion location: a systematic review," *The Lancet*, vol. 356, no. 9224, pp. 122–126, 2000.
- [19] P. L. Francis, N. Herrmann, G. Tennen, and K. L. Lanctot, "A brief history of poststroke depression neuroimaging," *Aging Health*, vol. 5, no. 1, pp. 79–88, 2009.
- [20] N. Wei, W. Yong, X. Li et al., "Post-stroke depression and lesion location: a systematic review," *Journal of Neurology*, vol. 262, no. 1, pp. 81–90, 2015.
- [21] K. Noonan, L. M. Carey, and S. G. Crewther, "Meta-analyses indicate associations between neuroendocrine activation, deactivation in neurotrophic and neuroimaging markers in depression after stroke," *Journal of Stroke and Cerebrovascular Diseases*, vol. 22, no. 7, pp. e124–e135, 2013.
- [22] W. C. Drevets, J. L. Price, and M. L. Furey, "Brain structural and functional abnormalities in mood disorders: implications for neurocircuitry models of depression," *Brain Structure & Function*, vol. 213, no. 1–2, pp. 93–118, 2008.
- [23] C. Diener, C. Kuehner, W. Brusniak, B. Ubl, M. Wessa, and H. Flor, "A meta-analysis of neurofunctional imaging studies of emotion and cognition in major depression," *NeuroImage*, vol. 61, no. 3, pp. 677–685, 2012.
- [24] P. B. Fitzgerald, A. R. Laird, J. Maller, and Z. J. Daskalakis, "A meta-analytic study of changes in brain activation in depression," *Human Brain Mapping*, vol. 29, no. 6, pp. 683–695, 2008.
- [25] S. M. Palmer, S. G. Crewther, L. M. Carey, and The START Project Team, "A meta-analysis of changes in brain activity in clinical depression," *Frontiers in Human Neuroscience*, vol. 8, article 1045, 2015.

- [26] B. B. Biswal, M. Mennes, X. N. Zuo et al., "Toward discovery science of human brain function," *Proceedings of the National Academy of Sciences*, vol. 107, no. 10, pp. 4734–4739, 2010.
- [27] D. Cordes, V. M. Haughton, K. Arfanakis et al., "Mapping functionally related regions of brain with functional connectivity MR imaging," *American Journal of Neuroradiology*, vol. 21, no. 9, pp. 1636–1644, 2000.
- [28] N. K. Logothetis, J. Pauls, M. Augath, T. Trinath, and A. Oeltermann, "Neurophysiological investigation of the basis of the fMRI signal," *Nature*, vol. 412, no. 6843, pp. 150–157, 2001.
- [29] Y.-F. Wang, F. Liu, Z. L. Long et al., "Steady-state BOLD response modulates low frequency neural oscillations," *Scientific Reports*, vol. 4, no. 1, article 7376, 2014.
- [30] M. D. Fox and M. E. Raichle, "Spontaneous fluctuations in brain activity observed with functional magnetic resonance imaging," *Nature Reviews. Neuroscience*, vol. 8, no. 9, pp. 700–711, 2007.
- [31] Z. Yu-Feng, H. Yong, Z. Chao-Zhe et al., "Altered baseline brain activity in children with ADHD revealed by resting-state functional MRI," *Brain & Development*, vol. 29, no. 2, pp. 83–91, 2007.
- [32] Q.-H. Zou, C. Z. Zhu, Y. Yang et al., "An improved approach to detection of amplitude of low-frequency fluctuation (ALFF) for resting-state fMRI: fractional ALFF," *Journal of Neuroscience Methods*, vol. 172, no. 1, pp. 137–141, 2008.
- [33] X. di, E. H. Kim, C. C. Huang, S. J. Tsai, C. P. Lin, and B. B. Biswal, "The influence of the amplitude of low-frequency fluctuations on resting-state functional connectivity," *Frontiers in Human Neuroscience*, vol. 7, article 118, 2013.
- [34] X.-N. Zuo, A. di Martino, C. Kelly et al., "The oscillating brain: complex and reliable," *NeuroImage*, vol. 49, no. 2, pp. 1432–1445, 2010.
- [35] J. H. Zhang, J. Badaut, J. Tang, A. Obenaus, R. Hartman, and W. J. Pearce, "The vascular neural network—a new paradigm in stroke pathophysiology," *Nature Reviews. Neurology*, vol. 8, no. 12, pp. 711–716, 2012.
- [36] G. Buzsáki and A. Draguhn, "Neuronal oscillations in cortical networks," *Science*, vol. 304, no. 5679, pp. 1926–1929, 2004.
- [37] M. Penttonen and G. Buzsáki, "Natural logarithmic relationship between brain oscillators," *Thalamus & Related Systems*, vol. 2, no. 2, pp. 145–152, 2003.
- [38] L. Wang, W. Dai, Y. Su et al., "Amplitude of low-frequency oscillations in first-episode, treatment-naive patients with major depressive disorder: a resting-state functional MRI study," *PLoS One*, vol. 7, no. 10, article e48658, 2012.
- [39] L. Wang, Q. Kong, K. Li et al., "Frequency-dependent changes in amplitude of low-frequency oscillations in depression: a resting-state fMRI study," *Neuroscience Letters*, vol. 614, pp. 105–111, 2016.
- [40] S. Lassalle-Lagadec, I. Sibon, B. Dilharreguy, P. Renou, O. Fleury, and M. Allard, "Subacute default mode network dysfunction in the prediction of post-stroke depression severity," *Radiology*, vol. 264, no. 1, pp. 218–224, 2012.
- [41] J. E. Vicentini, M. Weiler, S. R. M. Almeida, B. M. de Campos, L. Valler, and L. M. Li, "Depression and anxiety symptoms are associated to disruption of default mode network in subacute ischemic stroke," *Brain Imaging and Behavior*, vol. 11, no. 6, pp. 1571–1580, 2017.
- [42] H. Liu, L. Song, and T. Zhang, "Changes in brain activation in stroke patients after mental practice and physical exercise: a functional MRI study," *Neural Regeneration Research*, vol. 9, no. 15, pp. 1474–1484, 2014.
- [43] V. Balaev, I. Orlov, A. Petrushevsky, and O. Martynova, "Functional connectivity between salience, default mode and frontoparietal networks in post-stroke depression," *Journal of Affective Disorders*, vol. 227, pp. 554–562, 2018.
- [44] N. Egorova, M. Veldsman, T. Cumming, and A. Brodtmann, "Fractional amplitude of low-frequency fluctuations (fALFF) in post-stroke depression," *NeuroImage: Clinical*, vol. 16, pp. 116–124, 2017.
- [45] R. C. Kessler, P. Berglund, O. Demler, R. Jin, K. R. Merikangas, and E. E. Walters, "Lifetime prevalence and age-of-onset distributions of DSM-IV disorders in the National Comorbidity Survey Replication," *Archives of General Psychiatry*, vol. 62, no. 6, pp. 593–602, 2005.
- [46] P. M. Lewinsohn, A. Solomon, J. R. Seeley, and A. Zeiss, "Clinical implications of 'subthreshold' depressive symptoms," *Journal of Abnormal Psychology*, vol. 109, no. 2, pp. 345–351, 2000.
- [47] L. M. Carey, S. Crewther, O. Salvado et al., "STroke imAging pRevention and Treatment (START): a longitudinal stroke cohort study: clinical trials protocol," *International Journal of Stroke*, vol. 10, no. 4, pp. 636–644, 2015.
- [48] T. Brott, H. P. Adams Jr., C. P. Olinger et al., "Measurements of acute cerebral infarction: a clinical examination scale," *Stroke*, vol. 20, no. 7, pp. 864–870, 1989.
- [49] J. B. W. Williams and K. A. Kobak, "Development and reliability of a structured interview guide for the Montgomery Asberg Depression Rating Scale (SIGMA)," *The British Journal of Psychiatry: the Journal of Mental Science*, vol. 192, no. 1, pp. 52–58, 2008.
- [50] U. Sagen, T. G. Vik, T. Moum, T. Mørland, A. Finset, and T. Dammen, "Screening for anxiety and depression after stroke: comparison of the hospital anxiety and depression scale and the Montgomery and Asberg depression rating scale," *Journal of Psychosomatic Research*, vol. 67, no. 4, pp. 325–332, 2009.
- [51] P. Goodin, G. Lamp, R. Vidyasagar, D. McArdle, R. J. Seitz, and L. M. Carey, "Altered functional connectivity differs in stroke survivors with impaired touch sensation following left and right hemisphere lesions," *NeuroImage: Clinical*, vol. 18, pp. 342–355, 2018.
- [52] R. W. Cox, "AFNI: software for analysis and visualization of functional magnetic resonance neuroimages," *Computers and Biomedical Research*, vol. 29, no. 3, pp. 162–173, 1996.
- [53] B. B. Avants, N. J. Tustison, G. Song, P. A. Cook, A. Klein, and J. C. Gee, "A reproducible evaluation of ANTs similarity metric performance in brain image registration," *NeuroImage*, vol. 54, no. 3, pp. 2033–2044, 2011.
- [54] S. van der Walt, S. C. Colbert, and G. Varoquaux, "The NumPy Array: a structure for efficient numerical computation," *Computing in Science & Engineering*, vol. 13, no. 2, pp. 22–30, 2011.
- [55] T. E. Oliphant, "Python for scientific computing," *Computing in Science & Engineering*, vol. 9, no. 3, pp. 10–20, 2007.
- [56] K. Gorgolewski, C. D. Burns, C. Madison et al., "Nipype: a flexible, lightweight and extensible neuroimaging data processing framework in python," *Frontiers in Neuroinformatics*, vol. 5, article 13, 2011.

- [57] K. J. Friston, S. Williams, R. Howard, R. S. J. Frackowiak, and R. Turner, "Movement-related effects in fMRI time-series," *Magnetic Resonance in Medicine*, vol. 35, no. 3, pp. 346–355, 1996.
- [58] Y. Behzadi, K. Restom, J. Liao, and T. T. Liu, "A component based noise correction method (CompCor) for BOLD and perfusion based fMRI," *NeuroImage*, vol. 37, no. 1, pp. 90–101, 2007.
- [59] C.-G. Yan, B. Cheung, C. Kelly et al., "A comprehensive assessment of regional variation in the impact of head micro-movements on functional connectomics," *NeuroImage*, vol. 76, pp. 183–201, 2013.
- [60] Z. S. Saad, S. J. Gotts, K. Murphy et al., "Trouble at rest: how correlation patterns and group differences become distorted after global signal regression," *Brain Connectivity*, vol. 2, no. 1, pp. 25–32, 2012.
- [61] Z. S. Saad, R. C. Reynolds, H. J. Jo et al., "Correcting brain-wide correlation differences in resting-state FMRI," *Brain Connectivity*, vol. 3, no. 4, pp. 339–352, 2013.
- [62] A. Eklund, T. E. Nichols, and H. Knutsson, "Cluster failure: why fMRI inferences for spatial extent have inflated false-positive rates," *Proceedings of the National Academy of Sciences*, vol. 113, no. 28, pp. 7900–7905, 2016.
- [63] N. Tzourio-Mazoyer, B. Landeau, D. Papathanassiou et al., "Automated anatomical labeling of activations in SPM using a macroscopic anatomical parcellation of the MNI MRI single-subject brain," *NeuroImage*, vol. 15, no. 1, pp. 273–289, 2002.
- [64] J. A. Maldjian, P. J. Laurienti, and J. H. Burdette, "Precentral gyrus discrepancy in electronic versions of the Talairach atlas," *NeuroImage*, vol. 21, no. 1, pp. 450–455, 2004.
- [65] J. A. Maldjian, P. J. Laurienti, R. A. Kraft, and J. H. Burdette, "An automated method for neuroanatomic and cytoarchitectonic atlas-based interrogation of fMRI data sets," *NeuroImage*, vol. 19, no. 3, pp. 1233–1239, 2003.
- [66] R Core Team, *R: A Language and Environment for Statistical Computing*, R Foundation for Statistical Computing, Vienna, Austria, 2018, <https://www.R-project.org/>.
- [67] D. Sliz and S. Hayley, "Major depressive disorder and alterations in insular cortical activity: a review of current functional magnetic imaging research," *Frontiers in Human Neuroscience*, vol. 6, article 323, 2012.
- [68] T. Tse, T. Linden, L. Churilov, S. Davis, G. Donnan, and L. M. Carey, "Longitudinal changes in activity participation in the first year post-stroke and association with depressive symptoms," *Disability and Rehabilitation*, pp. 1–8, 2018.
- [69] L. Wang, D. F. Hermens, I. B. Hickie, and J. Lagopoulos, "A systematic review of resting-state functional-MRI studies in major depression," *Journal of Affective Disorders*, vol. 142, no. 1–3, pp. 6–12, 2012.
- [70] A. T. Drysdale, L. Grosenick, J. Downar et al., "Resting-state connectivity biomarkers define neurophysiological subtypes of depression," *Nature Medicine*, vol. 23, no. 1, pp. 28–38, 2017.
- [71] L. M. Carey, R. J. Seitz, M. Parsons et al., "Beyond the lesion: neuroimaging foundations for post-stroke recovery," *Future Neurology*, vol. 8, no. 5, pp. 507–527, 2013.
- [72] A. R. Carter, G. L. Shulman, and M. Corbetta, "Why use a connectivity-based approach to study stroke and recovery of function?," *NeuroImage*, vol. 62, no. 4, pp. 2271–2280, 2012.
- [73] P. Zhang, Q. Xu, J. Dai, J. Wang, N. Zhang, and Y. Luo, "Dysfunction of affective network in post ischemic stroke depression: a resting-state functional magnetic resonance imaging study," *BioMed Research International*, vol. 2014, Article ID 846830, 7 pages, 2014.
- [74] R. M. Bonelli and J. L. Cummings, "Frontal-subcortical circuitry and behavior," *Dialogues in Clinical Neuroscience*, vol. 9, no. 2, pp. 141–151, 2007.
- [75] A. T. Beck, "The evolution of the cognitive model of depression and its neurobiological correlates," *The American Journal of Psychiatry*, vol. 165, no. 8, pp. 969–977, 2008.
- [76] I. H. Gotlib and J. Joormann, "Cognition and depression: current status and future directions," *Annual Review of Clinical Psychology*, vol. 6, no. 1, pp. 285–312, 2010.
- [77] J. Joormann and I. H. Gotlib, "Updating the contents of working memory in depression: interference from irrelevant negative material," *Journal of Abnormal Psychology*, vol. 117, no. 1, pp. 182–192, 2008.
- [78] S. M. Levens and E. A. Phelps, "Insula and orbital frontal cortex activity underlying emotion interference resolution in working memory," *Journal of Cognitive Neuroscience*, vol. 22, no. 12, pp. 2790–2803, 2010.
- [79] J. L. Price and W. C. Drevets, "Neural circuits underlying the pathophysiology of mood disorders," *Trends in Cognitive Sciences*, vol. 16, no. 1, pp. 61–71, 2012.
- [80] J. D. Henry, W. von Hippel, P. Molenberghs, T. Lee, and P. S. Sachdev, "Clinical assessment of social cognitive function in neurological disorders," *Nature Reviews Neurology*, vol. 12, no. 1, pp. 28–39, 2016.
- [81] C. L. McGrath, M. E. Kelley, B. W. Dunlop, P. E. Holtzheimer III, W. E. Craighead, and H. S. Mayberg, "Pretreatment brain states identify likely nonresponse to standard treatments for depression," *Biological Psychiatry*, vol. 76, no. 7, pp. 527–535, 2014.
- [82] H. D. Critchley, "Neural mechanisms of autonomic, affective, and cognitive integration," *The Journal of Comparative Neurology*, vol. 493, no. 1, pp. 154–166, 2005.
- [83] M. A. Eckert, V. Menon, A. Walczak et al., "At the heart of the ventral attention system: the right anterior insula," *Human Brain Mapping*, vol. 30, no. 8, pp. 2530–2541, 2009.
- [84] I. Mutschler, A. Schulze-Bonhage, V. Glauche, E. Demandt, O. Speck, and T. Ball, "A rapid sound-action association effect in human insular cortex," *PLoS One*, vol. 2, no. 2, pp. e259–e259, 2007.
- [85] C. Willer, S. C. Ramsay, R. J. S. Wise, K. J. Friston, and R. S. J. Frackowiak, "Individual patterns of functional reorganization in the human cerebral cortex after capsular infraction," *Annals of Neurology*, vol. 33, no. 2, pp. 181–189, 1993.
- [86] E. D. Adrian, "Afferent areas in the cerebellum connected with the limbs," *Brain*, vol. 66, no. 4, pp. 289–315, 1943.
- [87] W. Grodd, E. Hülsmann, M. Lotze, D. Wildgruber, and M. Erb, "Sensorimotor mapping of the human cerebellum: fMRI evidence of somatotopic organization," *Human Brain Mapping*, vol. 13, no. 2, pp. 55–73, 2001.
- [88] J. A. Bernard, R. D. Seidler, K. M. Hassevoort et al., "Resting state cortico-cerebellar functional connectivity networks: a comparison of anatomical and self-organizing map approaches," *Frontiers in Neuroanatomy*, vol. 6, article 31, 2012.
- [89] N. Y. Kim, S. C. Lee, J.-C. Shin, J. E. Park, and Y. W. Kim, "Voxel-based lesion symptom mapping analysis of depressive

- mood in patients with isolated cerebellar stroke: a pilot study,” *NeuroImage: Clinical*, vol. 13, pp. 39–45, 2017.
- [90] R. L. Buckner, F. M. Krienen, A. Castellanos, J. C. Diaz, and B. T. T. Yeo, “The organization of the human cerebellum estimated by intrinsic functional connectivity,” *Journal of Neurophysiology*, vol. 106, no. 5, pp. 2322–2345, 2011.
- [91] J. Gross, S. Baillet, G. R. Barnes et al., “Good practice for conducting and reporting MEG research,” *NeuroImage*, vol. 65, pp. 349–363, 2013.
- [92] D. Millett, “Hans Berger: from psychic energy to the EEG,” *Perspectives in Biology and Medicine*, vol. 44, no. 4, pp. 522–542, 2001.
- [93] K. A. Lindquist, T. D. Wager, H. Kober, E. Bliss-Moreau, and L. F. Barrett, “The brain basis of emotion: a meta-analytic review,” *The Behavioral and Brain Sciences*, vol. 35, no. 3, pp. 121–143, 2012.
- [94] M. P. Austin, P. Mitchell, K. Wilhelm et al., “Cognitive function in depression: a distinct pattern of frontal impairment in melancholia?,” *Psychological Medicine*, vol. 29, no. 1, pp. 73–85, 1999.
- [95] M. A. Diego, T. Field, and M. Hernandez-Reif, “CES-D depression scores are correlated with frontal EEG alpha asymmetry,” *Depression and Anxiety*, vol. 13, no. 1, pp. 32–37, 2001.
- [96] W. C. Drevets, “Prefrontal cortical-amygdalar metabolism in major depression,” *Annals of the New York Academy of Sciences*, vol. 877, pp. 614–637, 1999.
- [97] D. J. Bauer and P. J. Curran, “Probing interactions in fixed and multilevel regression: inferential and graphical techniques,” *Multivariate Behavioral Research*, vol. 40, no. 3, pp. 373–400, 2005.
- [98] R. M. Birn, J. B. Diamond, M. A. Smith, and P. A. Bandettini, “Separating respiratory-variation-related fluctuations from neuronal-activity-related fluctuations in fMRI,” *NeuroImage*, vol. 31, no. 4, pp. 1536–1548, 2006.
- [99] J. S. Siegel, G. L. Shulman, and M. Corbetta, “Measuring functional connectivity in stroke: approaches and considerations,” *Journal of Cerebral Blood Flow and Metabolism*, vol. 37, no. 8, pp. 2665–2678, 2017.
- [100] M. Küblböck, M. Woletz, A. Höflich et al., “Stability of low-frequency fluctuation amplitudes in prolonged resting-state fMRI,” *NeuroImage*, vol. 103, pp. 249–257, 2014.
- [101] J. S. Siegel, A. Z. Snyder, L. Ramsey, G. L. Shulman, and M. Corbetta, “The effects of hemodynamic lag on functional connectivity and behavior after stroke,” *Journal of Cerebral Blood Flow and Metabolism*, vol. 36, no. 12, pp. 2162–2176, 2016.

Research Article

MMP-9 Contributes to Dendritic Spine Remodeling Following Traumatic Brain Injury

Barbara Pijet , Marzena Stefaniuk, and Leszek Kaczmarek 

Laboratory of Neurobiology, BRAINCITY, Nencki Institute of Experimental Biology of Polish Academy of Sciences, Pasteura 3, 02-093 Warsaw, Poland

Correspondence should be addressed to Barbara Pijet; b.pijet@nencki.gov.pl and Leszek Kaczmarek; l.kaczmarek@nencki.gov.pl

Received 23 November 2018; Accepted 3 April 2019; Published 6 May 2019

Guest Editor: Michael Nilsson

Copyright © 2019 Barbara Pijet et al. This is an open access article distributed under the Creative Commons Attribution License, which permits unrestricted use, distribution, and reproduction in any medium, provided the original work is properly cited.

Traumatic brain injury (TBI) occurs when a blow to the head causes brain damage. Apart from physical trauma, it causes a wide range of cognitive, behavioral, and emotional deficits including impairments in learning and memory. On neuronal level, TBI may lead to circuitry remodeling and in effect imbalance between excitatory and inhibitory neurotransmissions. Such change in brain homeostasis may often lead to brain disorders. The basic units of neuronal connectivity are dendritic spines that are tiny protrusions forming synapses between two cells in a network. Spines are dynamic structures that undergo morphological transformation throughout life. Their shape is strictly related to an on/off state of synapse and the strength of synaptic transmission. Matrix metalloproteinase-9 (MMP-9) is an extrasynaptically operating enzyme that plays a role in spine remodeling and has been reported to be activated upon TBI. The aim of the present study was to evaluate the influence of MMP-9 on dendritic spine density and morphology following controlled cortical impact (CCI) as animal model of TBI. We examined spine density and dendritic spine shape in the cerebral cortex and the hippocampus. CCI caused a marked decrease in spine density as well as spine shrinkage in the cerebral cortex ipsilateral to the injury, when compared to sham animals and contralateral side both 1 day and 1 week after the insult. Decreased spine density was also observed in the dentate gyrus of the hippocampus; however, in contrast to the cerebral cortex, spines in the DG became more filopodia-like. In mice lacking MMP-9, no effects of TBI on spine density and morphology were observed.

1. Introduction

Traumatic brain injury caused by an external mechanical force evokes a variety of brain responses, including focal extrasynaptic matrix degradation, neuronal loss within hippocampus area, glia activation, synaptic remodeling, and ion channels activity changes [1, 2]. On a neurotransmission level, a massive glutamate efflux, increased level of extracellular glutamate, and hyperactivation of NMDAR receptor channels followed by their loss are observed [3]. These events are also strictly related to dendritic spine remodeling [4]. Dendritic spines are small membranous protrusions that undergo plastic morphological changes under both physiological (e.g., development or learning and memory) and pathological (e.g., neurodegeneration, psychiatric disorders) conditions [5–7]. Several recent reports have described changes in dendritic spine density and size following brain trauma [8–16].

MMP-9 is pericellularly acting endopeptidase, classified as a gelatinase due to its ability to cleave gelatin [17–21]. Through involvement in extracellular matrix remodeling, it regulates numerous cell processes and physiological functions [22–26]. Aside from physiological role, MMP-9 takes part in such central nervous system pathological events as injury, stroke, or epileptogenesis, as well as neuropsychiatric disorders such as schizophrenia or addiction [27–35]. Importantly, previous reports have also indicated that MMP-9 is a crucial dendritic spine shape modulator [36–41] and its level is altered posttrauma [28, 40, 42–45]. To what extent upon brain injury MMP-9 is involved in altering dendritic spines number and shape is yet unknown. To bridge this gap, we set out to analyze the effects of MMP-9 levels on TBI-stimulated plastic changes of the dendritic spines in the mouse brain. For this, we used controlled cortical impact (CCI) as an animal model of traumatic brain injury [46].

First, we describe influence of CCI on density and morphology of dendritic spines in the cerebral cortex and hippocampus 24 hours and 7 days of postbrain injury. Next, we assess the effects of missing MMP-9 due to the gene knockout (KO) on spine density and shape following TBI.

2. Materials and Methods

2.1. Animals. The study was performed on adult (12–14 weeks old) C57BL/6J male mice (Animal House, Center for Experimental Medicine, Białystok, Poland), MMP-9 homozygous knockout mice (MMP-9 KO), and their WT siblings (MMP-9 WT) on a C57BL/6J background [47]. All mice were maintained in the Animal House of the Nencki Institute. Animals were housed in individual cages under controlled environment (temperature $22 \pm 1^\circ\text{C}$, humidity 50–60%, with free access to food and water and a 12 h light/dark cycle). All procedures were performed in accordance with the Animal Protection Act in Poland, directive 2010/63/EU, and were approved by the 1st Local Ethics Committee (Permissions Numbers: 383/2012; 609/2014).

2.2. Induction of TBI with CCI. Mice were subjected to unilateral cortical contusion using the controlled cortical impact protocol [28, 46, 48] following anesthesia evoked with 4% isoflurane (Aerrane; Baxter, UK) in 100% oxygen with a delivery rate of 4 l/min. During the surgery, concentration of isoflurane was maintained at the level of 3% in 100% oxygen with delivery of 0.6 l/min (Combi Vet Anesthesia System; Rothacher; Switzerland). For deeper sedation, briefly before the injury, mice were injected subcutaneously with butorphanol ($10 \mu\text{g}/30 \text{ g}$ body weight). After skull exposure by midline scalp incision, craniectomy was performed using a 5 mm \varnothing trephine (Fine Science Tools FST; Germany) over the left parietotemporal cortex between the lambda and bregma (Figure 1(a)). The bone piece was carefully removed without disrupting the dura. For TBI execution, we used Leica Impact One device equipped with an electrically driven metallic piston controlled by a linear velocity displacement transducer (Leica Biosystems, KAWA.SKA; Poland). After craniectomy, the adjustable CCI equipment was mounted on the left stereotaxic arm at an angle of 20° from vertical. CCI was delivered according to the protocol [28] using the following parameters: \varnothing 3 mm: flat tip; depth: 0.5 mm from the dura; velocity: 5 m/s, and dwell time: 100 ms. After injury, bleeding was strictly controlled, a piece of sterile plastic was placed over the craniectomy area, and the incision was sutured with nylon stitches (Sigmed; Poland). Next, the animals were returned to the heated home cages for postsurgical recovery. Sham-injured animals underwent identical anesthesia and craniectomy procedures, but were not subjected to CCI. The following number of animals was subjected to procedure per each time point: C57BL/6J ($n = 5$ CCI, $n = 5$ sham), MMP-9 WT ($n = 5$ CCI, $n = 3$ sham), and MMP-9 KO ($n = 5$ CCI, $n = 3$ sham).

2.3. Nissl Staining. To verify cerebral cortex degeneration, we performed Nissl staining. 24 hours and 7 days after the injury, mice were anesthetized and perfused with 0.37%

sulfide solution (5 ml/min, 4°C) for 5 min followed by perfusion with 4% paraformaldehyde in 0.1 M sodium phosphate buffer, pH 7.4 (5 ml/min, 4°C) for 10 min. The brains were removed from the skull and postfixed in buffered 4% paraformaldehyde for 4 h at 4°C , and then cryoprotected in a solution containing 30% glycerol in 0.02 M potassium phosphate-buffered saline for 48 h. Samples were then frozen on dry ice and stored at -80°C . Frozen brains were sectioned in the coronal plane ($40 \mu\text{m}$) with a sliding cryostat (Leica Biosystems, KAWA.SKA; Poland). The sections were mounted on microscope gelatin-covered slides, dried, and stained with cresyl violet. Pictures of Nissl-stained sections were taken using the light microscope Nikon Eclipse Ni equipped with PlanApo 2x objective.

2.4. Dendritic Spine Analysis. Dendritic spines were visualized using lipophilic dye Dil (1,1'-dioctadecyl-3,3,3',3'-tetramethylindocarbocyanine perchlorate, #D282 Life Technologies, Warsaw, Poland). 24 hours and 7 days after CCI, mice were sacrificed and their brains were collected. Next, they were cut into $130 \mu\text{m}$ sections on vibratome (Leica VT 1000S, Leica Biosystems Nussloch GmbH, Wetzlar, Germany). Slices were processed for Dil staining. Random dendrite labeling was performed using $1.6 \mu\text{m}$ tungsten particles (Bio-Rad, Hercules, CA, USA) coated with Dil. Dye was delivered to cells using Gene Gun (Bio-Rad). After staining, slices were fixed with 0.4% paraformaldehyde in phosphate-buffered saline (PBS; overnight at 4°C) and placed on microscopic slides. Z-stacks of dendrites from the 2nd and 3rd layers of the perilesional cortex and the dentate gyrus (DG) were acquired using the LSM780 confocal system equipped with 40x objective (Plan Achromat 40x/1.4 Oil DIC) (Zeiss, Poznań, Poland). Dil emission was excited using a HeNe 594 nm laser. For each image, the following parameters were applied: 70 nm pixel size, 300 nm Z-intervals, averaging 4. Maximum intensity projections of Z-stacks covering the length of dendrite were analyzed using semiautomatic SpineMagick! software [49]. It allows marking dendritic spine head and base manually. Next, the software marks automatically spine edges that can be adjusted manually to fully reflect the spine shape [49]. For each animal, 5–7 single dendrites from selected brain areas (one dendrite per neuron per image) were analyzed. First, dendritic spine density was calculated. In the next step, dendritic spines were examined according to the following morphological parameters: spine area, head width, spine length, and a scale-free parameter - the length divided by the width (length to width ratio) (Figure 2(a)). This parameter reflects the spine shape—the higher the ratio, the more filopodial spine is.

To determine group size, we used assumption on the basis of sample size determination and the following equation:

$$n = 1 + 2C \left(\frac{s}{d} \right)^2, \quad (1)$$

where n is the group size, C is a constant dependent on the value of α and power selected (here it equals 10.51 for 0.9 power and 0.05 significance level), s is an estimate of the

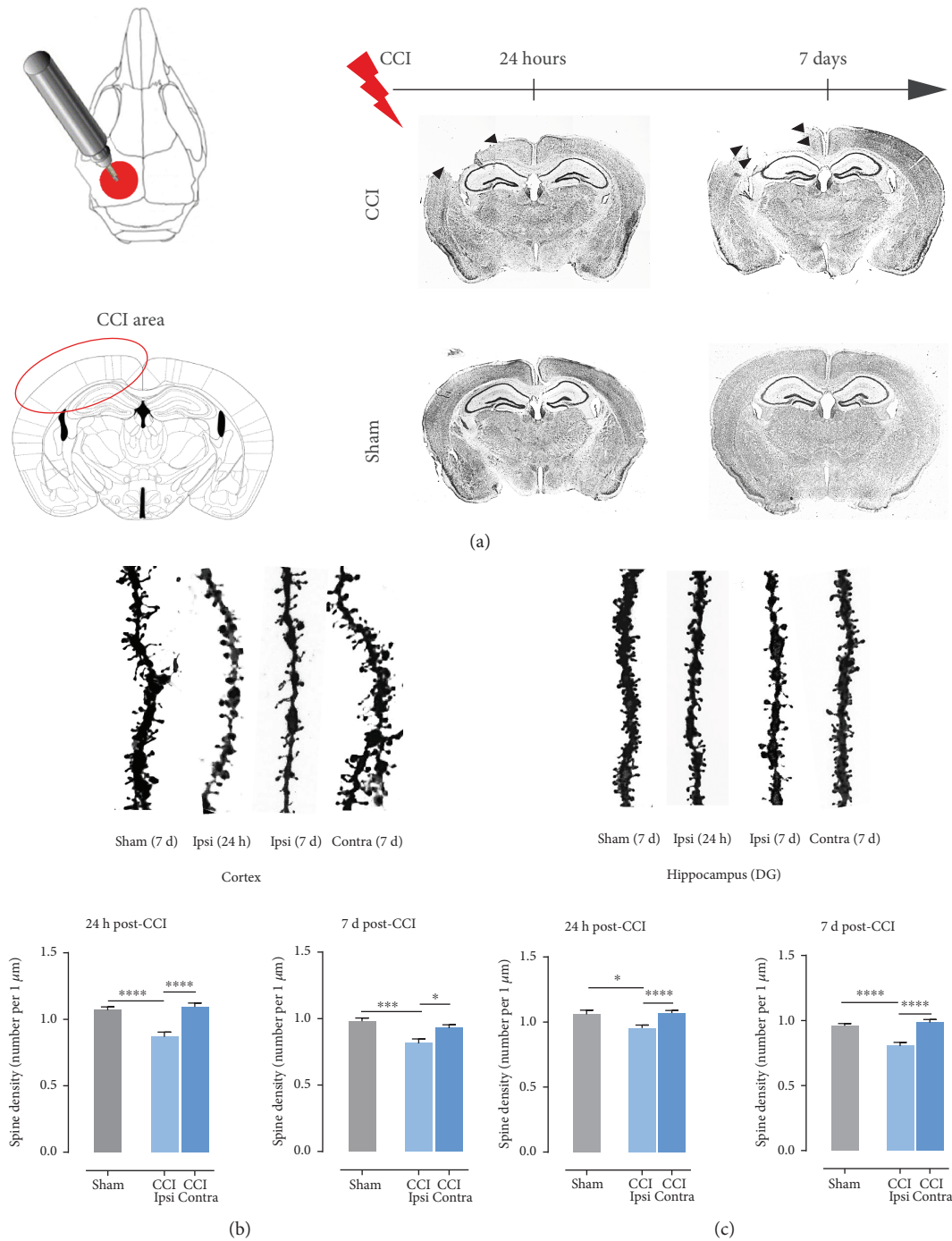
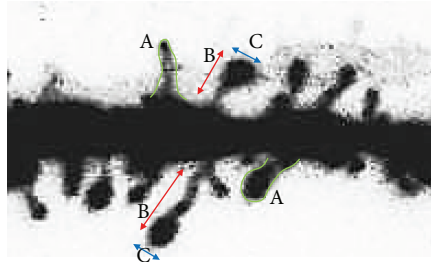


FIGURE 1: Decrease in spine density after controlled cortical impact (CCI). (a) Schematic representation of injured area. Nissl-stained brain sections from animals at 1 and 7 days after CCI (CCI: animals after controlled cortical impact; sham: animals subjected to craniectomy without cortical injury). (b) Spine density (number of spines per 1 μm of dendrite length) in ipsi- and contralateral 2nd and 3rd cortex layers of C57Bl6/J mice, 1 and 7 days after CCI and sham procedures; right panel shows representative dendrites pictures. (c) Spine density in ipsi- and contralateral dentate gyrus of C57Bl6/J mice, 1 and 7 days after CCI and sham procedures; right panel shows representative dendrite pictures. Data are presented as mean \pm SEM. Statistical analysis was carried out using one-way ANOVA followed by Tukey's post hoc test. Asterisks indicate statistical significance from the CCI and sham groups, respectively. * $P < 0.05$; *** $P \leq 0.001$; **** $P < 0.0001$.

population standard deviation of the variable, and d is the magnitude of the difference. With the above-estimated values, the group size is 10. In our experiments, we

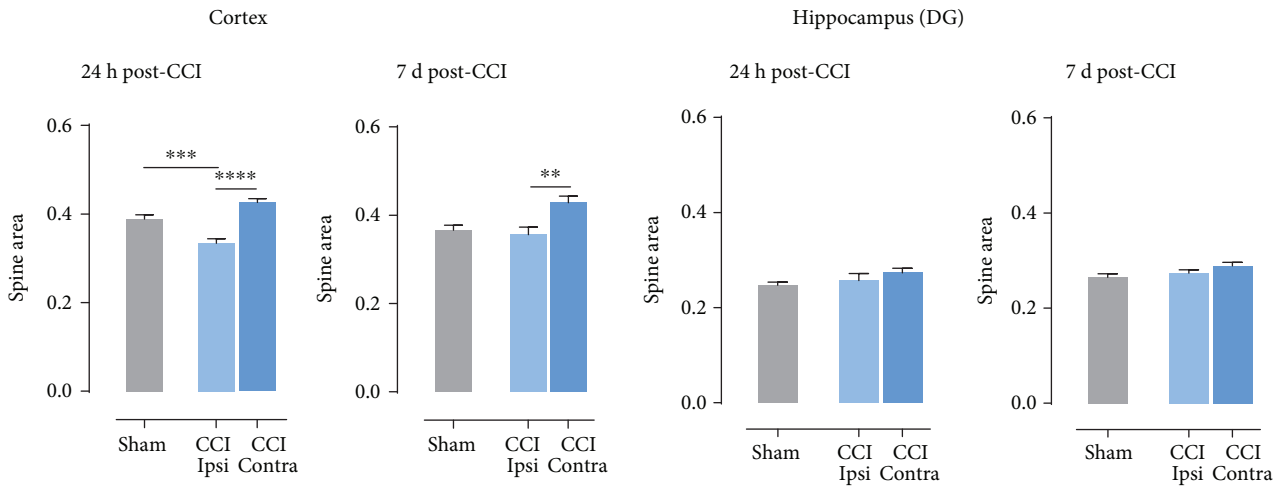
increased the group size and it varied between 15 and 25 depending on the experiment (5 to 7 pictures per animal, 3-5 animals per group).



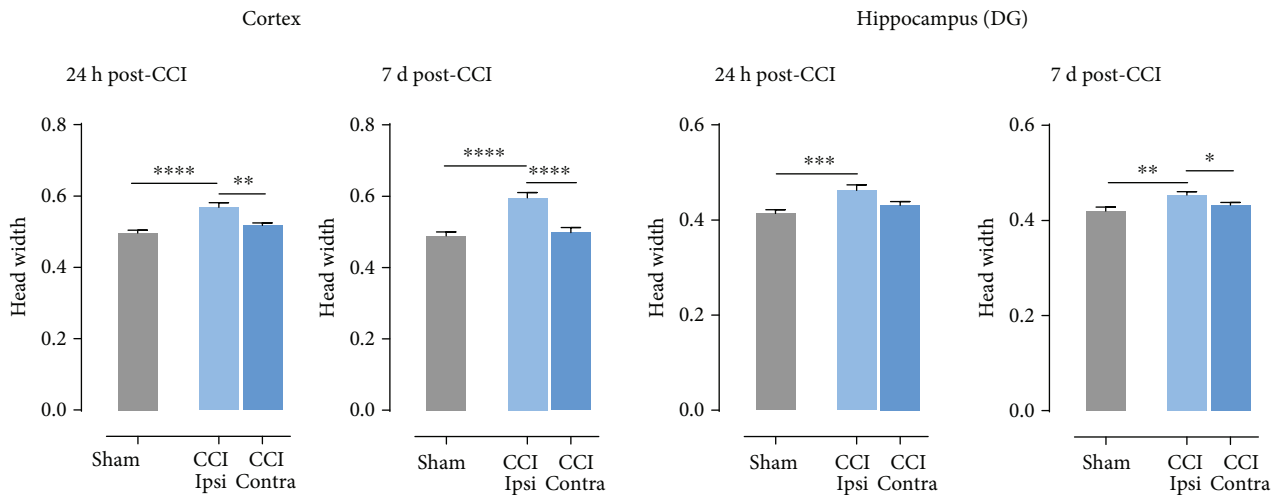
Dendritic spine
shape parameters

- A : spine area
- B : spine length
- C : head width
- B/C : length/width ratio

(a)



(b)



(c)

FIGURE 2: Continued.

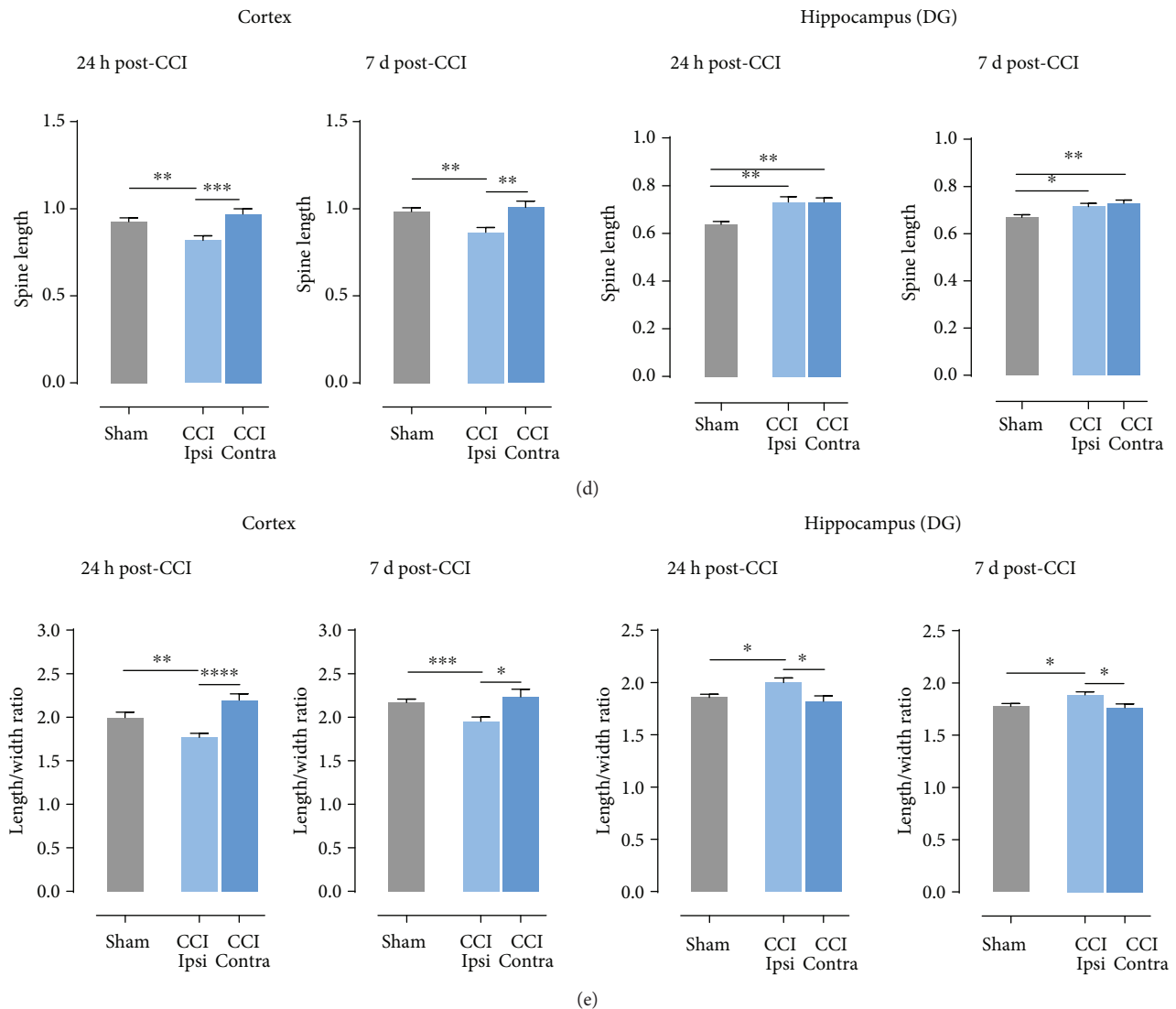


FIGURE 2: Time-dependent changes in dendritic spines shape after controlled cortical impact (CCI). (a) Spine shape parameters: A: spine area; B: spine length; C: head width; B/C: length/width ratio. (b) Spine area calculated in the ipsi- and contralateral cortex and hippocampus of C57Bl6/J mice, 1 and 7 days after CCI and sham procedures. (c) Head width calculated in the ipsi- and contralateral cortex and hippocampus of C57Bl6/J mice, 1 and 7 days after CCI and sham procedures. (d) Spine length calculated in the ipsi- and contralateral cortex and hippocampus of C57Bl6/J mice, 1 and 7 days after CCI and sham procedures. (e) Length/width ratio calculated in the ipsi- and contralateral cortex and hippocampus of C57Bl6/J mice, 1 and 7 days after CCI and sham-operated animals. Data are presented as mean \pm SEM. Statistical analysis was carried out using one-way ANOVA followed by Tukey's post hoc test. Asterisks indicate statistical significance from the CCI and sham groups, respectively. * $P < 0.05$; ** $P \leq 0.01$; *** $P \leq 0.001$; **** $P < 0.00013.3$.

2.5. Statistical Analyses. All results are expressed as mean \pm SEM. The appropriate tests were chosen (see below), taking into account whether data had normal distribution and equal variation. All analyses were conducted using GraphPad Prism, version 7.02 (GraphPad Software Inc., La Jolla, CA). Differences between the experimental groups were considered significant if the type 1 error was less than 5%.

3. Results

3.1. Decrease in Spine Density in the Cerebral Cortex and the Hippocampus Evoked by Controlled Cortical Impact (CCI). To induce TBI in mice, we used controlled cortical impact

(CCI) as described by Bolkvadze and Pitkänen [46]. To describe morphological changes evoked by injury, the brains were collected 24 hours and 7 days post-CCI. Control animals (sham-operated) were subjected to craniectomy only and sacrificed together with the animals that underwent CCI. The Nissl staining revealed time-dependent cerebral cortex degeneration within the injured area (Figure 1(a)). In sham-operated animals, hardly any tissue damage was observed. A separate batch of animals was used to perform dendritic spine analyses. Animals were subjected to CCI or sham surgery. Twenty-four hours or 7 days later, their brains were collected to perform analyses of dendritic spines from ipsi- and contralateral sides. For this, we used lipophilic dye that incorporates into cell membranes and marks the whole

cell contour. Sections were imaged using a confocal microscope, as described in Materials and Methods. Spine density was calculated as a number of protrusions per $1\ \mu\text{m}$ of dendrite length. Twenty-four hours and 7 days after CCI, spine density was decreased in the 2nd and 3rd layers of the ipsilateral cerebral cortex, as compared to the contralateral hemisphere (24 h **** $P < 0.0001$; 7 d * $P = 0.0135$) and sham animals (24 h **** $P < 0.0001$; 7 d *** $P = 0.0003$; Figure 2(b)). Similar effect was observed in the DG where 24 hours and 7 days after TBI spine density were significantly lower compared to the contralateral side (24 h * $P < 0.0001$; 7 d * $P = 0.0001$; Figure 1(c)) and sham-operated animals (24 h * $P = 0.0251$; 7 d **** $P < 0.0001$; Figure 1(c)).

3.2. Dendritic Spines Become Shorter and Wider in Injured Cerebral Cortex Area. Next, we aimed at more detailed analysis of morphological alterations following trauma. For this, we used a semiautomatic software to evaluate dendritic spine shapes on the basis of the following parameters: length, head width, and length to width ratio that describes the spine shape, with its increase reflecting filopodial shape (Figure 2(a)). The parameters were measured at two time points, 1 and 7 days after CCI. Dendritic spines shrank in the ipsilateral cerebral cortex following trauma as their areas were smaller both 24 hours and 7 days after brain injury, compared to the contralateral cortex (24 h **** $P < 0.0001$; 7 d ** $P = 0.0057$; Figure 1(b)). Significant difference between ipsilateral hemisphere and sham-operated animals was observed only after 24 hours (*** $P = 0.0005$), while in the DG, no significant differences were observed (Figure 2(b)). Head width (width at the widest point of the spine) increased both in the cortex and DG in injured hemispheres, compared to the contralateral hemisphere (cortex: 24 h ** $P < 0.0015$; 7 d **** $P > 0.0001$; DG: 7 d * $P = 0.033$) and animals that underwent sham surgeries (cortex: 24 h **** $P > 0.0001$; 7 d **** $P > 0.0001$; DG: 24 h **** $P = 0.0005$; 7 d ** $P = 0.0086$) (Figure 2(c)). Next parameter, spine length, reflects the distance from the bottom to the top of the spine (Figure 2(d)). In the ipsilateral cortex, spine length was decreased compared to the contralateral hemisphere in both time points (24 h *** $P = 0.0006$; 7 d ** $P = 0.0097$) and sham-operated animals (24 h *** $P = 0.0021$; 7 d * $P = 0.0043$). In contrast, in the ipsilateral DG, spines were longer than in animals after sham operation (24 h ** $P = 0.0021$; 7 d * $P = 0.0166$), and no difference compared to the contralateral hemisphere was observed. Decrease of the ratio between the length and width of the spine was observed in the ipsilateral cerebral cortex when compared to the contralateral side (Figure 2(e), 24 h: ** $P < 0.0001$; 7 d * $P = 0.0182$) and sham animals (24 h: ** $P = 0.0061$; 7 d **** $P = 0.0010$). While in the ipsilateral DG, opposite effect was noticed, where the length/width ratio increases in response to TBI compared to contralateral DG (24 h * $P = 0.0166$; 7 d * $P = 0.026$) as well as in comparison to sham animals (24 h * $P = 0.0402$; 7 d * $P = 0.037$; Figure 2(e)).

3.3. Deficiency of MMP-9 Impairs the Effect of Brain Injury on Spine Density Decline. Since MMP-9 is one of the key

modulators of dendritic spines shape and its role in TBI and subsequent epileptogenesis has been recently highlighted [28], we set out to evaluate whether the lack of MMP-9 affects morphological changes observed in WT animals. For this, we used mice missing MMP-9 (MMP-9 KO) and their wild-type littermates (WT MMP-9). We focused on 7-day post-CCI time point. As we reported in the previous report, MMP-9 activity was the highest during first week after brain injury [28]. After CCI in WT and KO MMP-9 animals, we analyzed dendritic spines as described above. 1 week after the brain injury, spine density was decreased in the ipsilateral cerebral cortex of WT animals as compared to the contralateral side of the injured brain (** $P = 0.0011$; Figure 3(a)) and sham-operated animals (** $P = 0.0067$; Figure 3(a)). However, this phenomenon was not observed in MMP-9 KO mice (Figures 3(a) and 3(b)).

3.4. MMP-9 Is Required for Spine Shape Remodeling upon Injury. To further unravel the influence of MMP-9 on the postinjury morphological changes of dendritic spines, we analyzed basic spine parameters (Figure 2(a)). We focused on length to width ratio and spine head width as these parameters indicate whether protrusions undergo plastic changes. In WT animals, in the ipsilateral cerebral cortex area, we observed increase in head width compared to contralateral hemisphere (**** $P < 0.0001$; Figure 4(a)) and sham-operated animals (* $P = 0.0477$; Figure 4(a)). Similarly, to the cerebral cortex, in the ipsilateral dentate gyrus of hippocampus WT MMP-9 mice, head width was significantly bigger compared to the contralateral hippocampus (** $P = 0.0020$; Figure 5(a)) and sham-operated animals (** $P = 0.0061$; Figure 5(a)). On the contrary, in MMP-9 KO animals, following CCI, no alterations in dendritic spine morphology were detected in both analyzed structures (Figures 4(a) and 5(a)). In the injured cerebral cortex, WT MMP-9 mice length/width ratio decreased, while in the ipsilateral dentate gyrus increased (Figures 4(b) and 5(b)). The changes in the ipsilateral cortex was significant compared to the contralateral side of the brain (** $P = 0.0048$; Figure 4(b)) and sham animals (* $P = 0.0316$; Figure 4(b)), whereas in MMP-9 KO mice, no differences were observed (Figure 4(b)). In the DG, ratio between the spine length and width in ipsilateral hemisphere was significantly higher compared only to sham animals (** $P = 0.0016$; Figure 5(b)). Similarly, to the cortex, the changes between the CCI and sham groups were not significant (Figure 5(b)).

4. Discussion

Here, we show that traumatic brain injury caused by the controlled cortical impact induces acute (within 1 day post-TBI) changes in the dendritic spine number and morphology, as well as prolonged (up to 7 days after the injury) spine remodeling. Spine density decreases following brain trauma in the ipsilateral side both in the cerebral cortex and the dentate gyrus of the hippocampus. Following trauma dendritic spines in the ipsilateral cerebral cortex shrink, get shorter and their heads get wider, thus being converted into more mushroom-like shape. On the other hand, spines in the DG on the

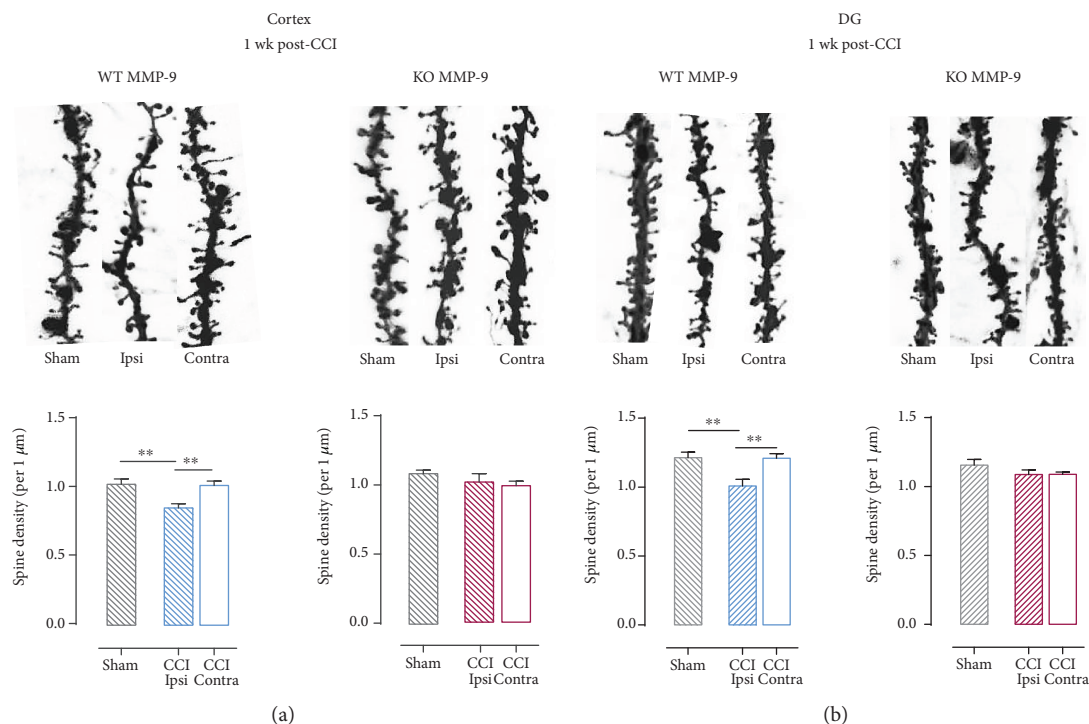


FIGURE 3: Effect of lack of functional MMP-9 on spine density in animals after controlled cortical impact (CCI). (a) Spine density in ipsi- and contralateral 2nd and 3rd cortex layers of animals with different *mmp-9* gene expression levels 1 week after CCI and sham surgeries; upper panel shows representative dendrites pictures. (b) Spine density in the ipsi- and contralateral dentate gyrus of animals with different *mmp-9* gene expression levels 1 week after CCI and sham surgeries; upper panel shows representative dendrite pictures. Data are presented as mean \pm SEM. Statistical analysis was carried out using one-way ANOVA followed by Tukey's post hoc test. Asterisks indicate statistical significance from the CCI and sham groups, respectively. $**P \leq 0.01$.

ipsilateral side get longer and thinner, assuming more filopodial form. Lack of MMP-9 activity in the brain abrogates the effects evoked by the trauma, both as far as the spine dynamics (reflected by changes in the density) and morphological plasticity are concerned.

Dendritic spines are protrusions containing the majority of excitatory synapses, thus gating inputs received by the nerve cell [4, 50]. The density and morphology of dendritic spines are regulated by synaptic activity, and so spines undergo dynamic turnover throughout life. Filopodia-shaped spines are more prominent in the developing brain and are considered "immature" [51]. Some reports indicate that these are spine precursors during synapse formation [52]. Spines considered "mature" are more mushroom-shaped, allowing stabilizing the spine by gathering more neurotransmitter receptors in the head [53]. Other feature of such shape is that the narrow spine neck might also compartmentalize calcium necessary for synaptic transmission to occur [54]. When the brain is challenged by injury, spines respond accordingly to maintain milieu homeostasis [7].

First, we measured dendritic spine density. Spine number has been shown to be related to overall synaptic activity, e.g., in the hippocampus transient enhancement of dendritic spine density accompanies early long-term potentiation (LTP) in the dentate gyrus [55]. Previous studies on dendritic spine plasticity evoked by TBI in animal models showed decreased spine density in the hippocampus and the cerebral cortex at various times after brain injury (24 hours to 35

days) [9, 11, 13, 16]. Furthermore, one study expands these observations up to 1.5 years, showing changes that last not only shortly after brain injury but also continue into chronic stages of TBI. Moreover, they take place in widespread regions beyond the site of acute trauma [12].

Dendritic spine loss is accompanied by dendrite deformation and swelling [15]. Our results are essentially in agreement with the abovementioned data; however, they extend those observations by describing the detailed shape parameters. In the present study, we show that 24-hour postinjury dendritic spine density decreases in the ipsilateral side in the cortex and the hippocampus, which is consistent with the previous report [8, 11]. We further demonstrate that 7 days after injury the number of spines per dendrite length is still decreased in the cortex and the DG. Dendritic spine loss one-week posttrauma was also shown in the CA1 of the hippocampus [12]. Since our TBI conditions were far less severe, we conclude that even mild injury then can result in substantial changes in the brain.

Furthermore, we also show a detailed morphological analysis of dendritic spines in the cortex and hippocampus after traumatic brain injury. Here, we demonstrate that after brain trauma induced by CCI, dendritic spines in the cerebral cortex, ipsilaterally to the injury side, are getting shorter and their heads become wider, when compared to sham-operated animals and the contralateral side of the injured cerebral cortex. Overall, the spine plasticity observed in the cerebral cortex ipsilateral to the

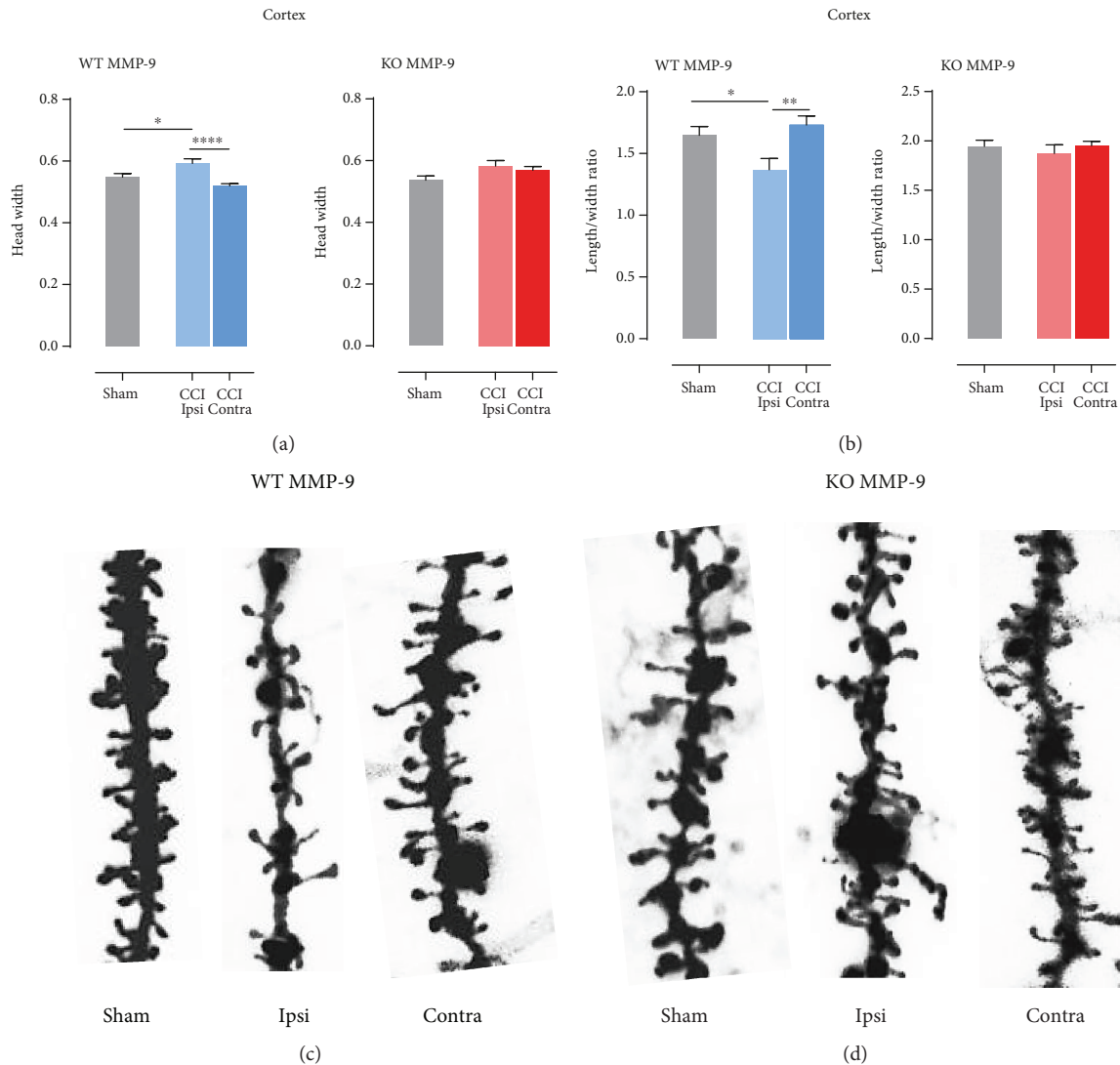


FIGURE 4: Effects of MMP-9 on spine shape changes in the cerebral cortex layers of animals 1 week post-CCI. (a) Head width calculated in the ipsi- and contralateral cortex and hippocampus of C57Bl6/J mice, 7 days after CCI and sham procedures. (b) Length/width ratio calculated in the ipsi- and contralateral cortex and hippocampus of C57Bl6/J mice, 7 days after CCI and sham-operated animals. (c) Dendrite pictures from the ipsi- and contralateral cortex and sham animals. (d) Representative dendrite pictures from the ipsi- and contralateral cortex and sham animals. Data are presented as mean \pm SEM. Statistical analysis was carried out using one-way ANOVA followed by Tukey's post hoc test. Asterisks indicate statistical significance from the CCI and sham groups, respectively. * $P < 0.05$; ** $P \leq 0.01$.

injury and in a deeper located DG showed similar pattern of spine morphological alterations, except for the length/width ratio. This morphological parameter is believed to reflect spine maturity [4, 39, 52]. The greater this value, the spine is more filopodial-shaped, i.e., immature. This finding deserves a special comment. The filopodia-like spines are presumably prone to support initiation of synaptic plasticity processes [4, 36, 50]. Therefore, this result may suggest that DG may undergo synaptic plasticity that may predispose this brain structure to support epileptogenesis that is a frequent consequence of TBI [56, 57].

In the present study, we show that TBI-driven dynamics and morphological plasticity of dendritic spines are MMP-9-dependent. Increases in MMP-9 following TBI have previously been reported both in the animal brain and human cerebrospinal fluid, blood plasma, and serum [9, 30, 44–47,

58, 59]. The possible role of MMP-9 in controlling spine dynamics has been previously demonstrated in the DG, following treatment with excitotoxic kainic acid, where MMP-9 KO mice were found to be resistant to spine loss [60, 61]. Similarly, recently, Nagaoka et al. [62] have reported that MMP-9 controls spine dynamics in the neocortex of fragile X mental retardation protein KO mice.

Furthermore, in our study, missing MMP-9 has entirely abrogated dendritic spine morphological plasticity provoked by TBI, both in the cerebral cortex ipsilateral to the injury and in the dentate gyrus. This finding goes well along with multiple data showing a pivotal role of MMP-9 in regulation of dendritic spine size and shape [29, 63, 64].

Finally, we shall stress that previous studies [28, 40] demonstrated that MMP-9 KO mice brain showed limited brain damage after CCI. However, the extend of this

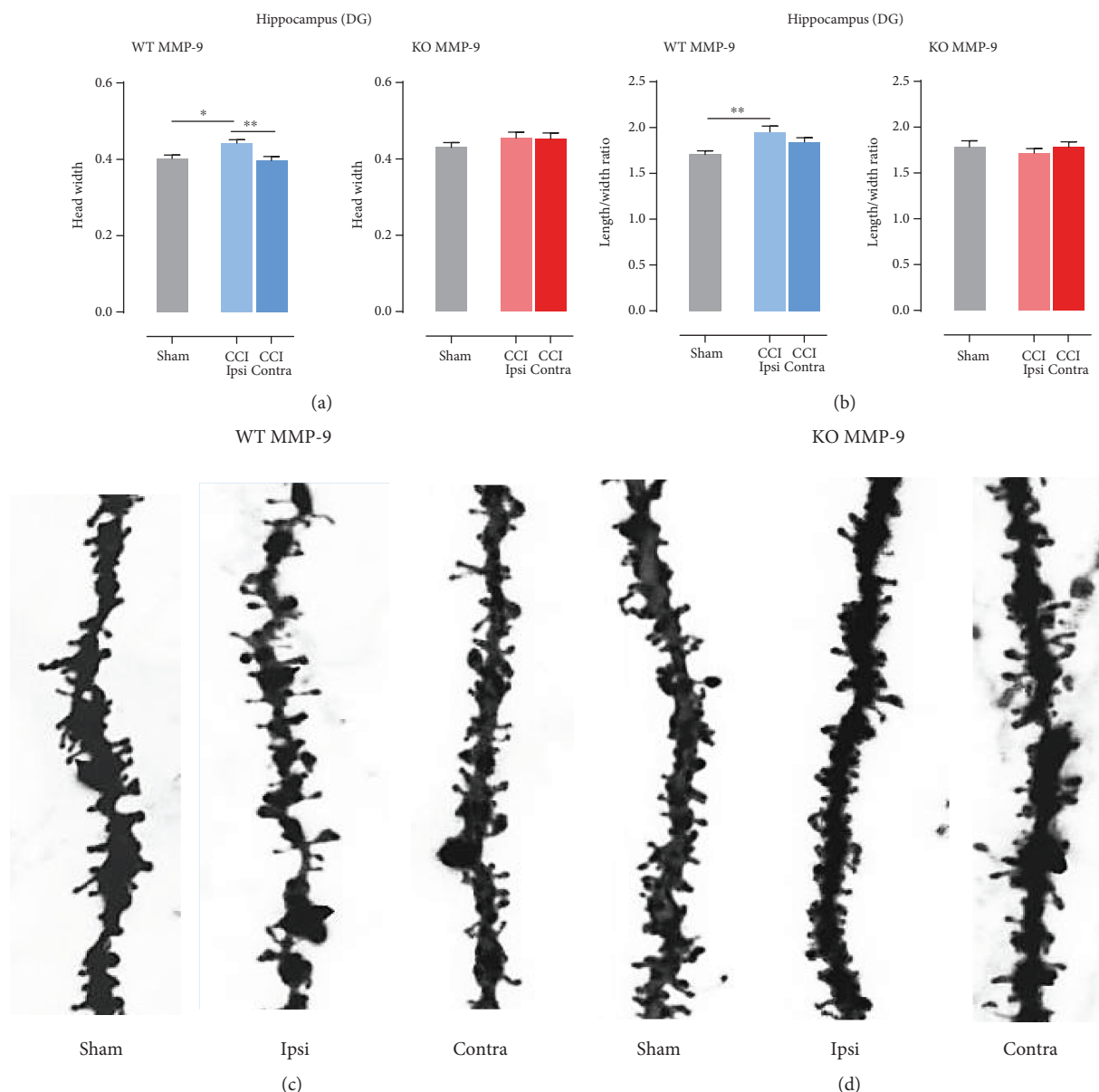


FIGURE 5: Effects of MMP-9 on spine shape changes in the dentate gyrus of animals 1 week post-CCI. (a) Head width calculated in the ipsi- and contralateral hippocampus of C57Bl6/J mice, 7 days after CCI and sham procedures. (b) Length/width ratio calculated in the ipsi- and contralateral hippocampus of C57Bl6/J mice, 7 days after CCI and sham-operated animals. (c) Dendrite pictures from the ipsi- and contralateral dentate gyrus and sham animals. (d) Representative dendrite pictures from the ipsi- and contralateral dentate gyrus and sham animals. Data are presented as mean \pm SEM. Statistical analysis was carried out using one-way ANOVA followed by Tukey's post hoc test. Asterisk indicate statistical significance from the CCI and sham groups, respectively. * $P < 0.05$; ** $P \leq 0.01$.

protection against brain damage (MMP-9 KO still demonstrated almost 40% of the cortical injury area as compared to WT) does not seem to explain the entire abrogation of TBI effects on the spines in the MMP-9 KO brains.

5. Conclusions

Herein, we have provided a detailed analysis of TBI-evoked density and morphological plasticity of the dendritic spines. We have found that in result of the injury, there is a decrease in spine density both very close (ipsilateral cerebral cortex) and more distal (hippocampal dentate gyrus on the ipsilateral

side) to the locus of the injury. However, the spines located on neurons close to the injury assume more mushroom-like shape, whereas those in DG become more filopodia-like. Missing MMP-9 previously shown to exert control of the spine density and morphology abrogated the aforementioned plasticity entirely. Considering the previously reported role of MMP-9 in posttraumatic epileptogenesis (PTE) that might be supported by abnormal synaptic plasticity, and a well-documented role of this enzyme in the plasticity of dendritic spines, it is tempting to suggest that MMP-9-dependent dendritic spine dynamics and morphological plasticity contribute to PTE.

Data Availability

Previously reported (MMP-9 activity after CCI; role of MMP-9 in posttraumatic epileptogenesis) data were used to support this study and are available at doi:10.1007/s12035-018-1061-5. These prior studies (and datasets) are cited at relevant places within the text as reference [28].

Conflicts of Interest

The authors declare that there is no competing interest relevant to the publication of this paper.

Acknowledgments

The study was supported by a grant from the National Center of Research and Development (NCBiR) grants: ERA-NET Neuron grant (NEURON/09/13) and (PBS/A8/36/2015) and the Foundation for Polish Science BRAINCITY MAB/2018/10. The BRAINCITY project is carried out within the International Research Agendas programme of the Foundation for Polish Science cofinanced by the European Union under the European Regional Development Fund.

References

- [1] C. M. Atkins, "Decoding hippocampal signaling deficits after traumatic brain injury," *Translational Stroke Research*, vol. 2, no. 4, pp. 546–555, 2011.
- [2] T. M. Reeves, M. L. Prins, J. P. Zhu, J. T. Povlishock, and L. L. Phillips, "Matrix metalloproteinase inhibition alters functional and structural correlates of deafferentation-induced sprouting in the dentate gyrus," *The Journal of Neuroscience*, vol. 23, no. 32, pp. 10182–10189, 2003.
- [3] E. Shohami and A. Biegon, "Novel approach to the role of NMDA receptors in traumatic brain injury," *CNS & Neurological Disorders - Drug Targets*, vol. 13, no. 4, pp. 567–573, 2014.
- [4] C. Sala and M. Segal, "Dendritic spines: the locus of structural and functional plasticity," *Physiological Reviews*, vol. 94, no. 1, pp. 141–188, 2014.
- [5] E. G. Gray, "Axo-somatic and axo-dendritic synapses of the cerebral cortex: an electron microscope study," *Journal of Anatomy*, vol. 93, pp. 420–433, 1959.
- [6] K. M. Harris and S. B. Kater, "Dendritic spines: cellular specializations imparting both stability and flexibility to synaptic function," *Annual Review of Neuroscience*, vol. 17, no. 1, pp. 341–371, 1994.
- [7] R. F. McCann and D. A. Ross, "A fragile balance: dendritic spines, learning, and memory," *Biological Psychiatry*, vol. 82, no. 2, pp. e11–e13, 2017.
- [8] J. N. Campbell, D. Register, and S. B. Churn, "Traumatic brain injury causes an FK506-sensitive loss and an overgrowth of dendritic spines in rat forebrain," *Journal of Neurotrauma*, vol. 29, no. 2, pp. 201–217, 2012.
- [9] X. Gao, P. Deng, Z. C. Xu, and J. Chen, "Moderate traumatic brain injury causes acute dendritic and synaptic degeneration in the hippocampal dentate gyrus," *PLoS One*, vol. 6, no. 9, article e24566, 2011.
- [10] E. Schwarzbach, D. P. Bonislawski, G. Xiong, and A. S. Cohen, "Mechanisms underlying the inability to induce area CA1 LTP in the mouse after traumatic brain injury," *Hippocampus*, vol. 16, no. 6, pp. 541–550, 2006.
- [11] C. N. Winston, D. Chellappa, T. Wilkins et al., "Controlled cortical impact results in an extensive loss of dendritic spines that is not mediated by injury-induced amyloid-beta accumulation," *Journal of Neurotrauma*, vol. 30, no. 23, pp. 1966–1972, 2013.
- [12] A. Ertürk, S. Mentz, E. E. Stout et al., "Interfering with the chronic immune response rescues chronic degeneration after traumatic brain injury," *The Journal of Neuroscience*, vol. 36, no. 38, pp. 9962–9975, 2016.
- [13] X. Gao and J. Chen, "Mild traumatic brain injury results in extensive neuronal degeneration in the cerebral cortex," *Journal of Neuropathology & Experimental Neurology*, vol. 70, no. 3, pp. 183–191, 2011.
- [14] Y. Zhang, Z. G. Zhang, M. Chopp et al., "Treatment of traumatic brain injury in rats with N-acetyl-seryl-aspartyl-lysyl-proline," *Journal of Neurosurgery*, vol. 126, no. 3, pp. 782–795, 2017.
- [15] S. Zhao, X. Gao, W. Dong, and J. Chen, "The role of 7,8-dihydroxyflavone in preventing dendrite degeneration in cortex after moderate traumatic brain injury," *Molecular Neurobiology*, vol. 53, no. 3, pp. 1884–1895, 2016.
- [16] J. R. Chen, T. J. Wang, Y. J. Wang, and G. F. Tseng, "The immediate large-scale dendritic plasticity of cortical pyramidal neurons subjected to acute epidural compression," *Neuroscience*, vol. 167, no. 2, pp. 414–427, 2010.
- [17] M. Dziembowska and J. Włodarczyk, "MMP9: a novel function in synaptic plasticity," *The International Journal of Biochemistry & Cell Biology*, vol. 44, no. 5, pp. 709–713, 2012.
- [18] H. Frankowski, Y. H. Gu, J. H. Heo, R. Milner, and G. J. Del Zoppo, "Use of gel zymography to examine matrix metalloproteinase (gelatinase) expression in brain tissue or in primary glial cultures," in *Astrocytes*, vol. 814 of *Methods in Molecular Biology*, pp. 221–233, 2012.
- [19] T. Klein and R. Bischoff, "Physiology and pathophysiology of matrix metalloproteases," *Amino Acids*, vol. 41, no. 2, pp. 271–290, 2011.
- [20] P. E. Van den Steen, B. Dubois, I. Nelissen, P. M. Rudd, R. A. Dwek, and G. Opdenakker, "Biochemistry and molecular biology of gelatinase B or matrix metalloproteinase-9 (MMP-9)," *Critical Reviews in Biochemistry and Molecular Biology*, vol. 37, no. 6, pp. 375–536, 2002.
- [21] J. Vandooren, J. van Damme, and G. Opdenakker, "On the structure and functions of gelatinase B/matrix metalloproteinase-9 in neuroinflammation," *Progress in Brain Research*, vol. 214, pp. 193–206, 2014.
- [22] C. Bonnans, J. Chou, and Z. Werb, "Remodelling the extracellular matrix in development and disease," *Nature Reviews Molecular Cell Biology*, vol. 15, no. 12, pp. 786–801, 2014.
- [23] I. M. Ethell and D. W. Ethell, "Matrix metalloproteinases in brain development and remodeling: synaptic functions and targets," *Journal of Neuroscience*, vol. 85, no. 13, pp. 2813–2823, 2007.
- [24] M. Ferrer-Ferrer and A. Dityatev, "Shaping synapses by the neural extracellular matrix," *Frontiers in Neuroanatomy*, vol. 12, p. 40, 2018.
- [25] J. D. Mott and Z. Werb, "Regulation of matrix biology by matrix metalloproteinases," *Current Opinion in Cell Biology*, vol. 16, no. 5, pp. 558–564, 2004.
- [26] G. Opdenakker, "On the roles of extracellular matrix remodeling by gelatinase B," *Verhandelingen - Koninklijke Academie*

- Voor Geneeskunde Van België*, vol. 59, no. 6, pp. 489–514, 1997.
- [27] L. L. Phillips, T. M. Reeves, J. L. Chan, and A. E. Doperalski, “Time dependent integration of matrix metalloproteinases and their targeted substrates directs axonal sprouting and synaptogenesis following central nervous system injury,” *Neural Regeneration Research*, vol. 9, no. 4, pp. 362–376, 2014.
- [28] B. Pijet, M. Stefaniuk, A. Kostrzevska-Ksiezzyk, P. E. Tsilibary, A. Tzinia, and L. Kaczmarek, “Elevation of MMP-9 levels promotes epileptogenesis after traumatic brain injury,” *Molecular Neurobiology*, vol. 55, no. 12, pp. 9294–9306, 2018.
- [29] B. Vafadari, A. Salamian, and L. Kaczmarek, “MMP-9 in translation: from molecule to brain physiology, pathology, and therapy,” *Journal of Neurochemistry*, vol. 139, no. 2, pp. 91–114, 2016.
- [30] D. Neuhofer and P. Kalivas, “Metaplasticity at the addicted tetrapartite synapse: a common denominator of drug induced adaptations and potential treatment target for addiction,” *Neurobiology of Learning and Memory*, vol. 154, pp. 97–111, 2018.
- [31] P. Penzes, M. E. Cahill, K. A. Jones, J. E. VanLeeuwen, and K. M. Woolfrey, “Dendritic spine pathology in neuropsychiatric disorders,” *Nature Neuroscience*, vol. 14, no. 3, pp. 285–293, 2011.
- [32] A. Pitkänen, X. E. Nnode-Ekane, K. Łukasiuk et al., “Neural ECM and epilepsy,” *Progress in Brain Research*, vol. 214, pp. 229–262, 2014.
- [33] S. M. Reinhard, K. Razak, and I. M. Ethell, “A delicate balance: role of MMP-9 in brain development and pathophysiology of neurodevelopmental disorders,” *Frontiers in Cellular Neuroscience*, vol. 9, p. 280, 2015.
- [34] K. Lepeta and L. Kaczmarek, “Matrix metalloproteinase-9 as a novel player in synaptic plasticity and schizophrenia,” *Schizophrenia Bulletin*, vol. 41, no. 5, pp. 1003–1009, 2015.
- [35] M. Verslegers, K. Lemmens, I. Van Hove, and L. Moons, “Matrix metalloproteinase-2 and -9 as promising benefactors in development, plasticity and repair of the nervous system,” *Progress In Neurobiology*, vol. 105, pp. 60–78, 2013.
- [36] M. Magnowska, T. Gorkiewicz, A. Suska et al., “Transient ECM protease activity promotes synaptic plasticity,” *Scientific Reports*, vol. 6, no. 1, article 27757, 2016.
- [37] P. Michaluk, M. Wawrzyniak, P. Alot et al., “Influence of matrix metalloproteinase MMP-9 on dendritic spine morphology,” *Journal Of Cell Science*, vol. 124, no. 19, pp. 3369–3380, 2011.
- [38] Z. Szepesi, E. Hossy, B. Ruszczycki et al., “Synaptically released matrix metalloproteinase activity in control of structural plasticity and the cell surface distribution of GluA1-AMPA receptors,” *PLoS One*, vol. 9, no. 5, article e98274, 2014.
- [39] L. Tian, M. Stefanidakis, L. Ning et al., “Activation of NMDA receptors promotes dendritic spine development through MMP-mediated ICAM-5 cleavage,” *Journal Of Cell Biology*, vol. 178, no. 4, pp. 687–700, 2007.
- [40] X. Wang, J. Jung, M. Asahi et al., “Effects of matrix metalloproteinase-9 gene knock-out on morphological and motor outcomes after traumatic brain injury,” *The Journal of Neuroscience*, vol. 20, no. 18, pp. 7037–7042, 2000.
- [41] X. Wang, O. Bozdagi, J. S. Nikitczuk, Z. W. Zhai, Q. Zhou, and G. W. Huntley, “Extracellular proteolysis by matrix metalloproteinase-9 drives dendritic spine enlargement and long-term potentiation coordinately,” *Proceedings of the National Academy of Sciences of the United States of America*, vol. 105, no. 49, pp. 19520–19525, 2008.
- [42] T. Hayashi, Y. Kaneko, S. Yu et al., “Quantitative analyses of matrix metalloproteinase activity after traumatic brain injury in adult rats,” *Brain research*, vol. 1280, pp. 172–177, 2009.
- [43] J. S. Truettner, O. F. Alonso, and W. D. Dietrich, “Influence of therapeutic hypothermia on matrix metalloproteinase activity after traumatic brain injury in rats,” *Journal of Cerebral Blood Flow & Metabolism*, vol. 25, no. 11, pp. 1505–1516, 2005.
- [44] E. Suehiro, H. Fujisawa, T. Akimura et al., “Increased matrix metalloproteinase-9 in blood in association with activation of interleukin-6 after traumatic brain injury: influence of hypothermic therapy,” *Journal of Neurotrauma*, vol. 21, no. 12, pp. 1706–1711, 2004.
- [45] D. Vajtr, O. Benada, J. Kukacka et al., “Correlation of ultrastructural changes of endothelial cells and astrocytes occurring during blood brain barrier damage after traumatic brain injury with biochemical markers of BBB leakage and inflammatory response,” *Physiological Research*, vol. 58, no. 2, pp. 263–268, 2009.
- [46] T. Bolkvadze and A. Pitkänen, “Development of post-traumatic epilepsy after controlled cortical impact and lateral fluid-percussion-induced brain injury in the mouse,” *Journal of Neurotrauma*, vol. 29, no. 5, pp. 789–812, 2012.
- [47] T. H. Vu, J. M. Shipley, G. Bergers et al., “MMP-9/gelatinase B is a key regulator of growth plate angiogenesis and apoptosis of hypertrophic chondrocytes,” *Cell*, vol. 93, no. 3, pp. 411–422, 1998.
- [48] D. H. Smith, H. D. Soares, J. S. Pierce et al., “A model of parasagittal controlled cortical impact in the mouse: cognitive and histopathologic effects,” *Journal of Neurotrauma*, vol. 12, no. 2, pp. 169–178, 1995.
- [49] B. Ruszczycki, Z. Szepesi, G. M. Wilczynski et al., “Sampling issues in quantitative analysis of dendritic spines morphology,” *BMC Bioinformatics*, vol. 13, no. 1, p. 213, 2012.
- [50] H. Kasai, M. Fukuda, S. Watanabe, A. Hayashi-Takagi, and J. Noguchi, “Structural dynamics of dendritic spines in memory and cognition,” *Trends in Neurosciences*, vol. 33, no. 3, pp. 121–129, 2010.
- [51] M. Miller, “Maturation of rat visual cortex. III. Postnatal morphogenesis and synaptogenesis of local circuit neurons,” *Brain Research*, vol. 390, no. 2, pp. 271–285, 1986.
- [52] J. D. Jontes and S. J. Smith, “Filopodia, spines, and the generation of synaptic diversity,” *Neuron*, vol. 27, no. 1, pp. 11–14, 2000.
- [53] E. A. Nimchinsky, B. L. Sabatini, and K. Svoboda, “Structure and function of dendritic spines,” *Annual Review of Physiology*, vol. 64, no. 1, pp. 313–353, 2002.
- [54] R. Yuste, “Dendritic spines and distributed circuits,” *Neuron*, vol. 71, no. 5, pp. 772–781, 2011.
- [55] M. Wosiski-Kuhn and A. M. Stranahan, “Transient increases in dendritic spine density contribute to dentate gyrus long-term potentiation,” *Synapse*, vol. 66, no. 7, pp. 661–664, 2012.
- [56] J. Jarero-Basulto, Y. Gasca-Martínez, M. Rivera-Cervantes, M. Ureña-Guerrero, A. Feria-Velasco, and C. Beas-Zarate, “Interactions between epilepsy and plasticity,” *Pharmaceuticals*, vol. 11, no. 1, p. 17, 2018.
- [57] T. P. Sutula and F. E. Dudek, “Unmasking recurrent excitation generated by mossy fiber sprouting in the epileptic dentate gyrus: an emergent property of a complex system,” *Progress In Brain Research*, vol. 163, pp. 541–563, 2007.

- [58] O. Hadass, B. N. Tomlinson, M. Gooyit et al., “Selective inhibition of matrix metalloproteinase-9 attenuates secondary damage resulting from severe traumatic brain injury,” *PLoS One*, vol. 8, no. 10, article e76904, 2013.
- [59] M. Grossetete, J. Phelps, L. Arko, H. Yonas, and G. A. Rosenberg, “Elevation of matrix metalloproteinases 3 and 9 in cerebrospinal fluid and blood in patients with severe traumatic brain injury,” *Neurosurgery*, vol. 65, no. 4, pp. 702–708, 2009.
- [60] A. Szklarczyk, J. Lapinska, M. Rylski, R. D. G. McKay, and L. Kaczmarek, “Matrix metalloproteinase-9 undergoes expression and activation during dendritic remodeling in adult hippocampus,” *The Journal of Neuroscience*, vol. 22, no. 3, pp. 920–930, 2002.
- [61] G. M. Wilczynski, F. A. Konopacki, E. Wilczek et al., “Important role of matrix metalloproteinase 9 in epileptogenesis,” *Journal of Cell Biology*, vol. 180, no. 5, pp. 1021–1035, 2008.
- [62] A. Nagaoka, H. Takehara, A. Hayashi-Takagi et al., “Abnormal intrinsic dynamics of dendritic spines in a fragile X syndrome mouse model in vivo,” *Scientific Reports*, vol. 6, no. 1, article 26651, 2016.
- [63] A. Dityatev, M. Schachner, and P. Sonderegger, “The dual role of the extracellular matrix in synaptic plasticity and homeostasis,” *Nature Reviews Neuroscience*, vol. 11, no. 11, pp. 735–746, 2010.
- [64] G. W. Huntley, “Synaptic circuit remodelling by matrix metalloproteinases in health and disease,” *Nature Reviews Neuroscience*, vol. 13, no. 11, pp. 743–757, 2012.

Research Article

Stroke Induces a BDNF-Dependent Improvement in Cognitive Flexibility in Aged Mice

Josh Houlton, Lisa Y. Y. Zhou, Deanna Barwick, Emma K. Gowing,
and Andrew N. Clarkson 

Department of Anatomy, Brain Health Research Centre and Brain Research New Zealand, University of Otago, Dunedin 9054, New Zealand

Correspondence should be addressed to Andrew N. Clarkson; andrew.clarkson@otago.ac.nz

Received 23 November 2018; Revised 10 March 2019; Accepted 4 April 2019; Published 5 May 2019

Guest Editor: Lara Boyd

Copyright © 2019 Josh Houlton et al. This is an open access article distributed under the Creative Commons Attribution License, which permits unrestricted use, distribution, and reproduction in any medium, provided the original work is properly cited.

Stroke remains a leading cause of disability worldwide. Recently, we have established an animal model of stroke that results in delayed impairment in spatial memory, allowing us to better investigate cognitive deficits. Young and aged brains show different recovery profiles after stroke; therefore, we assessed aged-related differences in poststroke cognition. As neurotrophic support diminishes with age, we also investigated the involvement of brain-derived neurotrophic factor (BDNF) in these differences. Young (3–6 months old) and aged (16–21 months old) mice were trained in operant touchscreen chambers to complete a visual pairwise discrimination (VD) task. Stroke or sham surgery was induced using the photothrombotic model to induce a bilateral prefrontal cortex stroke. Five days poststroke, an additional cohort of aged stroke animals were treated with intracerebral hydrogels loaded with the BDNF decoy, TrkB-Fc. Following treatment, animals underwent the reversal and rereversal task to identify stroke-induced cognitive deficits at days 17 and 37 poststroke, respectively. Assessment of sham animals using Cox regression and log-rank analyses showed aged mice exhibit an increased impairment on VD reversal and rereversal learning compared to young controls. Stroke to young mice revealed no impairment on either task. In contrast, stroke to aged mice facilitated a significant improvement in reversal learning, which was dampened in the presence of the BDNF decoy, TrkB-Fc. In addition, aged stroke control animals required significantly less consecutive days and correction trials to master the reversal task, relative to aged shams, an effect dampened by TrkB-Fc. Our findings support age-related differences in recovery of cognitive function after stroke. Interestingly, aged stroke animals outperformed their sham counterparts, suggesting reopening of a critical window for recovery that is being mediated by BDNF.

1. Introduction

Poststroke disability can include impairments in motor, sensory, visual, and cognitive functions [1]. Cognitive impairments, like motor impairments, can persist for years, leading to increased burden on caregivers and society [2, 3]. An added complication of cognitive impairments is that epidemiological evidence shows that impairments arising from strokes to the prefrontal cortex (PFC) or parietal cortex can take several months before becoming apparent [2, 4–6]. Whilst cognitive impairments are present in the traditional middle cerebral artery occlusion models of stroke, cognitive assessment in these models are often confounded by the presence of gross

motor impairments that are required to be intact in order to complete the cognitive tasks themselves [7]. Furthermore, our knowledge of the mechanisms that underlie cognitive impairments following stroke remains inadequate and additional research is still required to determine which intervention to use and at what time point should treatment begin.

In an effort to assess changes in cognition following stroke, several groups have established stroke models targeting the PFC, reporting deficits in spatial memory and executive function in the absence of motor impairment [8–10]. The rationale for targeting the PFC is that it is one of several key areas involved in higher order cognitive processing, such as executive function, attention, behavioural inhibition, and

goal-directed learning [11, 12]. In addition, the PFC region is linked with normal age-related cognitive decline, as well as behavioural impairments in neurodegenerative disorders in both rodents and humans [13–15]. As many as 92% of stroke survivors report some form of cognitive decline, including impairments in attention, working memory, and executive function, which includes cognitive flexibility [16, 17]. Cognitive flexibility is what allows one to adapt to new and unexpected conditions in our day-to-day lives; without it, even the smallest of tasks would become a huge ordeal.

Preclinical assessment of cognitive impairments is limited by the absence of tests that are considered to be translational. This, however, has changed in recent years with the development of touchscreen-based cognitive testing for rodents that allow us to assess components of human-based cognition which are assessed using the Cambridge Neuropsychological Test Automated Battery (CANTAB) assessment tools [18–21]. Importantly, various behavioural tests have been developed to assess cognitive impairments linked to disease-based genetic mutations using identical paradigms in both humans and rodents [18, 19]. In addition, lesions to the medial PFC (mPFC) have been shown to play a role in impaired reversal learning, specifically when rodents are presented with complex images using touchscreens [22, 23].

Given the translatability of the touchscreen technology, we aimed to further characterise our PFC stroke model to see if this extends to impaired cognitive flexibility as assessed using the visual discrimination (VD), reversal, and rereversal tasks. As 75-89% of all strokes occur in people aged 65 and over [24], we also aimed to assess how aged mice would perform on this task. Moreover, neurotrophins such as brain-derived neurotrophic factor (BDNF), which play an important role in regulating plasticity, have been shown to diminish with age [25, 26]. Therefore, we also investigated the involvement of BDNF in the poststroke recovery of cognitive function as we and others have previously reported this neurotrophin to be critical for poststroke recovery of motor function [27–30].

2. Methods

2.1. Animals and Surgical Procedures. All procedures described in this study were carried out in accordance with the guidelines on the care and use of laboratory animals set out by the University of Otago, Animal Research Committee and the Guide for Care and Use of Laboratory Animals (NIH Publication No. 85-23, 1996). Mice were housed under a 12-hour light/dark cycle with ad libitum access to food and water. All young animals were paired based on initial learning rates on the VD task and then randomly assigned to either sham or stroke surgery. Aged animals were also grouped based on their initial learning rate and randomly assigned to either sham, stroke, or stroke+TrkB-Fc treatments. All assessments were carried-out by observers blind as to the treatment group. For the initial experiment comparing the effect of age and stroke, focal stroke to the PFC of young (3-6 months old, $n=13$) and aged (16-21 months old, $n=10$) male C57BL/6J mice was induced by photothrombosis as previously described [10]. Under isoflurane anaesthesia (2-2.5% in O_2), mice were placed in a

TABLE 1: Summary showing treatment group sizes included for analysis at the start of the experiment and for both the reversal and rereversal tasks. Animal numbers that were excluded for both the reversal and rereversal tasks are shown in brackets.

Treatment group	Starting n	Final n for reversal	Final n for rereversal
Young sham	13	12 (1)	12 (1)
Young stroke	13	11 (2)	11 (2)
Aged sham	9	7 (2)	7 (2)
Aged stroke	10	8 (2)	7 (3)
Aged stroke+IgG-Fc	10	8 (2)	7 (3)
Aged stroke+TrkB-Fc	16	11 (5)	10 (6)

stereotactic apparatus and the skull was exposed through a midline incision, cleared of connective tissue, and dried. A cold light source (KL1500 LCD, Zeiss) attached to a 40x objective giving a 2 mm diameter illumination was positioned 1.2 mm anterior to Bregma, and 0.2 mL of Rose Bengal solution (Sigma-Aldrich; 10 g/L in normal saline) was administered through intraperitoneal (i.p.) injection. After five minutes, the brain was illuminated through the intact skull for 22 minutes, creating bilateral lesions to the PFC [10]. Young ($n=13$) and aged ($n=9$) sham animals received the same surgery as above, with a 0.2 mL injection of saline (i.p.) instead of Rose Bengal. Another cohort of aged mice (16-21 months old) also received the above stroke surgery prior to TrkB-Fc ($n=16$) or IgG-Fc ($n=10$) hydrogel administration, as described in Section 2.2.

Data obtained from animals in the study were collected across three cohorts due to the limited availability of the aged animals. We tried to keep treatment group size consistent across these cohorts; however, we noted the high attrition and mortality rates of our aged animals in some groupings, in particular the TrkB-Fc cohort. Therefore, some of the sham animals were reallocated and used in the stroke cohorts. A summary of the initial group sizes and number of mortalities between treatment groups can be seen in Table 1.

2.2. In Vivo Drug Dosing. A hyaluronan/heparan sulfate proteoglycan biopolymer hydrogel (HyStem-C, BioTime Inc., Alameda, CA) was employed to locally deliver TrkB-Fc or human IgG-Fc (antibody and vehicle control) five days poststroke to the peri-infarct cortex as described previously [27, 31]. The timing of treatment fits with the critical period when we know plasticity exists, that is, 3-14-days poststroke onset [32]. The stroke core is fully formed by 3 days, and we and others have shown that starting treatments 3-5 days poststroke does not interfere with the stroke itself but changes the state of plasticity and improves functional recovery, including treatments that alter BDNF and TrkB signalling [27, 28, 33]. Therefore, consistent with previous studies we administered TrkB-Fc or IgG-Fc five days poststroke. Following stroke, BDNF expression remains elevated for at least 3 weeks [27, 33, 34]. Similar profiles have been detected when using hydrogel delivery systems, with reports of small peptides (including TrkB-Fc) still being released 4 weeks after administration [25, 29, 30]. Therefore,

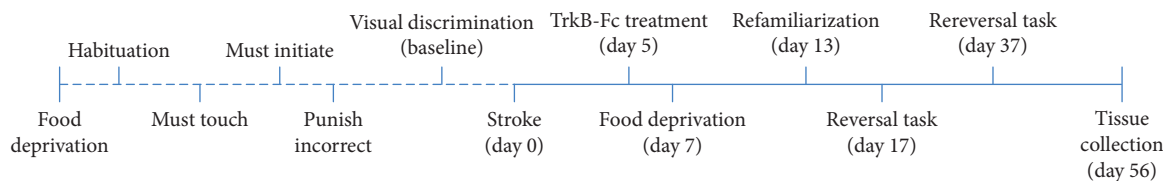


FIGURE 1: Experimental timeline illustrating the sequence of events in the current experiment. The dotted line represents pretraining prior to stroke surgery. The solid line refers to postsurgery events, with reference to the number of days after stroke.

hydrogel administration from 5 days poststroke would still be releasing TrkB-Fc or IgG-Fc at the start of the rereversal period, thereby inhibiting the later stroke-induced BDNF response and later BDNF-mediated learning.

A total of $7.5 \mu\text{L}$ of HyStem-C was impregnated with either TrkB-Fc ($5 \mu\text{g}/\text{mL}$) or human IgG-Fc ($5 \mu\text{g}/\text{mL}$). HyStem-C was prepared according to the manufacturer's instructions. In brief, TrkB-Fc or human IgG-Fc was added to the HyStem/-Gelin-S mix (component 1 of hydrogel), followed by the addition of Extralink (component 2 of the hydrogel) in a 4 : 1 ratio. The impregnated HyStem-C mix was injected immediately after preparation into the stroke cavity using a 30-gauge needle attached to a Hamilton syringe at stereotaxic coordinates 1.2 mm AP, 0 mm ML, and 0.75 mm DV.

2.3. Behavioural Assessment. The VD task has previously been used to identify an animal's perceptual ability, as well as testing their performance on an associative learning task [20]. Often, VD is paired with the reversal learning task in order to test behavioural flexibility, which can be disrupted as a consequence of have a neurological condition [20, 22].

Initial protocols for VD and reversal learning were adapted from those first described by Mar et al. and Brigman and Rothblat [21, 22]. Mice were trained to discriminate between two images, a solid white flash or wheel, presented in a spatially pseudorandomised manner, across a maximum of 30 trials per session. The two images were chosen following personal communication with a representative from Campden Instruments Ltd. (Julie Gill, personal communication, 2014), who observed equal salience following the presentation of both stimuli, which has been recently validated in environmentally enriched animals [35]. Animals were randomly allocated to learn either the flash or wheel stimuli during the initial VD learning task. When we established the randomisation, we also ensured that stimuli allocation was balanced between testing chambers and sequential runs. Correct responses for one stimulus resulted in an audio tone and reward ($S+$, correct), whilst responses for the other stimulus resulted in no reward ($S-$, incorrect) and a five second "time-out" period, during which time the house light was turned on. Incorrect responses were followed by a correction trial, where the same image was repeatedly presented in the same position, until a correct response was made.

Acquisition criterion for the VD task was $\geq 80\%$ correct responses across 30 trials within 60 minutes, with the criterion needing to be achieved over two consecutive days. Once the criterion was reached, animals were matched into groups based on initial learning rates (days to acquisition) before

being randomly allocated to one of the treatment groups. Following surgery, animals were allowed up to a week to recover before undergoing food deprivation, familiarization on the original VD stimuli for four sessions, and then beginning the reversal task at 17 days poststroke. In this task, the stimulus that previously elicited a reward becomes nonrewarded, and vice versa ($S+ \rightarrow S-$). Lastly, all animals then underwent the rereversal task at 3 days poststroke, where the correct and incorrect stimuli were switched back to their original responses. The criterion for the reversal and rereversal task was the same as the VD criterion. Animals were tested daily until criterion was met for all tasks. This experimental timeline is shown diagrammatically in Figure 1.

The data obtained for the VD and both the reversal and rereversal tasks include the number of consecutive days required to reach criteria, total number of trials to reach criteria, total number of correction trials made to reach criteria, and total intertrial interval (ITI) touches to make criteria.

2.4. Infarct Volume. At the completion of the VD task, animals were anaesthetised and transcardially perfused with 4% paraformaldehyde (PFA). The brains were removed and postfixed for 1 hour in 4% PFA before being transferred to 30% sucrose. The brains were cut coronally with a section thickness of $40 \mu\text{m}$ on a sliding microtome with a freezing stage, with all sections stored in cryoprotectant at -20°C . Infarct volume was determined by histological assessment using a previously published cresyl violet staining protocol [36]. Infarct volume was quantified using ImageJ (National Institutes of Health, USA) by an observer blind as to the treatment groups and was based on obtaining measurements from every 6th section through the entire infarct (area in mm^2), with infarct volume being quantified as follows:

$$\text{infarct volume (mm}^3\text{)} = (\text{area (mm}^2\text{)} \times \text{section thickness} \times \text{section interval}). \quad (1)$$

2.5. Statistical Analysis. The number of sessions required to complete the reversal task was plotted on a Kaplan-Meier curve, and group performance was compared using the Cox proportional-hazard regression model. Due to the effects of heteroscedasticity (collection of random variables) and positive skewing effects, all reversal and rereversal task variable data were log transformed prior to being analysed. Data from the other variables collected for both young and aged and stroke and sham animals were analysed using a two-way analysis of variance (ANOVA), followed by Sidak's multiple

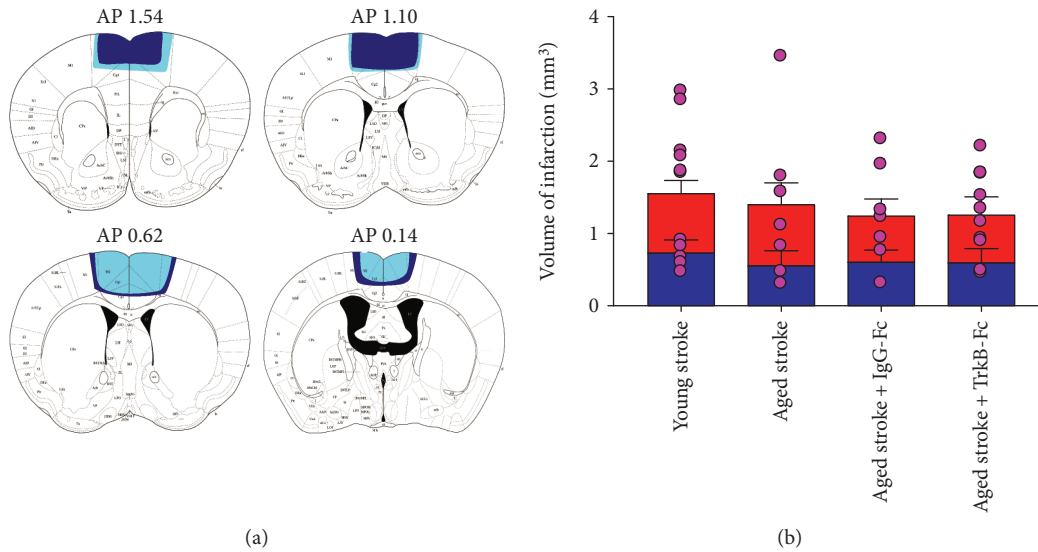


FIGURE 2: Schematic representation of the mean infarct area in aged (dark blue) and young (light blue) mice following a 22-minute bilateral PFC stroke. Stroke damage extends from 1.54 to 0.14 AP (a). Infarct volume was measured for both the left (blue bar) and right (red bar) hemispheres and for the whole brain (pink dots; b) in young stroke, aged stroke, and aged+TrkB-Fc stroke animals. Data are expressed as mean \pm S.E.M. for $n = 10-14$ per group.

comparisons post hoc test. Data from aged sham, aged stroke, and aged stroke+TrkB-Fc animals were analysed with a one-way ANOVA, followed by Sidak's multiple comparisons post hoc test. The Cox proportional hazard regression model was performed using STATA 13.0, with all remaining analyses being performed using Prism 6.0.

2.6. Exclusion Criteria. Conducting studies in aged rodents is notoriously difficult, with higher levels of attrition reported poststroke [37]. In the present study, one aged sham animal, one aged stroke+saline animal, one aged stroke+IgG-Fc animal, and three aged stroke+TrkB-Fc animals were sacrificed and excluded from reversal analysis due to attrition/mortality. Two young stroke animals, one aged stroke+saline animal, and one aged stroke+IgG-Fc animal were excluded because they showed no visible infarcts following cresyl violet staining. Furthermore, one aged sham animal, one young sham animal, and one aged stroke+TrkB-Fc animal were excluded from all analysis as they failed to meet the reversal criterion. Another aged stroke+TrkB-Fc animal was excluded due to an unsuccessful hydrogel injection. Furthermore, one aged stroke+saline animal, one aged stroke+IgG-Fc animal, and one aged stroke+TrkB-Fc animal also died during rereversal testing and were excluded from rereversal analysis. The final number of animals per treatment group for the reversal and rereversal tasks are shown in Table 1.

3. Results

3.1. Infarction Volume Quantification. Histological assessment of infarct volume was assessed at day 56 post-stroke, using cresyl violet staining (Figure 2). Damage following a stroke to the PFC extended into the primary motor cortex (M1), anterior cingulate cortex (ACC), and the supplementary motor cortex (Figure 2(a)). No differences

were found in asymmetry between damage to the left and right hemispheres following a bilateral PFC stroke in both young and aged animals treated with saline (young—left: $0.759 \pm 0.151 \text{ mm}^3$, right: $0.822 \pm 0.172 \text{ mm}^3$; aged—left: $0.581 \pm 0.172 \text{ mm}^3$, right: $0.845 \pm 0.276 \text{ mm}^3$; $p = 0.6816$, $F(1, 32) = 0.1714$; Figure 2(b)). Furthermore, no differences were found between the average total stroke volume between these groups (young: $1.58 \pm 0.274 \text{ mm}^3$; aged: $1.38 \pm 0.404 \text{ mm}^3$; $p = 0.5950$, $F(1, 32) = 0.2883$).

Aged stroke animals treated with IgG-Fc or TrkB-Fc showed no asymmetry between left and right hemispheres following a PFC stroke (IgG-Fc—left: $0.632 \pm 0.139 \text{ mm}^3$, right: $0.640 \pm 0.205 \text{ mm}^3$; TrkB-Fc—left: $0.621 \pm 0.170 \text{ mm}^3$, right: $0.665 \pm 0.221 \text{ mm}^3$; $p = 0.9247$, $F(1, 30) = 0.0090$; Figure 2(b)) and presented with average stroke volumes similar to aged and young stroke animals (IgG-Fc— $1.28 \pm 0.259 \text{ mm}^3$; TrkB-Fc, $1.29 \pm 0.186 \text{ mm}^3$; $p = 0.9739$, $F(1, 30) = 0.0011$). These data suggest that any behavioural differences seen *in vivo* between young and aged animals and also between aged animals treated with IgG-Fc and TrkB-Fc is unlikely to be due to differences in stroke volume.

3.2. Survival Curve of Reversal and Rereversal Tasks. Lesion studies have previously illustrated the involvement of the PFC in behavioural flexibility on the reversal task [20, 22]. Furthermore, the learning capacity of aged animals with stroke to the PFC during VD tasks in the operant touchscreen chambers has yet to be established. Therefore, the Kaplan-Meier survival curves and Cox regression analyses were used to look at the number of days each group needed in order to reach the criterion for the reversal task (assessed at poststroke day 17) and rereversal task (assessed at post-stroke day 37) (Figure 3). A test for proportional-hazard

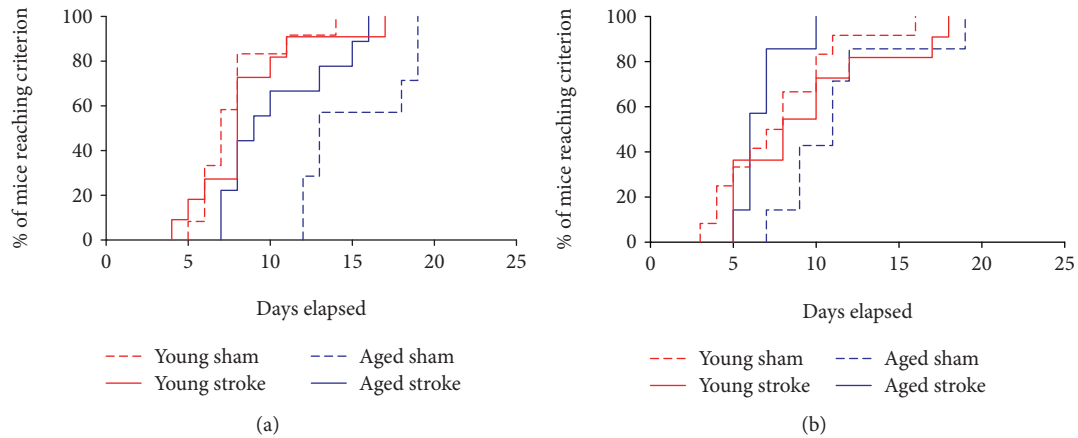


FIGURE 3: Survival curve of the number of sessions each animal is required to make to reach the criterion ($\geq 80\%$ accuracy across two consecutive days) in the reversal (a) or rereversal (b) tasks. Aged animals (sham—dotted blue line; stroke—solid blue line) take longer to learn both tasks compared to young animals (sham—dotted red line; stroke—solid red line). Aged stroke animals performed better than aged sham controls.

assumption showed that both the reversal and rereversal data sets showed no proportionality (data not shown).

A significant interaction effect of age and stroke was seen across the reversal task ($p < 0.0001$; $\chi^2 = 27.18$; $df = 4$; Figure 3(a)). Young sham animals completed the reversal task approximately 7.9 times faster than aged sham animals (hazard ratio (HR): 7.913, $p = 0.0004$, 95% confidence interval (CI): 2.498-25.07). Stroke to the PFC of young animals had no significant effect of learning in the reversal task (HR: 1.348, $p = 0.3814$, CI: 0.592-3.06). Interestingly, stroke to the PFC of aged animals facilitated improved learning in the reversal task, with aged stroke animals completing the task approximately 4.2 times faster than their aged-matched sham counterparts (HR: 4.283, $p = 0.0272$, CI: 2.460-11.221). No significant differences were seen between the performance of young animals and that of aged stroke animals in the reversal task (HR: 1.125, $p = 0.5936$, CI: 0.4662-2.715).

A significant interaction effect of age and stroke was also seen across all animals in the rereversal task ($p = 0.0007$; $\chi^2 = 15.02$; $df = 4$; Figure 3(b)). Young sham animals were found to master the rereversal task approximately 2.4 times faster than aged sham animals; however, this result only trended towards significance (HR: 2.447, $p = 0.0533$, CI: 0.829-5.136). Similar to the performance on the reversal task, there was no significant difference between young sham and young stroke animals on the rereversal task (HR: 1.848, $p = 0.2075$, CI: 0.7112-4.801). However, aged stroke animals were found to outperform their aged-matched sham counterparts, mastering the rereversal task 1.8 times faster (HR: 1.833, $p = 0.0473$, CI: 0.2166-4.006). No significant differences were seen between the performance of young and aged stroke animals in the rereversal task (HR: 1.333, $p = 0.1293$, CI: 0.5169-3.44).

These data indicate that there is an age-related decline in cognitive flexibility in mice. In addition, stroke to the PFC of aged mice appears to reopen a critical window for the improvement of recovery that results in the facilitation

of performance across both of these tasks, albeit, to different extents.

3.3. Performance in the Reversal Task after PFC Stroke. To investigate the performance of age-matched animals after PFC stroke in the reversal task, a two-way ANOVA was performed on log-transformed data (Figure 4). Throughout the reversal task, an overall effect of age and stroke surgery was seen in the number of consecutive days required to meet the criterion (stroke, $p = 0.0261$, $F(1, 35) = 5.394$; age, $p < 0.0001$, $F(1, 35) = 25.24$; Figure 4(a)), total number of correction trials (stroke, $p = 0.0054$, $F(1, 35) = 8.784$; age, $p < 0.0001$, $F(1, 35) = 20.49$; Figure 4(c)), and total number of ITI touches (stroke, $p = 0.0367$, $F(1, 35) = 4.71$; age, $p = 0.0015$, $F(1, 35) = 11.82$; Figure 4(d)). An age effect but not stroke effect was also observed in the total number of trials required to meet the reversal criterion (stroke, $p = 0.1546$, $F(1, 35) = 2012$; age, $p < 0.0001$, $F(1, 35) = 36.29$; Figure 4(b)). However, no significant interactions were observed between age and stroke effects across all of these measures (consecutive days, $p = 0.1509$, $F(1, 35) = 2.156$; total trials, $p = 0.0926$, $F(1, 35) = 2.994$; total correction trials, $p = 0.1460$, $F(1, 35) = 2.211$; and total ITI touches, $p = 0.1709$, $F(1, 35) = 1.9151$).

Sidak's multiple comparison test confirmed that aged sham animals require significantly more consecutive days ($p = 0.0003$), total trials ($p < 0.0001$), total correction trials ($p = 0.0008$), and total ITI touches ($p = 0.0090$) to make the criterion in the reversal task, relative to young sham animals. Furthermore, no significant differences were seen between young sham and young stroke animals across any of these variables (consecutive days, $p = 0.9163$; total trials, $p = 0.9969$; total correction trials, $p = 0.6816$; and total ITI touches, $p = 0.9384$). However, aged stroke animals were found to require significantly less consecutive days ($p = 0.0463$), total correction trials ($p = 0.0265$), and total ITI touches ($p = 0.0316$) to reach the criterion in the reversal task, relative to aged sham control animals. In contrast, there was

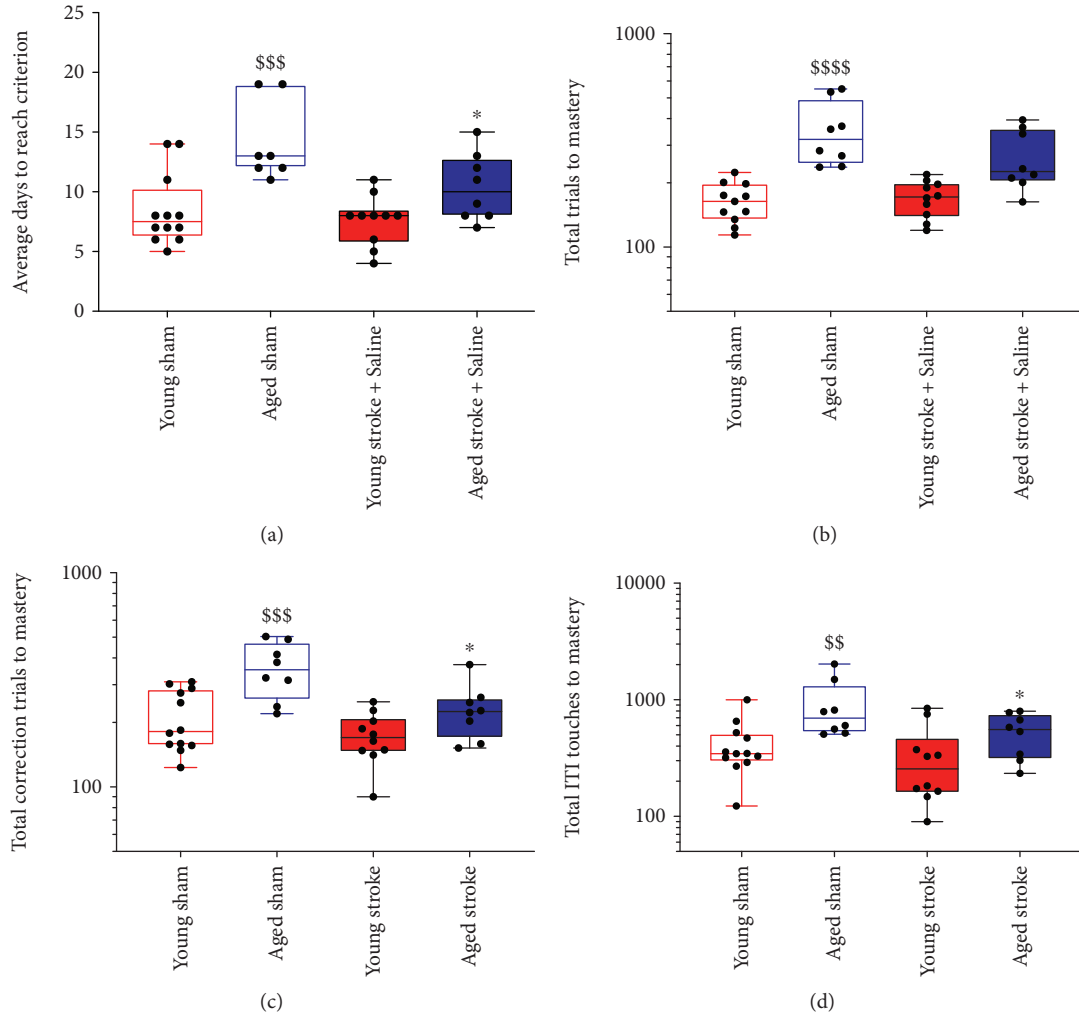


FIGURE 4: The effect of age (young (red) versus aged (blue)) and PFC stroke (filled boxes) on the number of consecutive days (a), total trials (b), total correction trials (c), and total ITI touches (d) required to master the reversal task compared to sham (open boxes) controls. \$\$ = $p < 0.01$, \$\$\$ = $p < 0.001$, and \$\$\$\$ = $p < 0.0001$ compared to young sham. * = $p < 0.05$ compared to aged-matched sham controls.

no significant difference seen in the number of total trials ($p = 0.1604$) that were required from aged stroke animals to make the reversal criteria relative to aged sham animals. Relative to young stroke animals, aged stroke animals were found to require significantly more total trials to master the reversal task ($p = 0.0217$); however, no other differences were observed between these two groups across the other variables (consecutive days, $p = 0.764$; total correction trials, $p = 0.1597$; and total ITI touches, $p = 0.4730$). Moreover, aged stroke animals required significantly more consecutive days to master the reversal task compared to young sham animals ($p = 0.0403$), but no differences were seen in the number of total trials ($p = 0.1136$), total correction trials ($p = 0.4319$), or total ITI touches ($p = 0.2664$).

Together these data support an age-related reduction of performance across the reversal task in aged sham mice. Moreover, stroke to aged mice appears to enhance reversal learning, an effect not observed in young mice.

3.4. Performance in the Rereversal Task after PFC Stroke.

To investigate the performance of age-matched animals after stroke to the PFC in the rereversal task, a two-way ANOVA was conducted on log-transformed data collected from day 37 poststroke (Figure 5). Assessment of the rereversal task revealed a greater variability in the data compared to the reversal task data. No effect of either age or stroke surgery was observed in the number of consecutive days (stroke, $p = 0.4563$, $F(1, 33) = 0.5853$; age, $p = 0.5686$, $F(1, 33) = 0.3317$; Figure 5(a)), total trials (stroke, $p = 0.3358$, $F(1, 33) = 0.953$; age, $p = 0.9121$, $F(1, 33) = 0.0123$; Figure 5(b)), and total ITI touches (stroke, $p = 0.1694$, $F(1, 33) = 1.976$; age, $p = 0.3378$, $F(1, 33) = 0.800$; Figure 5(d)). However, a significant effect of age but not stroke was seen in the total number of correction trials required to make the reversal criterion (stroke, $p = 0.4252$, $F(1, 33) = 0.652$; age, $p < 0.0140$, $F(1, 33) = 7.734$; Figure 5(c)). In addition, a significant interaction between age and stroke surgery was only seen in the

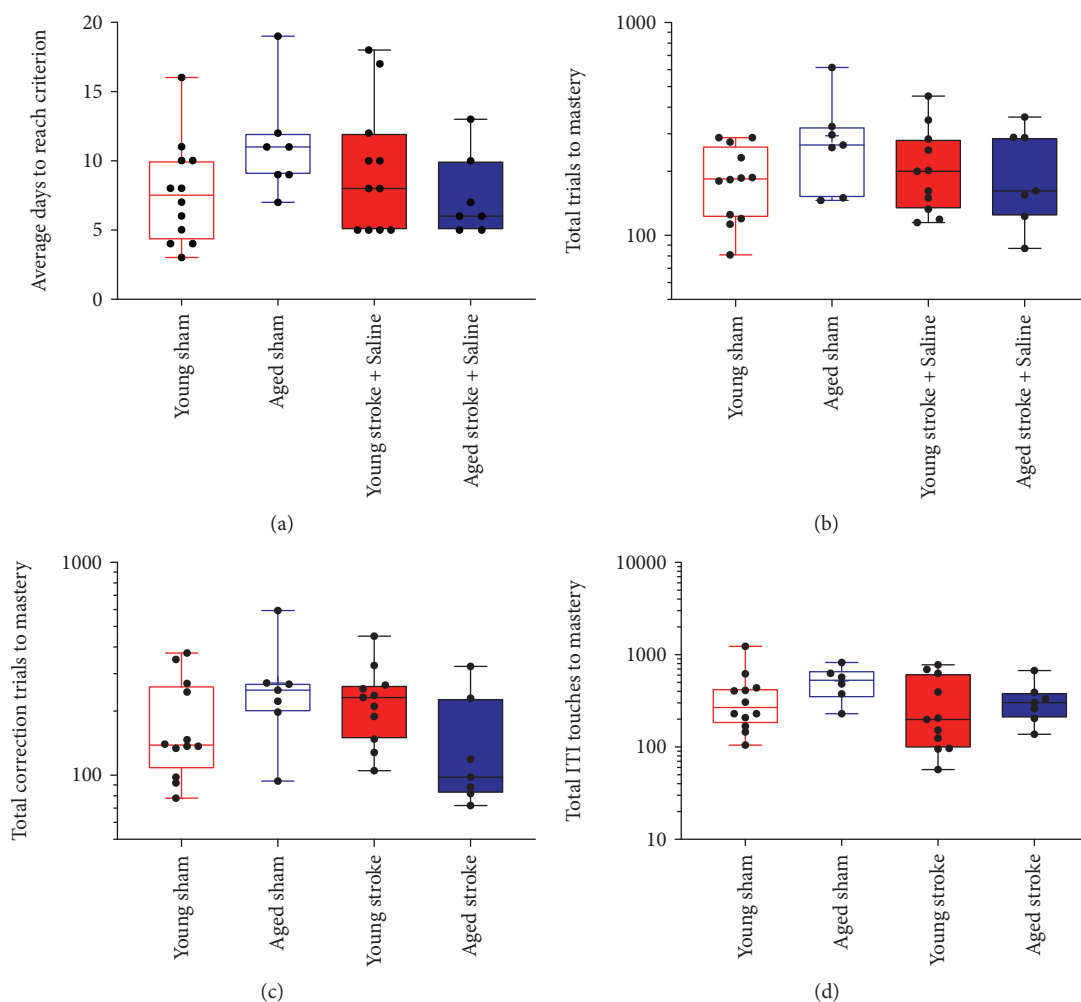


FIGURE 5: The effect of age (young (red) versus aged (blue)) and PFC stroke (filled boxes) on the number of consecutive days (a), total trials (b), total correction trials (c), and total ITI touches (D) required to master the rereversal task compared to sham (open boxes) controls.

total number of trials required to make the criterion (total trials, $p = 0.0288$, $F(1, 33) = 5.253$; consecutive days, $p = 0.0513$, $F(1, 33) = 4.089$; total correction trials, $p = 0.9596$, $F(1, 33) = 0.0263$; total ITIs, $p = 0.4912$, $F(1, 33) = 0.4849$).

Sidak's multiple comparison test failed to find a significant difference between the performance of young and aged sham animals in the rereversal task (consecutive days, $p = 0.2679$; total trials, $p = 0.3497$; total correction trials, $p = 0.2851$; and total ITI touches, $p = 0.6882$). Furthermore, no significant differences were found between young sham and young stroke animals (consecutive days, $p = 0.7331$; total trials, $p = 0.7229$; total correction trials, $p = 0.9267$; and total ITI touches, $p = 0.9341$) or between aged sham and stroke animals (consecutive days, $p = 0.3097$; total trials, $p = 0.1738$; total correction trials, $p = 0.9473$; and total ITI touches, $p = 5610$). Lastly, aged stroke animals performed similarly to both young sham (consecutive days, $p = 0$ to >0.9999 ; total trials, $p > 0.9999$; total correction trials, $p = 0.8266$; and total ITI touches, $p = 0.5451$) and young stroke animals (consecutive days, $p = 0.7297$;

total trials, $p = 0.1738$; total correction trials, $p = 0.2664$; and total ITI touches, $p = 0.9889$) in the rereversal task.

3.5. TrkB-Fc Blocks the Stroke-Induced Improvement in Performance. To investigate the involvement of BDNF signalling in reversal and rereversal learning after PFC stroke, performance was compared between aged sham animals and aged stroke animals treated with either IgG-Fc or the BDNF scavenger, TrkB-Fc (Figure 6). A Cox regression analysis of the Kaplan-Meier curves revealed a significant treatment effect ($p = 0.0124$, $\chi^2 = 9.16$, $df = 3$; Figure 6(a)). Specifically, aged stroke animals treated with IgG-Fc completed the reversal task approximately 1.3 times faster than aged sham animals (HR: 1.310, $p = 0.0272$, CI: 0.4369-3.684). Moreover, aged stroke animals treated with TrkB-Fc completed the reversal task approximately 3.1 times slower than aged stroke control animals (HR: 3.136, $p = 0.0073$, CI: 0.8256-11.91), performing similarly to aged sham animals (HR: 0.9144, $p = 0.8758$, CI: 0.297-2.811).

A one-way ANOVA was performed on log-transformed data from all animals, and it confirmed a significant

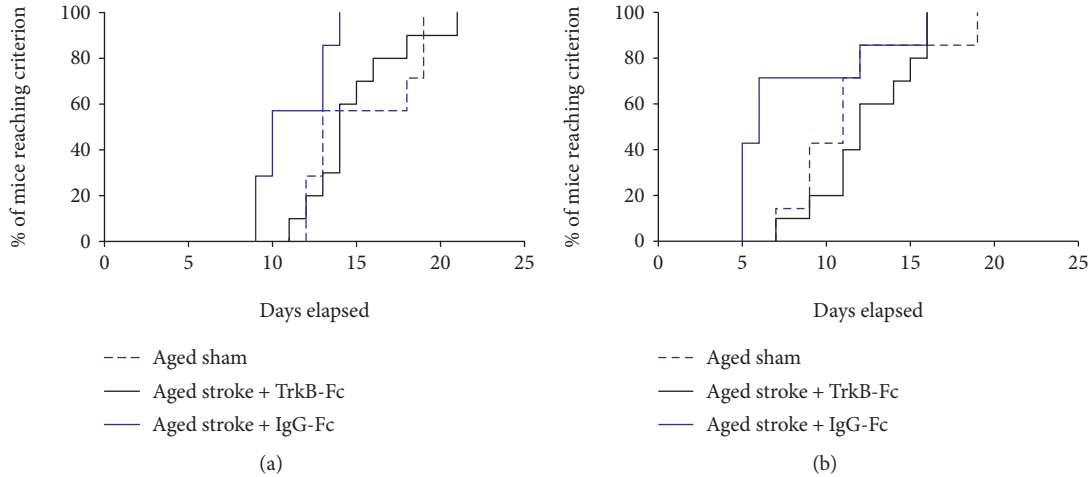


FIGURE 6: Survival curve of the number of sessions each animal is required to make to reach the criterion ($\geq 80\%$ accuracy across two consecutive days) in the reversal (a) or rereversal (b) tasks. Aged stroke animals (solid blue line) take longer to learn both tasks compared to aged sham controls (dotted blue line). Aged stroke animals performed better than aged sham controls. This effect was blocked following the administration of the BDNF decoy, TrkB-Fc (solid black line).

treatment effect for the number of consecutive days ($p = 0.0144$, $F(2, 23) = 5.174$; Figure 7(a)), total number of trials ($p = 0.0019$, $F(2, 23) = 8.346$; Figure 7(b)), total number of correction trials ($p = 0.0015$, $F(2, 23) = 8.757$; Figure 7(c)), and total number of ITI touches ($p = 0.0201$, $F(2, 23) = 4.656$; Figure 7(d)) to reach the criterion on the reversal task. Sidak's multiple comparison test further revealed that aged stroke animals treated with IgG-Fc required significantly less consecutive days ($p = 0.0346$), total trials ($p = 0.0013$), total correction trials ($p = 0.0048$), and total ITI touches ($p = 0.0184$) compared to aged sham animals. TrkB-Fc treatment was found to block this stroke-induced effect, with TrkB-Fc-treated aged stroke animals requiring significantly more consecutive days ($p = 0.0222$) and correction trials ($p = 0.0029$) to reach the criterion relative to aged stroke control animals. No significant differences were observed in the number of total trials ($p = 0.0538$) or total ITIs ($p = 0.0987$) between stroke +TrkB-Fc-treated animals and aged stroke controls on the reversal criterion. Finally, TrkB-Fc-treated aged stroke animals performed the same as aged sham animals across all variables (consecutive days, $p = 0.9992$; total trials, $p = 0.1405$; total correction trials, $p = 0.9798$; and total ITI touches, $p = 0.5304$).

Analysis of the rereversal task revealed a significant effect of treatment across all animals as detected using a Cox regression analysis of the Kaplan-Meier survival curves ($p = 0.0473$, $\chi^2 = 7.67$, $df = 3$; Figure 6(b)). Aged stroke animals treated with IgG-Fc completed the rereversal task similarly to aged sham animals (HR: 1.212, $p = 0.0831$, CI: 0.316-3.225). However, aged stroke animals treated with TrkB-Fc completed the rereversal task approximately 3.9 times slower than aged stroke control animals (HR: 3.911, $p = 0.0012$, CI: 0.722-6.014), with the performance of the TrkB-Fc-treated animals being similar to aged sham controls (HR: 1.142, $p = 8208$, CI: 0.363-3.59).

A one-way ANOVA was performed on log-transformed rereversal data, which confirmed a significant treatment effect on the total number of correction trials ($p = 0.0117$, $F(2, 21) = 5.598$; Figure 8(c)) and ITI touches ($p = 0.0049$, $F(2, 21) = 7.008$; Figure 8(d)) but not on the number of consecutive days ($p = 0.3397$, $F(2, 21) = 0.3397$; Figure 8(a)) or the total number of trials ($p = 0.1154$, $F(2, 21) = 2.41$; Figure 8(b)). In addition, Sidak's multiple comparisons revealed that aged stroke mice treated with IgG-Fc required significantly more total correction trials ($p = 0.0465$) and ITI touches ($p = 0.0315$) to make a rereversal compared to aged sham animals. However, no significant difference was seen in the number of consecutive days ($p = 0.6556$) or total number of trials ($p = 0.0426$) between these animals. Treatment with TrkB-Fc was shown to dampen the stroke-induced effect, with TrkB-Fc-treated stroke animals performing similarly to aged sham animals across all variables (consecutive days, $p = 0.8495$; total trials, $p = 0.5158$; total correction trials, $p = 0.5119$; and total ITI touches, $p = 0.8860$). Conversely, TrkB-Fc-treated aged stroke animals required significantly more total correction trials ($p = 0.0091$) and total ITI touches ($p = 0.0049$) to complete the rereversal task compared to aged stroke animals. However, no difference was observed between these treatment groups in regard to the number of consecutive days ($p = 0.3085$) or total trials taken ($p = 0.4114$).

4. Discussion

In recent years, touchscreen-based cognitive testing has been designed to target components of human-based cognition in rodents, thereby maximising the translational potential of preclinical experiments [18, 19, 21]. In the present study, we used this technology to demonstrate an age-related decline in cognitive flexibility on the VD task in mice. In addition, we showed that stroke to the PFC had no effect

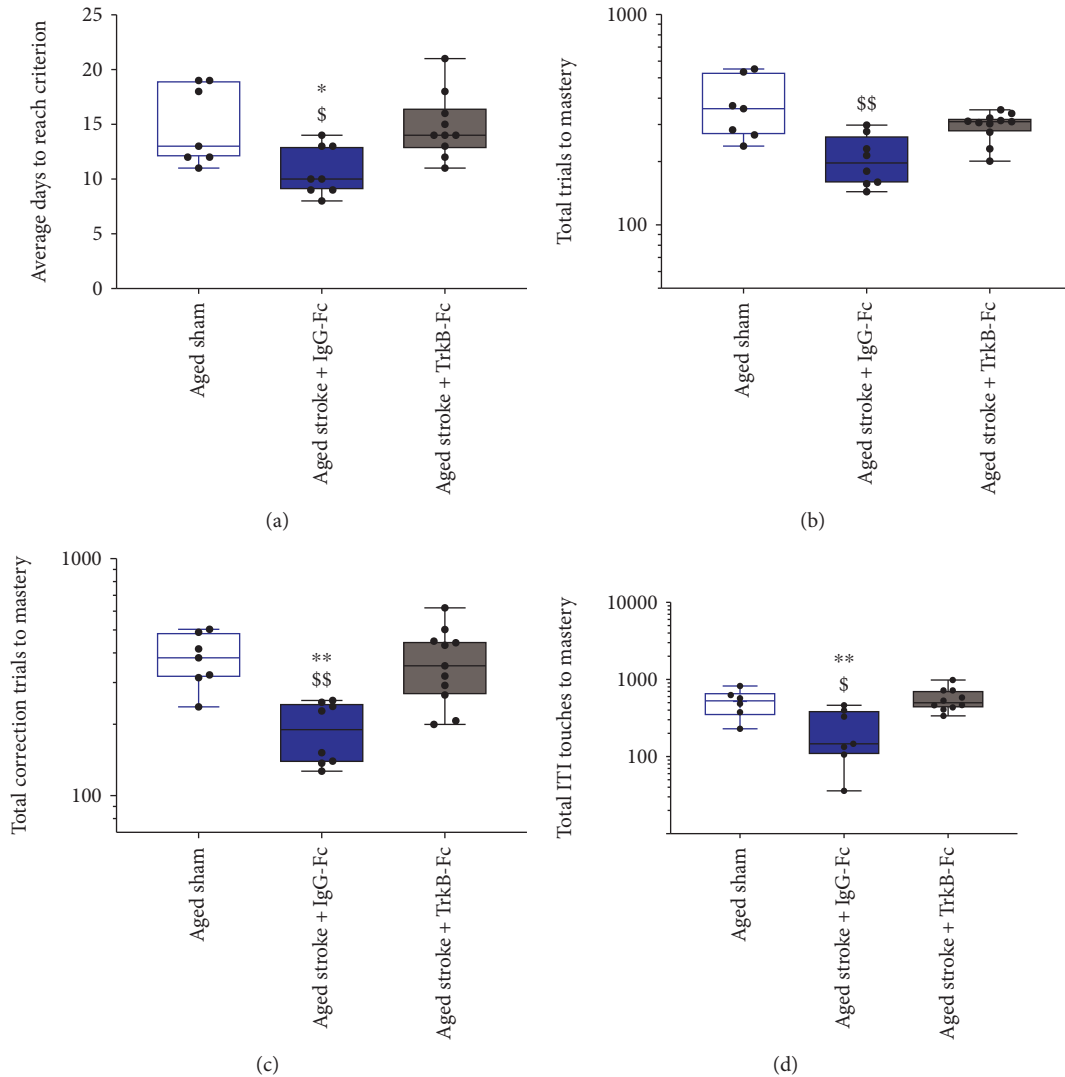


FIGURE 7: The effect of PFC stroke and TrkB-Fc treatment on the number of consecutive days (a), total trials (b), total correction trials (c), and total ITI touches (d) required to master the reversal task. Aged sham: nonfilled blue box; aged stroke+IgG-Fc (hydrogel control): filled blue box; aged stroke+TrkB-Fc: filled grey box. \$ = $p < 0.05$ and \$\$ = $p < 0.01$ compared to aged sham. * = $p < 0.05$ and ** = $p < 0.01$ compared to TrkB-Fc-treated aged stroke animals.

on reversal learning in young mice, but facilitated an improvement in learning in aged mice. Finally, we show that this stroke-induced improvement in learning observed in the aged mice was BDNF dependent, as the improvement in learning was blocked following administration of the BDNF decoy, TrkB-Fc.

The PFC is a region of the brain that is heavily involved with complex cognitive processes, such as behavioural flexibility [22]. Extensive evidence demonstrates that set-shifting performance is critically dependent on the dorsolateral prefrontal cortex (PFC) in primates or the medial prefrontal cortex (mPFC), which is the rodent homolog [38, 39]. Age-related alterations in both the architecture and molecular composition of the PFC are known to contribute to cognitive decline seen in healthy aged animals [40, 41]. Consistent with this, our study revealed an age-related decline in VD reversal learning, with aged sham animals requiring more consecutive days, trials, correction trials, and ITI

touches to reach the criterion compared to young sham animals. This finding is supported by human, primate, and rodent reversal studies that have reported cognitive slowing in aged cohorts using other cognitive assessments [40–43]. Moreover, this age-related cognitive slowing is not only applicable to behavioural flexibility but other cognitive domains such as spatial memory, attention, and working memory [43, 44]. Nonetheless, it is important to emphasise that these aged mice could still demonstrate the same degree of cognitive flexibility as young mice; however, they just required a longer period to reach this potential. It is also interesting to note that this age-related effect appears to be dampened in the rereversal task where the animals switch their learning back to the original stimuli pairing, indicating that the ability to adapt to previously learnt tasks remains intact in aged animals. The young versus age difference we report highlights the need to assess both young and aged cohorts as they respond differently to strokes, including eliciting a different

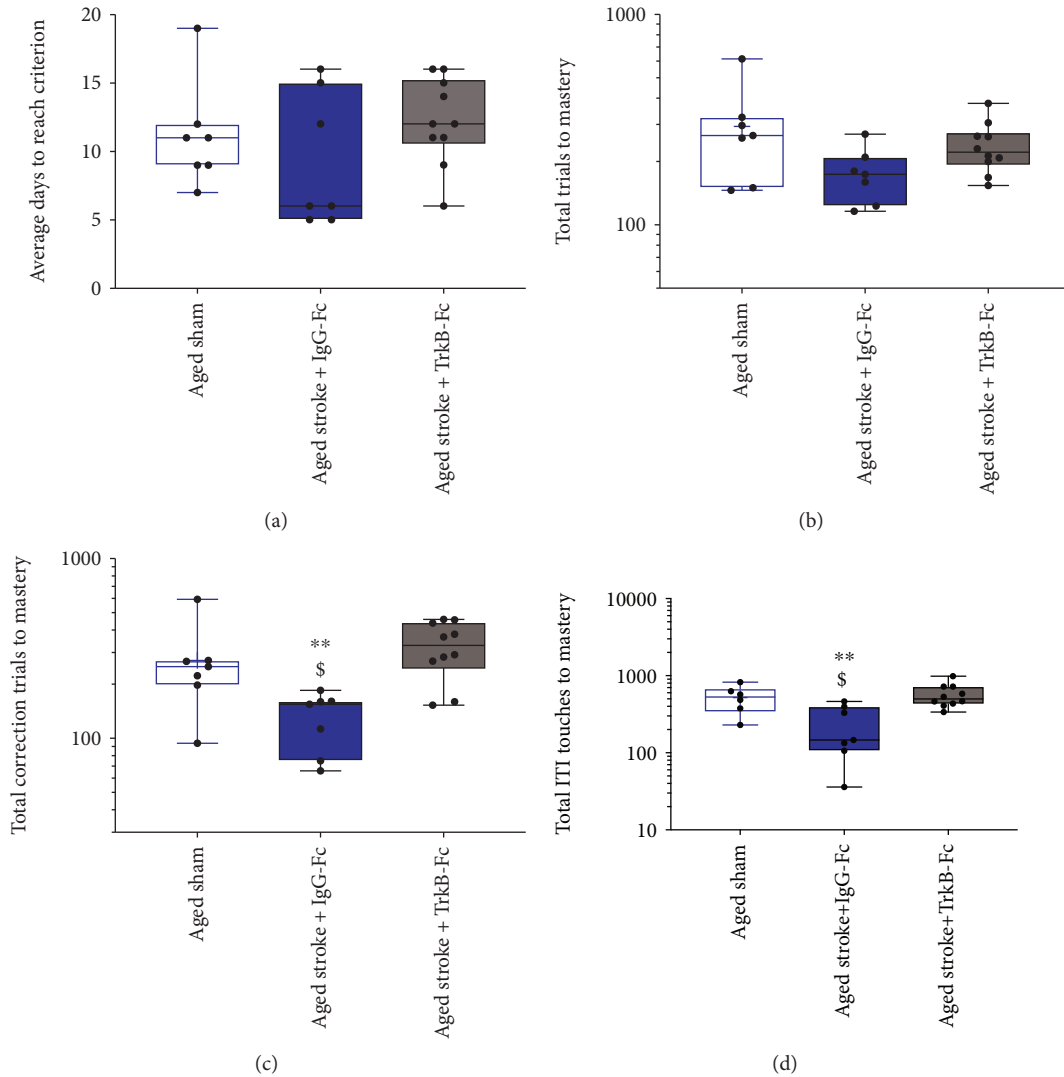


FIGURE 8: The effect of PFC stroke and TrkB-Fc treatment on the number of consecutive days (a), total trials (b), total correction trials (c), and total ITI touches (d) required to master the reversal task. Aged sham: nonfilled blue box; aged stroke: filled blue box; aged stroke+TrkB-Fc: filled grey box. \$ = $p < 0.05$, \$\$ = $p < 0.01$, and \$\$\$ = $p < 0.001$ compared to aged sham. * = $p < 0.05$ compared to TrkB-Fc-treated aged stroke animals.

molecular/transcriptional response [31, 45] and therefore potentially requiring different pharmacological and or physical therapies to enhance recovery.

In contrast to previous reports [22, 23], our findings showed that a stroke to the PFC had no effect on VD reversal and reversal learning in young mice, yet it improved performance in aged mice. There are a few possible explanations for these observations. Clinical studies have revealed that whilst unilateral lesions to the PFC fail to affect performance on a VD reversal task, bilateral lesions to the PFC cause severe impairments in this task [46]. This finding suggests that a larger lesion involving both cortices is required to create this deficit in cognitive flexibility in humans, which is also supported by reports of dementia in patients with global vascular impairment [47]. A second explanation for a lack of stroke-induced impairment seen in the present study may lie in the neural circuitry that has been proposed to control cognitive flexibility. Lesion and stroke

studies utilising touchscreen-based VD reversal tasks have highlighted the involvement of the mPFC, orbitofrontal cortex (OFC), and dorsolateral striatum in facilitating performance [8, 9, 48, 49], whereas the ventromedial PFC (vmPFC) and basolateral amygdala (BLA) play a role in restricting performance [48, 49]. It is possible then, that the site of the PFC strokes in the present experiment may have played an inhibitory role in reversal learning, similar to the BLA or vmPFC. In addition, we highlight that the age-associated improvement in cognitive flexibility is associated with an elevation in BDNF levels.

Human and rodent studies have both illustrated that younger brains recover more effectively than aged brains [50–52], possibly due to altered genetic and cellular responses observed in aged animals [53]. Whilst age-related differences in infarct volume have been investigated, these findings remain inconclusive [45, 54, 55], and age-related differences in infarct expansion and resolution and changes

in peri-infarct plasticity remain poorly understood. Furthermore, as the current study observed similar infarct volumes between young and aged animals, we propose that the remaining neurons in nuclei found in peri-infarct regions in young mice are likely to have a greater functional reserve, relative to old animals. The volume of the PFC has been reported to decrease with age, which could mean that the proportion of the PFC affected in the current stroke model may have been more detrimental to aged animals [56]. However, the exact function of this age-related loss of volume remains debated, with aged brains presenting with changes to dendritic arbour and sprouting profiles that have been proposed to help maintain the same number of synapses throughout the brain [57], thereby compensating for any cell death [58]. It is possible that the differences in functional reserve is solely plasticity mediated and dependent on changes in BDNF levels. However, much needed research is still needed to confirm these hypotheses.

The BDNF-mediated facilitation of reversal learning/cognitive flexibility that was observed in the current study may reflect a reopening of a critical window for functional recovery of cognition after stroke. Whilst the therapeutic potential of BDNF has been illustrated in preclinical stroke models [27–29], clinical success has been challenged by poor blood-brain barrier (BBB) permeability, short half-life, and off-target effects. However, with recent advances in technology, novel biomaterial drug-delivery systems offer the ability to circumvent these issues and provide regenerative agents directly to the injured brain. With this in mind, studies are underway assessing VD reversal task learning in aged stroke animals that receive recombinant human BDNF (rhBDNF) via a hydrogel implanted into the stroke cavity. We hope this may be able to “tap into” this BDNF-mediated mechanism to further promote recovery after stroke. It has also been postulated that a combinational treatment may be required to provide functional recovery in stroke patients especially in aged populations. Supporting this, Clarkson et al. have reported that aged mice receiving motor cortex strokes required treatment with BDNF and a BDNF-inducing AMPAkinase in order to gain the same level of functional recovery seen in young mice receiving BDNF treatment alone [28]. Future work in our lab hopes to investigate the therapeutic potential of this combinational approach, as this highlights the need to not only assess changes in BDNF but also the need to assess the role of AMPA receptor-mediated plasticity [28].

The lack of stroke-induced impairment seen in young mice is a limitation of the current study; however, this finding does match the clinical presentation of cognitive symptoms that are seen in humans following stroke. Cognitive impairments in elderly stroke patients are well documented; however, very few studies have reported these impairments in younger patients [55]. To improve our stroke model, future work could investigate the effect of focal lesions in Cerebral Autosomal Dominant Arteriopathy with Subcortical Infarcts and Leukoencephalopathy (CADASIL) mice. These genetically modified mice present with an abnormal regulation of blood flow and neurovascular dysfunction, which is known to be an underlying cause for vascular cognitive impairment

[59]. In light of this, we would expect our focal lesion models to have a more pronounced effect on cognitive flexibility in young mice, which may result in a detectable impairment in reversal learning.

The brain is known to undergo significant functional reorganisation in response to motor learning in the reaching task, and subsequent motor maps expand into neighbouring regions after stroke and brain injury, a process known as plasticity [60, 61]. Functional recovery resulting from this reorganisation has also been found to be dependent on BDNF signalling [27–30]. BDNF, like most neurotrophins, plays a critical role in neuronal development, differentiation, and survival. In addition, BDNF plays a central role in modulating components of synaptic plasticity both during development and throughout adulthood [62]. Such functions are mainly mediated via the release of BDNF that is regulated by neuronal activity [62, 63]. Collectively, these findings support the idea that BDNF is likely to play a role during the reparative phase after stroke, a period where the brain repairs itself to try compensate for the damaged tissue. Further support comes from clinical studies that have shown that aerobic exercise is sufficient to facilitate cognitive recovery (including cognitive flexibility) [64], an effect that is thought to be somewhat mediated by elevations in BDNF levels [65]. In conjunction with our study, these findings support the potential of BDNF to facilitate recovery of cognitive function in humans, not only after stroke but also with normal ageing.

BDNF is believed to have a beneficial effect on stroke recovery via several mechanisms: increased angiogenesis [66] and neurogenesis [67], increased brain repair [68], and enhanced synaptic plasticity [27, 69]. It is reasonable to predict that age-related changes in the BDNF-TrkB signalling pathway may have altered the responsiveness of the peri-infarct tissue to these mechanisms of plasticity in the aged mice of the current study. However, whether or not the expression of BDNF and its high-affinity receptor, TrkB, is reduced or increased in aged rodents remains a matter of debate [28, 70, 71]. We are currently investigating age-related changes in neurotrophin signalling pathways and treatments in the hope to better understand the functional role of BDNF throughout stroke-induced cognitive impairments. Because BDNF is associated with cognitive flexibility [48, 72], treatment with this trophic factor or other pharmacological agents that stimulate an increase in BDNF expression may be an effective therapy in alleviating slowing cognitive flexibility in other models of cognitive impairment.

The touchscreens require mice to be tested daily for an extended period of time in order to learn the task and then to perform both the reversal and rereversal tasks poststroke. Previous experiments have reported that PFC BDNF levels have been found to remain stable whilst rodents undergo classical learning, memory, and/or extinction tasks [73, 74]. These findings indicate that the learning experiences alone are not enough to significantly affect PFC BDNF expression. Therefore, the most parsimonious explanation for the stroke-induced improvement in cognitive flexibility observed in the current study in aged mice is that BDNF levels are elevated as a result of the stroke, which also fits with TrkB-Fc’s ability to dampen this response.

Overall, this study suggests that aged animals still have the capacity to learn and undertake complex cognitive tasks using an operant-based touchscreen, allowing the touchscreens to be used to investigate impairments and interventions in cognitive disorders. Furthermore, stroke to the PFC of young animals has no effect on cognitive flexibility, whereas stroke to the PFC of aged animals resulted in a significant improvement in performance in both the reversal and rereversal tasks. In addition, aged stroke mice treated with the BDNF decoy, TrkB-Fc, blocked the stroke-induced improvement in cognitive flexibility. Finally, we demonstrate that stroke to the PFC of aged mice reopens a critical window for functional recovery that is BDNF dependent.

Data Availability

All data used in the current manuscript have been placed in a repository at the University of Otago.

Disclosure

This work has been presented at two international conferences: (1) the 10th International Symposium on Neuroprotection and Neurorepair, October 9–11th, 2018, in Dresden, Germany, and (2) the 11th World Stroke Congress, October 17–20th, in Montreal, Canada.

Conflicts of Interest

The authors have nothing to declare.

Authors' Contributions

ANC, JH, and LYYZ designed the studies. JH, LYYZ, DB, and EKG collected the data. JH and LYYZ analysed the data and made the figures. JH, LYYZ, and ANC wrote the manuscript. All authors reviewed, edited, and approved the final version of this manuscript.

Acknowledgments

This work was supported by a Royal Society of New Zealand Project Grant and funding from the Ministry of Business, Innovation, and Employment, New Zealand (ANC). DB was supported by a University of Otago PhD Stipend. The authors would like to thank Mr. Andrew Gray for his statistical advice.

References

- [1] B. H. Dobkin, "Training and exercise to drive poststroke recovery," *Nature Clinical Practice Neurology*, vol. 4, no. 2, pp. 76–85, 2008.
- [2] A. Douiri, A. G. Rudd, and C. D. A. Wolfe, "Prevalence of poststroke cognitive impairment: South London Stroke Register 1995–2010," *Stroke*, vol. 44, no. 1, pp. 138–145, 2013.
- [3] H. Rigby, G. Gubitza, and S. Phillips, "A systematic review of caregiver burden following stroke," *International Journal of Stroke*, vol. 4, no. 4, pp. 285–292, 2009.
- [4] C. Loeb, C. Gandolfo, R. Croce, and M. Conti, "Dementia associated with lacunar infarction," *Stroke*, vol. 23, no. 9, pp. 1225–1229, 1992.
- [5] C. Ballard, E. Rowan, S. Stephens, R. Kalaria, and R. A. Kenny, "Prospective follow-up study between 3 and 15 months after stroke: improvements and decline in cognitive function among dementia-free stroke survivors >75 years of age," *Stroke*, vol. 34, no. 10, pp. 2440–2444, 2003.
- [6] D. Leys, H. Henon, M. A. Mackowiak-Cordoliani, and F. Pasquier, "Poststroke dementia," *The Lancet Neurology*, vol. 4, no. 11, pp. 752–759, 2005.
- [7] C. G. Markgraf, E. J. Green, B. E. Hurwitz et al., "Sensorimotor and cognitive consequences of middle cerebral artery occlusion in rats," *Brain Research*, vol. 575, no. 2, pp. 238–246, 1992.
- [8] C. A. Cordova, D. Jackson, K. D. Langdon, K. A. Hewlett, and D. Corbett, "Impaired executive function following ischemic stroke in the rat medial prefrontal cortex," *Behavioural Brain Research*, vol. 258, pp. 106–111, 2014.
- [9] R. A. Deziel, C. L. Ryan, and R. A. Tasker, "Ischemic lesions localized to the medial prefrontal cortex produce selective deficits in measures of executive function in rats," *Behavioural Brain Research*, vol. 293, pp. 54–61, 2015.
- [10] L. Y. Y. Zhou, T. E. Wright, and A. N. Clarkson, "Prefrontal cortex stroke induces delayed impairment in spatial memory," *Behavioural Brain Research*, vol. 296, pp. 373–378, 2016.
- [11] E. K. Miller and J. D. Cohen, "An integrative theory of prefrontal cortex function," *Annual Review of Neuroscience*, vol. 24, no. 1, pp. 167–202, 2001.
- [12] A. Miyake, N. P. Friedman, M. J. Emerson, A. H. Witzki, A. Howerter, and T. D. Wager, "The unity and diversity of executive functions and their contributions to complex 'Frontal Lobe' tasks: a latent variable analysis," *Cognitive Psychology*, vol. 41, no. 1, pp. 49–100, 2000.
- [13] L. Erraji-Benchekroun, M. D. Underwood, V. Arango et al., "Molecular aging in human prefrontal cortex is selective and continuous throughout adult life," *Biological Psychiatry*, vol. 57, no. 5, pp. 549–558, 2005.
- [14] A. Rozycka and M. Liguz-Leczna, "The space where aging acts: focus on the GABAergic synapse," *Aging Cell*, vol. 16, no. 4, pp. 634–643, 2017.
- [15] R. Schliebs and T. Arendt, "The cholinergic system in aging and neuronal degeneration," *Behavioural Brain Research*, vol. 221, no. 2, pp. 555–563, 2011.
- [16] S. Zinn, H. B. Bosworth, H. M. Hoenig, and H. S. Swartzwelder, "Executive function deficits in acute stroke," *Archives of Physical Medicine and Rehabilitation*, vol. 88, no. 2, pp. 173–180, 2007.
- [17] M. W. A. van Rijsbergen, R. E. Mark, P. L. M. de Kort, and M. M. Sitskoorn, "Prevalence and profile of poststroke subjective cognitive complaints," *Journal of Stroke and Cerebrovascular Diseases*, vol. 24, no. 8, pp. 1823–1831, 2015.
- [18] J. Nithianantharajah, N. H. Komiyama, A. McKechnie et al., "Synaptic scaffold evolution generated components of vertebrate cognitive complexity," *Nature Neuroscience*, vol. 16, no. 1, pp. 16–24, 2013.
- [19] J. Nithianantharajah, A. G. McKechnie, T. J. Stewart et al., "Bridging the translational divide: identical cognitive touchscreen testing in mice and humans carrying mutations in a disease-relevant homologous gene," *Scientific Reports*, vol. 5, article 14613, 2015.

- [20] A. E. Horner, C. J. Heath, M. Hvoslef-Eide et al., "The touchscreen operant platform for testing learning and memory in rats and mice," *Nature Protocols*, vol. 8, no. 10, pp. 1961–1984, 2013.
- [21] A. C. Mar, A. E. Horner, S. R. O. Nilsson et al., "The touchscreen operant platform for assessing executive function in rats and mice," *Nature Protocols*, vol. 8, no. 10, pp. 1985–2005, 2013.
- [22] J. Brigman and L. Rothblat, "Stimulus specific deficit on visual reversal learning after lesions of medial prefrontal cortex in the mouse," *Behavioural Brain Research*, vol. 187, no. 2, pp. 405–410, 2008.
- [23] T. J. Bussey, J. L. Muir, B. J. Everitt, and T. W. Robbins, "Triple dissociation of anterior cingulate, posterior cingulate, and medial frontal cortices on visual discrimination tasks using a touchscreen testing procedure for the rat," *Behavioral Neuroscience*, vol. 111, no. 5, pp. 920–936, 1997.
- [24] V. L. Feigin, M. H. Forouzanfar, R. Krishnamurthi et al., "Global and regional burden of stroke during 1990–2010: findings from the Global Burden of Disease Study 2010," *The Lancet*, vol. 383, no. 9913, pp. 245–255, 2014.
- [25] D. M. Yurek and A. Fletcher-Turner, "Lesion-induced increase of BDNF is greater in the striatum of young versus old rat brain," *Experimental Neurology*, vol. 161, no. 1, pp. 392–396, 2000.
- [26] M. J. Webster, C. S. Weickert, M. M. Herman, and J. E. Kleinman, "BDNF mRNA expression during postnatal development, maturation and aging of the human prefrontal cortex," *Developmental Brain Research*, vol. 139, no. 2, pp. 139–150, 2002.
- [27] A. N. Clarkson, J. J. Overman, S. Zhong, R. Mueller, G. Lynch, and S. T. Carmichael, "AMPA receptor-induced local brain-derived neurotrophic factor signaling mediates motor recovery after stroke," *Journal of Neuroscience*, vol. 31, no. 10, pp. 3766–3775, 2011.
- [28] A. N. Clarkson, K. Parker, M. Nilsson, F. R. Walker, and E. K. Gowing, "Combined ampakine and BDNF treatments enhance poststroke functional recovery in aged mice via AKT-CREB signaling," *Journal of Cerebral Blood Flow & Metabolism*, vol. 35, no. 8, pp. 1272–1279, 2015.
- [29] M. Ploughman, V. Windle, C. L. MacLellan, N. White, J. J. Doré, and D. Corbett, "Brain-derived neurotrophic factor contributes to recovery of skilled reaching after focal ischemia in rats," *Stroke*, vol. 40, no. 4, pp. 1490–1495, 2009.
- [30] C. L. Maclellan, M. B. Keough, S. Granter-Button, G. A. Chernenko, S. Butt, and D. Corbett, "A critical threshold of rehabilitation involving brain-derived neurotrophic factor is required for poststroke recovery," *Neurorehabilitation and Neural Repair*, vol. 25, no. 8, pp. 740–748, 2011.
- [31] S. Li, J. J. Overman, D. Katsman et al., "An age-related sprouting transcriptome provides molecular control of axonal sprouting after stroke," *Nature Neuroscience*, vol. 13, no. 12, pp. 1496–1504, 2010.
- [32] D. Corbett, S. T. Carmichael, T. H. Murphy et al., "Enhancing the alignment of the preclinical and clinical stroke recovery research pipeline: consensus-based core recommendations from the Stroke Recovery and Rehabilitation Roundtable Translational Working Group," *International Journal of Stroke*, vol. 12, no. 5, pp. 462–471, 2017.
- [33] D. J. Cook, C. Nguyen, H. N. Chun et al., "Hydrogel-delivered brain-derived neurotrophic factor promotes tissue repair and recovery after stroke," *Journal of Cerebral Blood Flow & Metabolism*, vol. 37, no. 3, pp. 1030–1045, 2017.
- [34] K. Ravina, D. Briggs, S. Kislal et al., "Intracerebral delivery of brain-derived neurotrophic factor using HyStem[®]-C hydrogel implants improves functional recovery and reduces neuroinflammation in a rat model of ischemic stroke," *International Journal of Molecular Sciences*, vol. 19, no. 12, p. 3782, 2018.
- [35] A. Zeleznikow-Johnston, E. L. Burrows, T. Renoir, and A. J. Hannan, "Environmental enrichment enhances cognitive flexibility in C57BL/6 mice on a touchscreen reversal learning task," *Neuropharmacology*, vol. 117, pp. 219–226, 2017.
- [36] A. N. Clarkson, L. Boothman-Burrell, Z. Dósa et al., "The flavonoid, 2'-methoxy-6-methylflavone, affords neuroprotection following focal cerebral ischaemia," *Journal of Cerebral Blood Flow & Metabolism*, 2018.
- [37] M. D. Lindner, V. K. Gribkoff, N. A. Donlan, and T. A. Jones, "Long-lasting functional disabilities in middle-aged rats with small cerebral infarcts," *Journal of Neuroscience*, vol. 23, no. 34, pp. 10913–10922, 2003.
- [38] S. B. Floresco, A. E. Block, and M. T. L. Tse, "Inactivation of the medial prefrontal cortex of the rat impairs strategy set-shifting, but not reversal learning, using a novel, automated procedure," *Behavioural Brain Research*, vol. 190, no. 1, pp. 85–96, 2008.
- [39] G. B. Bissonette and E. M. Powell, "Reversal learning and attentional set-shifting in mice," *Neuropharmacology*, vol. 62, no. 3, pp. 1168–1174, 2012.
- [40] B. S. Beas, J. A. McQuail, C. Bañuelos, B. Setlow, and J. L. Bizon, "Prefrontal cortical GABAergic signaling and impaired behavioral flexibility in aged F344 rats," *Neuroscience*, vol. 345, pp. 274–286, 2017.
- [41] B. L. Brim, R. Haskell, R. Awedikian et al., "Memory in aged mice is rescued by enhanced expression of the GluN2B subunit of the NMDA receptor," *Behavioural Brain Research*, vol. 238, pp. 211–226, 2013.
- [42] R. T. Bartus, R. L. Dean III, and D. L. Fleming, "Aging in the rhesus monkey: effects on visual discrimination learning and reversal learning," *Journal of Gerontology*, vol. 34, no. 2, pp. 209–219, 1979.
- [43] R. Schoenfeld, N. Foreman, and B. Leplow, "Ageing and spatial reversal learning in humans: findings from a virtual water maze," *Behavioural Brain Research*, vol. 270, pp. 47–55, 2014.
- [44] A. Gazzaley, J. W. Cooney, J. Rissman, and M. D'Esposito, "Top-down suppression deficit underlies working memory impairment in normal aging," *Nature Neuroscience*, vol. 8, no. 10, pp. 1298–1300, 2005.
- [45] S. Rosenzweig and S. T. Carmichael, "Age-dependent exacerbation of white matter stroke outcomes: a role for oxidative damage and inflammatory mediators," *Stroke*, vol. 44, no. 9, pp. 2579–2586, 2013.
- [46] J. Hornak, J. O'Doherty, J. Bramham et al., "Reward-related reversal learning after surgical excisions in orbito-frontal or dorsolateral prefrontal cortex in humans," *Journal of Cognitive Neuroscience*, vol. 16, no. 3, pp. 463–478, 2004.
- [47] W. M. van der Flier, I. Skoog, J. A. Schneider et al., "Vascular cognitive impairment," *Nature Reviews Disease Primers*, vol. 4, article 18003, 2018.
- [48] C. Graybeal, M. Feyder, E. Schulman et al., "Paradoxical reversal learning enhancement by stress or prefrontal cortical damage: rescue with BDNF," *Nature Neuroscience*, vol. 14, no. 12, pp. 1507–1509, 2011.

- [49] A. Izquierdo, C. Darling, N. Manos et al., "Basolateral amygdala lesions facilitate reward choices after negative feedback in rats," *Journal of Neuroscience*, vol. 33, no. 9, pp. 4105–4109, 2013.
- [50] H. Nakayama, H. S. Jorgensen, H. O. Raaschou, and T. S. Olsen, "The influence of age on stroke outcome. The Copenhagen Stroke Study," *Stroke*, vol. 25, no. 4, pp. 808–813, 1994.
- [51] L. Zhang, R. L. Zhang, Y. Wang et al., "Functional recovery in aged and young rats after embolic stroke: treatment with a phosphodiesterase type 5 inhibitor," *Stroke*, vol. 36, no. 4, pp. 847–852, 2005.
- [52] J. Suenaga, X. Hu, H. Pu et al., "White matter injury and microglia/macrophage polarization are strongly linked with age-related long-term deficits in neurological function after stroke," *Experimental Neurology*, vol. 272, pp. 109–119, 2015.
- [53] A. Popa-Wagner, S. T. Carmichael, Z. Kokaia, C. Kessler, and L. C. Walker, "The response of the aged brain to stroke: too much, too soon?," *Current Neurovascular Research*, vol. 4, no. 3, pp. 216–227, 2007.
- [54] K. M. Kelly, A. Kharlamov, T. M. Hentosz et al., "Photothrombotic brain infarction results in seizure activity in aging Fischer 344 and Sprague Dawley rats," *Epilepsy Research*, vol. 47, no. 3, pp. 189–203, 2001.
- [55] A. Popa-Wagner, A. M. Buga, and Z. Kokaia, "Perturbed cellular response to brain injury during aging," *Ageing Research Reviews*, vol. 10, no. 1, pp. 71–79, 2011.
- [56] R. Peters, "Ageing and the brain," *Postgraduate Medical Journal*, vol. 82, no. 964, pp. 84–88, 2006.
- [57] B. Kolb and R. Gibb, "Brain plasticity and behaviour in the developing brain," *Journal of Canadian Academy of Child and Adolescent Psychiatry*, vol. 20, pp. 265–276, 2011.
- [58] B. H. Anderton, "Ageing of the brain," *Mechanisms of Ageing and Development*, vol. 123, no. 7, pp. 811–817, 2002.
- [59] A. Joutel, M. Monet-Leprêtre, C. Gosele et al., "Cerebrovascular dysfunction and microcirculation rarefaction precede white matter lesions in a mouse genetic model of cerebral ischemic small vessel disease," *Journal of Clinical Investigation*, vol. 120, no. 2, pp. 433–445, 2010.
- [60] J. M. Conner, A. A. Chiba, and M. H. Tuszynski, "The basal forebrain cholinergic system is essential for cortical plasticity and functional recovery following brain injury," *Neuron*, vol. 46, no. 2, pp. 173–179, 2005.
- [61] R. J. Nudo, B. M. Wise, F. SiFuentes, and G. W. Milliken, "Neural substrates for the effects of rehabilitative training on motor recovery after ischemic infarct," *Science*, vol. 272, no. 5269, pp. 1791–1794, 1996.
- [62] S. J. Mowla, S. Pareek, H. F. Farhadi et al., "Differential sorting of nerve growth factor and brain-derived neurotrophic factor in hippocampal neurons," *Journal of Neuroscience*, vol. 19, no. 6, pp. 2069–2080, 1999.
- [63] A. Berretta, Y. C. Tzeng, and A. N. Clarkson, "Post-stroke recovery: the role of activity-dependent release of brain-derived neurotrophic factor," *Expert Review of Neurotherapeutics*, vol. 14, no. 11, pp. 1335–1344, 2014.
- [64] D. Rand, J. J. Eng, T. Liu-Ambrose, and A. E. Tawashy, "Feasibility of a 6-month exercise and recreation program to improve executive functioning and memory in individuals with chronic stroke," *Neurorehabilitation and Neural Repair*, vol. 24, no. 8, pp. 722–729, 2010.
- [65] M. S. El-Tamawy, F. Abd-Allah, S. M. Ahmed, M. H. Darwish, and H. A. Khalifa, "Aerobic exercises enhance cognitive functions and brain derived neurotrophic factor in ischemic stroke patients," *NeuroRehabilitation*, vol. 34, no. 1, pp. 209–213, 2014.
- [66] P. Kermani and B. Hempstead, "Brain-derived neurotrophic factor: a newly described mediator of angiogenesis," *Trends in Cardiovascular Medicine*, vol. 17, no. 4, pp. 140–143, 2007.
- [67] W.-R. Schäbitz, T. Steigleder, C. M. Cooper-Kuhn et al., "Intravenous brain-derived neurotrophic factor enhances poststroke sensorimotor recovery and stimulates neurogenesis," *Stroke*, vol. 38, no. 7, pp. 2165–2172, 2007.
- [68] L. A. Mamounas, C. A. Altar, M. E. Blue, D. R. Kaplan, L. Tessarollo, and W. E. Lyons, "BDNF promotes the regenerative sprouting, but not survival, of injured serotonergic axons in the adult rat brain," *Journal of Neuroscience*, vol. 20, no. 2, pp. 771–782, 2000.
- [69] E. G. Waterhouse and B. Xu, "New insights into the role of brain-derived neurotrophic factor in synaptic plasticity," *Molecular and Cellular Neurosciences*, vol. 42, no. 2, pp. 81–89, 2009.
- [70] M. Silhol, S. Arancibia, T. Maurice, and L. Tapia-Arancibia, "Spatial memory training modifies the expression of brain-derived neurotrophic factor tyrosine kinase receptors in young and aged rats," *Neuroscience*, vol. 146, no. 3, pp. 962–973, 2007.
- [71] F. Rage, M. Silhol, F. Biname, S. Arancibia, and L. Tapia-Arancibia, "Effect of aging on the expression of BDNF and TrkB isoforms in rat pituitary," *Neurobiology of Aging*, vol. 28, no. 7, pp. 1088–1098, 2007.
- [72] S. Kanoski, R. Meisel, A. Mullins, and T. Davidson, "The effects of energy-rich diets on discrimination reversal learning and on BDNF in the hippocampus and prefrontal cortex of the rat," *Behavioural Brain Research*, vol. 182, no. 1, pp. 57–66, 2007.
- [73] K. Vedovelli, E. Silveira, E. Velho et al., "Effects of increased opportunity for physical exercise and learning experiences on recognition memory and brain-derived neurotrophic factor levels in brain and serum of rats," *Neuroscience*, vol. 199, pp. 284–291, 2011.
- [74] J. Xin, L. Ma, T. Y. Zhang et al., "Involvement of BDNF signaling transmission from basolateral amygdala to infralimbic prefrontal cortex in conditioned taste aversion extinction," *Journal of Neuroscience*, vol. 34, no. 21, pp. 7302–7313, 2014.

Review Article

Finding the Intersection of Neuroplasticity, Stroke Recovery, and Learning: Scope and Contributions to Stroke Rehabilitation

Leeanne Carey ^{1,2}, Alistair Walsh ^{1,2}, Achini Adikari ³, Peter Goodin,^{2,4}
Damminda Alahakoon,³ Daswin De Silva,³ Kok-Leong Ong,³ Michael Nilsson ^{1,5,6}
and Lara Boyd ⁷

¹Occupational Therapy, School of Allied Health, Human Sciences and Sport, College of Science, Health and Engineering, La Trobe University, Bundoora, VIC 3086, Australia

²Neurorehabilitation and Recovery, Stroke Division, Florey Institute of Neuroscience and Mental Health, Heidelberg VIC 3084, Australia

³Research Centre for Data Analytics and Cognition, La Trobe University, Bundoora, VIC 3086, Australia

⁴Department of Medicine and Neurology, Melbourne Brain Centre, Royal Melbourne Hospital, Parkville, VIC 3050, Australia

⁵Faculty of Health and Medicine and Centre for Rehab Innovations, The University of Newcastle, Callaghan NSW 2308, Australia

⁶LKC School of Medicine, Nanyang Technological University (NTU), 308232, Singapore

⁷Djavad Mowafaghian Centre for Brain Health, Faculty of Medicine, University of British Columbia, Vancouver, BC, Canada V6T 1Z3

Correspondence should be addressed to Leeanne Carey; l.carey@latrobe.edu.au, Michael Nilsson; Michael.nilsson@newcastle.edu.au, and Lara Boyd; lara.boyd@ubc.ca

Received 24 November 2018; Revised 4 February 2019; Accepted 24 March 2019; Published 2 May 2019

Academic Editor: Yasuo Terao

Copyright © 2019 Leeanne Carey et al. This is an open access article distributed under the Creative Commons Attribution License, which permits unrestricted use, distribution, and reproduction in any medium, provided the original work is properly cited.

Aim. Neural plastic changes are experience and learning dependent, yet exploiting this knowledge to enhance clinical outcomes after stroke is in its infancy. Our aim was to search the available evidence for the core concepts of neuroplasticity, stroke recovery, and learning; identify links between these concepts; and identify and review the themes that best characterise the intersection of these three concepts. **Methods.** We developed a novel approach to identify the common research topics among the three areas: neuroplasticity, stroke recovery, and learning. A concept map was created *a priori*, and separate searches were conducted for each concept. The methodology involved three main phases: data collection and filtering, development of a clinical vocabulary, and the development of an automatic clinical text processing engine to aid the process and identify the unique and common topics. The common themes from the intersection of the three concepts were identified. These were then reviewed, with particular reference to the top 30 articles identified as intersecting these concepts. **Results.** The search of the three concepts separately yielded 405,636 publications. Publications were filtered to include only human studies, generating 263,751 publications related to the concepts of neuroplasticity ($n = 6,498$), stroke recovery ($n = 79,060$), and learning ($n = 178,193$). A cluster concept map (network graph) was generated from the results; indicating the concept nodes, strength of link between nodes, and the intersection between all three concepts. We identified 23 common themes (topics) and the top 30 articles that best represent the intersecting themes. A time-linked pattern emerged. **Discussion and Conclusions.** Our novel approach developed for this review allowed the identification of the common themes/topics that intersect the concepts of neuroplasticity, stroke recovery, and learning. These may be synthesised to advance a neuroscience-informed approach to stroke rehabilitation. We also identified gaps in available literature using this approach. These may help guide future targeted research.

1. Introduction

Neuroplasticity can be defined as the ability of the nervous system to respond to intrinsic or extrinsic stimuli by reorganizing its structure, function, and connections [1]. Neural plastic changes are associated with development [2] and learning [3, 4]. They occur throughout the lifespan [5] and may be enhanced following injury [6]. They are influenced by experience [7] and the context [8, 9] in which that experience occurs. The major drivers of neuroplastic change are meaningful behavior [10]. Evidence of neural plastic changes can be observed at various levels, e.g., cellular/synaptic changes, changes in the structure and function of brain regions and networks, and changes in behavior such as improved skill and adaptability [11, 12]. Strong scientific evidence demonstrates that the brain has remarkable capacity for plasticity and reorganisation, yet exploiting this knowledge to enhance clinical outcomes is in its infancy.

After a brain injury, such as stroke, the person is challenged to sense, move, communicate, and engage in daily activities with the brain and body that are impacted by the stroke. Immediate and long-term effects of stroke include impairment in sensation, movement, cognition, psychological and emotional functions, and reduced independence and quality of life. There may be evidence of improvement and some regaining of lost skill. A trajectory of spontaneous and supported recovery over the days, weeks, and months after stroke has been described [13, 14]. Yet rehabilitation outcomes are currently suboptimal and variable [15, 16], and evidence supporting novel or more effective treatments is limited.

Neural plastic changes occur following brain injury, such as stroke [17]. The changes may occur in the days, weeks, months, and years following stroke [11, 13]. They may be adaptive or maladaptive [18, 19]. For example, a person can learn nonuse of the limb or develop dystonic postures following sensory loss [20]. However, we have yet to harness this window of opportunity for ongoing recovery both short- and long-term after stroke. The continuum of recovery after stroke presents opportunities for targeted rehabilitation to harness and enhance these mechanisms of neural plasticity for improved outcomes.

Neural plastic changes are *experience* and *learning dependent*. *Learning* is the process of acquiring a relatively lasting change in knowledge and skills [21]. Learning cannot be measured directly, and assessment may address different criterion indicators of learning [21]. The potential exists for the phenomenon of neural plasticity to be shaped by the experiences that occur following stroke [8, 9, 19] and to be positively impacted by rehabilitation [9, 19, 22]. The question is how can we build on and shape this experience and drive positive plasticity to achieve better outcomes for stroke survivors?

Neurorehabilitation may be defined as “facilitation of adaptive learning” [23]. *Stroke rehabilitation* founded on neuroscience is now recognised for its capacity to achieve more restorative outcomes [1, 19]. Experience and learning-dependent plasticity are core to this change [12, 23]. There are different conditions under which that plasticity may be

enhanced, facilitated, and/or consolidated. These different conditions likely impact the type of neuroplasticity facilitated and behavioral outcomes observed. An advanced understanding of these will help guide the development of neuroscience-based interventions.

The aim of our scoping review was (i) to search the evidence available in relation to the three core concepts of neural plasticity, stroke recovery, and learning; (ii) to identify how these concepts are linked to each other; and (iii) to identify and discuss the themes/topics that best characterise the intersection of these three concepts, in order to better inform the neuroscience basis of stroke rehabilitation and stroke recovery.

In relation to neural plasticity, we were interested in the identification of evidence of neuroplastic changes, e.g., at cellular and neural network levels. This included evidence such as synaptic changes, brain networks, and functional connectivity. We anticipated this literature would be primarily found in neuroscience and neuroimaging type journals. For the concept of stroke recovery, we were interested in outcomes related to impairment, performance, participation, and quality of life, at different times in the recovery trajectory and in relation to rehabilitation. The concept of *learning* focused on the process of change and included domains such as experience, different types of learning, attention and cognition, adaptation, environment, motivation, and goal. Investigation of the *links and intersection* between these concepts has the potential to reveal the following: (1) the type of learning experience that can enhance neural plasticity; (2) the evidence that links neural plasticity and improved outcomes for stroke survivors; and (3) how the different learning experiences linked with neural plasticity might influence/contribute to better stroke outcomes.

In achieving our aim, we sought to develop and use a methodology that would enable a broad and comprehensive scoping of the current literature. This included identification of key topics represented in the literature that relate to the three core concepts and an approach that permits searching and identification of related terms that may be used by authors. This was important to maximise the likelihood that a broad range of terms that are likely to have similar or overlapping meaning was able to be searched and accessed.

2. Methodology

A series of steps were conducted to identify the common research interests among the three research areas: neuroplasticity, stroke recovery, and learning. A concept map was first developed to guide the review in relation to our aim. Figure 1 depicts the concept map comprising (a) the three main concepts (neuroplasticity, stroke recovery, and learning); (b) example main keywords related to each of the concepts; (c) arrows depicting the associations among each of the main concepts; and (d) numbers to indicate our key foci/associations of interest. The target population was adult humans with stroke. Health outcomes included improved function, such as skill, performance, and quality of life.

Following the initial creation of the concept map, our approach was to scope the literature available in relation to

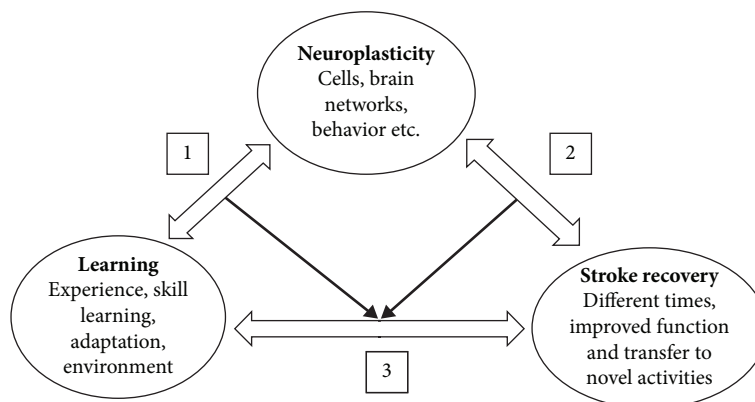


FIGURE 1: Concept map depicting the three main concepts and the potential associations between them.

each of the three core concepts separately and then identify the relationship (link) between each other. Given the amount of literature for each of the concepts, we adopted a novel approach to searching and clustering the large number of papers and identifying the links and intersection. In particular, we employed an automatic text processing engine (Section 2.3) to aid the process and identify the unique and common topics among these research concepts. In this way, we were able to map the identified topics to components 1, 2, and 3 in the proposed concept map. A narrative review was then conducted of the common themes and the top articles that were identified as intersecting the three concepts.

Our novel approach consisted of three main phases: data collection and filtering, development of a clinical vocabulary, and the development of an automatic clinical text processing engine. The methodology to build the vocabulary and text processing engine is comprised of three main technical approaches: *text mining* [24]—to extract relevant information from the research articles and structure data according to our analysis; *natural language processing* (NLP) [25]—to create word embeddings and topic ontology; and *text analysis* [26]—to derive insights on how the three concepts are linked together based on the identified topic associations. The details of the techniques are further described in Sections 2.2 and 2.3.

2.1. Data Collection and Filtering. A comprehensive literature search was conducted using PubMed to assemble research studies addressing neuroplasticity, stroke recovery, and learning. First, we conducted three separate and broad searches. We used the tree of MeSH headings associated with each of these concepts to ensure broad and comprehensive inclusion of data. For example, under the heading of learning [F02.463.425], this included 25 subheadings and further 32 subheadings under these subheadings. As an inclusion criteria for the collected studies, we selected research where experiments were conducted on humans.

The PubMed database was accessed using the Entrez Programming Utilities (E-utilities), a set of eight server side programs that provide a programmatic interface to the National Center for Biotechnology Information (NCBI) database system [27]. A python helper library, used to interact with the E-utilities and perform other formatting and

data managing tasks, is available at <https://github.com/alistairwalsh/informatician>.

The three separate requests with the query terms “neuroplasticity[MeSH],” “stroke[MeSH],” and “learning[MeSH]” returned associated PubMed ID numbers, which were then used to retrieve all the information available for those articles. The resulting XML documents were then searched for an English abstract along with their article title, abstract, and index terms (i.e., mesh terms and/or keyword lists) to produce a collection of studies that were searched for terms of interest.

Three sources of data were collected and analysed for each article retrieved: title, abstract, and index terms, as identified in the article by the authors. This data was not only selected for its availability but also based on the expectation that key topic words should be captured in these sources. Further, data collected across these data sources should be comparable as the type of information included in abstracts is relatively uniform, with clear expectations, and is usually word limited, thus minimising bias due to variance in article length.

2.2. Development of a Clinical Vocabulary. Following the filtering of the collected documents, text mining tasks were performed to gain insights on the associations between the three concepts. Text mining is the process of extracting useful information from unstructured data and customization according to the requirements. For this purpose, it was necessary to build a vocabulary/initial seed word list, which could be used as the guide for text mining to extract relevant information. Therefore, a clinical vocabulary comprising of prominent topics in all three research areas was required. The following steps were undertaken to develop the vocabulary.

2.2.1. Domain Knowledge from Experts. An initial vocabulary was formed using the domain knowledge from experts. These topic vocabulary terms are listed in Table 1. This initial vocabulary included keywords as well as key phrases. Three knowledge experts (LC, MN, and LB) contributed to the list.

2.2.2. Incorporating Index Terms Provided by Authors in Articles Retrieved. Index terms (keywords provided by

TABLE 1: Domain knowledge from experts used for each of the three concept areas.

Concept 1: Neural Plasticity	Concept 2: Stroke Recovery	Concept 3: Learning	Concept 3: Learning <i>cont.</i>
Cells	Post-stroke	Experience-dependent	Activity-dependent
Synapses	Time	Experience	Adaptation
BDNF	Trajectory	Spontaneous	Transfer
Brain	Function	Implicit	Complex, complexity
Brain regions	Skill	Enriched environment	Metacognition
Neuroimaging	Impairment	Multisensory	Strategy
Learning systems	Movement	Multimodal	Problem solve
White matter	Sensation	Cross-modal	Generalise
Functional connectivity	Language	Long-term	Novel
Brain activation	Speech	Potiation	Relearning
Reorganisation	Physical	Environment	Consolidation
Frontal	Cognition	Stimulation	Well learnt
Networks/systems	Mood	Performance	Overlearn
Brain network	Activity	Learning-dependent	Personal experience
Connection	Task	Skill learning	Environment
Behavior change	Work	Motor learning	Task complexity
Consolidation	Participation	Perceptual learning	Task switching
Experience-dependent plasticity		Sensory learning	Performance
Learning-dependent plasticity		Discrimination	Human
Activity-dependent plasticity		Generalisation	Individual
Glial cells		Reinforcement learning	Motivation
Microglia		Task-specific	Cognition/cognitive
Astrocytes		Sequence	Concentration
Gliosis		Errorful	Transmitters
Neuroimmunology		Errorless	Receptors
Blood brain barrier		Challenge point	Vision
Axons			Hearing
Dendrites			Perception
Circulation			Emotion
Neurogenesis			Mood
Progenitor cells			Fatigue
			Stress

authors) and MESH terms used by the authors for each article were included to further enrich the vocabulary.

2.2.3. Word Embedding Technique to Expand the Vocabulary.

Word embedding is a machine learning technique that intelligently captures the context of a word in a document, i.e., capturing semantic and syntactic similarity as well as identifying the relation with other words. This technique was used to extract synonyms for the original list of terms (i.e., as outlined in Table 1). The extracted model was applied to the three sources of data from each article (i.e. title, abstract, and index terms). A word2vec model was trained from the collection of publications that can identify terms that were being used in a similar context. For instance, the word “consolidation” generated a similarly used word list (“formation,” “reconsolidation,” “storage,” and “acquisition”). The generated similar words were manually reviewed for relevance before adding to the vocabulary.

2.3. Development of an Automatic Clinical Text Processing Engine. To analyse the associations between the concepts, we developed an automatic clinical text processing engine, which is capable of automatically extracting key terms from documents and generating a concept link map. A series of natural language processing (NLP) techniques and text analysis were used for this purpose. NLP is known as the application of computational techniques to analyse natural language which is unstructured textual data [28]. The developed text processing engine is comprised of an array of NLP techniques to extract topics, calculate similarity, and create a concept link map which was used for the analysis of topic associations. The primary tasks of the developed engine are explained below.

2.3.1. Automatic Term Extraction. Intelligent search algorithms [29] were used to automatically extract relevant terms from the abstracts, titles, and index terms provided by the

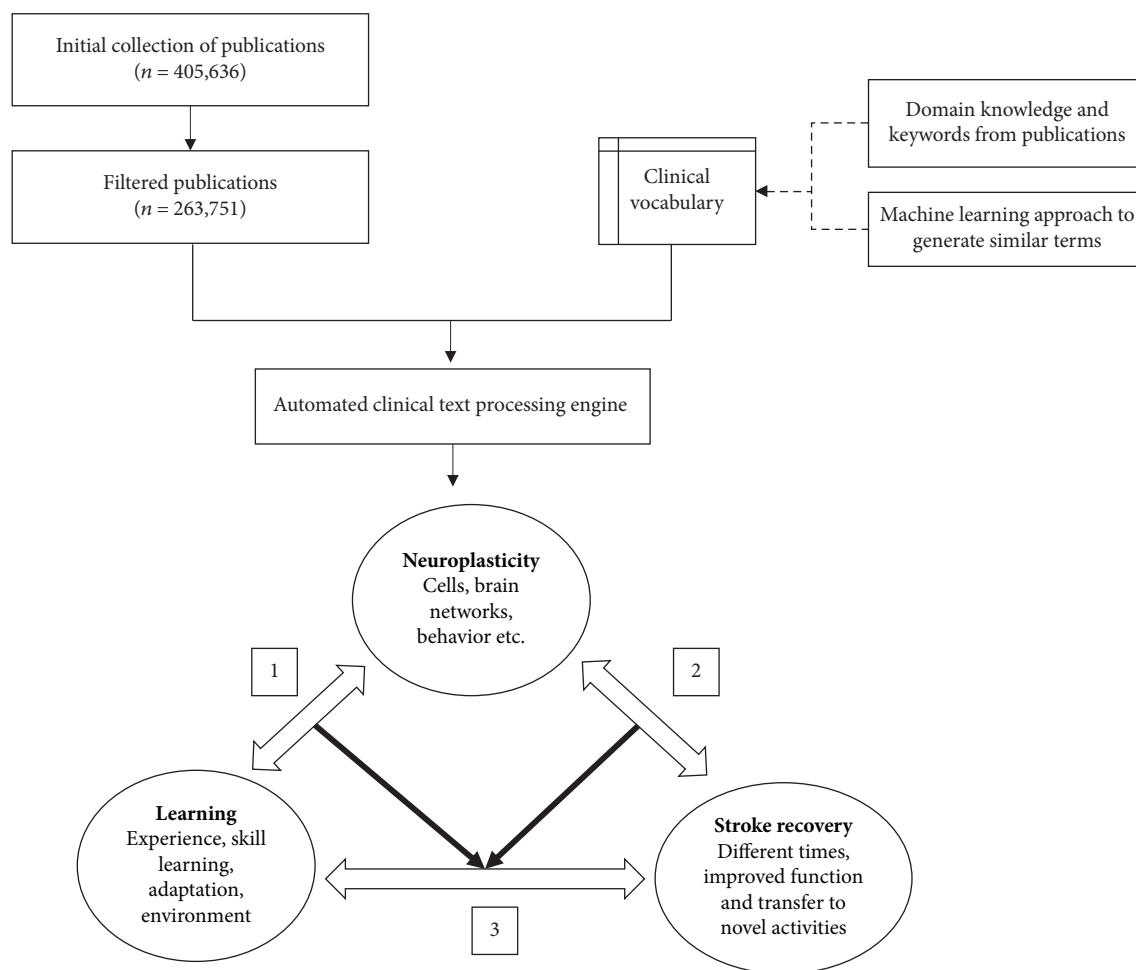


FIGURE 2: The high-level process of the methodology.

authors of the publications. The developed vocabulary was used for this purpose. The process generated lists of topics being discussed for each publication.

2.3.2. Term Similarity Identification. Once the terms were extracted, it was essential to identify the common terms between the three groups. We used NLP techniques to automatically group publications that have similar topics and thereby identify unique and common clusters of topics.

2.3.3. Weight Concept Link Map. The results were then used to generate a weighted concept link map illustrating the topics that connect the concepts together. The output concept map represented an overview of the topics that link the three concepts together. Each connection was given a score based on the number of publications, therefore allowing filtering out only the important connections.

The high-level process of the text analysis engine is illustrated in Figure 2.

2.4. Investigation of Time-Linked Patterns in Keywords Used for Each Concept. We conducted a post hoc analysis to explore if any time-related patterns emerged in relation to the emergence of topics for each of the three concepts over

time. First, the three core concepts were analysed with the date of the publication and for each topic; a percentage was calculated for each year indicating the use of that topic in a particular year (i.e., based on sum of times, each keyword was mentioned each year, from 1975 to 2018). We then analysed how the three concepts have been linked together from 1975 to 2018 to explore the emergence of patterns in the linking of concepts over time.

3. Results

Searching the three core concepts separately yielded 405,636 publications. Publications were filtered to include only studies of humans, generating 263,751 publications from the three groups. This included studies related to the concepts of neuroplasticity ($n = 6,498$), stroke recovery ($n = 79,060$), and learning ($n = 178,193$).

Figure 3 illustrates the topical associations between the three main concepts generated from the automatic text processing engine following the concept map. The three main nodes in the generated concept map represent the focus areas: neuroplasticity, stroke recovery, and learning. Each line connected to the nodes represents topics discussed related to the respective research area. The strength of

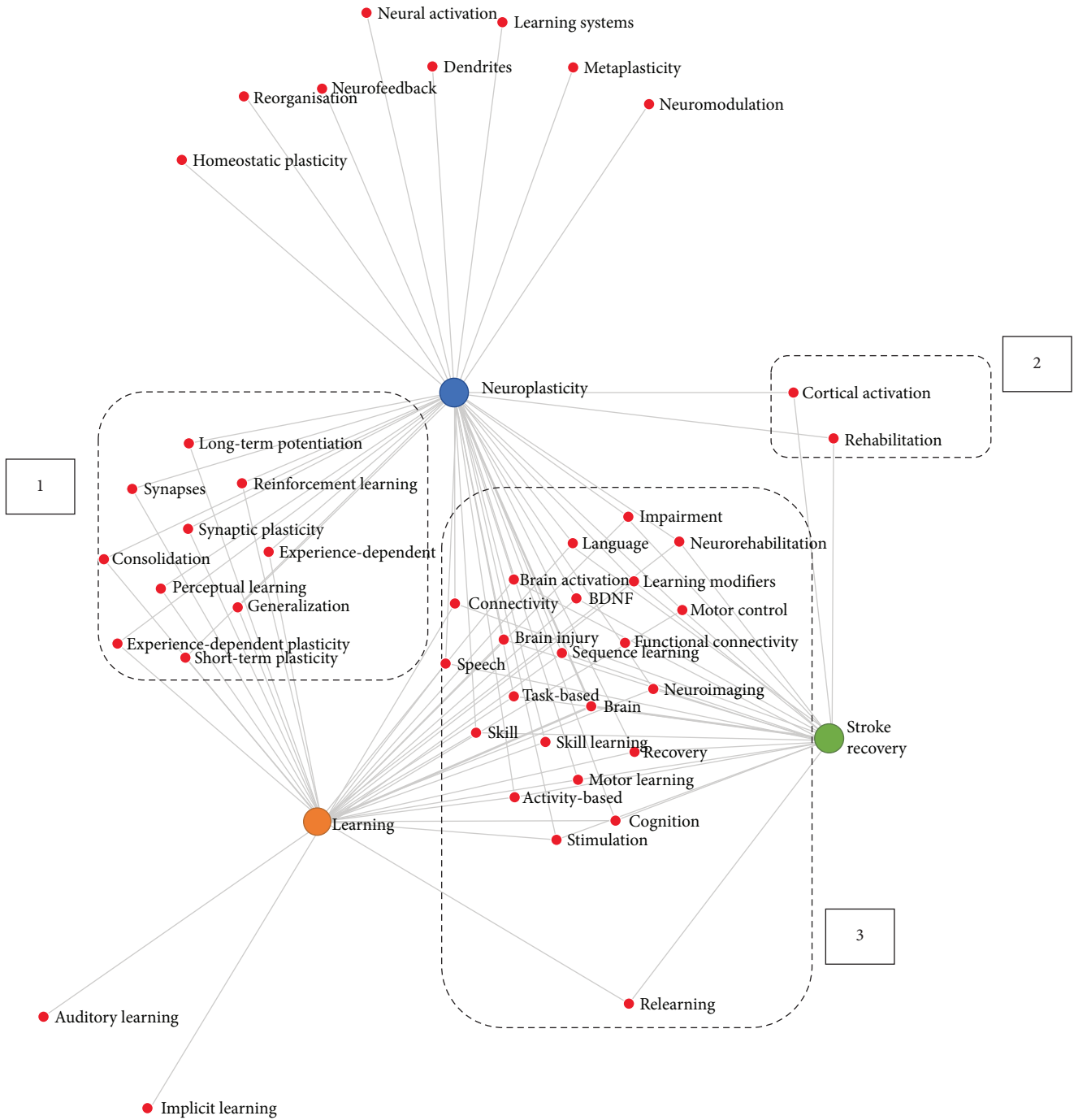


FIGURE 3: Generated concept map using the automatic text processing engine—showing 3 main *concepts* (nodes), strength of link between nodes (number of publications), identification of *common themes* being discussed based on the proposed concept link map (encircled areas 1, 2, and 3), and *topics* (words) that help to characterise the concept and/or the links between them.

each line is an indication of the quantity of publications. The encircled components of the generated diagram are based on the proposed concept link map in the methodology. The numbers indicate the links between the concepts as follows:

- (1) Common themes being discussed in neuroplasticity and learning

- (2) Common themes being discussed in neuroplasticity and stroke recovery
- (3) Common themes being discussed in learning and stroke recovery with common themes in neuroplasticity

The common themes identified between the main concepts are listed in Table 2, together with an indication of

TABLE 2: Common themes identified linking concepts of neuroplasticity, stroke recovery, and learning.

Topic	Normalized score	Publication count
Common themes between neuroplasticity and learning (Link 1)		
Synaptic plasticity	0.314	778
Consolidation	0.231	360
Long-term potentiation	0.145	340
Perceptual learning	0.145	280
Experience-dependent learning	0.059	150
Generalization	0.038	99
Experience-dependent plasticity	0.025	67
Short-term plasticity	0.022	58
Reinforcement learning	0.021	55
Common themes between neuroplasticity and stroke recovery (Link 2)		
Cortical activation	0.562	113
Rehabilitation	0.438	86
Common themes between neuroplasticity, stroke recovery, and learning (Link 3)		
Cognition	0.279	4032
Brain	0.141	3762
Stimulation	0.113	2830
Task-based learning	0.085	2136
Activity-based learning	0.073	1834
Motor learning	0.043	1090
Learning modifiers	0.041	1018
Skills	0.036	910
Movement	0.030	760
Impairment	0.029	732
Language	0.024	613
Connectivity	0.019	472
Speech	0.017	429
Neuroimaging	0.014	344
Neurorehabilitation	0.009	242
Motor control	0.008	203
BDNF	0.008	192
Skill learning	0.007	188
Functional connectivity	0.006	164
Brain injury	0.006	162
Brain activation	0.006	160
Sequence learning	0.004	107
Relearning	0.003	105

the number of publications and normalised score (weights) for each theme.

The top 30 articles identified that intersect all three main concepts: neuroplasticity, learning, and stroke recovery, are listed in Table 3. These articles were selected according to their weighting and are ordered with the most recent at the top. It is noted that 15 articles are reviews and nine are controlled trials. The full text of these articles was downloaded and reviewed for the narrative review.

3.1. A Time-Based Analysis of the Terminology and the Evolution of Topics over Time. A post hoc analysis of the use of keywords (topics) for each concept and the evolution of how the topics link together over time revealed two outcomes: (1) overall topic distribution over time—this indicated how frequently a given topic was addressed in research studies each year thereby demonstrating the patterns over time; (2) the emergence of topics—this indicated when certain topics first appeared and how they evolved over time. Based on the patterns identified by these outcomes, we further examined the time-based topical associations to observe how the link (intersection) between the three concepts (neuroplasticity, learning, and stroke) had emerged over time. For demonstration purposes, we created three sets of publications based on the patterns detected by the time-based topic distribution. Three time periods emerged: (1) Early era (1975-1990); (2) Emerging era (1997-2003); and (3) Recent era (2012-2018). These time periods emerged primarily from the topic flow graph of neuroplasticity. Using the publications in these three groups, we analysed the evolution of the link between the three concepts. This process was automated by the proposed text mining approach.

Figure 4 highlights the outcomes of this analysis showing the associations of the concepts according to the aforementioned time periods. The Early era (1975-1990) was characterised by only a few topics in neuroplasticity. Prominent topics were “Stimulation,” “Consolidation,” and “Synapses.” The links between neuroplasticity, stroke, and learning are established. This was followed by the Emerging era (1997-2003), a time where many new topics (keywords) first appeared, particularly in relation to neuroplasticity, and more new directions of research were formed. The Recent period (2012-2018) revealed the latest research topics. Many new topics appeared in relation to all three concepts during this period. The link, Neuroplasticity-Stroke, was expanded with “Neurostimulation” and “Cortical activation” other than “Brain”; the link Neuroplasticity-Learning became stronger, with many more research studies; and the link Learning-Stroke emerged, linking all three concepts together.

4. Discussion

The aim of this review was to identify the literature that links neuroplasticity, stroke recovery, and learning in order to advance our understanding of and provide direction for a neuroscience-informed approach to stroke rehabilitation. The concept map generated by the text processing engine provides an efficient and rigorous approach to identify associations between different research areas as well as insights on important research themes and topics within a large pool of research publications. Moreover, the weighted link map provided a quantitative measure of the significance of the relationship between the themes; thus, the important topics could be identified. Finally, the intersection between all three concepts was defined and common topics identified. Time-linked patterns emerged from our analysis of the evolution of the link between the three concepts.

TABLE 3: Top 30 filtered articles that address common themes being discussed in learning and stroke recovery with common themes in neuroplasticity.

Author	Date	Title	Journal	Type
Charalambous et al. [30]	2018	The Feasibility of an Acute High-Intensity Exercise Bout to Promote Locomotor Learning after Stroke	<i>Topics in Stroke Rehabilitation</i>	Controlled trial
Fan et al. [31]	2017	Transcranial Direct Current Stimulation over Multiple Days Enhances Motor Performance of a Grip Task	<i>Annals of Physical and Rehabilitation Medicine</i>	Controlled trial
van der Vliet et al. [32]	2017	BDNF Val66Met but Not Transcranial Direct Current Stimulation Affects Motor Learning after Stroke	<i>Brain Stimulation</i>	Controlled trial
Pearson-Fuhrhop et al. [33]	2017	Genetic Variation in the Human Brain Dopamine System Influences Motor Learning and Its Modulation by L-Dopa	<i>PloS One</i>	Controlled trial
Horton et al. [34]	2017	Adaptation, Perceptual Learning, and Plasticity of Brain Functions	<i>Graefe's Archive for Clinical and Experimental Ophthalmology</i>	Review
Divya et al. [35]	2017	Post-Stroke Cognitive Impairment - A Cross-Sectional Comparison Study between Mild Cognitive Impairment of Vascular and Non-Vascular Etiology	<i>Journal of the Neurological Sciences</i>	Comparative study
Wadden et al. [36]	2017	Predicting Motor Sequence Learning in Individuals with Chronic Stroke	<i>Neurorehabilitation and Neural Repair</i>	Controlled trial
Censor et al. [37]	2016	Altered Human Memory Modification in the Presence of Normal Consolidation	<i>Cerebral Cortex</i>	Controlled trial
Siegel et al. [38]	2016	Disruptions of Network Connectivity Predict Impairment in Multiple Behavioral Domains after Stroke	<i>Proceedings of the National Academy of Sciences</i>	Clinical trial
Buma et al. [39]	2016	Brain Activation Is Related to Smoothness of Upper Limb Movements after Stroke	<i>Experimental Brain Research</i>	Clinical trial
Reinkensmeyer et al. [40]	2016	Computational Neurorehabilitation: Modeling Plasticity and Learning to Predict Recovery	<i>Journal of NeuroEngineering and Rehabilitation</i>	Review
Soekadar et al. [41]	2015	Brain-Machine Interfaces in Neurorehabilitation of Stroke	<i>Neurobiology of Disease</i>	Review
Kitago et al. [42]	2015	Robotic Therapy for Chronic Stroke: General Recovery of Impairment or Improved Task-Specific Skill?	<i>Journal of Neurophysiology</i>	Clinical trial
Lefebvre et al. [43]	2015	Neural Substrates Underlying Stimulation-Enhanced Motor Skill Learning after Stroke	<i>Brain: A Journal of Neurology</i>	Controlled trial
Winstein et al. [44]	2014	Infusing Motor Learning Research into Neurorehabilitation Practice: A Historical Perspective with Case Exemplar from the Accelerated Skill Acquisition Program	<i>Journal of Neurologic Physical Therapy: JNPT</i>	Case study
Mang et al. [45]	2013	Promoting Neuroplasticity for Motor Rehabilitation after Stroke: Considering the Effects of Aerobic Exercise and Genetic Variation on Brain-Derived Neurotrophic Factor	<i>Physical Therapy</i>	Review
Buma et al. [46]	2013	Understanding Upper Limb Recovery after Stroke	<i>Restorative Neurology and Neuroscience</i>	Review
Byl et al. [47]	2013	Effectiveness of Sensory and Motor Rehabilitation of the Upper Limb following the principles of Neuroplasticity: Patients Stable Poststroke	<i>Neurorehabilitation and Neural Repair</i>	Controlled trial
Bowden et al. [48]	2013	Promoting Neuroplasticity and Recovery after Stroke: Future Directions for Rehabilitation Clinical Trials	<i>Current Opinion in Neurology</i>	Review

TABLE 3: Continued.

Author	Date	Title	Journal	Type
Albert and Kesselring [49]	2012	Neurorehabilitation of Stroke	<i>Journal of Neurology</i>	Review
Arya et al. [50]	2011	Movement Therapy Induced Neural Reorganization and Motor Recovery in Stroke: A Review.	<i>Journal of Bodywork and Movement Therapies</i>	Review
Duret [51]	2010	[Contributions of Robotic Devices to Upper Limb Poststroke Rehabilitation]	<i>Revue Neurologique</i>	Review
Graham et al. [52]	2009	The Bobath Concept in Contemporary Clinical Practice	<i>Topics in Stroke Rehabilitation</i>	Review
Ween [53]	2008	Functional Imaging of Stroke Recovery: An Ecological Review from a Neural Network Perspective with an Emphasis on Motor Systems	<i>Journal of Neuroimaging</i>	Review
Ziemann and Siebner [54]	2008	Modifying Motor Learning through Gating and Homeostatic Metaplasticity	<i>Brain Stimulation</i>	Review
Daly and Ruff [55]	2007	Construction of Efficacious Gait and Upper Limb Functional Interventions Based on Brain Plasticity Evidence and Model-Based Measures for Stroke Patients	<i>The Scientific World Journal</i>	Discussion paper
Hlustik and Mayer [56]	2006	Paretic Hand in Stroke: From Motor Cortical Plasticity Research to Rehabilitation	<i>Cognitive and Behavioral Neurology</i>	Review
Krakauer [57]	2006	Motor Learning: Its Relevance to Stroke Recovery and Neurorehabilitation	<i>Current Opinion in Neurology</i>	Review
Forrester et al. [58]	2005	Exercise-Mediated Locomotor Recovery and Lower-Limb Neuroplasticity after Stroke	<i>Journal of Rehabilitation Research and Development</i>	Review
Winstein et al. [59]	1999	Motor Learning after Unilateral Brain Damage	<i>Neuropsychologia</i>	Controlled trial

learning-based rehabilitation was evident. For example, a dissociation between disrupted memory modifications in the presence of normal consolidation was reported and may be related to differences in a lesioned brain structure linked with macrostructure network anatomy and microstructural white matter integrity [37]. Clearly, cognition is important, highlighting the need to recognise and assess cognitive profiles of stroke survivors, even those with reported mild neurological impairment. The issue of cognitive decline [60, 61] also needs to be considered.

As expected, *Brain* was also a topic that was represented in a large number of publications. As well as being a focus in its own right, it was often linked with terms such as brain function, brain damage, brain injury, brain plasticity, brain stimulation, brain imaging, brain activation, and brain networks. *Stimulation* was primarily referred to in the context of brain stimulation and adjunct therapeutic stimulation techniques, such as functional electrical stimulation (FES) [41]. This theme highlights the search for and possible role of adjunctive stimulation techniques to enhance neural plastic changes and stroke recovery. It highlights an area of research focus and proof of concept exploration of new therapies to try to manipulate plasticity and recovery.

Different types of learning were identified in the context of neuroplasticity and stroke recovery, representing a clear intersection of all three concepts (Link 3). These included *task-based learning* and *activity-based learning*. The common focus on learning in the context of tasks and/or activities ($n = 3,970$ publications) was identified using this approach. The topic of task-specific training, a term often used in clinical settings, was also aligned. These learning approaches are seen as potential enhancers of neural plasticity [49]. Task-based learning and activity-based learning map to concepts of learning-dependent plasticity. The role of learning that is task- and/or activity-based appears to have relevance in the context of stroke recovery and rehabilitation. For example, changes in central nervous system (CNS) structure and function may be modified by “activity,” together with motor learning principles [55]. In fact, both neuroscience and learning approaches that are integrated into rehabilitation included *task-based training* as a core element of therapy, consistent with recommendations [1, 9, 12, 23, 57].

Aligned with this focus on task- and activity-based learning is *skill* and *skill learning*, focusing on the outcomes of learning. Skill learning in the context of stroke recovery and neurorehabilitation links learning-dependent plasticity with restorative therapies. The goal of learning-dependent plasticity is often the learning of a skill, such as juggling and playing a musical instrument. In the context of stroke recovery, it may be learning a sensorimotor skill, such as learning to grasp a cup in a more normal manner following paresis. We have clear evidence from animal studies that training is a critical ingredient to this change [10, 62]. In human studies, evidence suggests that skill learning, but not strength training, induces cortical reorganization and cortical changes may only occur with learning of new skills and not just with repetitive use [9, 63]. For example, recent evidence highlights that motor skill learning of a repeated sequence altered cortical activation by inducing a more normal,

contralateral pattern of brain activation, whereas increasing general arm use did not induce motor learning or alter brain activity [63].

A relatively large proportion of the publications (20.78%) were focused on *motor learning*, *movement*, and *motor control*. This finding highlights the current focus on movement outcomes, potentially at the expense of other functions or more complex outcomes. A relatively small proportion of articles focused on language and speech (9.2%). In comparison, focus on sensation (vision or touch) appeared to be missing as did more complex outcomes such as daily activities and or transfer to novel and/or complex activities. This likely reflects where the field currently is, i.e., in its infancy, in relation to applying knowledge that integrates neural plasticity with learning and valued stroke recovery outcomes. Nevertheless, the value of learning paradigms, in particular motor learning paradigms, is growing and a push to “infuse” motor learning research into neurorehabilitation practice is argued for in this literature [44]. An interesting observation was that the capacity for functional restitution after brain damage was different in sensory and motor systems [34]. The authors identified the role of adaptation and perceptual learning and their linkages with plasticity, as potentially important. Such findings further highlight the importance of systematic investigation across different functions.

Interestingly, *experience-dependent learning* was identified as a topic linking only neuroplasticity and learning (not the 3-way intersection) in our review (Link 1). Experience-dependent learning is closely aligned with experience-dependent plasticity [12]. Experience-dependent plasticity refers to the brain’s capacity to change in response to environmental stimuli (and learning). It has been a major focus of preclinical studies and has culminated in the evidence of “enriched environments” to enhance recovery. Key features of this type of plasticity include exposure to environments that have multiple sensory attributes, social context etc. [12]. The potential for enriched environments to impact neural plastic changes and stroke recovery has been identified [8]; however, it did not emerge from the current review that represents the collective focus of the field. Given the existing link between experience and neural plasticity, the potential to connect this link more strongly with stroke recovery through targeted research is highlighted.

A few topics highlighted outcomes and/or mechanisms of change at a neurobiological level. Those topics that spanned underlying mechanisms or biomarkers included *connectivity*, *neuroimaging*, *BDNF*, *functional connectivity*, and *brain activation*. The neurobiological mechanisms underlying recovery in patients with varying severity of impairment and in the longer term, are incompletely understood. New technologies are emerging and have a role in providing new insights [64] and in helping to predict recovery and ability to benefit from interventions [36, 65]. For example, a predictive relationship was elucidated between the type of behavior, e.g., specific visual or distributed memory, and the brain lesion and network disruption [38]. This was possible using machine learning and multiple measures of the brain and behavior, i.e., resting functional connectivity (FC), lesion

topography, and behavior in multiple domains (attention, visual memory, verbal memory, language, motor, and visual). A key role of distributed brain network disruption, beyond focal damage, was highlighted [38].

The process of and application of learning, including *sequence learning* to *relearning* and *neurorehabilitation*, were also identified as themes. Given the focus on learning and search terms used, it was interesting to note that the current literature often *did not* include topics that reflect a greater specificity in the nature of the learning, e.g., implicit and explicit learning. An exception was the identification of sequence learning as the approach to motor skill learning by Wadden et al. [36]. Again, this likely reflects the state of the science in the application these concepts to stroke rehabilitation. The issue of restitution of function, e.g., motor, versus adaptive motor learning strategies to compensate for motor impairments was identified but not resolved [39]. Nevertheless, we recommend this topic as an important avenue for future research on the basis that the process of learning is dynamic and could be disrupted following brain injury, and specific types of learning might be more beneficial following certain types of brain injury [23].

Of further interest is the fact that learning terms such as *generalization* and *transfer* (included in the MESH term for learning) did not emerge in any of the common themes. This is of potential concern given that outcomes associated with training and therapy need to be able to transfer to novel tasks and complex settings. The issue of sustainable and generalizable gains in motor skills and associated behaviors is highlighted in the rehabilitation literature [23, 57]. It is known that transfer to tasks that have not been directly trained in therapy is often very limited [57]. Transfer of gains in skills to personally-important real-life activities is rarely spontaneous and relatively rarely reported. Improvement in personally important, real-life activities is critical [23]. However, sensorimotor rehabilitation is historically focused on impairment reduction, with limited focus given to transfer of gains to real-life activities. Greater attention to outcomes that demonstrate different gradients of transfer and generalisation is recommended.

Neuroplasticity, learning, and transfer to novel tasks may be promoted by task complexity [12, 66, 67]. Different neural networks are implicated for learning of sensorimotor skills and transfer [68] and the value of metacognition strategies suggested [69]. The need for specific strategies to enhance transfer is supported by evidence from motor learning and neuroscience [68, 69]. Activity-dependent plasticity, defined as a form of neuroplasticity that arises from the use of cognitive functions and personal experience [67], would appear to be particularly relevant in this context. Interestingly, preliminary evidence suggests combined cognitive strategy and task-specific training improve transfer to untrained activities in subacute stroke [70].

Finally, *learning modifiers* was also identified as a topic. Factors that modify learning, its effectiveness, and impact at different times in the recovery trajectory are of interest. These factors ranged from factors such as BDNF [32] to adjunctive therapies, such as transcranial direct current stimulation

[31] and robotics [42, 51]. One of the top 30 articles addressed the time course of skill reacquisition after stroke [46]. Other factors that might be modifiers of learning such as stress, concentration, perception, emotion, mood, and fatigue were not identified as topics despite being included as search terms.

4.3. The Evolution of Themes and Topics over Time. Further analysis was carried out to explore the evolution and associations of topics over time. Our objective was to observe how the topics in neuroplasticity, stroke recovery, and learning had evolved over time (1975-2018) using the collected sample of research studies from 1975 to 2018. Only a few topics were identified in the early time period (1975-1990). The link between neuroplasticity and stroke was established via research focused on “Brain,” while the link between neuroplasticity and learning was established via studies on “Stimulation” and “Consolidation.” In contrast, the Emerging era (1997-2003) showed the appearance of many more topics in neuroplasticity and the links have more weight indicating the availability of more research studies. The analysis of research in the Recent era (2012-2018) disclosed the emergence of many new topics. The link between neuroplasticity and stroke recovery was further expanded by studies on “cortical activation” and “neurostimulation.” It was also observed that the link between stroke recovery and learning was established in this time period, thus linking all three concepts together.

As this analysis was automated by the text mining approach described, further analysis and comparison using different time periods will allow disclosing other interesting patterns and insights regarding the associations among the three concepts. We present this time-based topic analysis as further contribution to the proposed approach as it enables researchers to mine useful time-based patterns from many publications without manual processing.

4.4. Recommendations for Future Research. Some recommendations for future research emerge from our review. The development of computational models of salient neural processes [40], including plasticity and learning systems of the brain in the context of stroke rehabilitation, is recommended. While focus to date has been primarily on motor function, we should not lose sight of the need to target other functions, such as language and sensation. Further, systematic investigation of outcomes across a profile of outcomes, including impairment and performance, activities, and participation is recommended [71] to achieve the valued outcomes articulated by people living with stroke [72]. We should also give greater attention to the processes of learning and how they map to different types of neural plastic changes, i.e. experience-dependent, learning-dependent, and activity-dependent plasticity. This is important as the different types of plasticity are aligned with specific goals, experiences, and learning conditions and may be more able to be enhanced at different times in the recovery trajectory. It is unlikely that one type of learning or principle of training, such as intensity, is likely to meet the skill and activity outcomes valued.

The development of future interventions should match neuroscience and learning principles to specific outcomes. In particular, the need to systematically target the intersect between neural plasticity and learning to achieve better generalisation of training effects and transfer to novel tasks in the context of stroke rehabilitation is critical. With further understanding, the potential to individualise therapy emerges. This may include the recognition of underlying capacities that support a particular type of learning, through genetic variations and strategies that influence modifiers of learning, such as BDNF. Finally, future research should be directed at discovering drivers of the different types of plasticity, as well as when they might best be applied at different times in the recovery trajectory.

5. Conclusions

In summary, the novel approach taken in this review allowed us to identify and characterise not only the topics that are currently being investigated in the literature but also those that are not or are only infrequently mentioned. Identification of the common intersecting themes linked with the core concepts proposed now provides a foundation of literature that may be synthesised to advance a neuroscience-informed approach to stroke rehabilitation. Further, such an approach helps to identify gaps in the field that may be important, as researched and recommended in related fields. For example, the topics of transfer and generalisation have been extensively researched in the field of learning, but did not emerge as an intersection with neural plasticity and stroke recovery. The review of the concepts of neural plasticity, learning, and stroke recovery and the common themes and topics that link them has provided direction for future research, important in the development of new neuroscience and learning-based therapeutic approaches. Finally, the potential also exists to develop theoretical frameworks by which new interventions may be conceptualised, incorporating knowledge of the intersection between contributing fields of research.

Conflicts of Interest

The authors have no conflict of interest to declare.

Acknowledgments

We acknowledge the support for the analysis, write-up, and researchers from the James S. McDonnell Foundation 21st Century Science Initiative in Cognitive Rehabilitation-Collaborative Award (# 220020413). We also acknowledge the support from the National Health and Medical Research Council of Australia (NHMRC) Project grant (# 1022694), Career Development Award (# 307905), Centre of Research Excellence (# 1077898), and Partnership grant (# 1134495).

References

- [1] S. C. Cramer, M. Sur, B. H. Dobkin et al., "Harnessing neuroplasticity for clinical applications," *Brain*, vol. 134, no. 6, pp. 1591–1609, 2011.
- [2] W. T. Greenough, J. E. Black, and C. S. Wallace, "Experience and brain development," *Child Development*, vol. 58, no. 3, pp. 539–559, 1987.
- [3] Y. Chang, "Reorganization and plastic changes of the human brain associated with skill learning and expertise," *Frontiers in Human Neuroscience*, vol. 8, p. 35, 2014.
- [4] L. G. Ungerleider, J. Doyon, and A. Karni, "Imaging brain plasticity during motor skill learning," *Neurobiology of Learning and Memory*, vol. 78, no. 3, pp. 553–564, 2002.
- [5] A. May, "Experience-dependent structural plasticity in the adult human brain," *Trends in Cognitive Sciences*, vol. 15, no. 10, pp. 475–482, 2011.
- [6] N. Dancause, S. Barbay, S. B. Frost et al., "Extensive cortical rewiring after brain injury," *The Journal of Neuroscience*, vol. 25, no. 44, pp. 10167–10179, 2005.
- [7] A. Holtmaat and K. Svoboda, "Experience-dependent structural synaptic plasticity in the mammalian brain," *Nature Reviews Neuroscience*, vol. 10, no. 9, pp. 647–658, 2009.
- [8] H. Janssen, J. Bernhardt, J. M. Collier et al., "An enriched environment improves sensorimotor function post-ischemic stroke," *Neurorehabilitation and Neural Repair*, vol. 24, no. 9, pp. 802–813, 2010.
- [9] R. J. Nudo, "Adaptive plasticity in motor cortex: implications for rehabilitation after brain injury," *Journal of Rehabilitation Medicine*, vol. 35, pp. 7–10, 2003.
- [10] R. J. Nudo, "Postinfarct cortical plasticity and behavioral recovery," *Stroke*, vol. 38, no. 2, pp. 840–845, 2007.
- [11] T. H. Murphy and D. Corbett, "Plasticity during stroke recovery: from synapse to behaviour," *Nature Reviews Neuroscience*, vol. 10, no. 12, pp. 861–872, 2009.
- [12] M. Pekna, M. Pekny, and M. Nilsson, "Modulation of neural plasticity as a basis for stroke rehabilitation," *Stroke*, vol. 43, no. 10, pp. 2819–2828, 2012.
- [13] L. M. Carey and R. Seitz, "Functional neuroimaging in stroke recovery and neurorehabilitation: conceptual issues and perspectives," *International Journal of Stroke*, vol. 2, no. 4, pp. 245–264, 2007.
- [14] J. Bernhardt, K. S. Hayward, G. Kwakkel et al., "Agreed definitions and a shared vision for new standards in stroke recovery research: the stroke recovery and rehabilitation roundtable taskforce," *Neurorehabilitation and Neural Repair*, vol. 31, no. 9, pp. 793–799, 2017.
- [15] National Stroke Foundation, *National Stroke Audit- Rehabilitation Services Report*, Melbourne, Australia, 2016.
- [16] P. van Vliet, L. M. Carey, and M. Nilsson, "Targeting stroke treatment to the individual," *International Journal of Stroke*, vol. 7, no. 6, pp. 480–481, 2012.
- [17] S. C. Cramer and J. D. Riley, "Neuroplasticity and brain repair after stroke," *Current Opinion in Neurology*, vol. 21, no. 1, pp. 76–82, 2008.
- [18] R. J. Nudo, "Recovery after damage to motor cortical areas," *Current Opinion in Neurobiology*, vol. 9, no. 6, pp. 740–747, 1999.
- [19] L. M. Carey, *Stroke Rehabilitation: Insights from Neuroscience and Imaging*, Oxford University Press, New York, NY, USA, 2012.
- [20] L. M. Carey, "Loss of somatic sensation," in *Textbook of Neural Repair and Rehabilitation*, M. E. Selzer, L. G. Cohen, S. Clarke, and P. W. Duncan, Eds., Cambridge University Press, Cambridge, UK, 2012.

- [21] E. R. Skidmore, "Training to optimize learning after traumatic brain injury," *Current Physical Medicine and Rehabilitation Reports*, vol. 3, no. 2, pp. 99–105, 2015.
- [22] L. M. Carey, "Neuroplasticity and learning lead a new era in stroke rehabilitation," *International Journal of Therapy and Rehabilitation*, vol. 14, no. 6, pp. 250–251, 2007.
- [23] L. M. Carey, H. J. Polatajko, and C. M. Baum, "Stroke rehabilitation: a learning perspective," in *Stroke Rehabilitation: Insights from Neuroscience and Imaging*, L. M. Carey, Ed., pp. 11–23, Oxford University Press, New York, NY, USA, 2012.
- [24] R. Feldman and J. Sanger, *The Text Mining Handbook: Advanced Approaches in Analyzing Unstructured Data*, Cambridge University Press, UK, 2007.
- [25] R. Collobert, J. Weston, L. Bottou, M. Karlen, K. Kavukcuoglu, and P. Kuksa, "Natural language processing (almost) from scratch," *Journal of Machine Learning Research*, vol. 12, pp. 2493–2537, 2011.
- [26] G. Salton, C. S. Yang, and C. T. Yu, "A theory of term importance in automatic text analysis," *Journal of the American Society for Information Science*, vol. 26, no. 1, pp. 33–44, 1975.
- [27] National Center for Biotechnology Information, "Entrez programming utilities help," 2010, <http://www.ncbi.nlm.nih.gov/books/NBK25501>.
- [28] E. D. Liddy, "Natural language processing," in *Encyclopedia of Library and Information Science*, Marcel Decker, Inc., New York, NY, USA, 2001.
- [29] D. Minnie and S. Srinivasan, "Intelligent search engine algorithms on indexing and searching of text documents using text representation," in *2011 International Conference on Recent Trends in Information Systems*, pp. 121–125, India Kolkata, December 2011.
- [30] C. C. Charalambous, E. E. Helm, K. A. Lau, S. M. Morton, and D. S. Reisman, "The feasibility of an acute high-intensity exercise bout to promote locomotor learning after stroke," *Topics in Stroke Rehabilitation*, vol. 25, no. 2, pp. 83–89, 2018.
- [31] J. Fan, J. Voisin, M. H. Milot, J. Higgins, and M. H. Boudrias, "Transcranial direct current stimulation over multiple days enhances motor performance of a grip task," *Annals of Physical and Rehabilitation Medicine*, vol. 60, no. 5, pp. 329–333, 2017.
- [32] R. van der Vliet, G. M. Ribbers, Y. Vandermeeren, M. A. Frens, and R. W. Selles, "BDNF Val66Met but not transcranial direct current stimulation affects motor learning after stroke," *Brain Stimulation*, vol. 10, no. 5, pp. 882–892, 2017.
- [33] K. M. Pearson-Fuhrhop, B. Minton, D. Acevedo, B. Shahbaba, and S. C. Cramer, "Genetic variation in the human brain dopamine system influences motor learning and its modulation by L-Dopa," *PLoS One*, vol. 8, no. 4, article e61197, 2013.
- [34] J. C. Horton, M. Fahle, T. Mulder, and S. Trauzettel-Klosinski, "Adaptation, perceptual learning, and plasticity of brain functions," *Graefes Archive for Clinical and Experimental Ophthalmology*, vol. 255, no. 3, pp. 435–447, 2017.
- [35] K. P. Divya, R. N. Menon, R. P. Varma et al., "Post-stroke cognitive impairment - a cross-sectional comparison study between mild cognitive impairment of vascular and non-vascular etiology," *Journal of the Neurological Sciences*, vol. 372, pp. 356–362, 2017.
- [36] K. P. Wadden, K. De Asis, C. S. Mang et al., "Predicting motor sequence learning in individuals with chronic stroke," *Neurorehabilitation and Neural Repair*, vol. 31, no. 1, pp. 95–104, 2017.
- [37] N. Sensor, E. R. Buch, K. Nader, and L. G. Cohen, "Altered human memory modification in the presence of normal consolidation," *Cerebral Cortex*, vol. 26, no. 9, pp. 3828–3837, 2016.
- [38] J. S. Siegel, L. E. Ramsey, A. Z. Snyder et al., "Disruptions of network connectivity predict impairment in multiple behavioral domains after stroke," *Proceedings of the National Academy of Sciences of the United States of America*, vol. 113, no. 30, article 10.1073/pnas.1521083113, pp. E4367–E4376, 2016.
- [39] F. E. Buma, J. van Kordelaar, M. Raemaekers, E. E. H. van Wegen, N. F. Ramsey, and G. Kwakkel, "Brain activation is related to smoothness of upper limb movements after stroke," *Experimental Brain Research*, vol. 234, no. 7, pp. 2077–2089, 2016.
- [40] D. J. Reinkensmeyer, E. Burdet, M. Casadio et al., "Computational neurorehabilitation: modeling plasticity and learning to predict recovery," *Journal of NeuroEngineering*, vol. 13, no. 1, p. 42, 2016.
- [41] S. R. Soekadar, N. Birbaumer, M. W. Slutzky, and L. G. Cohen, "Brain-machine interfaces in neurorehabilitation of stroke," *Neurobiology of Disease*, vol. 83, pp. 172–179, 2015.
- [42] T. Kitago, J. Goldsmith, M. Harran et al., "Robotic therapy for chronic stroke: general recovery of impairment or improved task-specific skill?," *Journal of Neurophysiology*, vol. 114, no. 3, pp. 1885–1894, 2015.
- [43] S. Lefebvre, L. Dricot, P. Laloux et al., "Neural substrates underlying stimulation-enhanced motor skill learning after stroke," *Brain*, vol. 138, no. 1, pp. 149–163, 2015.
- [44] C. Winstein, R. Lewthwaite, S. R. Blanton, L. B. Wolf, and L. Wishart, "Infusing motor learning research into neurorehabilitation practice: a historical perspective with case exemplar from the accelerated skill acquisition program," *Journal of Neurologic Physical Therapy*, vol. 38, no. 3, pp. 190–200, 2014.
- [45] C. S. Mang, K. L. Campbell, C. J. D. Ross, and L. A. Boyd, "Promoting neuroplasticity for motor rehabilitation after stroke: considering the effects of aerobic exercise and genetic variation on brain-derived neurotrophic factor," *Physical Therapy*, vol. 93, no. 12, pp. 1707–1716, 2013.
- [46] F. Buma, G. Kwakkel, and N. Ramsey, "Understanding upper limb recovery after stroke," *Restorative Neurology and Neuroscience*, vol. 31, no. 6, pp. 707–722, 2013.
- [47] N. Byl, J. Roderick, O. Mohamed et al., "Effectiveness of sensory and motor rehabilitation of the upper limb following the principles of neuroplasticity: patients stable poststroke," *Neurorehabilitation and Neural Repair*, vol. 17, no. 3, pp. 176–191, 2003.
- [48] M. G. Bowden, M. L. Woodbury, and P. W. Duncan, "Promoting neuroplasticity and recovery after stroke: future directions for rehabilitation clinical trials," *Current Opinion in Neurology*, vol. 26, no. 1, pp. 37–42, 2013.
- [49] S. J. Albert and J. Kesselring, "Neurorehabilitation of stroke," *Journal of Neurology*, vol. 259, no. 5, pp. 817–832, 2012.
- [50] K. N. Arya, S. Pandian, R. Verma, and R. K. Garg, "Movement therapy induced neural reorganization and motor recovery in stroke: a review," *Journal of Bodywork and Movement Therapies*, vol. 15, no. 4, pp. 528–537, 2011.
- [51] C. Duret, "Contributions of robotic devices to upper limb poststroke rehabilitation," *Revue Neurologique*, vol. 166, no. 5, pp. 486–493, 2010.

- [52] J. V. Graham, C. Eustace, K. Brock, E. Swain, and S. Irwin-Carruthers, "The Bobath concept in contemporary clinical practice," *Topics in Stroke Rehabilitation*, vol. 16, no. 1, pp. 57–68, 2009.
- [53] J. E. Ween, "Functional imaging of stroke recovery: an ecological review from a neural network perspective with an emphasis on motor systems," *Journal of Neuroimaging*, vol. 18, no. 3, pp. 227–236, 2008.
- [54] U. Ziemann and H. R. Siebner, "Modifying motor learning through gating and homeostatic metaplasticity," *Brain Stimulation*, vol. 1, no. 1, pp. 60–66, 2008.
- [55] J. J. Daly and R. L. Ruff, "Construction of efficacious gait and upper limb functional interventions based on brain plasticity evidence and model-based measures for stroke patients," *ScientificWorldJournal*, vol. 7, pp. 2031–2045, 2007.
- [56] P. Hlustik and M. Mayer, "Paretic hand in stroke: from motor cortical plasticity research to rehabilitation," *Cognitive and Behavioral Neurology*, vol. 19, no. 1, pp. 34–40, 2006.
- [57] J. W. Krakauer, "Motor learning: its relevance to stroke recovery and neurorehabilitation," *Current Opinion in Neurology*, vol. 19, no. 1, pp. 84–90, 2006.
- [58] L. W. Forrester, L. A. Wheaton, and A. R. Luft, "Exercise-mediated locomotor recovery and lower-limb neuroplasticity after stroke," *Journal of Rehabilitation Research & Development*, vol. 45, no. 2, pp. 205–220, 2008.
- [59] C. J. Winstein, A. S. Merians, and K. J. Sullivan, "Motor learning after unilateral brain damage," *Neuropsychologia*, vol. 37, no. 8, pp. 975–987, 1999.
- [60] H. Brodaty, A. Withall, A. Altendorf, and P. S. Sachdev, "Rates of depression at 3 and 15 months poststroke and their relationship with cognitive decline: the Sydney Stroke Study," *American Journal of Geriatric Psychiatry*, vol. 15, no. 6, pp. 477–486, 2007.
- [61] T. A. D. Jolly, P. S. Cooper, S. A. Wan Ahmadul Badwi et al., "Microstructural white matter changes mediate age-related cognitive decline on the Montreal Cognitive Assessment (MoCA)," *Psychophysiology*, vol. 53, no. 2, pp. 258–267, 2016.
- [62] R. J. Nudo, B. M. Wise, F. SiFuentes, and G. W. Milliken, "Neural substrates for the effects of rehabilitative training on motor recovery after ischemic infarct," *Science*, vol. 272, no. 5269, pp. 1791–1794, 1996.
- [63] L. Boyd, E. Vidoni, and B. Wessel, "Motor learning after stroke: is skill acquisition a prerequisite for contralesional neuroplastic change?," *Neuroscience Letters*, vol. 482, no. 1, pp. 21–25, 2010.
- [64] L. M. Carey, R. J. Seitz, M. Parsons et al., "Beyond the lesion: neuroimaging foundations for post-stroke recovery," *Future Neurology*, vol. 8, no. 5, pp. 507–527, 2013.
- [65] L. A. Boyd, K. S. Hayward, N. S. Ward et al., "Biomarkers of stroke recovery: consensus-based core recommendations from the stroke recovery and rehabilitation roundtable," *Neurorehabilitation and Neural Repair*, vol. 31, no. 10-11, pp. 864–876, 2017.
- [66] J. R. Carey, E. Bhatt, and A. Nagpal, "Neuroplasticity promoted by task complexity," *Exercise and sport sciences reviews*, vol. 33, no. 1, pp. 24–31, 2005.
- [67] K. Ganguly and M. Poo, "Activity-dependent neural plasticity from bench to bedside," *Neuron*, vol. 80, no. 3, pp. 729–741, 2013.
- [68] R. D. Seidler, "Neural correlates of motor learning, transfer of learning, and learning to learn," *Exercise and Sport Sciences Reviews*, vol. 38, no. 1, pp. 3–9, 2010.
- [69] E. R. Skidmore, D. R. Dawson, M. A. Butters et al., "Strategy training shows promise for addressing disability in the first 6 months after stroke," *Neurorehabilitation and Neural Repair*, vol. 29, no. 7, pp. 668–676, 2015.
- [70] S. McEwen, H. Polatajko, C. Baum et al., "Combined cognitive-strategy and task-specific training improve transfer to untrained activities in subacute stroke: an exploratory randomized controlled trial," *Neurorehabilitation and Neural Repair*, vol. 29, no. 6, pp. 526–536, 2015.
- [71] L. M. Carey, "Directions for stroke rehabilitation clinical practice and research," in *Stroke Rehabilitation: Insights from Neuroscience and Imaging*, L. M. Carey, Ed., pp. 240–249, Oxford University Press, New York, NY, USA, 2012.
- [72] A. Pollock, B. St George, M. Fenton, and L. Firkins, "Top ten research priorities relating to life after stroke," *The Lancet Neurology*, vol. 11, no. 3, p. 209, 2012.

Research Article

Motor Control System for Adaptation of Healthy Individuals and Recovery of Poststroke Patients: A Case Study on Muscle Synergies

Fady S. Alnajjar ^{1,2}, Juan C. Moreno ³, Ken-ichi Ozaki,⁴ Izumi Kondo,⁴
and Shingo Shimoda²

¹College of Information Technology (CIT), The United Arab Emirates University, Al Ain, UAE

²RIKEN BSI-Toyota Collaboration Center, Aichi, Japan

³Neural Rehabilitation Group, Cajal Institute, National Council for Scientific Research (CSIC), Madrid, Spain

⁴National Center for Geriatrics and Gerontology, Aichi, Japan

Correspondence should be addressed to Fady S. Alnajjar; fady.alnajjar@uaeu.ac.ae

Received 26 October 2018; Accepted 24 February 2019; Published 27 March 2019

Guest Editor: Lara Boyd

Copyright © 2019 Fady S. Alnajjar et al. This is an open access article distributed under the Creative Commons Attribution License, which permits unrestricted use, distribution, and reproduction in any medium, provided the original work is properly cited.

Understanding the complex neuromuscular strategies underlying behavioral adaptation in healthy individuals and motor recovery after brain damage is essential for gaining fundamental knowledge on the motor control system. Relying on the concept of muscle synergy, which indicates the number of coordinated muscles needed to accomplish specific movements, we investigated behavioral adaptation in nine healthy participants who were introduced to a familiar environment and unfamiliar environment. We then compared the resulting computed muscle synergies with those observed in 10 moderate-stroke survivors throughout an 11-week motor recovery period. Our results revealed that computed muscle synergy characteristics changed after healthy participants were introduced to the unfamiliar environment, compared with those initially observed in the familiar environment, and exhibited an increased neural response to unpredictable inputs. The altered neural activities dramatically adjusted through behavior training to suit the unfamiliar environment requirements. Interestingly, we observed similar neuromuscular behaviors in patients with moderate stroke during the follow-up period of their motor recovery. This similarity suggests that the underlying neuromuscular strategies for adapting to an unfamiliar environment are comparable to those used for the recovery of motor function after stroke. Both mechanisms can be considered as a recall of neural pathways derived from preexisting muscle synergies, already encoded by the brain's internal model. Our results provide further insight on the fundamental principles of motor control and thus can guide the future development of poststroke therapies.

1. Introduction

Behavioral adaptation to unpredictable environmental changes is one of the most powerful capabilities for performing activities of daily living (ADL). For example, we can walk not only on flat asphalt but also on gravel and we can easily move from the living room to the kitchen no matter how the furniture is arranged or even how frequently it is rearranged. Moreover, behavioral adaptation has been found to be essential for enhancing the quality of communication between people [1]. Thus, without adaptability to our surroundings, we would be unable to complete even simple ADL. Clarifying the computational mechanisms that underlie

behavioral adaptation is necessary for understanding the fundamental principles of the motor control system and developing treatment for related disorders.

There have been many attempts to explain behavioral adaptation in humans, by analyzing neuronal activity [2–7] and biological control architectures [8–11] and by proposing learning mechanisms based on biological systems [12–16]. However, the computational mechanism that governs behavioral adaptation remains unsolved.

From the viewpoint of behavioral adaptation, the redundancy of the musculoskeletal system plays a leading role in adjusting our behavior to the environment, as Bernstein pointed out half a century ago [17]. For instance, even the

relatively simple motion of the shoulder joint is achieved by the complex combination of at least nine muscles [18]. Investigating how the central nervous system (CNS) groups and recruits muscles depending on the task and knowledge of the surrounding environment may provide a fundamental clue behind neuromuscular adaptability.

To explain the plausible biological computational mechanism for choosing the appropriate combination of muscles to control point-to-point movements, several researchers have proposed the notion of muscle synergy [19–23]. Muscle synergy, defined as the relative weight of muscle activations driven by common excitation primitives, provides a simple control algorithm, yet allowing for complex motor behavior [7].

Some motor characteristics of human behavior could be deciphered when behaviors were analyzed based on muscle synergy [24, 25]. In our previous study [26], we introduced two indices, based on muscle synergies, and experimentally showed that they represent the efficiency by which basic movement skills (e.g., upright balance skills) are adapted to the environment. The purpose of the current study was to determine whether neuromuscular control strategies are comparable between healthy individuals during their adaptation to an unfamiliar environment and stroke survivors during their recovery. Note that we do not compare here how the muscle synergy pattern is shaped in each case but how the increasing or decreasing of muscle synergy dimensionality is similar between adaptation/recovery. This similarity could be related to the model adopted by the CNS to represent how much it knows about the environment. We considered that this would provide crucial insight and better understanding for developing poststroke rehabilitation systems, better tailored to the treatment of specific motor deficits. To facilitate this study, we have focused on investigating the muscle synergy adaptability of a well-understood single-joint motor task, such as shoulder flexion, which was introduced to the poststroke patients and shoulder adduction introduced to the healthy participants [27]. The reason for presenting two different types of movements to each type of participants is due to the nature level of the participants. Shoulder flexion task was introduced to the patients due to their constrained range of joint motion. For healthy participants, on the other hand, shoulder adduction was introduced due to limitation of the need of using robotic manipulandum capable to produce hard enough task to stimulate their muscle synergy adaptation. Despite focusing on this task, we believe in the generalization of synergy features [28].

We hypothesized that, in poststroke patients with motor dysfunctions, the brain responds as if experiencing an unknown environment due to the interruption of established neural pathways, similar to what occurs when healthy individuals experience an unfamiliar environment. We also argue that the use of muscle synergy analysis for clarifying the pathology of poststroke patients with unilateral motor impairment could provide greater diagnostic accuracy and may help to design more effective poststroke rehabilitation programs than using common clinical tests, which cannot illustrate progress at a neural level during rehabilitation [29–32].

In this study, we compared the behaviors of poststroke patients during an eleven-week recovery phase with those of healthy participants during performance of movements in familiar and unfamiliar environments/tasks. We also analyzed changes in muscle synergy in both scenarios.

2. Materials and Methods

2.1. Experimental Setup and Protocol

2.1.1. Healthy Participants: Experimental Setup

(1) *Participants.* Nine healthy adults (age: 38.1 ± 7.8 years (mean \pm standard deviation (SD))) participated in this experiment. All participants were right handed and reported no neurological or upper limb muscular impairments. The experimental protocol was approved by the RIKEN ethics committee. Written informed consent was obtained from all participants.

(2) *Robotic Manipulandum.* Participants were asked to control the gripper position of a robotic manipulandum (Force Dimension, Nyon, Switzerland) by using their right arm (see Figure 1(a)). The manipulandum contains a bilateral control system, allowing participants to experience the computer-generated virtual space through the forces generated. The robot manipulandum was used to constrain motion and generate an “unfamiliar” environment to healthy participants, by introducing random stiffness “resistance” to the arm movement, in various levels; three types of resistance were used: 4, 7, and 10 N. During the experiment, participants were seated on an adjustable chair with the right hand holding the knob of the manipulandum from the side. A monitor display showing the virtual space was placed in front of the participant to provide feedback for the performance on the assigned tasks.

(3) *Electromyography (EMG).* Six surface EMG electrodes were placed on the participant’s right shoulder to record the activity of primary muscles. Due to the nature of the assigned task, comprising right hand horizontal shoulder adduction, the following muscles were recorded: pectoralis major (PM), deltoid anterior (AD), infraspinatus (IS), teres major (TM), latissimus dorsi (LD), and biceps brachii (BI). EMG electrodes were positioned in accordance with the guidelines of Surface EMG for the Non-Invasive Assessment of Muscles—European Community project [33]. EMG signals were sampled at 1 kHz, high-pass filtered with a cutoff frequency of 30 Hz, root-mean-square rectified, and smoothed using a moving average with a window length of 10 samples. The EMG from each muscle was normalized to its peak value from the experimental set. EMG data were synchronized with the manipulandum data through the use of a common clock and trigger.

2.1.2. *Healthy Participants: Experiment Protocol.* The participants were asked to perform tasks in three different environments:

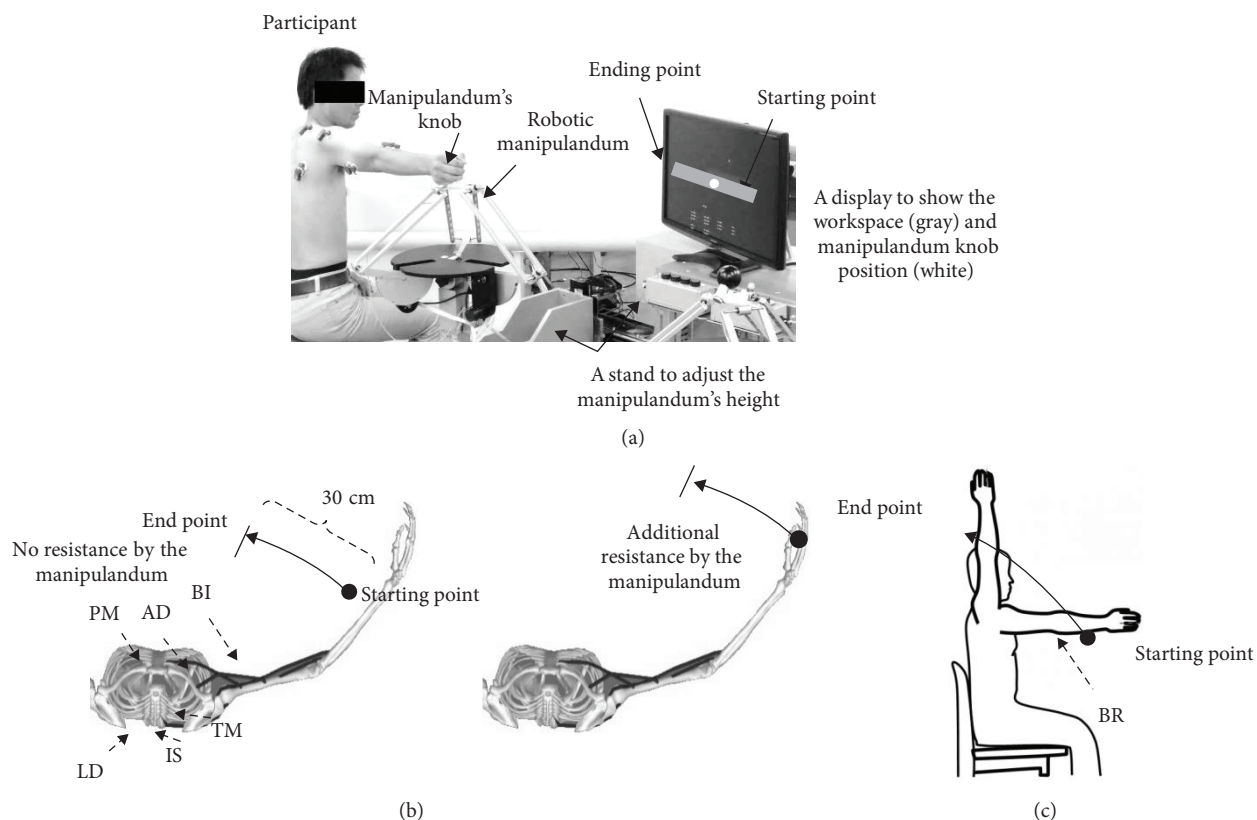


FIGURE 1: Experimental setup and protocol for healthy participants (more details are in [37]). (a) Participant posture, manipulandum, display positions, and workspace (30 cm long). The white circle in the display illustrates the position of the manipulandum knob in the space. The knob position was displayed to the participant to simplify tracking in the assigned task (the display moved horizontally with the knob from the starting point to the ending point of the workspace). (b) Top view illustrating the relevant muscles in the upper torso and right arm in the two tasks for the healthy group—left: the task in the standard environment; right: the task in the modified and adaptation environment. *Standard environment*: move the knob from the starting point to the ending point 10 times (no resistance applied). *Modified environment*: move the knob from the starting point to the ending point 20 times (no resistance and various resistances applied randomly). *Adaptation environment*: move the knob from the starting point to the ending point 15 times for two sessions separated by resting time (7-N resistance applied by the manipulandum at all trials). PM: pectoralis major; AD: deltoid anterior; IS: infraspinatus; TM: teres major; LD: latissimus dorsi; BI: biceps brachii. (c) Side view illustrating the task for the poststroke group. Five muscles were recorded in both the intact and the affected shoulder. Muscles that were shared with healthy participants are the PM, AD, IS, and BI. While BR, brachioradialis, was newly introduced to accommodate the task.

- (1) *Standard Environment*. We asked each participant to grasp the knob of the manipulandum and perform 10 trials of horizontal shoulder adduction from a predefined starting position (see Figure 1(b)). To ensure that the experimental constraints were similar across individuals, we instructed participants not to use their elbow, to maintain a constant contraction of their shoulder muscles, and to complete each trial in 1 s. In this environment, the manipulandum did not produce any significant resistance on the participant's arm. The starting and ending points of the movement were denoted by the manipulandum knob position and displayed on the screen in front of the participants. Particularly for this environment, participants were asked to perform 20 practice trials for familiarizing themselves with the environment before the start of data collection
- (2) *Modified Environment*. To introduce an unfamiliar environment to the participants, we modified the manipulandum responses, compared to those used in the standard environment. In this environment, the manipulandum randomly applied resistance varying from 4 ~ 10 N on the participant's arm, opposite to the movement's direction (see Figure 1(b)). The resistances were applied randomly. Thus, participants could not predict the resistance, thereby reducing the possibility of adaptation at this stage. We asked each participant to repeat the horizontal shoulder adduction task 20 times
- (3) *Adaptation Environment*. Here, we examined the participants' adaptability to the unfamiliar environment through training. We determined this environment as unfamiliar, because even healthy participants could not master the movement in a single trial [34].

TABLE 1: Patients' demographics table.

Patient no.	Sex/age	SIAS	Stroke type
P1	M/49	3	Cerebral infarction
P2	M/58	4	Cerebral infarction
P3	M/75	2	Cerebral infarction
P4	M/63	2	Brainstem infarction
P5	M/70	4	Cerebral infarction
P6	F/64	3	Acute subdural hematoma
P7	M/85	4	Cerebral infarction
P8	F/51	3	Cerebral infarction
P9	F/76	2	Cerebral infarction
P10	M/74	3	Cerebral infarction

P: patient; M: male; F: female; SIAS: stroke impairment assessment set.

At this stage, we asked participants to perform 30 trials of horizontal shoulder adduction. The participants were given a rest period of 120 s after the first 15 trials to minimize muscle fatigue. In this environment, a resistance of 7 N was applied continuously for all trials (although we have done a pilot of resistance varying from 4, 7, to 10 N, the 7 N resistance is the one which we could see little change on the initial computed muscle synergy. The 4 N resistance showed no muscle synergy changes, and in the 10 N resistance, it was hard for the participant to adapt due to muscle fatigue)

2.1.3. Poststroke Patients: Experimental Setup

(1) *Participants.* Ten poststroke patients (age: 66.5 ± 11.6 years (mean \pm SD)) participated in this experiment (see Table 1). All patients were recruited 1.5~2 months after stroke onset and were diagnosed with moderate unilateral motor impairment according to the stroke impairment assessment set (SIAS) (score, 2-4 out of 5) [35, 36]. The experiment protocol for stroke patients was approved by the ethics committee of the National Center for Geriatrics and Gerontology, Aichi, Japan.

(2) *Electromyography.* Surface EMG was recorded from muscles of the patient's affected and intact shoulders, while performing a shoulder flexion task, as described below. Five primary muscles were recorded in each shoulder: PM, AD, IS, BI, and brachioradialis (BR).

(3) *Experiment Protocol.* Due to the nature of the patients' impairment and their constrained range of joint motion, we asked the patients to do a simple bimanual shoulder flexion task. This was to compare muscle synergy in the intact and affected arms of the same patient, instead of just comparing it with that in the arm of a healthy individual. A set of 10 to 15 trials for each session was conducted by each patient, to avoid fatigue (see Figure 1(c)).

2.2. *Muscle Synergy Computation.* Muscle synergy has been described as a systematization method by which some

muscles are activated in synchrony to complete a task [22, 37]. It defines how muscles are synchronized using the following fixed matrix:

$$\begin{aligned} M &= WC, \\ M &\in \mathbb{R}^{m \times t}, \\ W &\in \mathbb{R}^{m \times n}, \\ C &\in \mathbb{R}^{n \times t}. \end{aligned} \quad (1)$$

Here, M refers to the time sequence signals activating m muscles and t is the length of the time sequence. W is the fixed matrix defining the synchronization of m muscles. n represents the number of synergies and should be smaller than m . W is normalized as

$$\begin{aligned} W &= \left[W^{(1)} W^{(2)} W^{(3)} \dots W^{(n)} \right], \\ |W^{(i)}| &= 1, \end{aligned} \quad (2)$$

where $W^{(i)}$ denotes the vector of size, expressed as

$$W^{(i)} \in \mathbb{R}^m. \quad (3)$$

We refer to W as the *synergy space*. C refers to the control signal activating m muscles. Note that n time sequence signals in C are changed to m signals in M using matrix W in equation (1). Therefore, the dimensionality for controlling m muscles is reduced from m to n using this system. The conceptual image of this signal transformation is shown in Figure 2(a).

We can estimate W and C from recorded EMG data using nonnegative matrix factorization (NMF) [38]. The synergy dimension (SyD) of the neural signal n is one of the important parameters in determining the characteristics of muscle synergy. An appropriate n must be chosen according to the behavior, to estimate W and C . Thus, we chose n using the following steps (see also the flowchart in Figure 2(b)):

- (i) Acquisition of EMG data for m muscles and generation of time sequence data for muscle activations (M) by filtering the raw EMG data
- (ii) Temporary definition of n as n_t and estimation of W_{nt} and C_{nt} using NMF
- (iii) Computation of the estimation error E as

$$E = M - W_{nt} C_{nt} \quad (4)$$

- (iv) Computation of the size of E , i.e., the variance accounted for (VAF), such that

$$\text{VAF} = 1 - \frac{\|E\|_F^2}{\|M\|_F^2}, \quad (5)$$

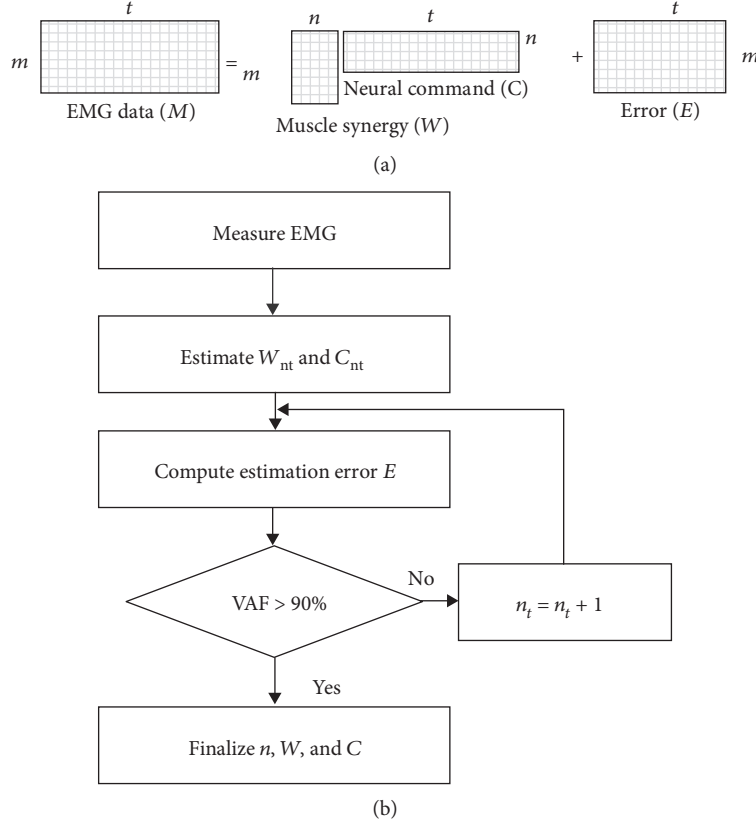


FIGURE 2: (a) A conceptual-mathematical model for identifying muscle synergies. (b) A flowchart that illustrates the process to estimate n , W , and C .

where $\|\cdot\|_F$ denotes the Frobenius norm. If VAF was smaller than a predefined threshold, we changed n_t to $(n_t + 1)$ and computed W_{n_t} and C_{n_t} again by NMF. VAF increases as n_t increases. The threshold is decided based on the behavior, but, in general, we used approximately 90% as a threshold, to indicate a good fit to the original data [38]. By such a threshold, we guarantee that each recorded muscle curve would be well reconstructed

The computation is continued by increasing n_t to $(n_t + 1)$ until VAF becomes larger than the threshold. We used the value of $n_t + 1$ as the dimension of the neural signal, thereby completing our selection of n and estimation of W and C .

2.3. Behavior Analysis Using Muscle Synergy. Both W and C represent interesting features of human motor behavior, as reported by Safavynia et al. [38]. Bizzi et al. [39] showed that W is not specific to individuals but is specific to behavior. Cheung et al. [40] analyzed muscle synergies in stroke survivors and showed that, at the beginning of recovery, some dimensions in synergy space W of the affected arm were merged, in comparison with those of the intact arm.

To analyze behavior by muscle synergy, we asked participants to repeat the assigned task several times (20-30 in healthy participants, 10-15 in stroke patients) and then computed n , W , and C for each trial, considering the time between the starting/ending of the movement (approximately 1.5 s). By comparing these parameters between trials, we derived the features of the behaviors. In our previous

study [26], we introduced indices of similar W and C at each trial and showed that they represent the ability of automatic posture response in healthy participants. Here, we used the same method for computing n , W , and C , to identify changes in behavior during adaptation to an unknown environment. In the case of adaptation analysis, n represents the level of adaptation to the environment.

3. Results

3.1. Healthy Participants. All healthy participants completed the assigned tasks successfully.

3.1.1. Dimensions of Synergy Space

(1) Standard Environment. Figure 3(a) shows the dimensionality of the resulting muscle synergies in participants performing the task in the standard environment. All participants needed two-dimensional muscle synergies to complete the task (i.e., the VAF SyD.2 was the minimum number of synergies that exceeded the assigned >90% threshold). The functional role of each synergy is illustrated in Figure 3(b): Synergy #1 (w_1) seems to mainly be involved in activating the prime mover muscles (PM and AD), which are primarily responsible for shoulder adduction. In contrast, Synergy #2 (w_2) seems to involve the manipulation of neutralizer muscles (BI, LD, IS, and TM), which assist the

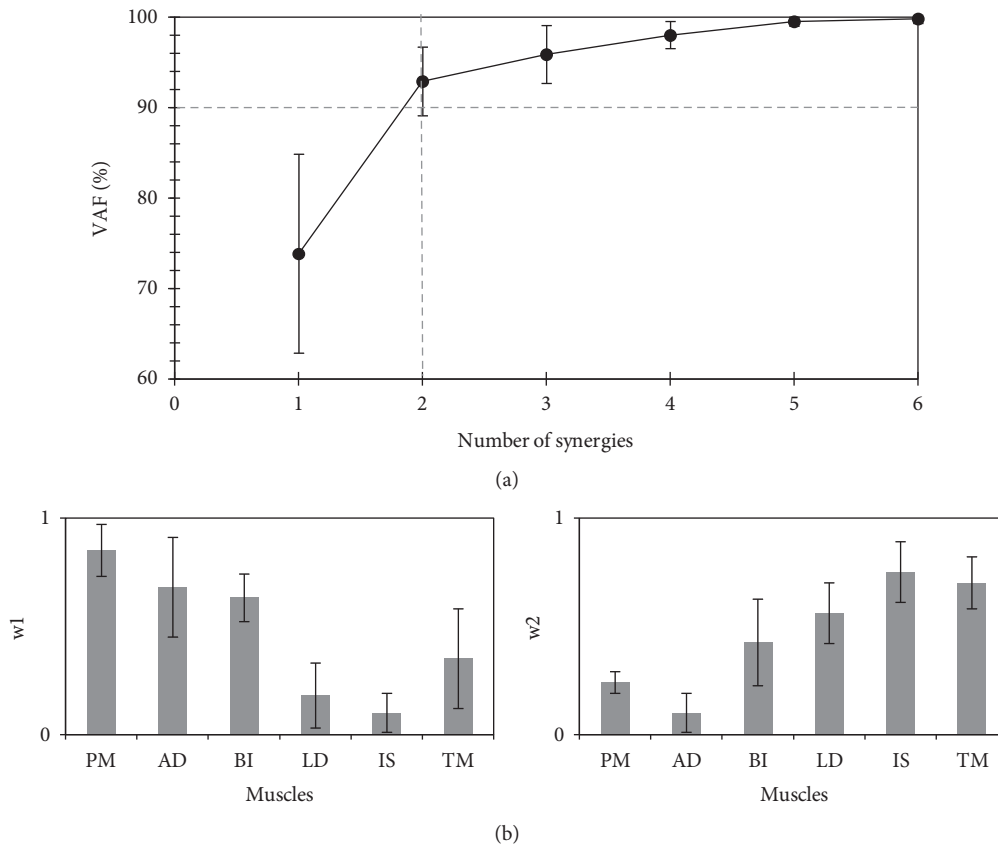


FIGURE 3: Synergy space at the standard (familiar) environment. (a) The variance accounted for (VAF) (%) all possible identified synergies from the recorded electromyograph while performing the task in the standard environment (mean \pm SD, 9 participants). The dashed vertical line identifies the estimated number of utilized synergies that exceeded the threshold (90%; represented by the horizontal dashed line). (b) Muscle synergy vectors (W) for two-dimensional muscle synergies (SyD.2; mean \pm SD, 9 participants). The orders of w_1 and w_2 were sorted based on their activation time (C). PM: pectoralis major; AD: deltoid anterior; BI: biceps brachii; LD: latissimus dorsi; IS: infraspinatus; TM: teres major.

internal rotation of the shoulder joint and are essential to complete the desired shoulder adduction.

(2) *Modified Environment.* Figure 4(a) shows the dimensionality of the resulting muscle synergies during task performance in the modified environment. When resistance was randomly applied, one-dimensional muscle synergy, on average, was observed in all participants for completing the task, instead of the original two-dimensional synergies. The identified synergy in this environment seemed to involve both the prime mover and neutralizer muscles (see Figure 4(b)), which could, in turn, have led to the reduction in the range of shoulder joint internal rotation, making the movement uncomfortable (participants reported of being tired after a few movements).

(3) *Adaptation Environment.* Figure 5(a) shows the dimensionality of the resulting muscle synergies in participants while performing the last 15 trials of the task in the modified environment (resistance was applied continuously). After behavioral adaptation to the unfamiliar environment, all participants returned to using two-dimensional muscle synergies to complete the task. The resulting synergies were

similar in function to those observed in the standard environment, i.e., w_1 and w_2 , which appeared to activate the prime mover and neutralizer muscles, respectively (see Figure 5(b)).

Figure 6(a) shows the gradual transformation from one-dimensional muscle synergy to two-dimensional muscle synergies over the 30 trials. The one-dimensional synergy (SyD.1) gradually decreased to below the threshold. After behavioral adaptation, the two-dimensional synergies (SyD.2) recovered to control the movement (SyD.2 > 90).

3.1.2. *Energy Consumption.* To understand the mechanism of muscle synergy formation during adaptation by the CNS, we included the energy consumption calculations [41]. To investigate the changes in system energy consumption required to complete the task in the adaptation environment [42, 43], we measured the average total muscle activations over the trials (see Figure 6(b)). We found that, after approximately 10 trials, lower muscle activation was needed to complete the task, indicating that joint movements and muscle activations are gradually improved by task repetition through environmental interaction, thus minimizing energy consumption by the movement, by finding more efficient motor solutions, i.e., correct muscle synergy recruitments, to complete the task.

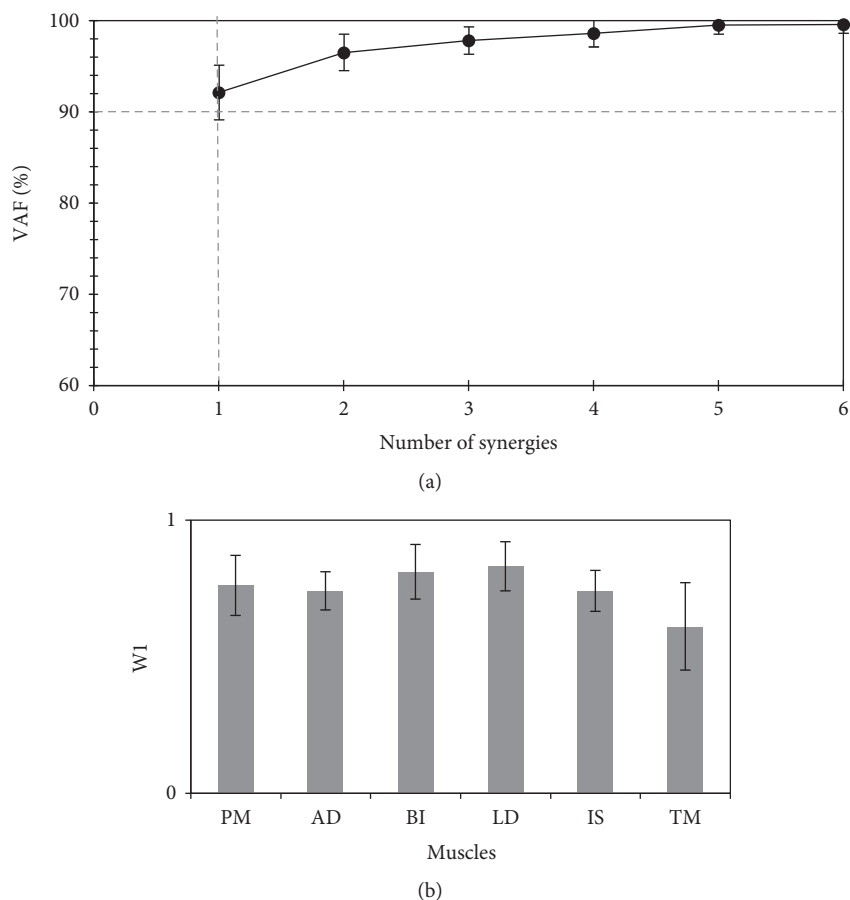


FIGURE 4: Synergy space at the disturbed (unfamiliar) environment. (a) The variance accounted for (VAF) (%) all possible identified synergies from the recorded electromyograph while performing the task in the *modified environment* (mean \pm SD, 9 participants). The dashed vertical line identifies the estimated number of utilized synergies that exceeded the threshold (90%; represented by the horizontal dashed line). (b) Muscle synergy vectors (W) for one-dimensional synergy, *SyD.1*. PM: pectoralis major; AD: deltoid anterior; BI: biceps brachii; LD: latissimus dorsi; IS: infraspinatus; TM: teres major.

3.2. *Poststroke Patients*. All poststroke patients completed the assigned tasks successfully.

3.2.1. *Muscle Synergy Dimensionality for the Stroke-Affected and Intact Arms*. Figure 7 shows the dimensionality of the resulting muscle synergies of the affected and intact arms of the 10 patients (mean \pm SD). On average, one-dimensional synergy was used to produce motion in the affected arm, while two-dimensional synergies were used to produce motion in the intact arm.

Regarding the functionality of the resulting synergies on the intact arm, similar to the healthy participants, w_1 was involved in activating the prime mover muscles, while w_2 was involved in activating the neutralizer muscles. The one-dimensional synergy in the affected arm, however, seemed to activate all recorded muscles in synchrony, revealing an abnormal synergy [44].

Figure 8 illustrates the adaptation process of the one-dimensional synergy (*SyD.1*) in all patients over the 11-week period in which they engaged in a regular rehabilitation program. Although the synergy remained one-dimensional, there were notable changes in the level of VAF, which resembled the formation of two synergies. Interestingly, these

results indicate the gradual improvement in muscle recruitment in patients. Instead, evaluation by SIAS was unable to demonstrate this improvement along the test period for most patients (SIAS index still unchanged).

4. Discussion

The results of this study suggest that the CNS utilizes similar neuromuscular strategies both in the case of healthy individuals, when they adapt to an unfamiliar environment, and in that of poststroke patients, when they recover their motor function. Despite the energy inefficiency of movements produced by low-dimensional muscle synergies, the CNS seems to opt for this module at the initial stages of facing a new situation (or when the internal model is unable to predict appropriately the system output), to handle any unpredictable environmental inputs. By interacting with the environment, the CNS progressively learns to recruit more muscle synergies to conserve energy when it ascertains that the environment is now safe or, in other words, when it rebuilds enough internal model and is able to rely on it.

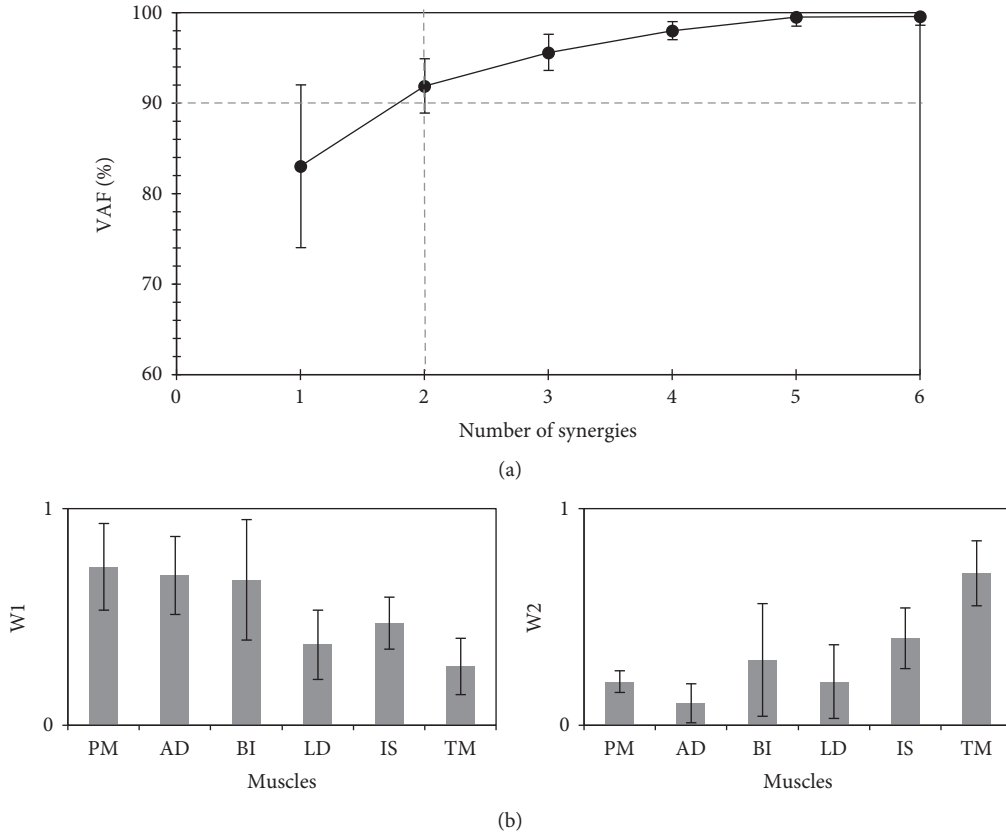


FIGURE 5: Synergy space after being adapted to the unfamiliar environment. (a) The variance accounted for (VAF) all possible identified synergies from the recorded electromyograph while performing the task in the *adaptation environment* (mean \pm SD, 9 participants). The dashed vertical line identifies the estimated number of utilized synergies that exceeded the threshold (90%; represented by the horizontal dashed line). (b) Muscle synergy vectors (W) in the two-dimensional synergies, *SyD.2*. PM: pectoralis major; AD: deltoid anterior; BI: biceps brachii; LD: latissimus dorsi; IS: infraspinatus; TM: teres major.

4.1. Features of Behavioral Adaptation in Healthy Participants. The experimental results in healthy participants revealed that the formation of muscle synergies is slightly altered when experiencing sudden changes in the familiar environment. The two-dimensional muscle synergies operating in the familiar environment were reduced to a single dimension when participants were first presented to the unfamiliar environment. However, this dimensionality reduction was accompanied by a simultaneous increase in muscle activations in response to the unfamiliar environmental inputs, suggesting that all muscles may be placed in a “standby” status, in order to promptly react to any unpredictable or unsafe input potentially occurring in the unseen environment/task, despite being energy inefficient. Nevertheless, our experiments show that training leads to a gradual adaptation to the new environment, resulting in the quick recovery of muscle synergy dimensionality to its original state. Moreover, the resulting energy consumption gradually decreases after the proper motor solutions are found. Note that the evaluation of the adaptation to the new environment, at this stage, was considered based on the computed muscle synergy of the healthy arm performing in a familiar environment.

The abovementioned findings are based on the assumption that movements required for the investigated task shared

a commonality across humans. While it is true that for some specific tasks, muscle synergy vectors could vary between individuals, for example, a bench press task at different velocities, Samani and Kristiansen [45], the investigated task and perturbation experiments in this study have led us to conclude that muscle synergy vectors adequately account for the EMG activity associated with elbow movements in the pool of investigated subjects. This is also coherent with prior findings that reported stereotyped patterns of motor modules or synergies underlying the control of this motor task in healthy humans, demonstrating complete muscle patterns for specified arm movement task goals [23, 46].

4.2. Features of Motor Recovery after Stroke. Instead of directly examining muscle synergies, the VAF level can be used as it also seems to encode motor impairments. Our results in poststroke patients showed a gradual decline in the VAF over the recovery period. This could be interpreted as an effort by the CNS to optimize arm movement by tuning possible motor solutions, similar to what happens in healthy participants dealing with unfamiliar environments. Notably, some patients showed recovery in the number of recruited muscle synergies, i.e., from one- to two-dimensional muscle synergies, and their clinical score also improved. These results suggest that the dimensionality of muscle synergy

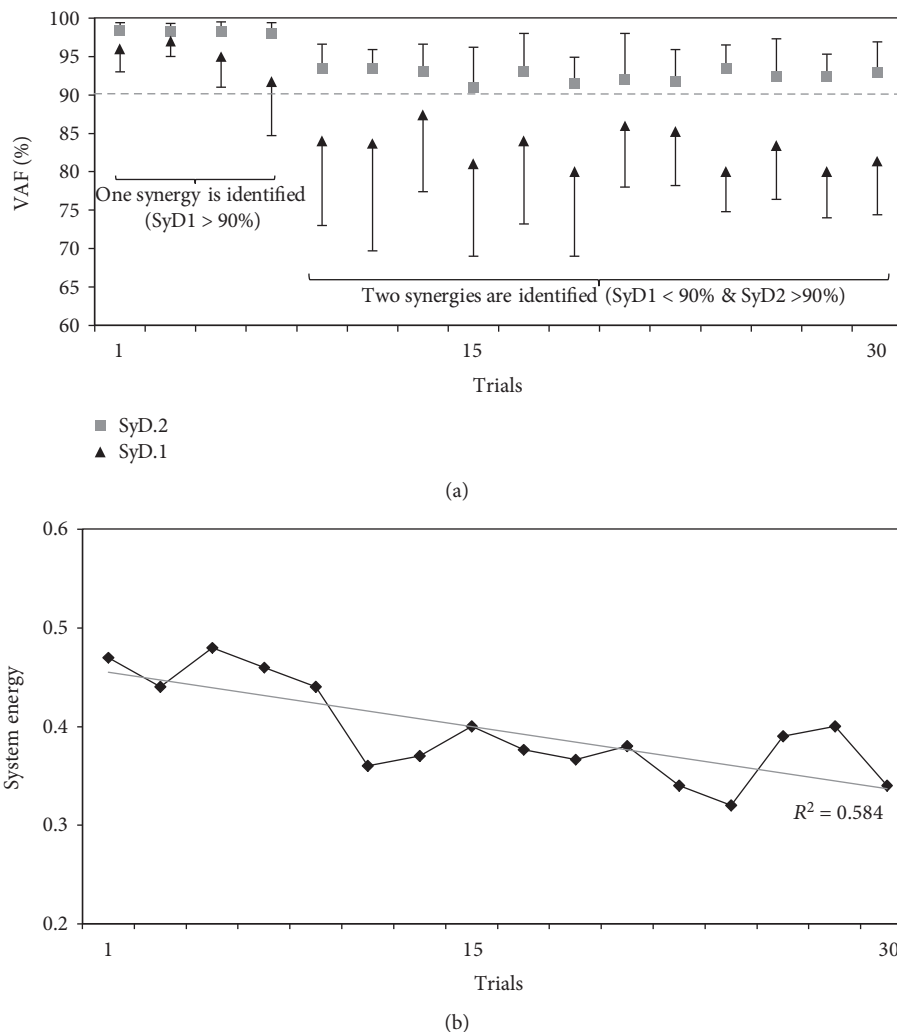


FIGURE 6: A gradual reduction in energy consumption as proper muscle synergies were recruited. (a) The gradual conversion of the one-dimensional synergy (SyD.1 > 90%) to two-dimensional synergies (SyD.1 < 90%) through training in the adaptive environment (mean \pm SD, 9 participants). (b) Changes in system energy through adaptation in the *adaptation environment*. Linear least-squares regression line ($R^2 = 0.5841$) to illustrate the adaptation direction. System energy was computed as the total muscle activation needed to complete a trial (mean, 9 participants). Greater muscle activations are associated with higher energy cost.

can be used to measure the level of motor function recovery. A similar conclusion was deduced in a study by Cheung et al. [40]. Note that at this stage, the recovery level was evaluated based on the computed muscle synergy from the intact arm of the same patient performing the same motor task.

4.3. Neurophysiological Interpretations of Adaptation and Recovery. The question of whether muscle synergy during stroke recovery is newly constructed or simply adapted from existing synergies is a long-standing debate in neuroscience [47]. Our results here suggest that muscle synergies during recovery from moderate stroke most likely represent an adaptation of existing synergies, similar to what occurs in healthy individuals when neurons adapt to an unfamiliar environment.

In this study, we found that both motor adaptation in healthy participants and recovery in poststroke patients have comparable features regarding synergy dimensionality.

Synergies in both cases varied as a function of the degree of control system adaptation to the environment. We postulate that, in healthy participants, the experience of the unfamiliar environment causes a temporal obstruction in CNS neural processes, as well as in muscles, which prevents the formation of efficient sets of muscle synergies, i.e., safety overcomes the efficiency. This can be inferred by the unregulated muscle activities and reduction in utilized muscle synergy dimensions. Similarly, in poststroke patients, lower dimension synergies operate in the stroke-affected arm than in the intact arm. Over time, however, we found that the dimensions of utilized synergies gradually increase in both healthy and poststroke participants, leading to the emergence of efficient motions.

4.4. Recruitment Strategies of Muscle Synergies and Internal Model Uncertainty. Behavioral studies have shown that the CNS employs various strategies during interaction with the

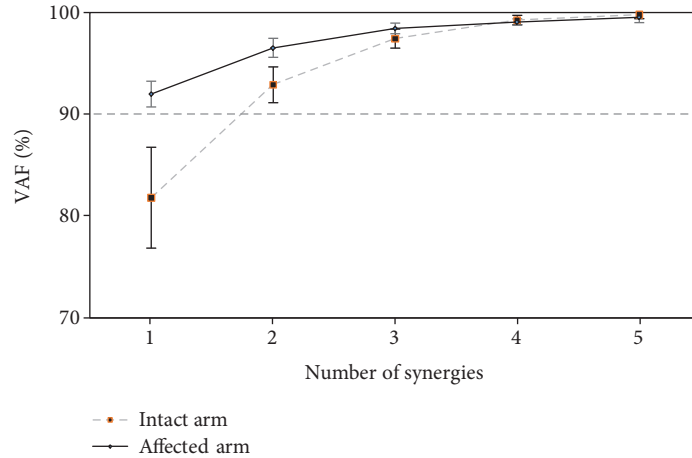


FIGURE 7: The variance accounted for (VAF) (%) all possible identified synergies from the recorded electromyograph while performing the task using the stroke-affected or intact arm, collected from ten patients with moderate stroke (mean \pm SD). One-dimensional synergy ($SyD.1 > 90\%$) is identified from the affected arm, while two-dimensional synergies ($SyD.1 < 90\%$ and $SyD.2 > 90\%$) are identified from the intact arm of the patients.

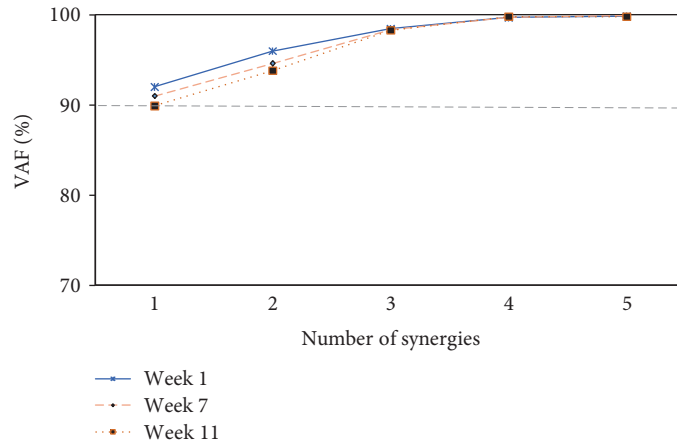


FIGURE 8: Muscle synergy dimensionality captures motor recovery. The variance accounted for (VAF) (%) all possible identified synergies from the recorded EMG while performing the task using the stroke-affected arm. Data were collected from 10 patients with moderate stroke (mean) at weeks: 1, 7, and 11 poststroke. The figure showing the gradual reduction of the one-dimensional synergy ($SyD.1$) towards the two-dimensional synergies ($SyD.2$) throughout the recorded period (mean \pm SD), i.e., $SyD = 1$ has moved towards < 90 VAF at week 11 (VAF = 89.8) compared to week 1 (VAF = 92). Thus, $SyD = 2$ became the representation of the recorded movement at week 11 instead of $SyD = 1$.

environment to ensure the best possible protection for the body with the lowest possible energy consumption [48, 49]. Hypothetically, these strategies are mainly chosen depending on the accuracy of existing internal models representing the surrounding environment. For instance, accreditation to anticipatory movements is higher, when the internal model is properly trained and the environment is stable and predictable. In contrast, compensatory and energy consuming reflex movements increase, when the internal model is tacitly inaccurate due to an unstable environment [48]. Other behavioral studies on limb postural control have shown that the activities of muscles around a joint can be modulated to minimize the perturbing effects of unknown external loads [50, 51]. These modulations gradually decrease over the course of learning a novel motor task [48, 52].

The abovementioned literature findings are consistent with our results. In our experimental conditions, both the behaviors observed in the modified environment (healthy participants) and in the initial stage of rehabilitation (post-stroke participants) can be regarded as pure compensatory movements in response to the new environmental condition, i.e., different dynamics of arm motion in healthy participants and different neural pathways in poststroke patients. However, these compensatory movements gradually change to anticipatory movements through training and interaction with the environment. The anticipatory movements correlate with the tuned muscle synergies, which interact efficiently with the familiar environment. In the unfamiliar environment, however, the simultaneous increase of muscle activities, although energetically expensive, may reflect a

compensatory strategy to overcome the yet untrained internal model. These otherwise inefficient muscle activities gradually decrease over the course of interaction with the environment. In line with our findings, Kawato et al. [53] argued that the alteration of muscle activities when first learning new skills is effective in learning schemes that take advantage of motor command errors resulting from the feedback controller as learning signals during building of internal models.

4.5. Towards Neurorehabilitation. Currently, most muscle synergy studies are limited to offline synergy analysis, which focuses on classifying motor skill or impairment levels. To move beyond this stage and towards real application for rehabilitation, a better understanding of synergy usage during learning and adaptation is required. Testing various training hypotheses directly in poststroke patients can be a complicated task, due to the age of typical stroke patients and related factors. Our muscle synergy analysis results suggest that motor function recovery in poststroke patients is comparable to adaptation to unfamiliar environments in healthy participants. A natural next step would be to investigate the introduction of multiple unfamiliar tasks, i.e., build a stroke-like scenario in healthy participants, and test various training/rehabilitation protocols to determine ways to enhance the adaptation process, before using such protocols in poststroke patients.

In our protocol, we tried to avoid/reduce muscle fatigue; although this might not be fully possible, especially in the case of more demanding scenarios (e.g., during repetitive training tasks for poststroke treatment), it should be noted that muscle fatigue reduces strength and increases perceived effort, as observed in joint kinematics and movement complexity analyses in healthy individuals [54]. However, these changes due to muscle fatigue do not reflect alterations in the overall principal component shape [55, 56]. In contrast, our results are in agreement with prior results by Simkins et al. [57], demonstrating that differences between joint movements in pathological conditions are comparable to the differences observed for able-bodied movement synergies, further supporting the hypothesis that altered synergies upon neurological injury are an expression of similar spinal mechanisms, as those regulating intact synergies in multi-joint movements. Furthermore, in their work, Simkins and colleagues [57] argue that alterations in pathological synergies during rehabilitation are shaped by plasticity at the spinal level. Interestingly, Jacobs et al. [58] discussed that, in tasks requiring high cortical involvement, the effect of training on the organization of intact muscle synergies is expressed with changes in modular organization, while in more basic, automated movements (e.g., walking), requiring less cortical activity, no changes in synergy number and structure are found. Equivalently, Torres-Oviedo et al. [22] investigated synergy organization during postural control (e.g., during walking) and showed that synergy robustness does not depend on reflex pathways or from biomechanical task constraints. In agreement with Krishnamoorthy et al. [59], our results demonstrate that muscle synergies and their organization are specific to the task, since they change with

changes in stability conditions and new muscle synergies emerge to account for changes in postural responses.

5. Conclusion

The goal of our study was to explore the computational mechanism behind behavioral adaptation in humans when encountering an unfamiliar environment and how it compares to behavioral recovery in poststroke patients. Uncovering this mechanism would enhance our understanding of motor control and recovery and offer guidance to develop new rehabilitation approaches for various neural disorders. These results suggest that the CNS monitors the familiarity of the internal model with the surrounding environment and, relying on that, predicts the suitable motor control strategy by tuning muscle synergy dimensionality. When the internal models are immature, the CNS utilizes more muscles with high activities, by recruiting fewer synergies, to compensate for unexpected interactions with unfamiliar environments. These extra utilized muscles may work as an additional neural feedback to update the internal model. When learning occurs and the internal model representations are built up, the CNS decreases the movement energy by increasing the recruited muscle synergies.

We conclude that abnormal muscle patterns in poststroke patients are similar to the patterns observed at the beginning of neuronal network adaption in new environments. Changes in muscle synergy can be used as an indicator of motor function recovery, as indicated by our experiments in healthy participants and also supported by prior results as a valid source to design metrics to quantify acquisition of motor skills in healthy humans [26]. We are currently developing an advanced rehabilitation system with an online assistive robot that takes into account patient pathology and interindividual synergy variability to support motor function recovery. Future studies are required to examine in more detail how muscle synergies are recruited over the course of complex and continuous movements, such as learning a sequence of whole-body movements while driving a car or riding a bike. Such understanding may not only enable finding new synergy-based indices indicating the level of motor impairment in poststroke patients but also predict their recovery level along with their rehabilitation.

Data Availability

The recorded electromyography data from both healthy and stroke patients used to support the findings of this study are available from the corresponding author upon request.

Conflicts of Interest

The authors declare that this work was conducted in the absence of any commercial and/or financial relationships that could be construed as any potential conflict of interest.

Acknowledgments

We are very grateful for the technical and financial assistance of Toyota Motor Co.

References

- [1] R. West and L. Turner, *Introducing Communication Theory: Analysis and Application*, McGraw-Hill, New York, NY, USA, 2009.
- [2] H. Markram and M. Tsodyks, "Redistribution of synaptic efficacy between neocortical pyramidal neurons," *Nature*, vol. 382, no. 6594, pp. 807–810, 1996.
- [3] F. S. Chance, S. B. Nelson, and L. F. Abbott, "Synaptic depression and the temporal response characteristics of V1 cells," *Journal of Neuroscience*, vol. 18, no. 12, pp. 4785–4799, 1998.
- [4] M. A. Castro-Alamancos, "Different temporal processing of sensory inputs in the rat thalamus during quiescent and information processing states in vivo," *Journal of Physiology*, vol. 539, no. 2, pp. 567–578, 2002.
- [5] L. A. Grade and W. J. Spain, "Synaptic depression as a timing device," *Physiology*, vol. 20, no. 3, pp. 201–210, 2005.
- [6] F. Alnajjar, Y. Yamashita, and J. Tani, "The hierarchical and functional connectivity of higher-order cognitive mechanisms: neurorobotic model to investigate the stability and flexibility of working memory," *Frontiers in Neurorobotics*, vol. 7, no. 2, 2013.
- [7] F. Alnajjar, M. Itkonen, V. Berenz, M. Tournier, C. Nagai, and S. Shimoda, "Sensory synergy as environmental input integration," *Frontiers in Neuroscience*, vol. 8, p. 436, 2015.
- [8] J. P. Swazey, *Reflexes and Motor Integration: Sherrington's Concept of Integrative Action*, Harvard University Press, 1969.
- [9] S. Shimoda and H. Kimura, "Bio-mimetic approach to tacit learning based on compound control," *IEEE Transactions on Systems, Man, and Cybernetics, Part B (Cybernetics)*, vol. 40, no. 1, pp. 77–90, 2010.
- [10] R. J. Tanaka and H. Kimura, "Mathematical classification of regulatory logics for compound environmental changes," *Journal of Theoretical Biology*, vol. 251, no. 2, pp. 363–379, 2008.
- [11] S. Shimoda, Y. Yoshihara, and H. Kimura, "Adaptability of tacit learning in bipedal locomotion," *IEEE Transactions on Autonomous Mental Development*, vol. 5, no. 2, pp. 152–161, 2013.
- [12] M. L. Minsky and S. A. Papert, *Perceptrons*, MIT Press, 1969.
- [13] A. G. Barto, R. S. Sutton, and C. W. Anderson, "Neuronlike adaptive elements that can solve difficult learning control problems," *IEEE Transactions on Systems, Man, and Cybernetics*, vol. SMC-13, no. 5, pp. 834–846, 1983.
- [14] R. A. Brooks, "A robust layered control system for a mobile robot," *IEEE Journal of Robotics and Automation*, vol. 2, no. 1, pp. 14–23, 1986.
- [15] Y. Kuniyoshi, Y. Yorozu, S. Suzuki et al., "Emergence and development of embodied cognition: a constructivist approach using robots," *Progress in Brain Research*, vol. 164, pp. 425–445, 2007.
- [16] F. Alnajjar and K. Murase, "A simple *aplysia*-like spiking neural network to generate adaptive behavior in autonomous robots," *Adaptive Behavior*, vol. 16, no. 5, pp. 306–324, 2008.
- [17] N. A. Bernstein, *The Coordination and Regulation of Movements*, Pergamon Press, 1967.
- [18] A. K. Saha, A. K. Das, and S. K. Dutta, "Mechanism of shoulder movements and a plea for the recognition of "zero position" of glenohumeral joint," *Clinical Orthopaedics and Related Research*, vol. 173, pp. 3–10, 1983.
- [19] G. Cappellini, Y. P. Ivanenko, R. E. Poppele, and F. Lacquaniti, "Motor patterns in human walking and running," *Journal of Neurophysiology*, vol. 95, no. 6, pp. 3426–3437, 2006.
- [20] V. C. K. Cheung, A. d'Avella, M. C. Tresch, and E. Bizzi, "Central and sensory contributions to the activation and organization of muscle synergies during natural motor behaviors," *The Journal of Neuroscience*, vol. 25, no. 27, pp. 6419–6434, 2005.
- [21] Y. P. Ivanenko, G. Cappellini, N. Dominici, R. E. Poppele, and F. Lacquaniti, "Coordination of locomotion with voluntary movements in humans," *Journal of Neuroscience*, vol. 25, no. 31, pp. 7238–7253, 2005.
- [22] G. Torres-Oviedo, J. M. Macpherson, and L. H. Ting, "Muscle synergy organization is robust across a variety of postural perturbations," *Journal of Neurophysiology*, vol. 96, no. 3, pp. 1530–1546, 2006.
- [23] A. D'Avella, A. Portone, and F. Lacquaniti, "Superposition and modulation of muscle synergies for reaching in response to a change in target location," *Journal of Neurophysiology*, vol. 106, no. 6, pp. 2796–2812, 2011.
- [24] A. D'Avella and F. Lacquaniti, "Control of reaching movements by muscle synergy combinations," *Frontiers in Computational Neuroscience*, vol. 7, p. 42, 2013.
- [25] J. Gonzalez-Vargas, M. Sartori, S. Dosen, D. Torricelli, J. L. Pons, and D. Farina, "A predictive model of muscle excitations based on muscle modularity for a large repertoire of human locomotion conditions," *Frontiers in Computational Neuroscience*, vol. 9, p. 114, 2015.
- [26] F. Alnajjar, T. Wojtara, H. Kimura, and S. Shimoda, "Muscle synergy space: learning model to create an optimal muscle synergy," *Frontiers in Computational Neuroscience*, vol. 7, p. 136, 2013.
- [27] E. Chiovetto, B. Berret, I. Delis, S. Panzeri, and T. Pozzo, "Investigating reduction of dimensionality during single-joint elbow movements: a case study on muscle synergies," *Frontiers in Computational Neuroscience*, vol. 7, p. 11, 2013.
- [28] E. Chiovetto, L. Patanè, and T. Pozzo, "Variant and invariant features characterizing natural and reverse whole-body pointing movements," *Experimental Brain Research*, vol. 218, no. 3, pp. 419–431, 2012.
- [29] G. K. Wakkal, B. J. Kollen, and R. C. Wagenaar, "Therapy impact on functional recovery in stroke rehabilitation: a critical review of the literature," *Physiotherapy*, vol. 85, no. 7, pp. 377–391, 1999.
- [30] A. Costa, M. Itkonen, H. Yamasaki, F. Alnajjar, and S. Shimoda, "Importance of muscle selection for EMG signal analysis during upper limb rehabilitation of stroke patients," in *2017 39th Annual International Conference of the IEEE Engineering in Medicine and Biology Society (EMBC)*, pp. 2510–2513, Seogwipo, South Korea, July 2017.
- [31] N. Yang, Q. An, H. Yamakawa et al., "Clarification of muscle synergy structure during standing-up motion of healthy young, elderly and post-stroke patients," in *2017 International Conference on Rehabilitation Robotics (ICORR)*, London, UK, July 2017.
- [32] F. Alnajjar and S. Shimoda, "Muscle synergies indices to quantify the skilled behavior in human," in *Converging Clinical and*

- Engineering Research on Neurorehabilitation II*, J. Ibáñez, J. González-Vargas, J. Azorín, M. Akay, and J. Pons, Eds., vol. 15 of *Biosystems & Biorobotics*, pp. 959–963, Springer, Cham, 2016.
- [33] H. J. Hermens, B. Freriks, R. Merletti et al., “European recommendations for surface electromyography,” in *Results of the SENIAM Project. Signal Processing*, Roessingh Research and Development, Enschede, The Netherlands, 1999.
- [34] G. Wulf and C. H. Shea, “Principles derived from the study of simple skills do not generalize to complex skill learning,” *Psychonomic Bulletin & Review*, vol. 9, no. 2, pp. 185–211, 2002.
- [35] N. Chino, S. Sonoda, K. Domen, E. Saitoh, and A. Kimura, “Stroke impairment assessment set (SIAS),” in *Functional Evaluation of Stroke Patients*, N. Chino and J. L. Melvin, Eds., pp. 19–31, Springer, Tokyo, 1996.
- [36] K. Domen, S. Sonoda, N. Chino, E. Saitoh, and A. Kimura, “Evaluation of motor function in stroke patients using the stroke impairment assessment set (SIAS),” in *Functional Evaluation of Stroke Patients*, N. Chino and J. L. Melvin, Eds., pp. 33–44, Springer, Tokyo, 1996.
- [37] F. S. Alnajjar, V. Berenz, O. Ken-ichi et al., “Muscle synergy features in behavior adaptation and recovery,” in *Repair, Restore, Relieve – Bridging Clinical and Engineering Solutions in Neurorehabilitation*, vol. 7 of *Biosystems & Biorobotics*, pp. 245–253, Springer, Cham, 2014.
- [38] G. Torres-Oviedo and L. H. Ting, “Muscle synergies characterizing human postural response,” *Journal of Neurophysiology*, vol. 98, no. 4, pp. 2144–2156, 2007.
- [39] E. Bizzi, V. C. K. Cheung, A. d’Avella, P. Saltiel, and M. C. Tresch, “Combining modules for movement,” *Brain Research Reviews*, vol. 57, no. 1, pp. 125–133, 2008.
- [40] V. C. Cheung, A. Turolla, M. Agostini et al., “Muscle synergy patterns as physiological markers of motor cortical damage,” *Proceedings of the National Academy of Sciences of the United States of America*, vol. 109, no. 36, pp. 14652–14656, 2012.
- [41] S. Oyama, S. Shimoda, F. S. K. Alnajjar et al., “Biomechanical reconstruction using the tacit learning system: intuitive control of prosthetic hand rotation,” *Frontiers in Neurorobotics*, vol. 10, 2016.
- [42] W. A. Sparrow and K. M. Newell, “Metabolic energy expenditure and the regulation of movement economy,” *Psychonomic Bulletin & Review*, vol. 5, no. 2, pp. 173–196, 1998.
- [43] W. F. Mommaerts, “Energetics of muscular contraction,” *Physiology reviews*, vol. 49, no. 3, pp. 427–508, 1969.
- [44] J. P. Dewald, P. S. Pope, J. D. Given, T. S. Buchanan, and W. Z. Rymer, “Abnormal muscle coactivation patterns during isometric torque generation at the elbow and shoulder in hemiparetic subjects,” *Brain*, vol. 118, no. 2, pp. 495–510, 1995.
- [45] A. Samani and M. Kristiansen, “Inter- and intrasubject similarity of muscle synergies during bench press with slow and fast velocity,” *Motor Control*, vol. 22, no. 1, pp. 100–115, 2018.
- [46] A. d’Avella, L. Fernandez, A. Portone, and F. Lacquaniti, “Modulation of phasic and tonic muscle synergies with reaching direction and speed,” *Journal of Neurophysiology*, vol. 100, no. 3, pp. 1433–1454, 2008.
- [47] S. A. Safavynia, G. Torres-Oviedo, and L. H. Ting, “Muscle synergies: implications for clinical evaluation and rehabilitation of movement,” *Topics in Spinal Cord Injury Rehabilitation*, vol. 17, no. 1, pp. 16–24, 2011.
- [48] R. Osu, D. W. Franklin, H. Kato et al., “Short- and long-term changes in joint co-contraction associated with motor learning as revealed from surface EMG,” *Journal of Neurophysiology*, vol. 88, no. 2, pp. 991–1004, 2002.
- [49] P. L. Gribble, L. I. Mullin, N. Cothros, and A. Mattar, “Role of cocontraction in arm movement accuracy,” *Journal of Neurophysiology*, vol. 89, no. 5, pp. 2396–2405, 2003.
- [50] M. L. Latash, “Independent control of joint stiffness in the framework of the equilibrium-point hypothesis,” *Biological Cybernetics*, vol. 67, no. 4, pp. 377–384, 1992.
- [51] T. E. Milner, “Adaptation to destabilizing dynamics by means of muscle cocontraction,” *Experimental Brain Research*, vol. 143, no. 4, pp. 406–416, 2002.
- [52] K. A. Thoroughman and R. Shadmehr, “Electromyographic correlates of learning an internal model of reaching movements,” *Journal of Neuroscience*, vol. 19, no. 19, pp. 8573–8588, 1999.
- [53] M. Kawato, K. Furukawa, and R. Suzuki, “A hierarchical neural-network model for control and learning of voluntary movement,” *Biological Cybernetics*, vol. 57, no. 3, pp. 169–185, 1987.
- [54] A. Costa-Garcia, M. Itkonen, H. Yamasaki, F. Alnajjar, and S. Shimoda, “A novel approach to the segmentation of sEMG data based on the activation and deactivation of muscle synergies during movement,” *IEEE Robotics and Automation Letters*, vol. 3, no. 3, pp. 1972–1977, 2018.
- [55] H. Kogami, Q. An, N. Yang et al., “Effect of physical therapy on muscle synergy structure during standing-up motion of hemiplegic patients,” *IEEE Robotics and Automation Letters*, vol. 3, no. 3, pp. 2229–2236, 2018.
- [56] J. C. Cowley and D. H. Gates, “Proximal and distal muscle fatigue differentially affect movement coordination,” *PLoS One*, vol. 12, no. 2, article e0172835, 2017.
- [57] M. Simkins, A. B. Jacobs, N. Byl, and J. Rosen, “Stroke-induced synergistic phase shifting and its possible implications for recovery mechanisms,” *Experimental Brain Research*, vol. 232, no. 11, pp. 3489–3499, 2014.
- [58] D. A. Jacobs, J. R. Koller, K. M. Steele, and D. P. Ferris, “Motor modules during adaptation to walking in a powered ankle exoskeleton,” *Journal of Neuroengineering and Rehabilitation*, vol. 15, no. 1, p. 2, 2018.
- [59] V. Krishnamoorthy, M. L. Latash, J. P. Scholz, and V. M. Zatsiorsky, “Muscle modes during shifts of the center of pressure by standing persons: effect of instability and additional support,” *Experimental Brain Research*, vol. 157, no. 1, pp. 18–31, 2004.

Clinical Study

White Matter Biomarkers Associated with Motor Change in Individuals with Stroke: A Continuous Theta Burst Stimulation Study

K. P. Wadden ¹, **S. Peters** ², **M. R. Borich** ³, **J. L. Neva** ², **K. S. Hayward**^{2,4,5},
C. S. Mang ⁶, **N. J. Snow**¹, **K. E. Brown**⁷, **T. S. Woodward**^{8,9}, **S. K. Meehan** ¹⁰
and **L. A. Boyd** ^{2,11}

¹Faculty of Medicine, Memorial University of Newfoundland, St. John's, Canada

²University of British Columbia, Department of Physical Therapy, Vancouver, Canada

³Division of Physical Therapy, Department of Rehabilitation Medicine, Emory University School of Medicine, Atlanta, USA

⁴Stroke Division, Florey Institute of Neuroscience and Mental Health, University of Melbourne, Melbourne, VIC 3084, Australia

⁵NHMRC Centre of Research Excellence in Stroke Rehabilitation and Brain Recovery, Australia

⁶University of Regina, Faculty of Kinesiology and Health Studies, Regina, Canada

⁷Department of Clinical and Movement Neurosciences, University College London, London, UK

⁸University of British Columbia, Department of Psychiatry, Vancouver, BC, Canada

⁹BC Mental Health and Addictions Research Institute, Vancouver, BC, Canada

¹⁰Department of Kinesiology, University of Waterloo, Waterloo, Canada

¹¹University of British Columbia, Centre for Brain Health, Vancouver, Canada

Correspondence should be addressed to L. A. Boyd; lara.boyd@ubc.ca

Received 10 August 2018; Accepted 8 November 2018; Published 4 February 2019

Academic Editor: Sergio Bagnato

Copyright © 2019 K. P. Wadden et al. This is an open access article distributed under the Creative Commons Attribution License, which permits unrestricted use, distribution, and reproduction in any medium, provided the original work is properly cited.

Continuous theta burst stimulation (cTBS) is a form of noninvasive repetitive brain stimulation that, when delivered over the contralesional hemisphere, can influence the excitability of the ipsilesional hemisphere in individuals with stroke. cTBS applied prior to skilled motor practice interventions may augment motor learning; however, there is a high degree of variability in individual response to this intervention. The main objective of the present study was to assess white matter biomarkers of response to cTBS paired with skilled motor practice in individuals with chronic stroke. We tested the effects of stimulation of the contralesional hemisphere at the site of the primary motor cortex (M1c) or primary somatosensory cortex (S1c) and a third group who received sham stimulation. Within each stimulation group, individuals were categorized into responders or nonresponders based on their capacity for motor skill change. Baseline diffusion tensor imaging (DTI) indexed the underlying white matter microstructure of a previously known motor learning network, named the constrained motor connectome (CMC), as well as the corticospinal tract (CST) of lesioned and nonlesioned hemispheres. Across practice, there were no differential group effects. However, when categorized as responders vs. nonresponders using change in motor behaviour, we demonstrated a significant difference in CMC microstructural properties (as measured by fractional anisotropy (FA)) for individuals in M1c and S1c groups. There were no significant differences between responders and nonresponders in clinical baseline measures or microstructural properties (FA) in the CST. The present study identifies a white matter biomarker, which extends beyond the CST, advancing our understanding of the importance of white matter networks for motor after stroke.

1. Introduction

Incomplete recovery of movement from stroke has led to interest in adjunct interventions. One such intervention is noninvasive brain stimulation that, when paired with therapy, may augment the effects of rehabilitation [1–3]. Continuous theta burst stimulation (cTBS) is a patterned form of repetitive transcranial magnetic stimulation (rTMS) that can suppress excitability of the primary motor cortex (M1) [4]. Following a stroke, there is evidence that the contralesional cortex exerts increased inhibition on the ipsilesional cortex through interhemispheric signaling [5]. In individuals with stroke, cTBS applied over the contralesional hemisphere may modulate interhemispheric imbalances to the ipsilesional hemisphere [6]. However, a large degree of individual variability in response to repetitive noninvasive brain stimulation techniques has been observed [2, 7]. As a result, there is an important focus on investigating biological markers (“biomarkers”) that characterize “responders” and “nonresponders” of noninvasive brain stimulation [2, 7].

To date, most research has focused on regional white matter (WM) tracts [2, 7] as biomarkers of recovery after stroke. However, recovery from stroke involves a network of bihemispheric pathways that extend between the contralesional and ipsilesional motor cortices, secondary motor areas, and ipsilesional cerebellum [8]. In the current work, we hypothesized that characterizing a specialized WM motor network associated with motor learning would explain response to cTBS paired with motor skill practice in individuals with chronic stroke [9]. We employed functional magnetic resonance imaging- (fMRI-) guided tractography to constrain WM connections associated with our previously identified gray matter (GM) motor learning network associated with motor learning in healthy individuals [9]. We named the resultant network the “constrained motor connectome” (CMC) and hypothesized that individual capacity for motor learning-related change following cTBS paired with motor skill practice would relate to residual integrity in the CMC [9].

The primary motor and somatosensory cortices (M1 and S1, respectively) are two brain areas that support motor recovery [10]. Hyperexcitability from both the contralesional M1 and S1 (M1c, S1c) correlates with reduced poststroke motor function [11]. Yet, few studies have extended noninvasive brain stimulation sites beyond contralesional M1 [1, 3]. Meehan et al. [3] compared the effects of cTBS over contralesional M1 versus S1 paired with motor practice and found comparable improvements in movement time during motor skill practice. Regardless of stimulation site, both M1 and S1 stimulation groups showed larger amounts of motor learning-related change compared to sham stimulation paired with motor skill practice [3]. During repetitive TMS over M1, stimulation spread of 2–3 cm over the cortex from the centre of coil [12] as well as strong connections between M1 and S1 [13] have been observed. Therefore, based on similar effects of cTBS over M1c and to S1c previously observed on movement time [3], and the proximity of the locus of stimulation sites (i.e., 2 cm apart), we hypothesized that improvements in motor performance would be *similar* for the M1c and S1c stimulation.

The overarching objective of the current study was to test whether a new brain-based biomarker, termed the CMC, could identify the capacity to respond to cTBS over M1c/S1c paired with motor skill practice. We first studied the effect of cTBS over M1c or S1c paired with motor skill practice on motor learning. We discovered highly variable responses to this intervention. We next categorized individuals in the M1c and S1c groups into responders or nonresponders based on the extent of their behavioural change. Given a lack of difference between individuals in the M1c and S1c groups, and to maintain power to consider responder status, we next combined responders from the two stimulation groups (M1c and S1c) into a sensorimotor (SM) cTBS group; the same was done for the nonresponders. We hypothesized that the integrity of the CMC [9] would explain response to cTBS over the SM paired with motor skill practice.

2. Methods

2.1. Participants. Twenty-eight individuals (mean age = 63.0 years; standard deviation (SD) = 12.88 years; 7 females) who demonstrated chronic stroke-related unilateral upper limb deficits were recruited. All experimental sessions were completed at the University of British Columbia (UBC). Ethical approval was granted from the Clinical Research Ethics Board of UBC. All participants provided written informed consent in accordance with the Declaration of Helsinki.

Inclusion criteria were (1) chronic cortical or subcortical stroke (≥ 6 months ago), (2) upper-extremity Fugl-Meyer (UE-FM) motor impairment score greater than or equal to 15, and (3) a Montreal Cognitive Assessment (MoCA) score greater than or equal to 26 [14]. Exclusion criteria were (1) history of seizure/epilepsy, head trauma, a major psychiatric diagnosis, neurodegenerative disorder, or substance abuse; (2) taking any gamma-aminobutyric acid (GABA) ergic, N-methyl-D-aspartate (NMDA) receptor antagonist, or other drug known to influence the neural receptors that facilitate neuroplasticity; or (3) contraindication to transcranial magnetic stimulation (TMS) or magnetic resonance imaging (MRI).

2.2. Experimental Design. Participants were pseudo-randomly assigned to one of three stimulation groups: (1) M1c cTBS (contralesional primary motor cortex), (2) S1c cTBS (contralesional primary somatosensory cortex), or (3) sham cTBS over contralesional M1 (Figures 1(a) and 1(b)). Pseudo-randomization was accomplished using a custom computer program that assigned individuals to a stimulation group while accounting for age, sex, and Fugl-Meyer (FM) score to ensure even distribution (M1c, $n = 9$; S1c, $n = 11$; and sham, $n = 8$). The experimental protocol consisted of seven sessions over 14 days. There were never more than two days between sessions, and the retention session was performed within 24 hours of the last practice session (Figure 1). In session 1, participants underwent MR scanning, clinical assessments of motor function and impairment (Wolf Motor Function Test (WMFT) and FM, respectively), and baseline performance on the experimental motor learning task, the serial targeting task (STT). During sessions 2

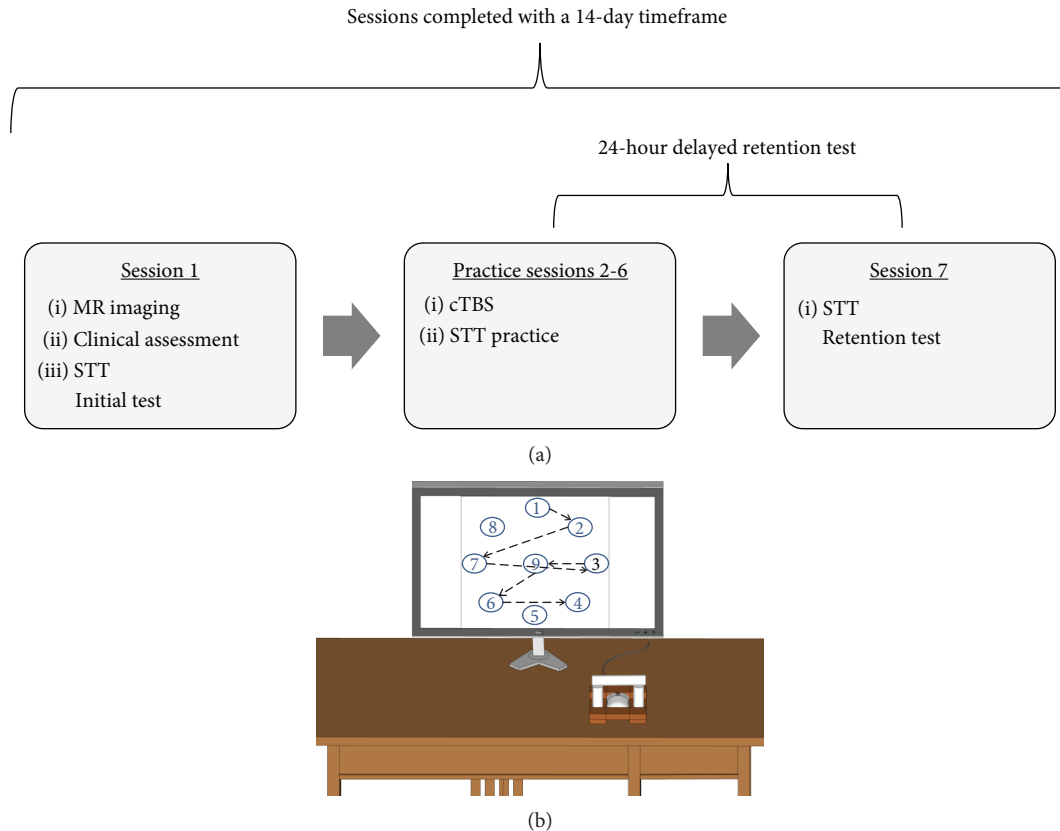


FIGURE 1: Experiment design and apparatus. (a) Experimental design and (b) serial tracking task (STT) apparatus and target locations.

to 6, participants received cTBS over the contralesional hemisphere according to the stimulation group (M1c, S1c, and sham) immediately before STT practice. In session 7, a no-cTBS STT retention test was employed to assess motor learning.

In session 1, to assess upper-extremity motor function, the WMFT was performed by a licensed physical therapist. Mean performance time to complete 15 items of the WMFT with the paretic and nonparetic arms was determined. Participants' WMFT rate was calculated to determine how many times an individual could complete the task continuously for 60 seconds (60 seconds divided by the performance time); if an individual could not perform the task in 120 seconds, a score of 0 was given [15]. In addition, individuals' physical impairment level was assessed via the upper-extremity (UE) FM scale (range 0-66; lower scores denote less paretic arm function). Participant characteristics are shown in Table 1.

2.3. Serial Targeting Task. Participants performed the STT seated. The paretic hand (pronated) was used to grasp a computer mouse (housed in a custom frame) to control the movements of an on-screen cursor (Wheel Mouse Optical, Microsoft Corporation, Redmond, Washington, USE). Individuals were instructed to move the cursor as quickly and accurately as possible to a series of sequentially appearing targets. The location of the participant's hand in space was occluded by an opaque surface affixed above the hand. Embedded within the series of targets was a repeated six-element sequence that was flanked by a six-element random

sequence. The participant performed four blocks of the STT during each practice session (2 to 6). Each block was comprised of nine random sequences that each contained six movements each, and eight repeated sequences that also contained six movements each. Participants performed one block of the STT in sessions 1 (baseline) and 7 (retention) to index motor learning [3].

2.4. Exponential Curve Fitting. The primary dependent measure was response total time (RTT). Participants' RTT was calculated as the time to initiate movement plus movement time. The sum RTT for all six movements within the repeated and random sequences was calculated separately. The RTT for repeated and random sequences in each block across the seven sessions (baseline, session 1; practice, sessions 2 to 6; and retention, session 7) of task performance for each participant was subsequently fit to separate exponential functions using the following equation [16, 17]:

$$E(\text{RTT}_N) = A + B e^{-\alpha N}. \quad (1)$$

$E(\text{RTT}_N)$ is the expected value of RTT on practice trial N . A is the expected values of RTT after practice has been completed (asymptote parameter). B is the expected change in RTT from session 1 to session 7 (change score parameter). Alpha (α) is the exponential motor skill acquisition rate parameter [18]. Our primary outcome measure was B , which reflects an individual's capacity for motor change. A custom MATLAB (Version R2013b, The

TABLE 1: Participant characteristics.

Participant	Stimulation group (M1c = 1; S1c = 2; sham = 3)	Lesion location (C = cortical; SC = subcortical)	MOCA	UE FM ^a	PSD ^b	Age
ST1	1	C	28.0	55.0	270.0	59.0
ST2	1	SC	26.0	63.0	37.0	50.0
ST3	1	SC	30.0	62.0	67.0	65.0
ST4	1	SC	26.0	56.0	94.0	64.0
ST5	1	SC	26.0	59.0	12.0	82.0
ST6	1	SC	23.0	41.0	196.0	46.0
ST7	1	SC	26.0	62.0	20.0	62.0
ST8	1	SC	26.0	16.0	22.0	57.0
ST9	1	SC	25.0	30.0	160.0	57.0
ST10	2	SC	25.0	59.0	82.0	67.0
ST11	2	C	27.0	60.0	142.0	73.0
ST12	2	SC	27.0	56.0	83.0	71.0
ST13	2	C	25.0	60.0	35.0	85.0
ST14	2	SC	29.0	62.0	81.0	76.0
ST15	2	SC	29.0	54.0	23.0	60.0
ST16	2	SC	24.0	7.0	94.0	57.0
ST17	2	C	21.0	62.0	24.0	55.0
ST18	2	SC	23.0	11.0	36.0	93.0
ST19	2	C	29.0	18.0	33.0	33.0
ST20	2	C	27.0	62.0	31.0	69.0
ST21	3	SC	28.0	23.0	41.0	63.0
ST22	3	SC	30.0	35.0	27.0	56.0
ST23	3	SC	28.0	58.0	20.0	71.0
ST24	3	SC	26.0	49.0	155.0	76.0
ST25	3	C	28.0	57.0	15.0	69.0
ST26	3	SC	24.0	61.0	18.0	79.0
ST27	3	SC	26.0	29.0	47.0	51.0
ST28	3	SC	21.0	57.0	27.0	83.0

C = cortical; M1c = contralesional primary motor cortex; PSD = poststroke duration; S1c = contralesional primary somatosensory cortex; SC = subcortical; UE FM = upper-extremity Fugl Meyer.

MathWorks Inc., Natick, Massachusetts, USA) script was used for all analyses.

2.4.1. Motor Practice Responder versus Nonresponder. The B score was used to differentiate between responders and non-responders. A positive B score reflects an individual's capacity for motor learning based on the performance plateau prediction, while a negative B score indicates an absence of motor learning-related change [19].

2.5. Transcranial Magnetic Stimulation Procedures. All participants were screened for contraindications to rTMS [20]. TMS was performed using Magstim Rapid² and Plus¹ magnetic stimulators and a 70 mm diameter air-cooled figure-of-eight coil (Magstim Co. Ltd., Whitland, Carmarthenshire, UK) on sessions 2 to 6. During all TMS procedures, participants were seated in a reclining chair with their hands placed in a relaxed position (elbow at 180 degrees flexion, forearm pronated). For all stimulation, coil positioning was continuously monitored using aBrainsight™ neuronavigation

system, which displayed each individual's T1-weighted MRI. The participants' motor hotspot (M1c) and resting motor threshold (RMT) were determined as the site that evoked a measurable MEP greater than or equal to 50 μ V peak-to-peak for 5 out of ten trials in the extensor carpi radialis (ECR) muscle, at the lowest stimulus intensity at rest. After identifying the ECR motor hotspot, the active motor threshold (AMT) was determined as the lowest intensity to evoke a 200 μ V MEP in at least five out of 10 TMS stimuli [21], while participants maintained a 20% maximal isometric voluntary hand grip contraction. Thereafter, cTBS was then applied with the participant at rest in the theta burst pattern of stimulation: three stimuli delivered at 50 Hz, grouped and delivered at 5 Hz, in continuous blocks for a total of 600 stimuli over 40 seconds [4] at an intensity of 80% AMT. Sham stimulation was performed with a dedicated coil that looked and sounded like active stimulation but did neither mimic the cutaneous sensation provided during active stimulation nor induce any current in the underlying cortex (Magstim Company Ltd.). Continuous TBS was delivered over the

determined M1c “hotspot” or two cm posterior to this location for S1c, consistent with previous work [1, 3], while sham was delivered over the M1c hotspot. Following cTBS completion on sessions 2 to 6, after a five-minute break, participants completed motor practice of the STT.

2.6. Magnetic Resonance Imaging Protocol. MR acquisition was conducted at the UBC MRI Research Centre on a Philips Achieva 3.0 T whole-body MRI scanner (Phillips Healthcare, Andover, Massachusetts) using an eight-channel sensitivity encoding head coil (SENSE factor = 2.4) and parallel imaging.

2.6.1. Anatomical Scan. A high-resolution T1-weighted anatomical scan (TR = 7.47 ms, TE = 3.65 ms, flip angle $\Theta = 6^\circ$, FOV = 256×256 mm, 160 slices, and 1 mm^3 isotropic voxel) was collected.

2.6.2. Diffusion-Weighted Magnetic Resonance Imaging (DW-MRI). One high-angular resolution diffusion imaging (HARDI) scan was performed using a single-shot echo-planar imaging (EPI) sequence (TR = 7096 ms, TE = 60 ms, FOV = 224×224 mm, 70 slices, and voxel dimensions = $2.2 \times 2.2 \times 2.2 \text{ mm}^3$). Diffusion weighting was applied across 60 independent noncollinear orientations ($b = 700 \text{ s/mm}^2$), along with five unweighted images ($b = 0 \text{ s/mm}^2$). Diffusion-weighted images (DWIs) were corrected for motion and distortion using the software package ExploreDTI v4.2.2 (<http://www.exploredti.com>; [22]). During motion and distortion correction, signal intensity was modulated and the b -matrix was rotated [22].

2.6.3. Corticospinal Tract (CST). Diffusion-weighted images were analyzed using ExploreDTI. All images remained in native space. At each voxel of the CST, constrained spherical deconvolution-based deterministic whole-brain fiber tractography was initiated using the following parameters: seedpoint resolution of 2 mm^3 , 0.2 mm step size, maximum turning angle greater than 40° , and fiber length range of 50 to 500 mm [23]. We used a constrained spherical deconvolution approach to analyze known pathways of the corticospinal tract (CST), to ensure the inclusion of all tracts where we could manually control their inclusion and exclusion and reduce false positives (see Figure 2 for methods).

2.6.4. Constrained Motor Connectome (CMC). Data from the CMC were first transformed into Montreal Neurological Institute Space. DTI analyses were completed using ExploreDTI. DTI is recommended when long-range axonal connectivity is of interest [24]. Therefore, for the CMC analysis we used the more conservative DTI tractography approach as we had no a priori guidelines to identify tracts within this motor network. At each voxel of the CMC, DTI-based deterministic whole-brain fiber tractography was initiated using the following parameters: seedpoint resolution of 2 mm^3 , FA threshold 0.2, 0.2 mm step size, maximum turning angle greater than 40° , and fiber length range of 50 to 500 mm. FA values, the most commonly reported measure of white matter microstructural integrity after stroke, were extracted from reconstructed tracts and used

for statistical analyses [25]. FA is a quantitative, unit-less measure of diffusion behaviour of water in the brain; a value of zero indicates diffusion of water as isotropic, and a value of one specifies a preferred direction of diffusion along one axis [26].

We used a previously defined functional motor network associated with motor learning in healthy individuals [9]. Selected binary masks of cortical GM clusters of activation were used as ROIs for WM tractography. Each of the four clusters encompassed multiple brain regions. Cluster one included the primary somatosensory cortex, motor cortex, precentral gyrus, bilaterally, and the right intraparietal, superior parietal, and inferior parietal cortices. Cluster two included lobule V, VI, VIIa, and VIIb of the cerebellum, bilaterally. Cluster three included right lobule VI and VIIa Crus of the cerebellum. Cluster four included left intraparietal and superior parietal cortices (Table 2 and Figure 2(b), b1). The GM cortical clusters from the functional motor network were derived from a whole-brain connectivity analysis in MNI space, allowing for the clusters of activation from the fMRI connectivity analysis to be overlaid on the DW images converted to MNI space. The functional motor network ROIs were used to isolate the underlying WM fiber tracts of the CMC (Figure 2(b), b1).

2.7. Statistical Analyses. Four main investigative steps were performed. These included (1) determining the effect of stimulation group (M1c, S1c, and sham) on motor sequence learning, (2) separating individuals into motor practice responders and nonresponders using the B score, (3) assessing differences in demographic and clinical measures between motor practice responders and nonresponders for the SMC-cTBS group, and (4) testing for differences in WM biomarkers between motor practice responders and nonresponders for the SMC-cTBS group.

2.8. Differences in Motor Sequence Learning between cTBS Groups in Individuals with Stroke during Practice and Retention

2.8.1. Baseline Performance. Session 1 (baseline) motor performance on the random and repeated sequences was evaluated with a two-factor GROUP (M1c, S1c, and sham) \times SEQUENCE (repeated, random) mixed-model analysis of variance (ANOVA) with mean RTT as the dependent variable.

2.8.2. Practice Performance. Performance of the repeated and random sequences during cTBS paired with motor skill practice (sessions 2 to 6) was examined using a three-factor GROUP (M1c, S1c, and sham) \times SEQUENCE (repeated, random) \times SESSION (sessions 2 to 6) mixed-model ANOVA with mean RTT as the dependent variable. There were two missing data points for practice days for two participants in the sham group ($n = 6$).

2.8.3. Retention Performance. To assess motor sequence learning at retention (session 7), a two-factor GROUP (M1c, S1c, and sham) \times SEQUENCE (repeated, random)

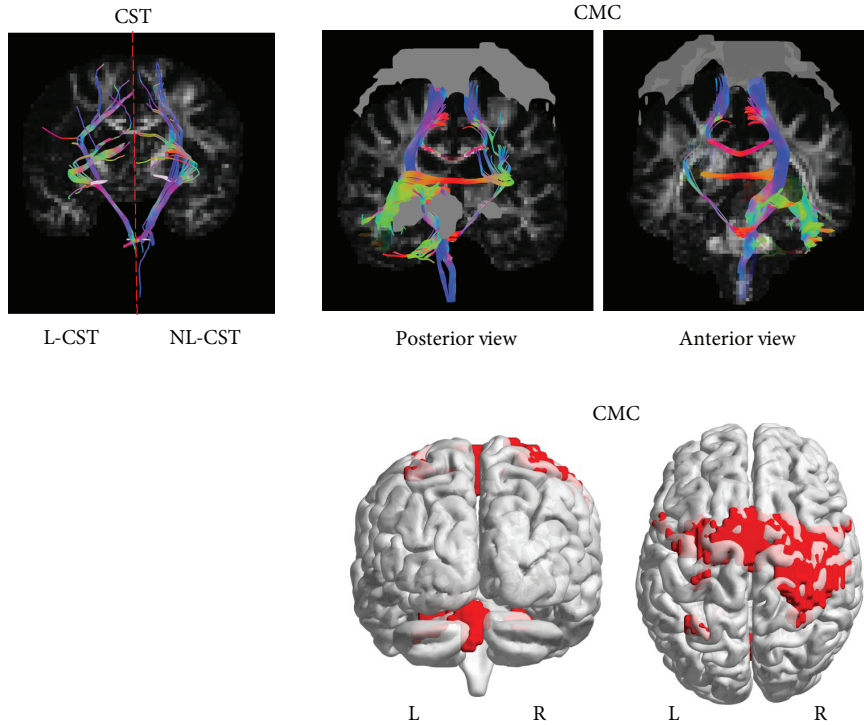


FIGURE 2: (a, b_1 , and b_2) Diffusion tensor imaging. Fractional anisotropy (FA) maps were created for individuals, followed by whole-brain tractography. This is an example of a single subject with a left hemispheric lesion. (a) Regions of interest (ROIs) for the nonlesioned (NL) and lesioned (L) corticospinal tracts (CST) were manually drawn on the native DW image, followed by tractography. The first cross-sectional ROI for the CST was delineated bilaterally (NL-CST and L-CST) in the axial plane [52]. First, a “SEED” ROI was constructed around the PLIC at the level of the anterior commissure [53]. Second, a logical “AND” ROI was constructed around the CST at the level of the mid-pons [54]. The “AND” function constrained the reconstruction to fibers passing through both the “SEED” and “AND” ROI. (b_1) The functional motor network mask (gray ROIs) was extracted and overlaid on the DW MNI image, followed by tractography of the CMC (posterior and anterior views). (b_2) The motor network mask (represented in red) was overlaid on the diffusion-weighted image to create the constrained motor connectome (CMC).

TABLE 2: Constrained motor connectome.

CMC	MNI coordinates ($X Y Z$)	mm^2
Right postcentral gyrus	36 -28 70	4171
Left cerebellum (V)	-16 -52 -22	704
Left superior parietal lobule	-32 -56 62	124
Right cerebellum (VI)	-26 -60 -26	114

The areas of the motor learning network were used as regions of interest, overlaid on diffusion-weighted images prior to tractography.

mixed-model ANOVA was performed with mean RTT as the dependent variable.

2.9. Effect of cTBS on Motor Sequence Learning for Motor Practice Responders. Motor practice responders were identified as individuals who demonstrated a positive B ($B > 0$) score for repeated sequences, and nonresponders were identified as individuals who demonstrated a negative B score ($B < 0$) (see Figure 3 for subject-specific examples). We tested the effect of stimulation (M1c, S1c, and sham) on performance for the *motor practice responder group*. Based on our hypothesis that there would be similarities between the effect of cTBS over M1c and S1c on RTT, we performed a planned

independent t -test on the B score between M1c and S1c groups for motor practice responders.

We had an a priori hypothesis that groups receiving inhibitory stimulation over the contralesional hemisphere (M1c, S1c groups) would demonstrate *greater* improvements in motor performance compared to individuals receiving sham stimulation (sham group) [3, 27–31]. To evaluate the effects of receiving stimulation, M1c and S1c groups were combined into a contralesional sensorimotor (SMc-cTBS group) group. To evaluate the effects of receiving active cTBS stimulation over SMc compared to sham stimulation, we performed a planned one-tailed independent t -test on B score between SMc-cTBS and sham groups for motor practice responders.

2.9.1. Clinical Measures for Motor Practice Responders and Nonresponders. To investigate whether differences existed in clinical measures between responders and nonresponders, we conducted independent group t -tests to assess differences in demographic and clinical characteristics. Demographic and clinical dependent variables included age, poststroke duration, UE-FM score, and paretic WMFT rate. Fisher’s exact test was used to assess differences between motor practice responders and nonresponders in stroke location

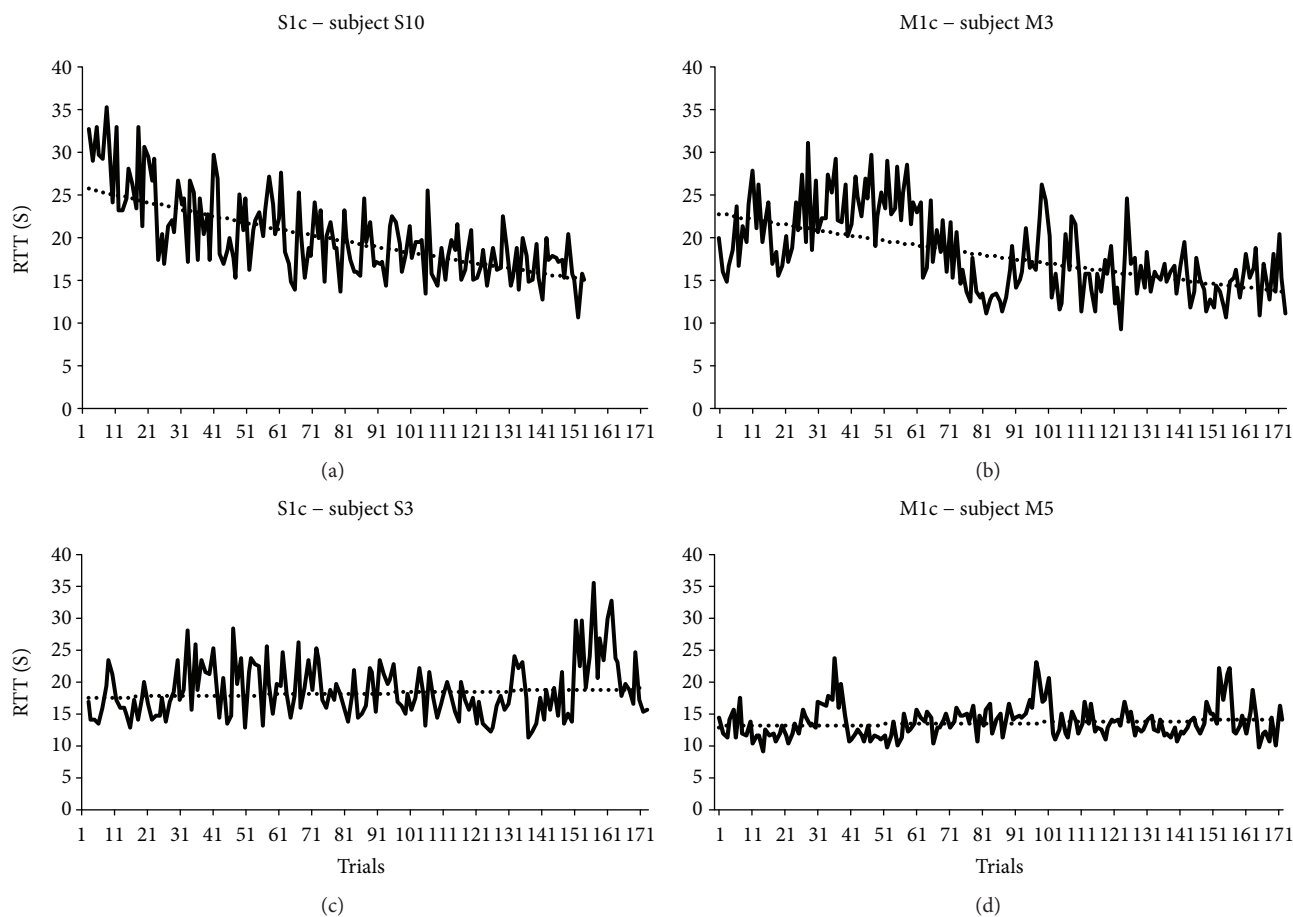


FIGURE 3: (a, b, c, and d) Active cTBS motor practice responder and nonresponders. The top panel represents motor practice responders (positive B score) following contralesional cTBS, delivered over the primary somatosensory cortex (S1c; B score = 14.27; (a)) or primary motor cortex (M1c; B score = 12.30; (b)), paired with motor skill practice. The bottom panel represents motor practice nonresponders (negative b score) following contralesional cTBS, delivered over the primary somatosensory cortex (S1c; B score = -4.35; (c)) or primary motor cortex (M1c; B score = -1.76; (d)) paired with motor skill practice.

TABLE 3: Participant characteristics for motor practice responders and nonresponders in M1c, S1c, and sham groups.

Group	Stim group	Age (yr)		Stroke location (C, SC)	PSD (months)		UE FM		Paretic WMFT rate	
		Mean	SD		Mean	SD	Mean	SD	Mean	SD
Responders $n = 17$	M1c = 5	66.3	14.41	C = 5	75.8	73.45	46.8	20.08	38.7	17.42
	S1c = 7			SC = 12						
	Sham = 5									
Nonresponders $n = 11$	M1c = 4	63.7	11.34	C = 2	54.7	45.43	49.1	20.11	40.2	19.12
	S1c = 4			SC = 9						
	Sham = 3									

C = cortical; M1c = contralesional primary motor cortex; PSD = poststroke duration; S1c = contralesional primary somatosensory cortex; SC = subcortical; UE FM = upper-extremity Fugl Meyer; WMFT = Wolf Motor Function Test.

(cortical, C; subcortical, SC) for these individuals (Table 3; see Figure 4 for stroke locations).

2.9.2. WM Tractography for Motor Practice Responders and Nonresponders. A multivariate analysis of variance (MANOVA) was used to assess differences in WM-FA from the CMC and NL- and L-CST between motor practice responders and

nonresponders within the SMC-cTBS group (S1c, M1c). The dependent variables for the MANOVA were FA values for each ROI (CMC, and NL- and L-CST). *Post hoc* univariate ANOVAs were performed on significant ($p \leq 0.05$) MANOVAs.

In the event of a violation of sphericity (significant Mauchly's test, $p \leq 0.05$), the Greenhouse-Geisser correction was applied. Levene's test for equality of variances was used

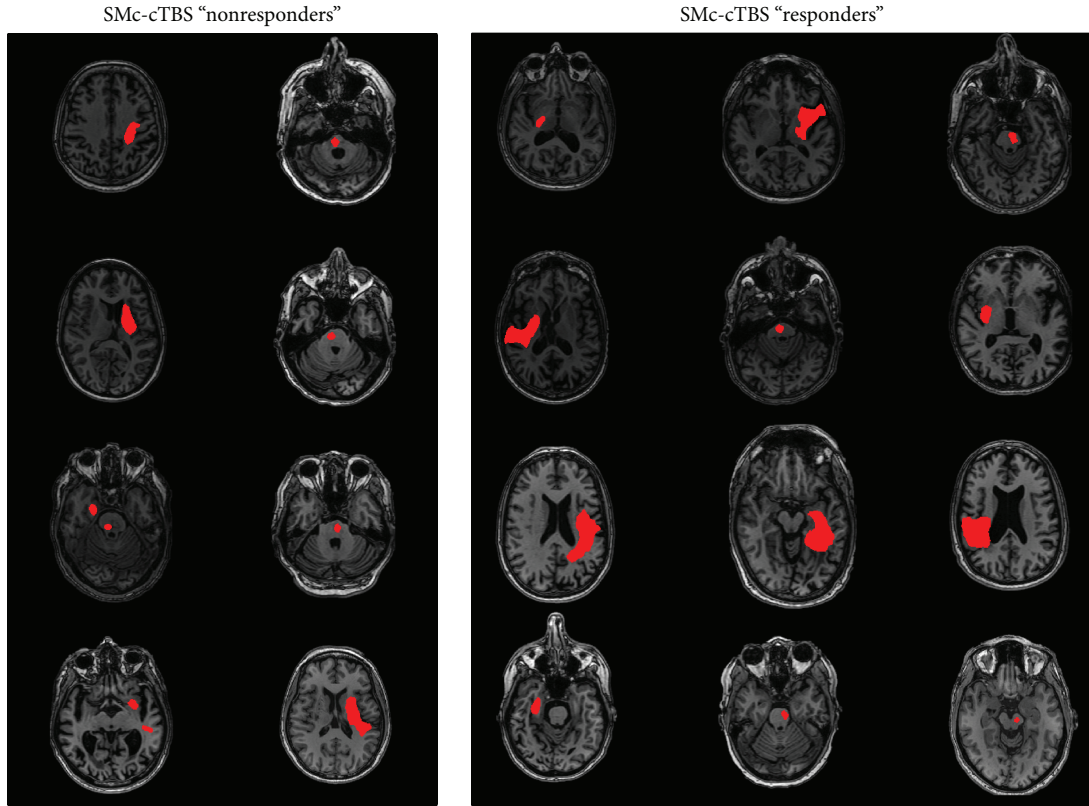


FIGURE 4: Lesion figure for M1c and S1c (sensorimotor- [SM]-) cTBS motor practice responders versus nonresponders.

to test for homogeneity of variance, and degrees of freedom were adjusted when the test was significant ($p \leq 0.05$). The 95% confidence intervals (CIs) of the mean difference (MD) were used to describe the effect of stimulation on improvements in motor performance (B score). Effect sizes were reported as partial eta-squared (η_p^2) where 0.01 is considered a relatively small effect, 0.06 moderate, and more than 0.14 a large effect [32]. Significance level for all statistical tests was set at $p \leq 0.05$, and post hoc tests, Bonferroni-corrected for multiple comparisons, were conducted when appropriate. Data are presented in the text as mean (M) plus or minus SD or standard error (SE). All statistical procedures were conducted using SPSS software (Version 21.0, IBM Corporation, Armonk, New York).

3. Results

3.1. Repeated versus Random Sequence Performance and Learning between cTBS Stimulation Groups

3.1.1. Baseline Performance. During initial STT performance (session 1), the random and repeated sequences trended towards, but were not, statistically different ($F_{(1,25)} = 4.09$, $p = 0.054$, $\eta_p^2 = 0.141$; Figure 5(a)). There was no baseline difference in performance level between groups (M1c, S1c, and sham) as shown by the lack of significant main effect of GROUP (M1c, S1c, and sham) ($F_{(2,23)} = 0.48$, $p = 0.63$, $\eta_p^2 = 0.037$). Additionally, there was no significant GROUP \times SEQUENCE interaction in session 1 ($F_{(2,23)} = 0.084$, $p = 0.92$, $\eta_p^2 = 0.007$).

3.1.2. Practice Performance. All groups (M1c, S1c, and sham) demonstrated improved motor performance on the STT, evidenced by an observed decrease in RTT across sessions 2 to 6 and a significant main effect of SESSIONS ($F_{(2.55,58.71)} = 4.51$, $p = 0.009$, $\eta_p^2 = 0.164$; Figure 5(b)). Mauchly's test indicated that the assumption of sphericity had been violated ($\chi^2(9) = 27.63$, $p = 0.001$); therefore, degrees of freedom were corrected using Greenhouse-Geisser estimate of sphericity ($\epsilon = 0.638$) for main effect of SESSIONS. In addition, individuals showed superior repeated ($M = 13.88$, $SE = 0.90$) compared to random sequence ($M = 15.59$, $SE = 0.99$) performance across practice sessions, as revealed by the significant main effect of SEQUENCE ($F_{(1,23)} = 19.63$, $p = 0.0019$, $\eta_p^2 = 0.46$). However, there was no main effect of GROUP (M1c, S1c, and sham) ($F_{(2,23)} = 0.066$, $p = 0.94$, $\eta_p^2 = 0.006$), no significant interaction for SEQUENCE \times SESSION ($F_{(4,92)} = 0.37$, $p = 0.83$, $\eta_p^2 = 0.016$), or for GROUP \times SEQUENCE ($F_{(2,23)} = 0.29$, $p = 0.749$, $\eta_p^2 = 0.025$).

3.1.3. Retention Test Performance. Motor learning-related change was shown by a main effect of SEQUENCE that confirmed all groups were faster for repeated ($M = 12.34$, $SE = 0.772$) compared to random sequence ($M = 14.20$, $SE = 0.861$) at retention ($F_{(1,25)} = 29.94$, $p < 0.001$, $\eta_p^2 = 0.55$; Figure 5(c)). However, the main effect of GROUP (M1c, S1c, and sham) ($F_{(2,25)} = 0.38$, $p = 0.68$, $\eta_p^2 = 0.030$) and the GROUP \times SEQUENCE interaction ($F_{(2,25)} = 0.64$, $p = 0.53$, $\eta_p^2 = 0.049$) were not significant.

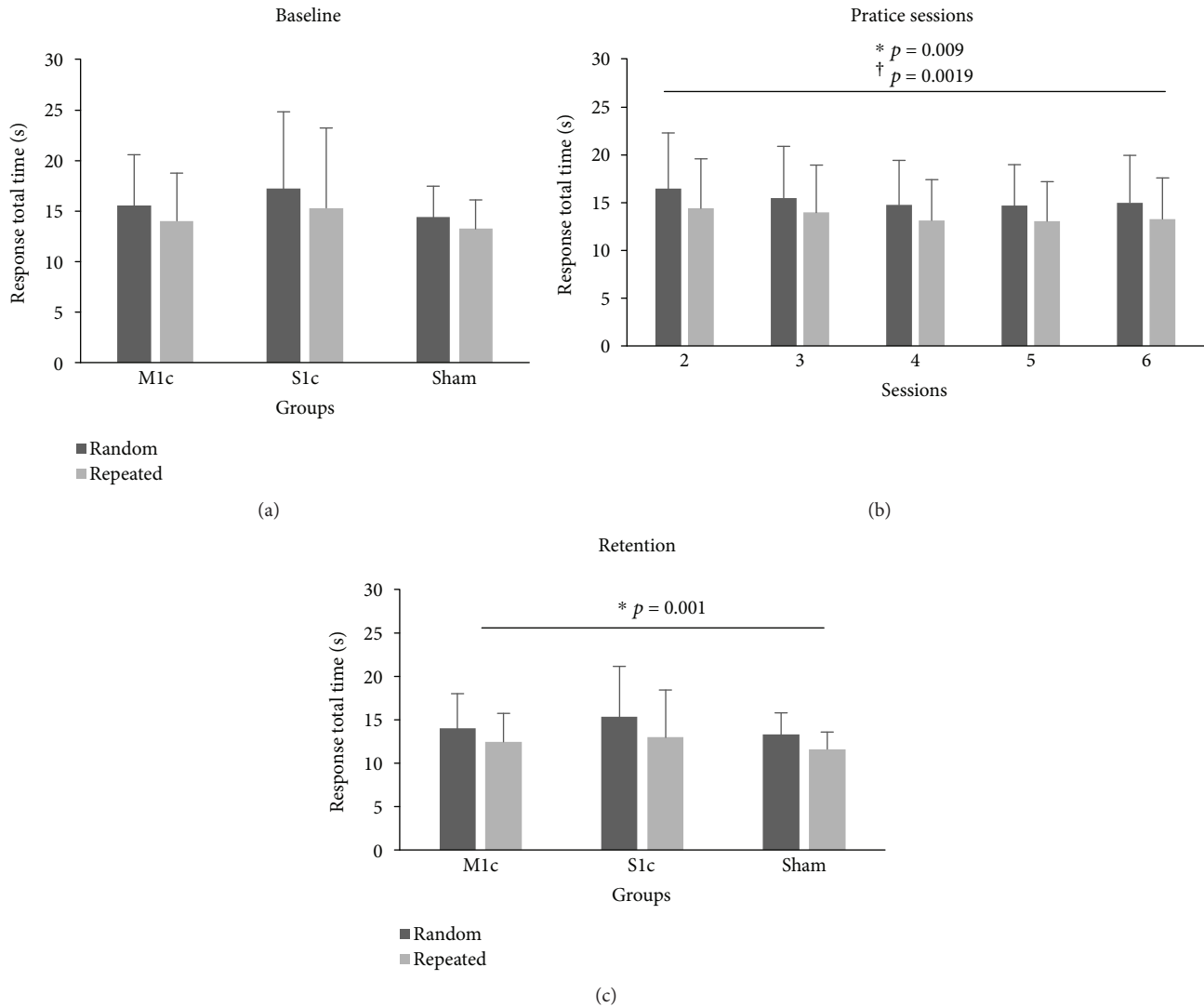


FIGURE 5: (a, b, and c) Mean response total time (RTT) for repeated and random sequences. Stimulation groups (M1c, S1c, and sham) demonstrated similar performances for repeated and random sequences on session 1 (baseline), 2 to 6, and 7 (retention). (a) All groups demonstrated initial faster RTTs for repeated compared to random sequence performance. (b) Collapsed across groups, all individuals demonstrated faster performance for repeated compared to random sequences across the five days of practice: $F_{(1,25)} = 29.94$, $p < 0.001$. (c) All groups demonstrated faster RTTs for repeated compared to random sequence during retention performance: $F_{(1,23)} = 19.63$, $p < 0.001$. Error bars are SD of the mean.

3.1.4. Motor Practice Responders. Overall, there were 17 motor practice responders and 11 nonresponders, as indicated by a positive B score for responders and a negative B score for nonresponders (M1c: 5 responders, 4 nonresponders; S1c: 7 responders, 4 nonresponders; and sham: 5 responders, 3 nonresponders) (see Figure 6 for normalized B score; normalization factor of $A + B$; A = asymptote value; B = change score). For motor practice responders, the first planned comparison showed no significant difference for B score between M1c ($M = 5.87$, $SD = 5.154$) and S1c ($M = 5.66$, $SD = 4.922$) groups for the performance of the repeated sequence ($t_{(10)} = 0.074$, $p = 0.94$, 95% CI $[-6.32, 6.76]$).

Following the amalgamation of M1c and S1c groups into the SMc-cTBS group, the second planned comparison demonstrated a significantly larger improvement in motor

performance (B score) for the SMc-cTBS group ($M = 5.74$, $SD = 4.784$) compared to the sham group ($M = 3.06$, $SD = 1.146$), $t_{(13.54)} = 1.82$, $p = 0.045$, 95% CI $[-0.48, 5.86]$.

3.1.5. Clinical Baseline Measures for the SMc cTBS Group. In the combined SMc-cTBS group, 12 of 20 participants responded positively to cTBS paired with motor skill training, as evidenced by a positive B score. When considering the individuals in the SMc-cTBS group, independent group t -tests and a Fisher's exact test (binary data for stroke location [C: 1; SC: 0]) demonstrated no significant differences in demographic (age: $t_{(18)} = 0.08$; $p = 0.93$) or clinical characteristics (stroke location: $p = 0.64$; PSD: $t_{(18)} = 0.70$, $p = 0.49$; UE-FM: $t_{(18)} = 0.25$, $p = 0.81$; and paretic WMFT

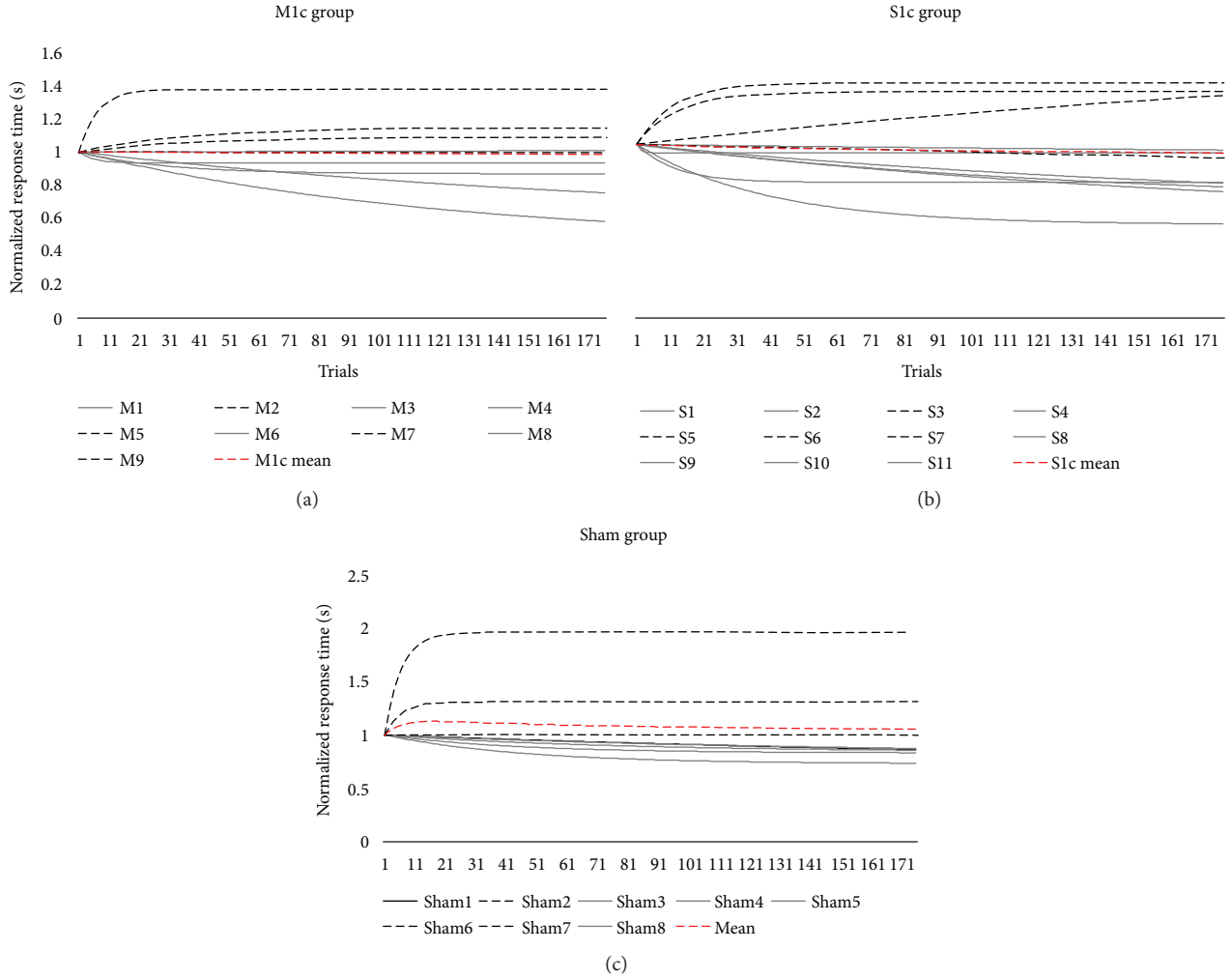


FIGURE 6: (a, b, and c) Motor skill acquisition curves for S1c, M1c, and sham stimulation groups. Single-subject normalized motor skill exponential curves for active cTBS stimulation groups (top panel) delivered over the contralesional primary somatosensory (S1c; (a)) and contralesional primary motor cortex (M1c; (b)) and for the sham stimulation group (bottom panel; (c)). Dotted black line indicates individuals with negative B scores and identified as motor skill nonresponders. Solid grey line indicates individuals with positive B scores and identified as motor practice responders. Dashed red line represents the mean motor skill acquisition curve for each stimulation group.

TABLE 4: Comparison (mean and SD) of responder versus nonresponder DWI characteristics in the SMc-cTBS group.

DWI	Responders		Nonresponders		F test $df_{(1,18)}$	p value
	Mean	SD	Mean	SD		
NL-CST	0.50	0.02	0.48	0.04	3.34	0.084
L-CST	0.42	0.08	0.46	0.05	0.94	0.345
CMC	0.48	0.01	0.46	0.01	7.69	0.013*

Significant effect of DW-FA between groups: Wilks' lambda = 0.62, $F_{(3,16)} = 3.24$, $p = 0.05$. Post hoc univariate tests revealed FA from tracts of the CMC ($F_{(1,18)} = 7.69$, $p = 0.013$) was significantly higher in responders versus nonresponders.

rate: $t_{(18)} = 0.44$, $p = 0.67$) between responders ($n = 12$) and nonresponders ($n = 8$).

3.1.6. White Matter Tractography for the SMc cTBS Group. In the combined SMc-cTBS group, following the GROUP (responder, nonresponder) \times WM-FA (NL-CST, L-CST, and CMC) MANOVA, there was a significant main effect of GROUP (responder, nonresponder) for WM-FA in NL-

and L-CST and CMC (Wilks' $\lambda = 0.62$, $F_{(3,16)} = 3.24$, $p = 0.05$, $\eta_p^2 = 0.38$). Post hoc univariate tests revealed that WM-FA from tracts within the CMC ($F_{(1,18)} = 7.69$, $p = 0.013$; see Table 4, Figure 7) were significantly higher (greater linear diffusion) in responders (CMC-FA: $M = 0.48$, $SD = 0.0149$) compared to nonresponders (CMC-FA: $M = 0.46$, $SD = 0.0113$). However, FA from the NL- and L-CST did not significantly differ between responders and nonresponders

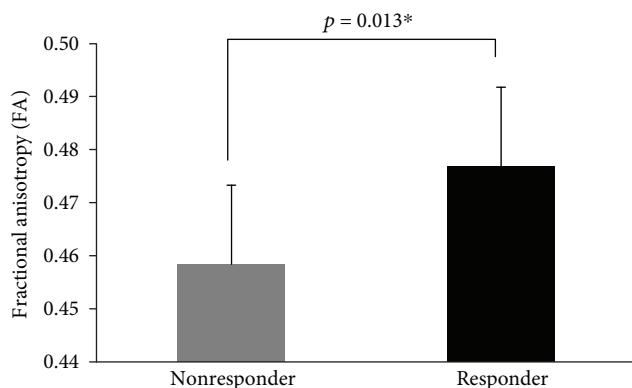


FIGURE 7: Comparison (mean [SD]) of responder versus nonresponder of CMC in the SM-cTBS group. Error bars represent SD.

($F_{(1,18)} \leq 3.34$, $p = 0.084$; see Table 4). Therefore, group differences in the microstructural integrity of the CMC network had higher predictive value than CST tracts (see Figure 8 for subject-specific examples of white matter tractography).

4. Discussion

We demonstrated that the residual white matter integrity of the CMC was significantly different between motor practice responders and nonresponders to contralesional cTBS paired with skilled motor practice. We showed that independent of receiving cTBS over the (1) contralesional primary motor cortex (M1c), (2) contralesional primary somatosensory cortex (S1), or (3) sham stimulation, individuals with chronic stroke demonstrated the ability to learn a motor sequence. This was supported by improved performance of both the repeated and random sequences at retention and lower RTTs for the repeated versus random sequence.

The lack of behavioural differences across stimulation groups is consistent with variable interindividual responses to noninvasive brain stimulation observed in previous studies [2, 7]. This finding motivated our investigation into a subgroup of “responders.” In the current work, motor practice responders who received cTBS (regardless of stimulation site) showed differences in RTT in comparison to data from individuals who underwent sham stimulation. However, similar to our past work [3], there was no motor learning-related difference between the two stimulation groups (see also [3, 13, 33]). This led us to combine the stimulation group and test whether a biomarker could be used to identify who would respond to cTBS paired with skilled motor practice. We discovered that the diffusivity properties of a network that has been previously identified as important for motor learning in healthy older adults, the CMC, also differed between responders and nonresponders.

Our finding, that a complex WM motor network (the CMC) is related to the responsiveness of individuals to cTBS paired with motor practice, extends previous findings, showing that greater anisotropy of white matter tracts is important in stroke recovery [1, 2, 34–36]. Similar to previous studies, responsiveness to noninvasive brain stimulation was not

explained by standard demographics, such as age, or stroke severity or paretic arm motor function [2, 7]. Contrary to prior literature, poststroke duration [37, 38], stroke location [39, 40], and corticospinal tract integrity [2, 7] did not characterize responsiveness to cTBS paired with motor practice. Inconsistency in measures that explain variability in response to noninvasive brain stimulation may reflect the lack of generalization between stimulation protocols (i.e., continuous versus intermittent TBS; brain region-stimulated [M1 versus S1]; contralesional versus ipsilesional hemisphere) [41]. To further the field of rTMS and poststroke recovery, future work is needed to define the specific impact of varying stimulation parameters and sites.

Following stroke, spared bihemispheric neuronal connections between direct pathways of the M1 and the CST, as well as indirect pathways such as the reticulospinal and/or rubrospinal, may contribute to positive capacity for motor change [8, 9, 42, 43]. Given the bihemispheric representation within the CMC, our findings may reflect the overlap between pathways in the CMC and those involved in interhemispheric signaling during cTBS stimulation and motor learning.

Our methodological approach for evaluating motor performance and stratifying responders and nonresponders was closely based on previous segregation procedures [2]. We employed a curve-fitting technique to categorize motor learning-related change from individual data across the entire practice period [17, 19]. Assessment of each individual’s capacity for motor learning-related change in this manner is not constrained to a predetermined set number of trials, but is based on the curvilinear pattern of performance change. As the field of stroke rehabilitation works to identify biomarkers, curve fitting presents a refined method for capturing behavioural states that could be applied to other interventions [44]. In the motor practice responder group (positive B score), there was a significant difference when comparing SM-cTBS stimulation with sham stimulation in change in response time. There was no difference between cTBS groups (M1c, S1c). Improvements in the performance of complex motor skills involve broad networks and strengthened connections between the sensory and motor cortices [3]. Shorter response times across practice may reflect enhancements in the encoding processes for force, target direction, and egocentric coordinate transformations that occur between motor and sensory cortices [3]. The interaction between M1 and S1 cortices during skill learning is critical, and our behavioural findings may reflect the reciprocal strengthening of connections in individuals with undisturbed WM linkage between regions. Alternately, our findings may indicate that individuals with a more intact motor network at baseline have a greater capacity for motor recovery. Rather than showing an isolated effect of cTBS on M1 versus S1, our data suggest that in individuals with a greater degree of WM integrity after stroke, it is likely that a broad network of regions responds to cTBS to promote motor learning.

4.1. Limitations. The identification of specific biomarkers that distinguish responders from nonresponders is an

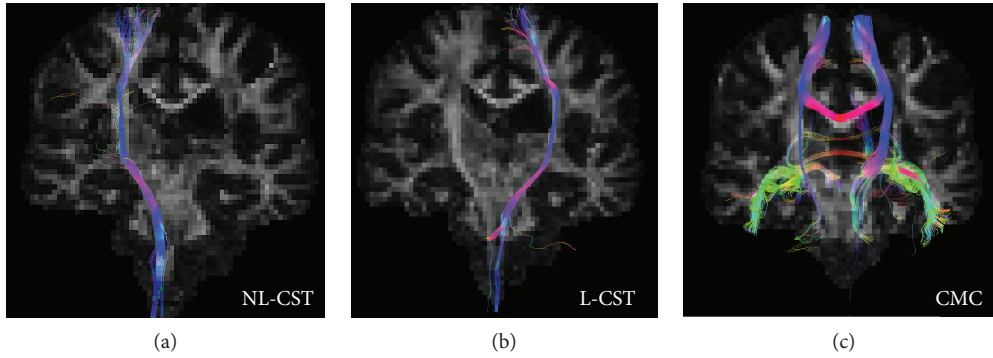


FIGURE 8: Subject-specific examples of white matter tractography. Fractional anisotropy (FA) and overlaid red-green-blue-colored FA tractography: red (left/right), green (anterior/posterior), and blue (superior/inferior). Examples of DW-WM tracts from the (a) nonlesioned corticospinal tract (NL-CST), (b) lesioned corticospinal tract (L-CST), and (c) constrained motor connectome (CMC) for a motor practice responder in the SMc-cTBS group.

important first step in understanding the mechanisms of action of noninvasive brain stimulation paired with motor practice [45]. A limitation of our study is the relatively small sample size ($n = 28$; M1c = 9, S1c = 11, and sham = 8). A larger sample may help to verify the CMC as a biomarker of cTBS response. Beyond our planned comparisons (two-tailed and one-tailed independent t -test), we observed a lack of behavioural effects and interactions between groups and sequences (random, repeated) using inferential statistics for performance of the serial tracking task. Furthermore, it is important to consider that the B value, which measures the expected change score, and was used to differentiate between motor practice responders and nonresponders, may be indicative of poor and good early performance, respectively. The motor skill nonresponders may have performed the task faster earlier in practice and therefore demonstrated a ceiling effect and less improvement in performance over the 5 days. While additional independent t -tests demonstrated that there was no statistical difference between the SM-cTBS motor practice responders and nonresponders for repeated sequence mean RTT at baseline, the group means showed motor practice responders had worse baseline performance ($M = 16.07$, $SD = 6.25$) compared to the motor skill nonresponders ($M = 12.70$, $SD = 6.81$). In addition, the predicted asymptote value, A , which reflects estimated plateau in performance, was not statistically different between motor practice responders and nonresponders, demonstrating similar practice-end motor performance levels. However, future research should investigate the response to cTBS over the contralesional hemisphere paired with motor practice in a more homogeneously impaired group of individuals with stroke.

An important alternative interpretation of our findings is that changes in motor performance may have been related to the preexisting white matter microstructural characteristics as opposed to a cTBS effect. With a larger sample, further comparisons between M1c and S1c cTBS and sham groups are needed to determine the underlying factor of change. In the current paper, we performed exploratory correlational analyses to evaluate the relationships between DWI data (CMC, NL-, and L-CST FA values) and exponential change score (B value). This was done in two ways: one using data

from individuals with stroke in the SM-cTBS group and the second using data from the entire group (SM-cTBS, sham groups). Only CMC white matter integrity showed a relationship with motor learning (B score) in the SM-cTBS group. This relationship was not observed for the group when individuals in the sham condition were included. These findings illustrate that greater integrity of the preexisting white matter microstructural of the CMC appears an important factor to drive larger change in motor performance when cTBS is applied over M1c/S1c and paired with motor skill practice, compared to motor skill practice alone.

The B value we calculated was based on the results of sessions 1 to 7; however, there were two missing data points for two participants in the sham group. We fit the data to the performance curve and calculated the B value with the missing data points omitted. Yet, performance curves are a robust method to capture the overall trend in performance data over time; curves are less susceptible to outliers, missing data, and random fluctuations than calculating the overall mean. Therefore, we believe utilizing curves to be an appropriate method to determine the capacity for performance change when missing data points exist; however, we acknowledge that missing data could bias the present findings and minimize the accuracy of predicting the trend in the data.

Finally, the CMC is a group-level approach; the diffusion-weighted images are normalized to MNI space to overlay a common motor network mask. Ideally, individualized masks created from an fMRI motor learning experiment prior to receiving a noninvasive brain stimulation intervention, in combination with the CMC, may help predict individualized responses to cTBS paired with skilled motor practice. Nevertheless, past work has shown that masks generated in native versus standard space do not yield significantly different information pertaining to WM microstructural integrity [46]. Our findings will support future work to investigate the possible usefulness of using fMRI-guided DWI as a methodological approach to identify biomarkers of recovery.

4.2. Future Studies. Individuals with stroke develop compensatory patterns of activation that promote rapid changes in motor function [47]. However, these compensatory patterns of activity may have long-term detrimental effects [48] that

are independent of improvements in motor impairment. Shifting individuals into a more normal pattern of activation early post-stroke may be an important mechanism for long-term motor recovery. As such, the capacity to determine responder and nonresponder biomarker profiles for noninvasive brain stimulation protocols is an important field of inquiry. Future studies need to determine individual functional and structural connectivity patterns associated with changes in motor function that evolve naturally (sham stimulation) compared to changes induced via noninvasive brain stimulation. Serial imaging of fMRI and DTI connectivity has been suggested as means for determining the relationship between behavioural and brain changes; however, many studies only examine changes pre- and post-intervention [44] and consider individuals in the chronic phase of recovery. Formulating experimental designs to investigate individual differences *throughout* interventions is essential to the understanding of variations in outcome measures and, furthermore, is central to derive maximal individualized treatment effects. Indeed, not all individuals demonstrate improvements over the same planned trajectory or number of practice sessions practice [17, 49]. Thus, individualized interventions are needed, based on persons' own potential for improvement.

5. Conclusions

The residual WM structure of a novel motor network in the brain, in the chronic phase of stroke, has emerged as a potential biomarker of motor recovery. The underlying neurophysiological mechanisms that yield the relationship between WM pathways and response to repetitive noninvasive brain stimulation needs further investigation. Findings from repetitive noninvasive brain stimulation studies have resulted in positive outcomes in stroke populations [50, 51]. However, the effects of noninvasive brain stimulation are known to be variable, which suggests that there are specific underlying mechanisms that drive activity-dependent plasticity following noninvasive brain stimulation paired with motor practice [51]. The findings from the present study demonstrate the potential importance of evaluating widespread, functionally relevant WM networks to characterize response profiles of individuals with stroke.

Data Availability

The behavioural and MRI data used to support the findings of this study are available from the corresponding author upon request.

Disclosure

A version of this manuscript has been published in chapter 5 of the doctoral dissertation: Wadden, K. P [17]. *The behavioural and neural science of motor skill learning in healthy individuals and people with stroke* (doctoral dissertation). University of British Columbia, Vancouver, Canada.

Conflicts of Interest

The authors declare that they have no conflicts of interest.

Acknowledgments

This study was funded by the Canadian Institutes for Health Research (CIHR) Grant (# MOP-106651). KSH was supported by the Michael Smith Foundation for Health Research, British Columbia, Canada (15980) and National Health and Medical Research Council of Australia (1088 449). KPW and KEB were supported by the Natural Sciences and Engineering Research Council (NSERC). JLN was supported by CIHR and the Michael Smith Foundation for Health Research.

References

- [1] S. M. Brodie, S. Meehan, M. R. Borich, and L. A. Boyd, "5 Hz repetitive transcranial magnetic stimulation over the ipsilesional sensory cortex enhances motor learning after stroke," *Frontiers in Human Neuroscience*, vol. 8, p. 143, 2014.
- [2] J. R. Carey, H. Deng, B. T. Gillick et al., "Serial treatments of primed low-frequency rTMS in stroke: characteristics of responders vs. nonresponders," *Restorative Neurology and Neuroscience*, vol. 32, no. 2, pp. 323–335, 2014.
- [3] S. K. Meehan, E. Dao, M. A. Lindsell, and L. A. Boyd, "Continuous theta burst stimulation over the contralesional sensory and motor cortex enhances motor learning post-stroke," *Neuroscience Letters*, vol. 500, no. 1, pp. 26–30, 2011.
- [4] Y.-Z. Huang, M. J. Edwards, E. Rounis, K. P. Bhatia, and J. C. Rothwell, "Theta burst stimulation of the human motor cortex," *Neuron*, vol. 45, no. 2, pp. 201–206, 2005.
- [5] N. Murase, J. Duque, R. Mazzocchio, and L. G. Cohen, "Influence of interhemispheric interactions on motor function in chronic stroke," *Annals of Neurology*, vol. 55, no. 3, pp. 400–409, 2004.
- [6] P. Talelli, R. J. Greenwood, and J. C. Rothwell, "Exploring theta burst stimulation as an intervention to improve motor recovery in chronic stroke," *Clinical Neurophysiology*, vol. 118, no. 2, pp. 333–342, 2007.
- [7] S. M. Brodie, M. R. Borich, and L. A. Boyd, "Impact of 5-Hz rTMS over the primary sensory cortex is related to white matter volume in individuals with chronic stroke," *European Journal of Neuroscience*, vol. 40, no. 9, pp. 3405–3412, 2014.
- [8] N. S. Ward, "Does neuroimaging help to deliver better recovery of movement after stroke?," *Current Opinion in Neurology*, vol. 28, no. 4, pp. 323–329, 2015.
- [9] K. P. Wadden, T. S. Woodward, P. D. Metzack et al., "Compensatory motor network connectivity is associated with motor sequence learning after subcortical stroke," *Behavioural Brain Research*, vol. 286, pp. 136–145, 2015.
- [10] L. M. Carey and R. J. Seitz, "Functional neuroimaging in stroke recovery and neurorehabilitation: conceptual issues and perspectives," *International Journal of Stroke*, vol. 2, no. 4, pp. 245–264, 2007.
- [11] C. Calautti, M. Naccarato, P. S. Jones et al., "The relationship between motor deficit and hemisphere activation balance after

- stroke: A 3T fMRI study," *NeuroImage*, vol. 34, no. 1, pp. 322–331, 2007.
- [12] T. Kammer, S. Beck, A. Thielscher, U. Laubis-Herrmann, and H. Topka, "Motor thresholds in humans: a transcranial magnetic stimulation study comparing different pulse waveforms, current directions and stimulator types," *Clinical Neurophysiology*, vol. 112, no. 2, pp. 250–258, 2001.
- [13] H. Enomoto, Y. Ugawa, R. Hanajima et al., "Decreased sensory cortical excitability after 1 Hz rTMS over the ipsilateral primary motor cortex," *Clinical Neurophysiology*, vol. 112, no. 11, pp. 2154–2158, 2001.
- [14] Z. S. Nasreddine, N. A. Phillips, V. Bédirian et al., "The Montreal Cognitive Assessment, MoCA: a brief screening tool for mild cognitive impairment," *Journal of the American Geriatrics Society*, vol. 53, no. 4, pp. 695–699, 2005.
- [15] T. M. Hodics, K. Nakatsuka, B. Upreti, A. Alex, P. S. Smith, and J. C. Pezzullo, "Wolf Motor Function Test for characterizing moderate to severe hemiparesis in stroke patients," *Archives of Physical Medicine and Rehabilitation*, vol. 93, no. 11, pp. 1963–1967, 2012.
- [16] S. Brown and A. Heathcote, "Averaging learning curves across and within participants," *Behavior Research Methods, Instruments, & Computers*, vol. 35, no. 1, pp. 11–21, 2003.
- [17] K. P. Wadden, K. D. Asis, C. S. Mang et al., "Predicting motor sequence learning in individuals with chronic stroke," *Neurorehabilitation and Neural Repair*, vol. 31, no. 1, pp. 95–104, 2017.
- [18] A. Heathcote, S. Brown, and D. J. K. Mewhort, "The power law repealed: the case for an exponential law of practice," *Psychonomic Bulletin & Review*, vol. 7, no. 2, pp. 185–207, 2000.
- [19] M. Yamashita, M. Kawato, and H. Imamizu, "Predicting learning plateau of working memory from whole-brain intrinsic network connectivity patterns," *Scientific Reports*, vol. 5, no. 1, p. 7622, 2015.
- [20] S. Rossi, M. Hallett, P. M. Rossini, and A. Pascual-Leone, "Screening questionnaire before TMS: an update," *Clinical Neurophysiology*, vol. 122, no. 8, p. 1686, 2011.
- [21] P. M. Rossini, A. T. Barker, A. Berardelli et al., "Non-invasive electrical and magnetic stimulation of the brain, spinal cord and roots: basic principles and procedures for routine clinical application. Report of an IFCN committee," *Electroencephalography and Clinical Neurophysiology*, vol. 91, no. 2, pp. 79–92, 1994.
- [22] A. Leemans and D. K. Jones, "The B-matrix must be rotated when correcting for subject motion in DTI data," *Magnetic Resonance in Medicine*, vol. 61, no. 6, pp. 1336–1349, 2009.
- [23] Y. D. Reijmer, A. Leemans, S. M. Heringa et al., "Improved sensitivity to cerebral white matter abnormalities in Alzheimer's disease with spherical deconvolution based tractography," *PLoS One*, vol. 7, no. 8, article e44074, 2012.
- [24] C. Nimsky, M. Bauer, and B. Carl, "Merits and limits of tractography techniques for the uninitiated," in *Advances and Technical Standards in Neurosurgery*, pp. 37–60, Springer, Cham, Switzerland, 2016.
- [25] S. H. Jang, "Prediction of motor outcome for hemiparetic stroke patients using diffusion tensor imaging: a review," *NeuroRehabilitation*, vol. 27, no. 4, pp. 367–372, 2010.
- [26] P. Mukherjee, J. I. Berman, S. W. Chung, C. P. Hess, and R. G. Henry, "Diffusion tensor MR imaging and fiber tractography: theoretic underpinnings," *American Journal of Neuroradiology*, vol. 29, no. 4, pp. 632–641, 2008.
- [27] P. S. Boggio, M. Alonso-Alonso, C. G. Mansur et al., "Hand function improvement with low-frequency repetitive transcranial magnetic stimulation of the unaffected hemisphere in a severe case of stroke," *American Journal of Physical Medicine & Rehabilitation*, vol. 85, no. 11, pp. 927–930, 2006.
- [28] F. Fregni, P. S. Boggio, A. C. Valle et al., "A sham-controlled trial of a 5-day course of repetitive transcranial magnetic stimulation of the unaffected hemisphere in stroke patients," *Stroke*, vol. 37, no. 8, pp. 2115–2122, 2006.
- [29] C. Grefkes, D. A. Nowak, L. E. Wang, M. Dafotakis, S. B. Eickhoff, and G. R. Fink, "Modulating cortical connectivity in stroke patients by rTMS assessed with fMRI and dynamic causal modeling," *NeuroImage*, vol. 50, no. 1, pp. 233–242, 2010.
- [30] N. Takeuchi, T. Chuma, Y. Matsuo, I. Watanabe, and K. Ikoma, "Repetitive transcranial magnetic stimulation of contralesional primary motor cortex improves hand function after stroke," *Stroke*, vol. 36, no. 12, pp. 2681–2686, 2005.
- [31] J. Tretriluxana, S. Kantak, S. Tretriluxana, A. D. Wu, and B. E. Fisher, "Low frequency repetitive transcranial magnetic stimulation to the non-lesioned hemisphere improves paretic arm reach-to-grasp performance after chronic stroke," *Disability and Rehabilitation: Assistive Technology*, vol. 8, no. 2, pp. 121–124, 2013.
- [32] C. D. Gray and P. R. Kinnear, *IBM SPSS Statistics 19 Made Simple*, Psychology Press, 2012.
- [33] H. Mochizuki, T. Furubayashi, R. Hanajima et al., "Hemoglobin concentration changes in the contralateral hemisphere during and after theta burst stimulation of the human sensorimotor cortices," *Experimental Brain Research*, vol. 180, no. 4, pp. 667–675, 2007.
- [34] R. Lindenberg, V. Renga, L. L. Zhu, D. Nair, and G. Schlaug, "Bihemispheric brain stimulation facilitates motor recovery in chronic stroke patients," *Neurology*, vol. 75, no. 24, pp. 2176–2184, 2010.
- [35] C. S. Mang, M. R. Borich, S. M. Brodie et al., "Diffusion imaging and transcranial magnetic stimulation assessment of transcallosal pathways in chronic stroke," *Clinical Neurophysiology*, vol. 126, no. 10, pp. 1959–1971, 2015.
- [36] L. L. Zhu, R. Lindenberg, M. P. Alexander, and G. Schlaug, "Lesion load of the corticospinal tract predicts motor impairment in chronic stroke," *Stroke*, vol. 41, no. 5, pp. 910–915, 2010.
- [37] J. H. Lee, S. B. Kim, K. W. Lee, M. A. Kim, S. J. Lee, and S. J. Choi, "Factors associated with upper extremity motor recovery after repetitive transcranial magnetic stimulation in stroke patients," *Annals of Rehabilitation Medicine*, vol. 39, no. 2, pp. 268–276, 2015.
- [38] D. K. Rose, C. Patten, T. E. McGuirk, X. Lu, and W. J. Triggs, "Does inhibitory repetitive transcranial magnetic stimulation augment functional task practice to improve arm recovery in chronic stroke?," *Stroke Research and Treatment*, vol. 2014, Article ID 305236, 10 pages, 2014.
- [39] M. Ameli, C. Grefkes, F. Kemper et al., "Differential effects of high-frequency repetitive transcranial magnetic stimulation over ipsilesional primary motor cortex in cortical and subcortical middle cerebral artery stroke," *Annals of Neurology*, vol. 66, no. 3, pp. 298–309, 2009.

- [40] T. Emara, N. El Nahas, H. A. Elkader, S. Ashour, and A. El Etrebi, "MRI can predict the response to therapeutic repetitive transcranial magnetic stimulation (rTMS) in stroke patients," *Journal of Vascular and Interventional Neurology*, vol. 2, no. 2, pp. 163–168, 2009.
- [41] A. M. Auriat, J. L. Neva, S. Peters, J. K. Ferris, and L. A. Boyd, "A review of transcranial magnetic stimulation and multimodal neuroimaging to characterize post-stroke neuroplasticity," *Frontiers in Neurology*, vol. 6, p. 226, 2015.
- [42] T. Rüber, G. Schlaug, and R. Lindenberg, "Compensatory role of the cortico-rubro-spinal tract in motor recovery after stroke," *Neurology*, vol. 79, no. 6, pp. 515–522, 2012.
- [43] R. Schulz, E. Park, J. Lee et al., "Synergistic but independent: the role of corticospinal and alternate motor fibers for residual motor output after stroke," *NeuroImage: Clinical*, vol. 15, pp. 118–124, 2017.
- [44] E. Burke and S. C. Cramer, "Biomarkers and predictors of restorative therapy effects after stroke," *Current Neurology and Neuroscience Reports*, vol. 13, no. 2, p. 329, 2013.
- [45] J. Bernhardt, K. Borschmann, L. Boyd et al., "Moving rehabilitation research forward: developing consensus statements for rehabilitation and recovery research," *International Journal of Stroke*, vol. 11, no. 4, pp. 454–458, 2016.
- [46] C.-h. Park, N. Kou, M.-H. Boudrias, E. D. Playford, and N. S. Ward, "Assessing a standardised approach to measuring corticospinal integrity after stroke with DTI," *NeuroImage: Clinical*, vol. 2, pp. 521–533, 2013.
- [47] L. Wang, C. Yu, H. Chen et al., "Dynamic functional reorganization of the motor execution network after stroke," *Brain*, vol. 133, no. 4, pp. 1224–1238, 2010.
- [48] M. F. Levin, J. A. Kleim, and S. L. Wolf, "What do motor 'recovery' and 'compensation' mean in patients following stroke?," *Neurorehabilitation and Neural Repair*, vol. 23, no. 4, pp. 313–319, 2009.
- [49] R. M. Hardwick, V. A. Rajan, A. J. Bastian, J. W. Krakauer, and P. A. Celnik, "Motor learning in stroke: trained patients are not equal to untrained patients with less impairment," *Neurorehabilitation and Neural Repair*, vol. 31, no. 2, pp. 178–189, 2016.
- [50] W.-Y. Hsu, C.-H. Cheng, K.-K. Liao, I.-H. Lee, and Y.-Y. Lin, "Effects of repetitive transcranial magnetic stimulation on motor functions in patients with stroke," *Stroke*, vol. 43, no. 7, pp. 1849–1857, 2012.
- [51] N. S. Ward, "Non-invasive brain stimulation for stroke recovery: ready for the big time?," *Journal of Neurology, Neurosurgery & Psychiatry*, vol. 87, no. 4, pp. 343–344, 2015.
- [52] J. H. Hong, S. M. Son, and S. H. Jang, "Somatotopic location of corticospinal tract at pons in human brain: a diffusion tensor tractography study," *NeuroImage*, vol. 51, no. 3, pp. 952–955, 2010.
- [53] M. R. Borich, K. P. Wadden, and L. A. Boyd, "Establishing the reproducibility of two approaches to quantify white matter tract integrity in stroke," *NeuroImage*, vol. 59, no. 3, pp. 2393–2400, 2012.
- [54] H. G. Kwon, D. G. Lee, S. M. Son et al., "Identification of the anterior corticospinal tract in the human brain using diffusion tensor imaging," *Neuroscience Letters*, vol. 505, no. 3, pp. 238–241, 2011.